THE CHIP-TOOL INTERFACE IN METAL CUTTING

by

John Gregory Horne

A dissertation submitted for the degree of Doctor of Philosophy at the University of Cambridge

St. John's College,
Cambridge

July 1978

PREFACE

This dissertation is a description of my own work, carried out in the Physics and Chemistry of Solids Group, Cavendish Laboratory, during the period between November 1975 and July 1978. It includes nothing which is the outcome of work done in collaboration and no part of it has been submitted for a degree at any other university.

The work was supervised by Professor David Tabor, whose inspiration and encouragement, and occasional scepticism, have been invaluable. For some of the time, the work was also supervised by Dr. Derry Doyle, whom I would also like to thank, for advice and companionship.

My thanks are also due to my wife; to the staff of the PCS Group, especially Mr. Alan Peck for reproducing the many photographs; to Mr. Terry Brown for help with preparation of specimens; to the Tube Investments Group and the Science Research Council for financial support and to Mrs. Denise Newman for typing the thesis so accurately.

July 1978

SUMMARY

The main aim of the work described in this dissertation has been to develop a description of the interface between the chip and the rake face of a cutting tool. This interface is of great importance in many manufacturing operations.

The experiments are conducted in a vacuum planing machine, which provides precise control of the atmospheric conditions during cutting. The chip/tool interface is studied directly, using a transparent (sapphire) cutting tool to machine various ductile metals, such as lead and aluminium, in air and in vacuum. On the basis of these observations a new classification is made of the zones of contact at the interface in continuous cutting. This description is extended to steel tools and harder workpieces such as copper.

The influence of oxygen on the rake face interaction is investigated. Previous workers have noted apparently anomalous behaviour; it is suggested that recent discoveries about the adhesion between metals and oxides help to explain these anomalies. The transparent tool is used to study the access of cutting lubricants to the chip/tool interface and the role of lubricants is examined in the light of the new description of the interface.

Continuous cutting with built-up edge formation, experienced with materials such as Duralumin and steel, and discontinuous cutting, experienced with materials such as magnesium and free-machining brass, are studied by means of these new techniques. Some suggestions are made concerning the material properties responsible for these types of cutting behaviour. The conditions of contact at the rake face of the tool are also studied.

A study is made of the influence of crystallographic orientation of the workpiece on the cutting process. Pure single crystals of aluminium, copper and magnesium are machined in various orientations. Some speculations are also made about the source of the instability in continuous cutting and on the mechanism of chip curl.

INDEX

CHAPTER ONE INTRODUCTION

ARRANGEMENT OF THE DISSERTATION 2

CHAPTER TWO THE STUDY OF ORTHOGONAL CUTTING

INTRODUCTION 4

2.1 ORTHOGONAL CUTTING GEOMETRY

2.1.1 Metal Cutting Geometry 5

2.1.2 Nomenclature 6

2.1.3 The Importance of the Shear Plane Angle 6

2.2 MODELS OF CONTINUOUS CUTTING

2.2.1 Simple Friction Models 7

2.2.2 Secondary Shear 8

2.2.3 Shear Zone Analysis 9

2.3 CONDITIONS AT THE CHIP/TOOL INTERFACE IN CONTINUOUS CUTTING

2.3.1 Nature of Contact 12

2.3.2 Stresses 12

2.4 CONTINUOUS CUTTING WITH BUILT-UP-EDGE AND DISCONTINUOUS CHIP FORMATION

2.4.1 Continuous Cutting with the Built-Up-Edge 14

2.4.2 Discontinuous Chip Formation 15

2.5 THE SHEARING PROCESS

2.5.1 Flow Stress in Metal Cutting 17

2.5.2 Instabilities in the Cutting Process 18

2.5.3 Chip Curl 19

2.6 CUTTING LUBRICANTS

Introduction 19

2.6.1 Gaseous Lubrication 20

2.6.2 Lubrication by Liquids 20

2.6.3 Access of the Lubricant 22

2.7 OTHER ASPECTS OF CUTTING RESEARCH 23

CHAPTER THREE EXPERIMENTAL ARRANGEMENT

3.1 THE VACUUM PLANING MACHINE

3.1.1 Mechanical 25

3.1.2 Vacuum System 26

3.1.3 Hydraulic System 27

3.1.4 Load Cell 28

3.1.5 Use of the Vacuum Planing Machine 29

3.2 TOOLING

Introduction 30

3.2.1 Tool Geometry 30

3.2.2 Steel Tools 31

3.2.3 Transparent Tool 31

3.2.4 Quick-Stop Device 33

3.3 PHOTOGRAPHIC EQUIPMENT 34

3.4 ANALYTICAL PROCEDURES

3.4.1 Calibration 34

3.4.2 Measurements of Cutting Geometry 35

3.4.3 Summary of Measured and Derived Quantities 36

3.4.4 Numerical Accuracy 37

CHAPTER FOUR THE CHIP-TOOL INTERFACE IN CONTINUOUS CUTTING

4.1 DIRECT OBSERVATIONS OF THE INTERFACE

Introduction 38

4.1.1 Cutting in Air 38

4.1.2 Cutting in Vacuum 40

4.2 ZONE 2 AND THE FORCES IN AIR AND VACUUM CUTTING 41

4.3 DETECTION OF MOTION IN ZONE 1

Introduction 42

4.3.1 Split Workpiece 42

4.3.2 Laminated Workpiece 42

4.3.3 Dispersed Particle Workpiece 43

4.4 FURTHER EXAMINATION OF THE CONTACT CONDITIONS

Introduction 44

4.4.1 Indium 44

4.4.2 Copper-Coated Tool 45

4.4.3 Quick-Stops with Steel Tools 46

4.4.4 Glow Discharge Cleaning 47
4.4.5 Negative Rake 48

4.5 MACHINING OF COPPER WITH STEEL TOOLS 48

4.6 DISCUSSION
Introduction 49
4.6.1 The Role of Oxygen 49
4.6.2 Movement in Zone 1 52
4.6.3 Zones 1a and 1b 53
4.6.4 Glow Discharge Cleaning 54
4.6.5 Effect with Different Tool Materials 55

4.7 A DESCRIPTION OF THE INTERFACE 57

CHAPTER FIVE CONTINUOUS CUTTING WITH BUILT-UP-EDGE FORMATION AND DISCONTINUOUS CUTTING

5.1 THE EFFECT OF BUILT-UP-EDGE ON CONTINUOUS CUTTING 59

5.2 OBSERVATIONS ON DURALUMIN WITH THE TRANSPARENT TOOL
Introduction 60
5.2.1 Alloy H 60
5.2.2 Alloy S 61

5.3 CUTTING OF MILD STEEL WORKPIECES 61

5.4 DISCUSSION OF BUILT-UP-EDGE 62

5.5 DISCONTINUOUS CUTTING 64

5.6 CONTACT CONDITIONS IN THE MACHINING OF MAGNESIUM
5.6.1 Cutting in Air 65
5.6.2 Cutting in Vacuum 65
5.6.3 Cutting Forces 66

5.7 FREE-MACHINING BRASS 66

5.8 DISCUSSION OF INTERFACE IN DISCONTINUOUS CUTTING 67

CHAPTER SIX MECHANICS OF THE CHIP-FORMING PROCESS

6.1 THE EFFECT OF ORIENTATION ON CUTTING
Introduction 69
6.1.1 Observations with a Coarse-Grained Polycrystalline Specimen 69

6.1.2 The Notion of a Constant Resolved Shear Stress 70

6.2 COPPER AND ALUMINIUM SINGLE CRYSTAL CUTTING

6.2.1 Experimental Details 71

6.2.2 Results 72

6.2.3 Discussion 73

6.3 MAGNESIUM SINGLE CRYSTAL CUTTING

6.3.1 Experimental Details 76

6.3.2 Results and Discussion 77

6.4 INSTABILITIES IN THE CUTTING PROCESS

Introduction 78

6.4.1 Tool Vibrations 78

6.4.2 Source of the Instability 79

6.4.3 Direct Observations of Lamellae 81

6.4.4 Discussion 81

6.5 CHIP CURL

6.5.1 Initial and Equilibrium Curl 82

6.5.2 Natural Curl 83

6.5.3 Ultra-tight Curl 87

CHAPTER SEVEN LUBRICANTS IN METAL CUTTING

INTRODUCTION 90

7.1 LUBRICATION BY GASES AND VAPOURS

7.1.1 The Role of Oxygen 90

7.1.2 Lubrication by Vapours 91

7.2 DIRECT OBSERVATIONS OF LIQUID LUBRICANT ACTION

7.2.1 Mechanism of Access 93

7.2.2 Carbon Tetrachloride 94

7.2.3 Water 94

7.2.4 Range of Organic Liquids 95

7.2.5 Discussion 95

7.3 LUBRICANT CHEMISTRY

Introduction 97

7.3.1 Experimental 98

7.3.2 Discussion 98

7.4 LUBRICANTS IN BUILT-UP-EDGE AND DISCONTINUOUS CUTTING

7.4.1 Lubrication in Continuous Cutting with Built-Up-Edge 101

7.4.2 Lubrication in Discontinuous Cutting 103

CHAPTER EIGHT THE ZONE 1a PROBLEM

INTRODUCTION 105

8.1 NATURE OF THE PROBLEM 105

8.2 FURTHER EXAMINATION OF THE EVIDENCE

Introduction 107

8.2.1 Contact 107

8.2.2 Stress 108

8.2.3 Movement 109

8.2.4 Adhesion 109

8.2.5 Surface Films 109

8.3 FURTHER EXPERIMENTS

8.3.1 Pulling on the Chip 110

8.3.2 Two Effects in Lubricated Cutting 111

8.3.3 More Copper Coatings 112

8.3.4 Internal and External Grids 112

8.4 DISCUSSION - POSSIBLE SLIDING MECHANISMS

8.4.1 Surface Buckling 113

8.4.2 The Effect of Roughness 114

8.4.3 Shear Stress Distribution 116

CHAPTER NINE SUMMARY OF MAIN CONCLUSIONS

SUMMARY 117

REFERENCES

CHAPTER ONE

INTRODUCTION

Metal cutting developed as a useful art long before there were analytical approaches to metal deformation. It remains a field of study in which very little real behaviour can be predicted by the application of theory alone. The deformation behaviour of metals, although complex, is in many cases amenable to analysis once the boundary conditions have been established. The development of good cutting theories is hindered by the difficulties in obtaining a realistic yet workable description of the way in which the tool and workpiece interact.

One of the major problems, preventing metal machining from being thoroughly investigated and understood, is the fact that the most important contact region in the process - the interface between the chip and the tool - is obscured from view during the cut. The work described in this dissertation includes the first comprehensive investigation into chip/tool contact conditions by means of direct observation of the interface. This is achieved by the use of a transparent cutting tool. Many of the most interesting results of this work are dynamic effects, seen when cutting is viewed from "inside" the tool. For this reason, a 16 mm cine film is included in the dissertation.

This worker has derived a considerable benefit from inheriting a working research machine-tool. Previous work with the vacuum planing machine (Williams, 1975) has been directed towards obtaining a better understanding of the role of lubricants in machining. With the ability to study directly the influence of lubricants on the rake face contact and the development of a better description of the interface, this

earlier work is extended. In addition to these speculations about the chip/tool interface, the process of forming the chip is studied, with reference to the shape of the chip, the metallurgical factors determining the mode of chip formation and the influence on cutting behaviour of the initial slip geometry of the workpiece.

ARRANGEMENT OF THE DISSERTATION

Some of the main theoretical approaches to metal cutting problems are surveyed in Chapter 2. An exhaustive review of the literature would be excessively long, so detailed discussion is concentrated in two main areas:

(a) the mechanics of the chip-forming process and form of the chip and

(b) the chip/tool interface in continuous cutting and influence of lubricants.

The apparatus is described in Chapter 3, together with the basic experimental techniques and procedures for analysing the data. Chapters 4 - 8 contain detailed descriptions of the experiments. Since the investigation often follows a progression from one conclusion to the next experiment, frequent discussion of results in the course of these Chapters is unavoidable. Wherever possible, however, several experimental situations are discussed together.

Chapter 4 is concerned with the interface between the chip and the rake face of the tool in continuous chip formation. Direct observations of the interface are first described. The transparent cutting tool is used to machine certain ductile metals in air and vacuum. The results of various modifications to the experimental technique are presented and discussed. The picture of the interface is extended to describe situations where steel tools and harder workpieces are employed.

Built-up-edge formation in continuous cutting, and discontinuous chip formation are considered in Chapter 5. With some workpiece materials, the transparent tool is used to reveal the contact conditions at the rake face. The behaviour of other materials which exhibit these modes of chip formation is discussed.

Chapter 6 includes the results of an investigation of the processes of slip in metal cutting. The influence of the crystal orientation of the workpiece is examined. Instabilities in continuous chip formation and the curl of the chip are also considered.

Lubrication in cutting is the subject of Chapter 7. The effect of gases and vapours, the access of liquid lubricant and the influence of lubricants on the chip/tool interface are investigated.

It emerges in the course of the investigation of continuous cutting that the region of chip/tool contact immediately adjacent to the cutting edge of the tool is not well understood. This region is discussed in Chapter 8.

The major conclusions of the work are summarised in Chapter 9.

CHAPTER TWO

THE STUDY OF ORTHOGONAL CUTTING

INTRODUCTION

The study of metal cutting has its origins about a hundred years ago and early studies (Thime, 1870; Tresca, 1878; Mallock, 1881) provide a description of the processes of chip formation. Mallock studied chips from a large number of materials and states "there is little difference in any of these", although his careful drawings suggest substantial variations. Thime observed that chips are formed by shear concentrated in a narrow band extending from the top of the tool to the free surface at the junction of the chip and workpiece.

Taylor (1907) adopted an empirical approach, making a monumental study of cutting tool materials and practice. The introduction of high speed steel tools in the 1900's and of cemented carbide tools in the 1920's enabled considerable advances in cutting technology to be made and promoted further theoretical studies of the machining process. Attempts were made to model the mechanism of chip formation (Ernst and Merchant, 1941) and continue to this day.

There has been a divergence between workers studying cutting from the fundamental point of view and those engaged in the development of practical cutting techniques. The complex nature of the process, with extreme conditions of stress, strain, strain rate and temperature, makes analytical approaches to the problem very difficult. Furthermore, many important aspects of the cutting process are connected with features which cannot easily be observed or measured and much doubt remains over the validity of the descriptions employed in analysis.

2.1 ORTHOGONAL CUTTING GEOMETRY

2.1.1 Metal Cutting Geometry

Metal cutting processes in general involve the passage of a wedge-shaped tool of hard material through the metal workpiece close to the surface. This results in the removal of workpiece material as a chip. The form of the tool, the nature of the workpiece and the characteristics of the chip vary with differences in the cutting geometry. Hand and machine tool processes are listed in Table 2.1 in order of increasing geometrical complexity. The list is not exhaustive, but contains the major cutting configurations.

For the purpose of fundamental study, the arrangement known as "Orthogonal cutting" is almost always employed, where the cutting edge, the direction of motion of the tool and the normal to the surface of generation are orthogonal. This leads to a considerable simplification of the mechanical principles involved, since the process may be tackled as a two-dimensional problem. Although very few practical metal cutting techniques have this configuration, the information derived from studies of orthogonal cutting may subsequently be applied to more complex geometries which are not so amenable to analysis.

Planing is an example of true orthogonal cutting, in which the workpiece is in the form of a strip. Tube cutting on a lathe approaches orthogonal geometry when the radius-to-thickness ratio is large, while disc cutting approximates to true orthogonal cutting when the depth of cut is small compared with the radius. In all these cases, the tool is wider than the section being machined. Away from the edges of the workpiece, the material flow approximates to plane strain and, as long as the depth of cut is small compared with the width of the workpiece,

TABLE 2.1 Hand and Machine Tool Processes

Cutting Process	Shape of Cutting Edge	Angle of Motion at Edge	Number of Cutting Edges	Motion of Tool	Motion of Workpiece
HAND					
Chisel	Straight	Normal	One	Linear	-
Saw	Straight	Normal	Many	Linear	-
File	Usually Straight	Oblique	Many	Linear	-
MACHINE					
Planing	Straight	Normal	One	Linear	-
Shaping	Curved	Normal	One	Linear	-
Broaching	Curved	Normal	Many	Linear	-
Tapping	Curved	Normal	Many	Circular (circumference)	-
Reaming	Curved	Oblique	Several	Circular (circumference)	-
Drilling	Curved	Oblique	Two	Circular (radial)	-
Turning	Straight	Oblique	One	Linear	Circular
Milling	Curved	Oblique	Several	Circular (circumference or radial)	Linear
Grinding	Not defined	Not defined	Very many	Circular	Linear or circular

TABLE 2.1 Hand and Machine Tool Processes

Cutting Process	Shape of Cutting Edge	Angle of Motion at Edge	Number of Cutting Edges	Motion of Tool	Motion of Workpiece
HAND					
Chisel	Straight	Normal	One	Linear	-
Saw	Straight	Normal	Many	Linear	-
File	Usually Straight	Oblique	Many	Linear	-
MACHINE					
Planing	Straight	Normal	One	Linear	-
Shaping	Curved	Normal	One	Linear	-
Broaching	Curved	Normal	Many	Linear	-
Tapping	Curved	Normal	Many	Circular (circumference)	-
Reaming	Curved	Oblique	Several	Circular (circumference)	-
Drilling	Curved	Oblique	Two	Circular (radial)	-
Turning	Straight	Oblique	One	Linear	Circular
Milling	Curved	Oblique	Several	Circular (circumference or radial)	Linear
Grinding	Not defined	Not defined	Very many	Circular	Linear or circular

the movement of material may be analysed in two dimensions.

2.1.2 Nomenclature

The essential features of this arrangement are shown in Figure 2.1. The cutting edge is formed at the apex of two faces, the clearance face, which is adjacent to the cut surface, and the rake face, which is adjacent to the chip. The angle between the clearance face and the cut surface is the "clearance angle". The angle between the rake face and the normal to the cut surface is the "rake angle", α . When the tip of the tool is the foremost point, this angle is defined as positive. In general, there will be a radius at the tip of the tool which is known as the "nose radius", but in most of the work that follows, we shall be concerned with ideally sharp tools.

A ribbon of material whose initial thickness, d, is the depth of cut is removed as a chip. When this chip is a continuous ribbon, of "chip thickness" t, the process may be idealised as continuous shear on a "shear plane" making an angle ϕ with the cut surface. Simple geometry yields the relationship:

$$\frac{d}{t} = \frac{\sin \phi}{\cos(\phi - \alpha)}$$

2.1.3 The Importance of the Shear Plane Angle

Metal cutting differs from most other metal working processes in that the flow of material is not constrained by the tooling. The amount of plastic work, which determines the cutting forces, may be expressed in terms of the shear plane angle ϕ, and in order to meet with any success, models of the cutting process must aim to predict this angle. Control of the shear plane angle is also of great importance in practical

Figure 2.1 Orthogonal cutting - nomenclature

Figure 2.2 Forces acting on the tool in orthogonal cutting

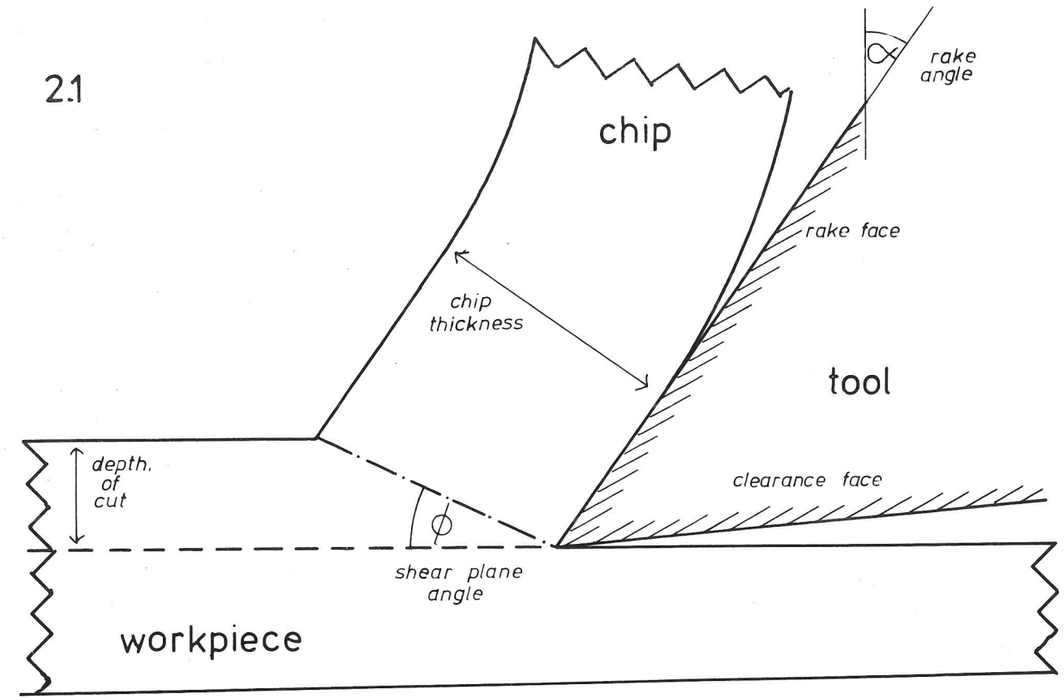

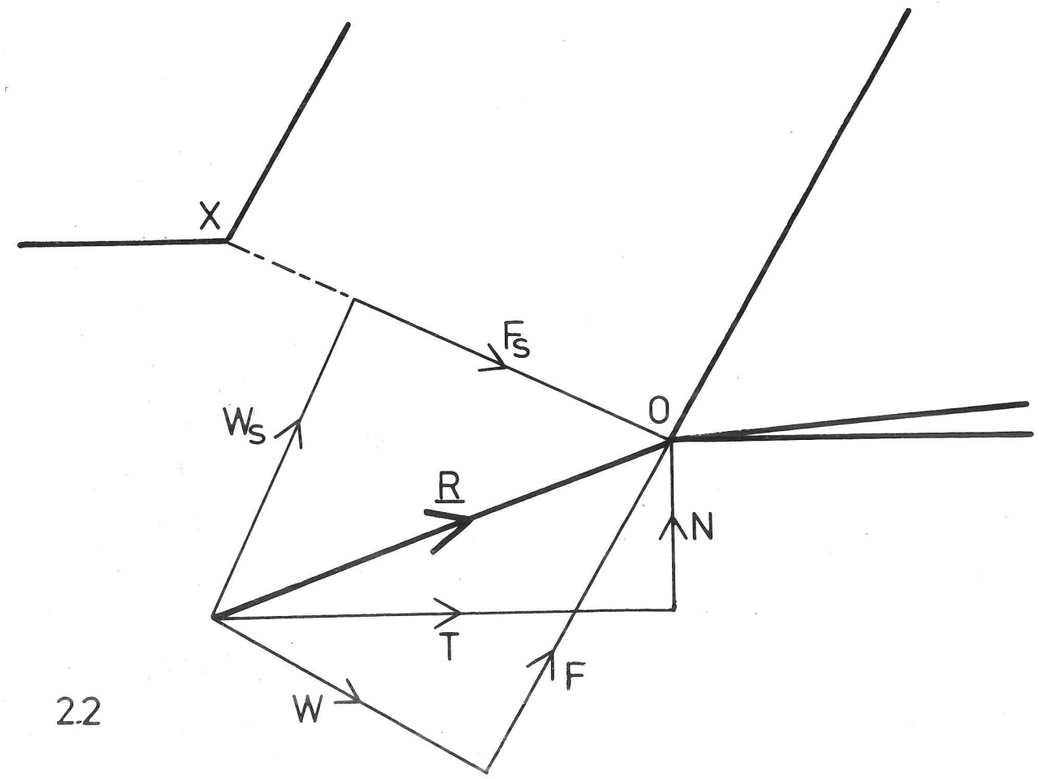

machining; in particular, a large frictional drag between the tool and the chip results in a low shear plane angle (Merchant, 1945).

2.2 MODELS OF CONTINUOUS CUTTING

2.2.1 Simple Friction Models

During continuous chip formation in the equilibrium state, a constant force R acts upon the cutting tool as shown in Figure 2.2. This may be resolved into components N and T normal and parallel to the cutting direction and it is these forces that are commonly measured in cutting experiments. R has components W and F normal and parallel to the rake face.

Several assumptions are made to develop a workable model:

(i) Shear occurs on a plane OX extending from the tool tip O to the free surface.

(ii) Forces are transmitted from the tool to the workpiece only at the rake face; the resultant forces on the shear plane are W_s and F_s normal and parallel to OX.

(iii) The normal force W and the friction force F on the rake face are related by the equation

$$F = W \tan \lambda$$

where λ is a constant friction angle.

The shear force F_s acting on the shear plane is then given by

$$F_s = \frac{R}{\cos (\lambda + \phi - \alpha)}$$

and the stress by

$$K = \frac{R \sin \phi}{dw \cos (\lambda + \phi - \alpha)}$$

where d and w are the depth and width of cut respectively.

This stress is equated to the flow stress of the material in plane strain. However, the equation is still far from instructive. It contains a friction angle, λ , whose value is as yet unknown. A more serious defect is the dependence on the shear plane angle, ϕ. It is assumed (Ernst and Merchant, 1941) that this angle takes the value which will minimise the energy consumed in the cutting process. This yields the solution

$$\phi = \frac{\pi}{4} + \frac{1}{2} (\alpha - \lambda).$$

In order to use this solution and assess its value, it is necessary to assign a value to λ. Friction angles are notorious for their variability, but when applying the principle that whatever value of λ best fits the data, the agreement of this model over a range of cutting conditions is not good. (Merchant, 1945; Kobayashi et al., 1960).

Several equations of the general form

$$\phi = f(\alpha, \lambda)$$

have been derived (Sata, 1963) with the originators often introducing additional angles, for example the angle between the shear plane and the direction of maximum shear stress (Shaw et al., 1953). All equations of this type are subject to the criticism that the friction angle, λ , is not known a priori and must be deduced for each cutting situation from experimental data. Other types of analysis have been made which incorporate different material properties or system parameters which are more amenable to independent verification.

2.2.2 Secondary Shear

It is found in practice that plastic flow occurs in a zone

extending from the vicinity of the tool tip to the free surface, known as the "primary shear zone", (Figure 2.3). In addition, observations suggest that there is always additional shearing of the chip on the underside i.e. adjacent to the rake face (Nakayama, 1962; Usui and Takada, 1967). This is described as the "secondary shear zone". The concept of frictional sliding along the rake face is replaced in newer models by the suggestion that the under-surface of the chip is affixed to the tool and relative movement occurs by internal shearing.

These models abandon the friction angle and, instead, describe the chip/tool contact in terms of a sticking length, under constant flow stress, (Rowe and Spick, 1967; Rowe and Wolstencroft, 1970). Certain assumptions in the Merchant model are retained, notably the approximation to a single shear plane and the use of a minimum energy criterion to predict ϕ. There is now, of course, the problem of assigning a value to the sticking length, which has replaced the friction angle. The work done in the primary and secondary shear zones is calculated and minimised algebraically with respect to ϕ, (Rowe and Spick, 1967). The agreement with experimental data is not particularly good but useful qualitative interpretation of cutting behaviour can be made (Rowe and Wolstencroft, 1970; Williams et al., 1970).

2.2.3 Shear Zone Analysis

A full theoretical treatment of the situation of Figure 2.3 has become possible through the use of slip line field theory (Hill, 1950; Childs and Rowe, 1973). The complexity of the slip line field (Lee and Shaffer, 1951; Kudo, 1965) and the number of parameters incorporated into the treatment (Palmer and Oxley, 1959; Hastings, Oxley and Stephenson, 1974) have grown, so that the theory in its most developed form is claimed to represent a close approximation to "real" machining

Figure 2.3 Shear zones in orthogonal cutting

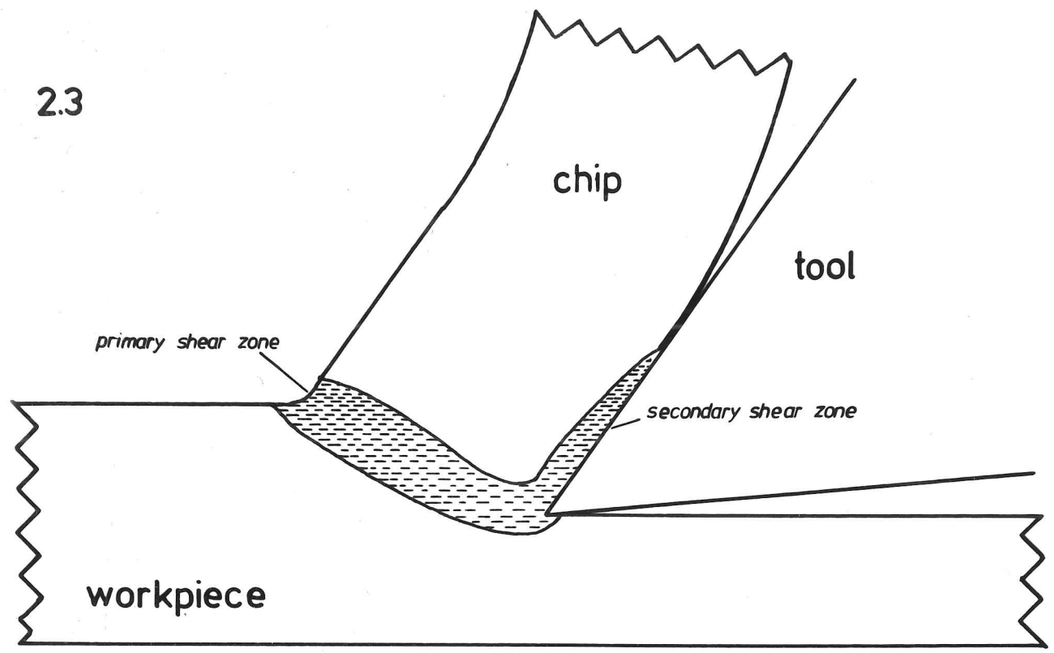

Figure 2.4 Stress distribution on the rake face of an orthogonal cutting tool (after Zorev).

τ = shear stress
σ = normal stress

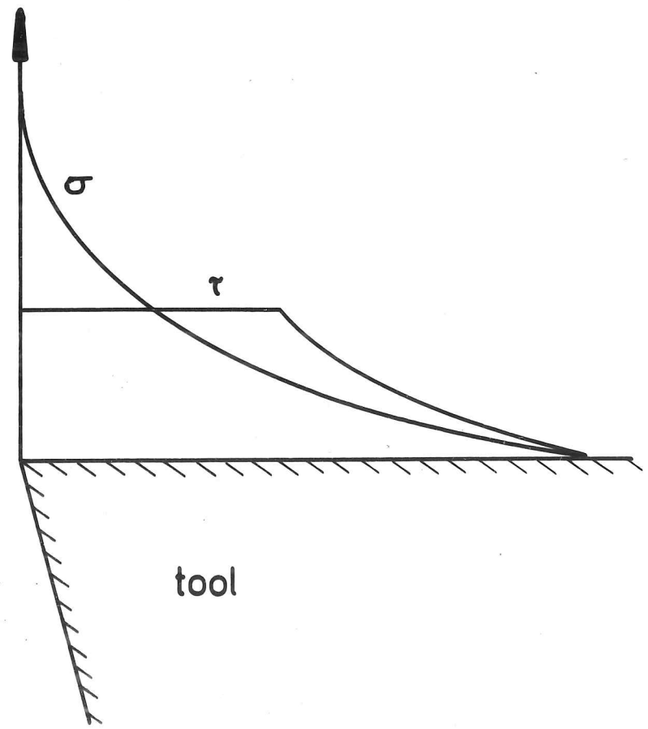

(Oxley and Hastings, 1977).

The shear plane OX in Figure 2.2 is a slip line, i.e. a direction of maximum shear strain rate (in this case infinite) and maximum shear stress. This is the simplest possible primary slip line field. Lee and Shaffer (1951) propose a straight-sided triangular secondary shear zone and predict

$$\phi = \frac{\pi}{4} + (\alpha - \lambda)$$

It will be noted that the concept of friction angle is retained. This model assumes a constant flow stress; Christopherson, Oxley and Palmer (1958) modify the analysis to take account of variations with strain (i.e. strain hardening).

Stephenson and Oxley (1970) used printed grids on the side of a workpiece in orthogonal configuration to measure the plastic flow in cutting. They conclude that the strain rate distribution is nearly symmetrical about OX, with large variations in the strain rate occurring through the primary shear zone. Childs (1971) and Usui and Takada (1967) have applied the grid method to strains on the rake face and conclude that shear strains of the order of 10 are common in this region. These techniques, unfortunately, suffer from the defect that plane strain conditions may not be maintained at the sides of the workpiece, although glass plates are usually glued to the side to restrict sideways flow. Observations may not, therefore, be representative of the strains within the workpiece and chip. In addition, the size of the grids employed is large compared with the width of the proposed secondary shear zone. The distortion of grain structure within the chip has also been used (Zorev, 1966) for estimating the strains and the size of the secondary shear zone. Specially-cast directional eutectic structures have also

been employed as "internal grids" (Cooke and Rice, 1973).

Temperature distributions lead to significant variations in the flow stress and the temperatures in the plastic zones are incorporated into recent models. Hastings, Oxley and Stephenson (1974) use empirical methods based upon experimental data of Boothroyd (1963).

Modelling the stresses on the rake face poses the greatest problems in this form of analysis (see Section 2.3). Oxley and Hastings (1977) in developing their model to predict strain rate in the primary shear zone use a "rectangular" rake face stress distribution, assuming that the normal and shearing stresses over the contact length are constant and related by a single friction angle. A significant advance is made, however, since a value for λ is not required for prediction of the stresses and strain rates. Childs (1971, 1972) has concentrated on obtaining accurate measurements of strain in the primary and secondary shear zones and developed a non-hardening theory to predict chip thickness, curvature and rake face contact length.

Recently-published work (Dewhurst, 1978) considers the pre-flow deformation at the free surface and the factors influencing curl of the chip. The author suggests that the machining process is not uniquely defined by a given set of steady-state conditions and that the mode of deformation depends in part on the build-up of deformation in the initial phase of cutting. It is also acknowledged that fluctuations in the cutting process may disturb the steady-state.

The success of slip line field theory in analysis of the cutting process is a matter of some dispute. In a recent paper considering the friction at the chip/tool interface, the authors (Oxley and Hastings, 1976) describe their results as "encouraging". Problems are encountered

in assigning values to the flow stress for the extreme conditions experienced in machining and the assessment of a particular treatment over a range of experimental situations is difficult.

2.3 CONDITIONS AT THE CHIP-TOOL INTERFACE IN CONTINUOUS CUTTING

2.3.1 Nature of Contact

The difficulties in obtaining a description of the chip/tool interface during cutting are related to the fact that it is hidden from view. Nakayama (1957, 1958) used a glass tool to machine lead at low cutting speeds and observes that the real and apparent areas of contact seem to be equal in the region adjacent to the cutting edge. Trent (1967) conducted metallographic examination of "quick-stop" sections when cutting steel with carbide and high speed steel tools and concludes that conditions of seizure are normal near the cutting edge in most metal cutting operations. Zorev (1958) and Wallace and Boothroyd (1964) observed that grinding marks on the tool are replicated on the underside of the chip and suggest that this indicates that the chip is seized to the tool. Bailey (1975), in a recent review, concludes that this picture of a sticking zone at the chip/tool interface near the tool tip is now almost universally accepted. There are, however, some reservations about the concept of seizure, since the chip is not usually adherent in this region when the cutting is stopped (Childs and Rowe, 1973).

2.3.2 Stresses

Studies have been made using photoelastic tools (Usui and Takeyama, 1960; Chandrasekeran and Kapoor, 1965) to cut lead workpieces in order to

examine the normal and shear stress distributions at the chip/tool interface. The fringe pattern in the photoelastic tool during cutting differs greatly from that obtained simply by pushing the tool against a ready-made chip. It is found that during cutting, the normal stress increases exponentially from the point at which the chip loses contact with the tool towards the cutting edge. The "frictional" stress, however, remains substantially constant over approximately half of the contact length from the tip, while over the remainder the stress decreases, roughly in proportion to the normal stress.

Studies using photoplastic workpieces (reviewed by Ramalingam, 1971) indicate that a continuous stress field exists in the primary and secondary shear zones, suggesting connections between the deformation processes. The fringes near the chip/tool interface are parallel to the rake face, except near the tip where a bowed-out appearance is noted. Caution, however, needs to be exercised in applying these results from a non-metal to the situation of metal cutting.

Further investigations into the possibility of two regions of stress at the interface have employed other techniques, such as a special dynamometer (Kamskov, 1959) or tools with controlled contact lengths (Wallace and Boothroyd, 1964). Wallace and Boothroyd propose the distinction of a sticking region, under constant frictional stress and a sliding region, where the coefficient of friction is constant. They consider that this transition is a sharp one, in contrast to the view of Finnie and Shaw (1956) who propose a gradual transition.

The model of the stress distribution that is most widely accepted is due to Zorev (1963) and is shown in Figure 2.4. Clearly a knowledge of the lengths of the sticking and sliding zones is of great importance, and an analytical method for determining the contact length is given

by Zorev (1966). The sticking region is thought to be one in which there is a steep velocity gradient from the rake face (zero velocity) to the body of the chip. In the sliding zone, the velocity at the rake face equals the chip velocity. The problem of how such a transition occurs (Scrutton, 1967) is largely unanswered.

2.4 CONTINUOUS CUTTING WITH BUILT-UP EDGE AND DISCONTINUOUS CHIP FORMATION

2.4.1 Continuous Cutting with the Built-up Edge

In certain cutting situations, the workpiece material forms a "built-up edge" (BUE) on the rake face of the tool (Ernst, 1938) and chip flow occurs over this static material, which effectively alters the geometry of the tool, increasing the rake angle (Figure 2.5). The BUE frequently breaks and reforms during cutting leading to poor surface finish. Classifications of the BUE in steels have been made (Trent, 1959, Heginbotham and Gogia, 1961) into four types according to the speed of cutting. Investigations have also been made into BUE formation in materials other than steel (Takeyama and Ono, 1968; Williams et al., 1970).

Early explanations of this phenomenon were based on the assumption that high friction and adhesion between the chip and the tool are sufficient to produce a built-up edge (Heginbotham and Gogia, 1961). Trent (1963, 1967, 1977) proposes that the BUE is composed of successive layers of chip material which seize to the tool face and to each other. However, some materials which adhere strongly to tool materials do not form BUE's (Takeyama and Ono, 1968). It is also observed that the BUE sometimes adheres preferentially to the chip (Childs and Rowe, 1973). Many additional mechanisms have been postulated as being necessary,

Figure 2.5 Continuous cutting with built-up edge.

Figure 2.6 Discontinuous chip formation.

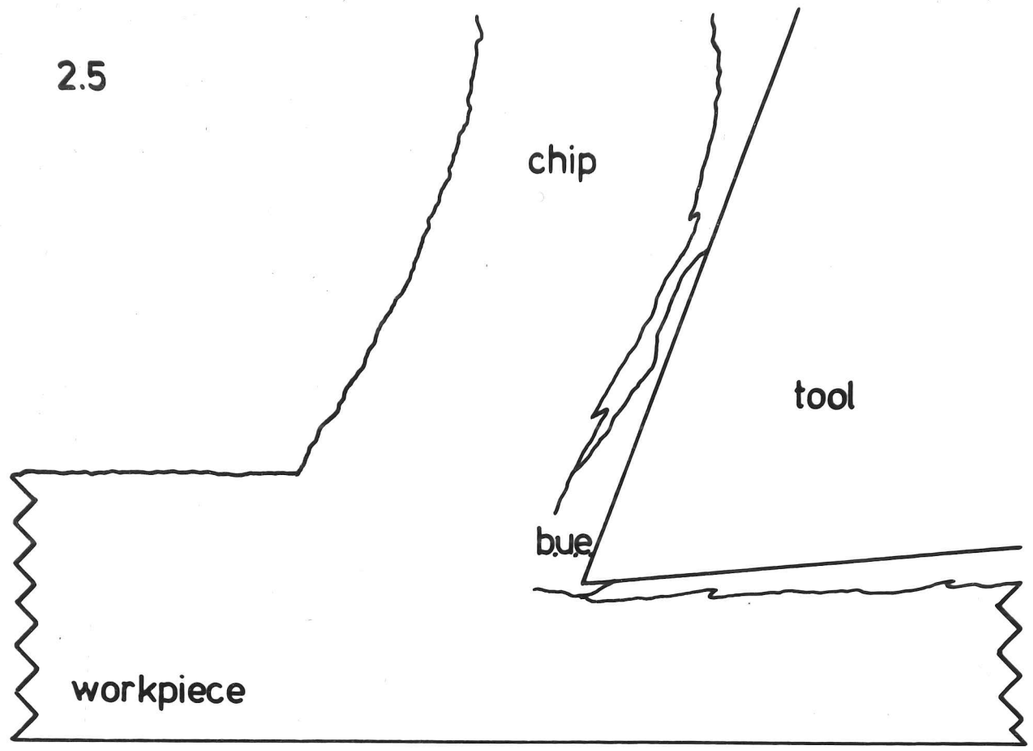

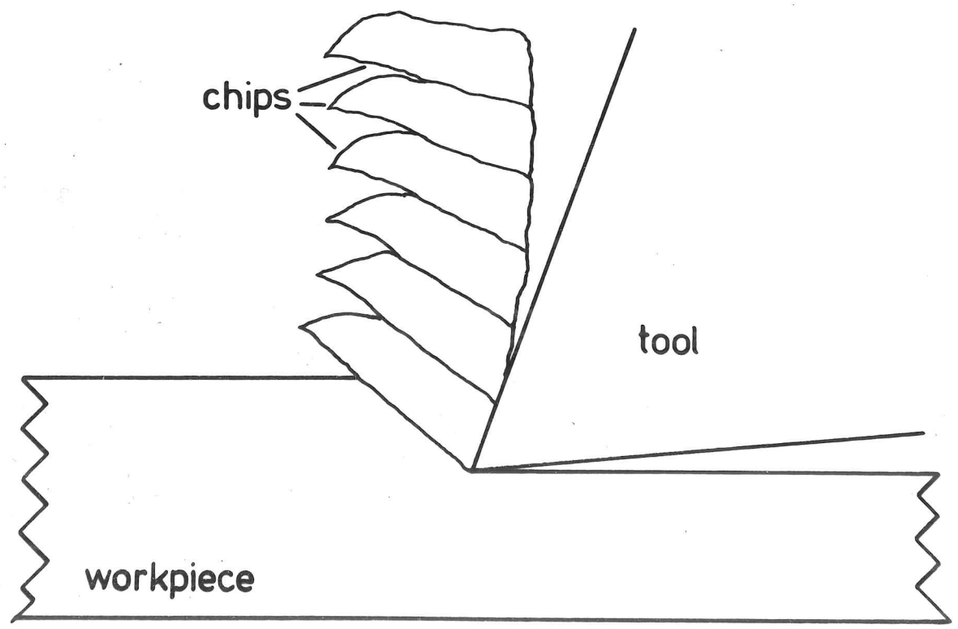

2.6

together with seizure conditions, for BUE formation to occur, including work hardening (Trent, 1963; Takeyama and Ono, 1968), strain ageing (Shaw, Smith and Cook, 1961) and solid solubility of the chip-tool combination (Iwata, Aihara and Okushima, 1971).

An alternative view is expressed by Williams et al. (1970) who suggest that only two-phase materials can form a built-up-edge. Work hardening of the chip material is held to be insufficient to stabilize a BUE while BUE's of hardness similar to the chip are sometimes capable of supporting the cutting action. The important parameters are cracking and separation between the chip and the material of the BUE, (Williams and Rollason, 1970).

Recent dynamic cutting experiments conducted inside a Scanning Electron Microscope (Doyle and Samuels, 1975) have indicated that fracture may play an important role in BUE formation and that the edge may not "build up" at all. It forms, instead, by a gross separation within the chip following the resistance to sliding on the rake face, this separation being initiated by second-phase particles.

2.4.2 Discontinuous Chip Formation

Large plastic strains are necessary for continuous chip formation, especially if the shear plane angle is low. When the workpiece material cannot support shear strains large enough to form a continuous chip, fracture can occur ahead of the tool (Figure 2.6).

The primary shear strain in continuous cutting may be expressed

$$\gamma = \frac{\cos \alpha}{\sin \phi \cos (\phi - \alpha)}$$

where the other symbols have the usual meaning. Field and Merchant

(1949) considered that discontinuous chips form if γ exceeds some critical value which depends on the material of the workpiece and the hydrostatic pressure. It has been suggested (Childs and Rowe, 1973) that the hydrostatic pressure may be approximately equated to the shear flow stress of the chip material, so a material criterion of maximum permissible shear strain can be adopted. Atkins (1974) indicates that the work of fracture should be incorporated in an analysis of the cutting situation and interprets variations in cutting behaviour in terms of fracture toughness.

In discontinuous cutting, the tool indents into the workpiece, pushing the material before it in a manner initially resembling continuous chip formation. The shear plane angle is initially large, but drops as the segment grows until failure occurs approximately along the shear plane. The crack may not propagate all the way to the free surface, since conditions at the tip of the moving crack are always changing, and a partially discontinuous mode may operate. The cycle repeats itself with the tool indenting once more into the fracture surface.

Ductile materials such as copper and iron can accommodate a large shear strain and only form discontinuous chips if the shear plane angle is constrained to be very low, which occurs at low speeds with low or negative rake angles and unlubricated conditions. The tendency is then to drag large lumps out of the machined surface. Lead additions to brass reduce its fracture toughness and induce discontinuous chip formation (Williams et al. 1970). However, there is also an effect on the rake face sliding due to the formation of a low strength interfacial lead film. Grey cast iron forms discontinuous chips but the more ductile nodular irons can form continuous chips (Cook, Finnie

and Shaw, 1954). Another commercially important class of materials to exhibit discontinuous chip formation is the Nimonic alloys.

2.5 THE SHEARING PROCESS

2.5.1 Flow Stress in Metal Cutting

Several attempts have been made to relate the primary shear process in metal cutting to shear processes in other types of deformation. The shear stress in cutting is found to be higher than in tensile experiments (Merchant, 1945). Comparison of the shear stress in slow cutting with values of the fully strain-hardened flow stress from static compression tests (Kobayashi et al., 1960) and hardness measurements (Williams and Gane, 1977) show better agreement. Dynamic testing methods (Wolak and Finnie, 1968) yield results nearer to actual cutting stresses at realistic cutting speeds.

Von Turkovich (1970) suggests a dislocation model predicting appropriate values for the shear stress. Studies of chips from micro-machining of single crystals of aluminium and copper, in the Scanning Electron Microscope (von Turkovich and Black, 1970) suggest that crystallographic orientation affects the shear process in cutting.

Ramalingam and Hazra (1973) machined aluminium single crystals and obtained force measurements for different orientations. Although variations in the shear plane angle and the cutting forces were observed, it was found that the resolved shear stress on the shear plane did not vary. The authors suggest that there is an invariant material property, the "dynamic shear stress". However, Williams and Gane (1977) in microtoming experiments with copper single crystals, found a difference in the material flow stress between "easy" and "difficult" orientations, the resolved shear stress being lower with

a specimen having a slip plane aligned with the shear plane.

2.5.2 Instabilities in the Cutting Process

Tresca (1878) and Mallock (1881) made the observation that, in continuous cutting, there are always fine striations, or "lamellae" on the free surface of the chip, indicative of some discontinuity in the process. This phenomenon has been largely overlooked in modelling the cutting process, although Shaw (1950) proposes that the presence of weak spots in the workpiece might give rise to the lamellae. With the introduction, with the Scanning Electron Microscope, of high magnification with large depths of field, closer studies have been made (Black, 1971, 1972; Ramalingam and Black, 1973). The shear process is thought to occur in an intermittent fashion, with the less deformed material separated by very thin plates of concentrated shear.

Marked variations in the lamellae spacing with differences in crystalline orientation have been noted (von Turkovich and Black, 1970). The view that thermal softening in the shear zone leads to catastrophic shear in shear fronts has received considerable support (Recht, 1964; von Turkovich, 1970). The phenomenon of "adiabatic shear" (Winter, 1975) is only elsewhere observed at very high rates of deformation, while lamellae are formed at all cutting speeds. However, the strain rates within shear fronts in the primary shear zone may be very high even at low cutting speeds (Ramalingam and Black, 1973).

An alternative description is offered by Rubenstein (1974). The tool indents into the workpiece with no interfacial slip between the chip and the rake face. When the stress necessary to produce shear on the most favourable plane is reached, shear occurs and the completed element slides up the rake face. All these approaches are considered

further in Chapter 6.

2.5.3 Chip Curl

Mallock (1881) remarks that "The curvature of shavings appears to be due to the crushing of the base of the laminae while passing over the face of the tool, thus making them thicker at that end than at the outer surface". Curly chip formation has been studied from the viewpoint of the slip line field theory (Kudo, 1965; Childs, 1971) and held to be due to the processes of secondary shear. The observation that initial chip curl is often tighter than the equilibrium curl has been attributed (Hahn, 1953) to thermal effects in the secondary shear zone.

Tight chip curl is usually associated with conditions of lubricated cutting (see Section 2.6) and unlubricated conditions, with greater rake face friction, cause straight chips to be produced (Childs, 1972). A new approach to the question of "natural curl" is presented in Chapter 6.

2.6 CUTTING LUBRICANTS

Introduction

Some manufacturing machining operations are performed "dry" but in most machine-shop situations cutting fluids are applied to the tool and workpiece. The main function of these fluids at higher cutting speeds (> 1 m sec^{-1}) is to remove heat from the cutting area and so reduce the temperature of the tool and prevent it from suffering thermal softening and wear. Lubricating properties of the cutting fluid become more important at lower cutting speeds.

Due to the contact geometry of the process, hydrodynamic and elastohydrodynamic effects are negligible and plain cutting oils can be

considered to act by boundary lubrication. Extreme pressure additives are frequently employed in metal cutting applications. Because of the highly chemically active nature of the freshly-generated metal surface formed from the body of the workpiece, the atmosphere itself is also extremely important in a study of the lubrication effects.

2.6.1 Gaseous Lubrication

The enclosure of a machine tool in a vacuum chamber has enabled workers to study cutting at low gas pressures. Cutting steel in a vacuum of 5×10^{-5} torr was found to increase the cutting forces over those experienced in atmospheric conditions (Rowe and Smart, 1963). Oxygen at pressures of 0.1 - 1 torr was found to be extremely effective in reducing the forces and it is suggested (Rollason, 1967) that the influence of oxygen is to prevent gross adhesion of the chip at the rake face. However, apparently anomalous effects have been noted when machining aluminium and copper with and without oxygen, when oxygen serves to increase the cutting forces (Rowe and Smart, 1964; Williams, 1975).

2.6.2 Lubrication by Liquids

It is widely believed that cutting oils act by preventing adhesion between the chip and the tool (Rollason, 1967; Bailey, 1975; Trent, 1977). In the case of materials that form a built-up edge, the lubricant sometimes eliminates this occurrence or else greatly reduces the BUE size. Plain oils were once widely used in cutting operations but oils with E.P. additives are now frequently employed. Chlorinated fluids are used to provide lubrication at temperatures up to about 350°C; beyond this temperature sulphonated fluids are used. Experiments

carried out by injecting fluids through a hole in the tool directly into the chip/tool interface (Sharma et al., 1971) showed that sulphonated fluids could be injected closer to the tip without the hole becoming blocked, supposedly reflecting the stability of the sulphide film at higher temperatures. It is interesting to find that these workers were unable to inject any cutting fluid closer to the cutting edge than about one and a half times the depth of cut. Fluids containing elemental sulphur have also been adopted, as well as fluids containing both sulphur and chlorine additives. Water-based synthetics are widely used in grinding operations and many have a combined surface-active and chemical role. Many factors apart from lubrication influence the development of cutting fluids, such as ease of handling and disposal. Since the operator of a machine tool necessarily comes into close contact with any cutting fluid, considerations of lubricant health hazards are of great importance.

Carbon tetrachoride, CCl_4, is frequently used in cutting research although its noxious fumes render it entirely unsuitable for machine-shop use. It is an extremely effective cutting fluid and is particularly efficient when used at the lower speeds often employed in research work (Williams et al., 1970). It is effective as a liquid or in the vapour phase but its lubricating ability is greater as a liquid (Rollason, 1967; Williams, 1975).

Childs (1972) observes that the elastic portion of the contact length is greatly reduced when using CCl_4, thus increasing the shear stress gradient over the remaining portion. Usui and Takada (1967) suggest that the formation of a low shear strength film in this region would cause the generation of a steep stress gradient.

A mechanism of cutting fluid action involving the alteration of the bulk mechanical properties of the workpiece has been put forward by

Rebinder and his co-workers (Epifanov et al., 1954; Rebinder et al., 1958) who suggest that the fluid diffuses into the metal and increases its plasticity. This view is not supported elsewhere; the effects noted by the Russian workers have been attributed to surface effects (Kramer, 1963). However, Shaw et al. (1961) and Kohn (1965) propose that CCl_4 may act by stabilising microcracks at the tool tip, which, it is suggested, reweld in the absence of lubricant. The fluid therefore has an embrittling effect. Although experiments designed to demonstrate these effects are frequently successful, there is no additional direct evidence although the presence of microcracks in continuous cutting situations has been demonstrated (Brown and Luong, 1975).

2.6.3 Access of the Lubricant

The observation that the lubricant cannot gain access to the "sticking" region adjacent to the tip of the tool is widely reported (Takeyama and Kasuya, 1961; Trent, 1967; Bailey, 1975). Considerable disagreement has arisen over the question of access of the fluid to the region between the chip and the tool close to the cutting edge.

Cassin and Boothroyd (1965), in experiments involving the use of CCl_4 as the lubricant, propose that, in the primary shear zone, diffusion occurs through the deforming workpiece material. This mechanism has been refuted on the grounds that the diffusion rate is orders of magnitude too slow (Williams, 1977) and studies using radioactively-tagged CCl_4 (Barlow, 1967) failed to produce evidence in support of this effect. The small reduction in cutting forces produced by applying lubricant to the free surface is attributed to the effect on dislocation emergence of the removal of hard oxide film on the workpiece or its replacement by a softer chloride (Barlow, 1967). If CCl_4 is applied to the workpiece

and then allowed to evaporate, the forces measured in the next cut are also reduced, but not in subsequent cuts.

A model involving the flow of liquid, against the flow of the chip, along microcapillaries in the chip/tool contact is offered by Merchant (1957) and elsewhere (Postikov, 1967). Numerical objections to this theory are made by Childs and Rowe (1973) who suggest that this mechanism imposes a severe restraint on the speed at which lubricants should be effective, lower than that observed in practice. The model has subsequently been developed to incorporate diffusion of gases and vapours (Williams and Tabor, 1976), where it is suggested that the vapour, rather than the liquid, is effective at higher cutting speeds. In spite of this, it is noted that the liquid is generally more effective than the vapour (Williams, 1977). This is because the controlling factor is the supply of liquid lubricant close to the contact region, which subsequently diffuses into the contact as a vapour.

In the only direct study of the behaviour of cutting fluid in the rake face contact which is reported in the literature (Takeyama and Kasuya, 1961), a transparent cutting tool was employed with lead work-pieces. It is reported that the access of oil to the contact occurs inwards from the sides rather than directly against the chip flow; the photographic evidence is unfortunately rather poor. This view of the mode of lubricant entry is also expressed by Mallock (1881). Some experiments described in Chapter 7 support this view.

2.7 OTHER ASPECTS OF CUTTING RESEARCH

Many approaches to the metal cutting problem involve the compilation of large bodies of data from measurements of cutting forces, chip geometry, tool wear and similar parameters in machining tests. It is probably fair

to say that advances in cutting technology are usually made on the basis of such tests rather than from an application of the principles derived from fundamental research. This reflects the progress still to be made in theoretical studies.

In "real" cutting situations, the tool is not perfectly sharp and interactions in the clearance region become important. Wear of the tool may be a more important economic factor than the cutting forces. The temperatures generated in metal cutting cause material properties to vary in a complex manner. Additionally, workpiece properties and behaviour are modified by alloying elements such as free-machining additives. Surface finish and condition are critical factors in assessing machining performance. Although these factors significantly affect real cutting techniques, in the study described in this dissertation they assume less importance. The emphasis is placed on obtaining a more valid description than hitherto available of the basic nature of the cutting process.

CHAPTER THREE

EXPERIMENTAL ARRANGEMENT

3.1 THE VACUUM PLANING MACHINE

3.1.1 Mechanical

A general view of the planing machine is seen in Figure 3.1 and a plan of the chamber is given in Figure 3.2. The rectangular base is constructed from welded stainless steel plate, and supported on a strong sectional steel framework. External welded ribs (e.g. (1)) increase the rigidity. The top plate of the chamber (not shown) is removable and is sealed to the chamber by a large Viton "O"-ring (2) in the top flange (3) and clamped through tapped holes (e.g. (4)) in the flange. The removable top plate is fitted with a 100 mm observation port located above the tool position.

The workpiece (5) is clamped to the carrier (6) at two points (7, 8) and located by means of hardened steel pins inserted through the carrier (e.g. (9)). This is attached to two shafts (10, 11) running through preloaded PTFE sleeve bearings in the chamber wall (12, 13). These shafts are driven by a hydraulic ram (14) and give the workpiece carrier a travel of 300 mm. Rotation of the carrier is prevented by a phosphor-bronze faced pin (15) sliding between two stainless steel rails (16) at the rear of the chamber.

The movement of the shafts is accommodated in the vacuum chamber by stainless steel bellows, (17, 18) supported at the centre by PTFE sleeves (19, 20) running on the shafts. The chamber is equipped with four FC38 ultra high vacuum flanges (21-24) sealed by copper gaskets. Pumping is through a 235 mm diameter hole in the base of the chamber (25).

Figure 3.1 General view of the vacuum planing machine.

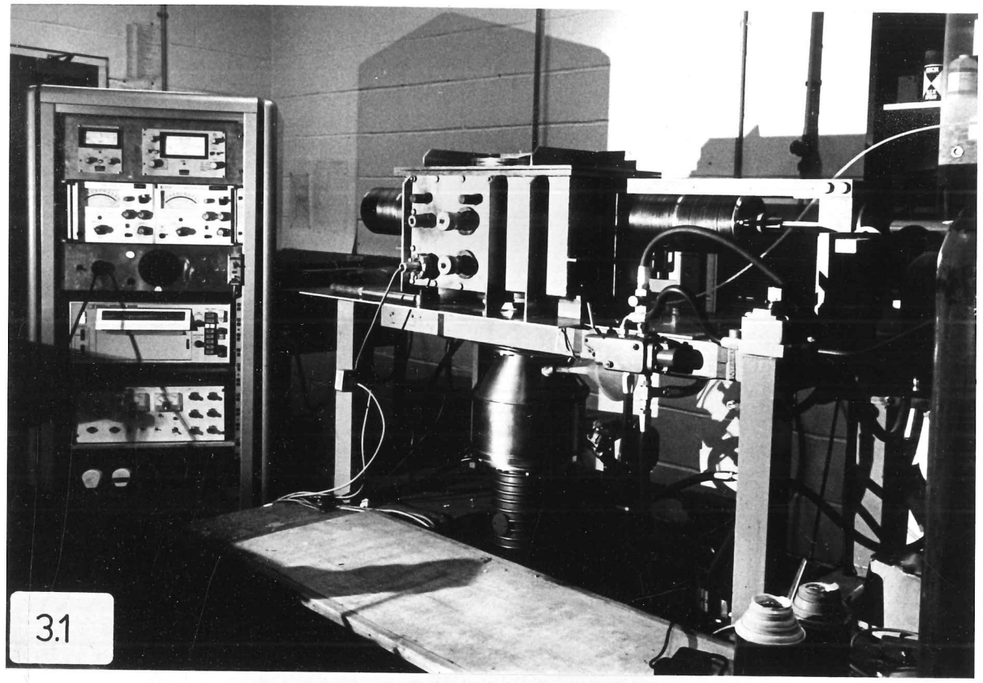

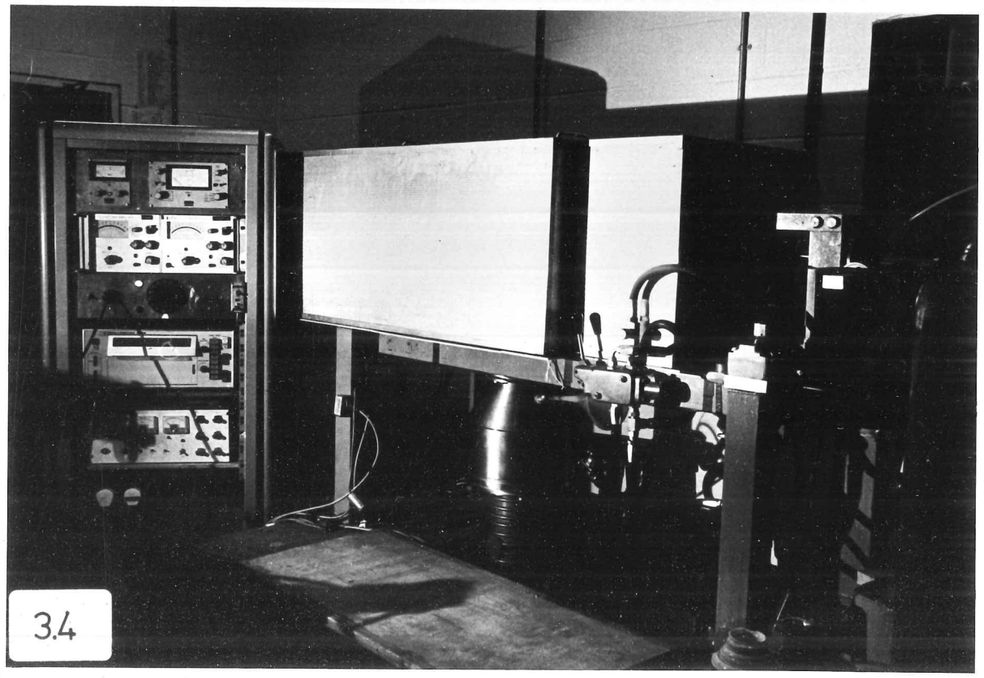

Figure 3.4 Planing machine with hot-box fitted.

Figure 3.2 Vacuum planing machine - plan of cutting chamber. Numbers indicate features described in text.

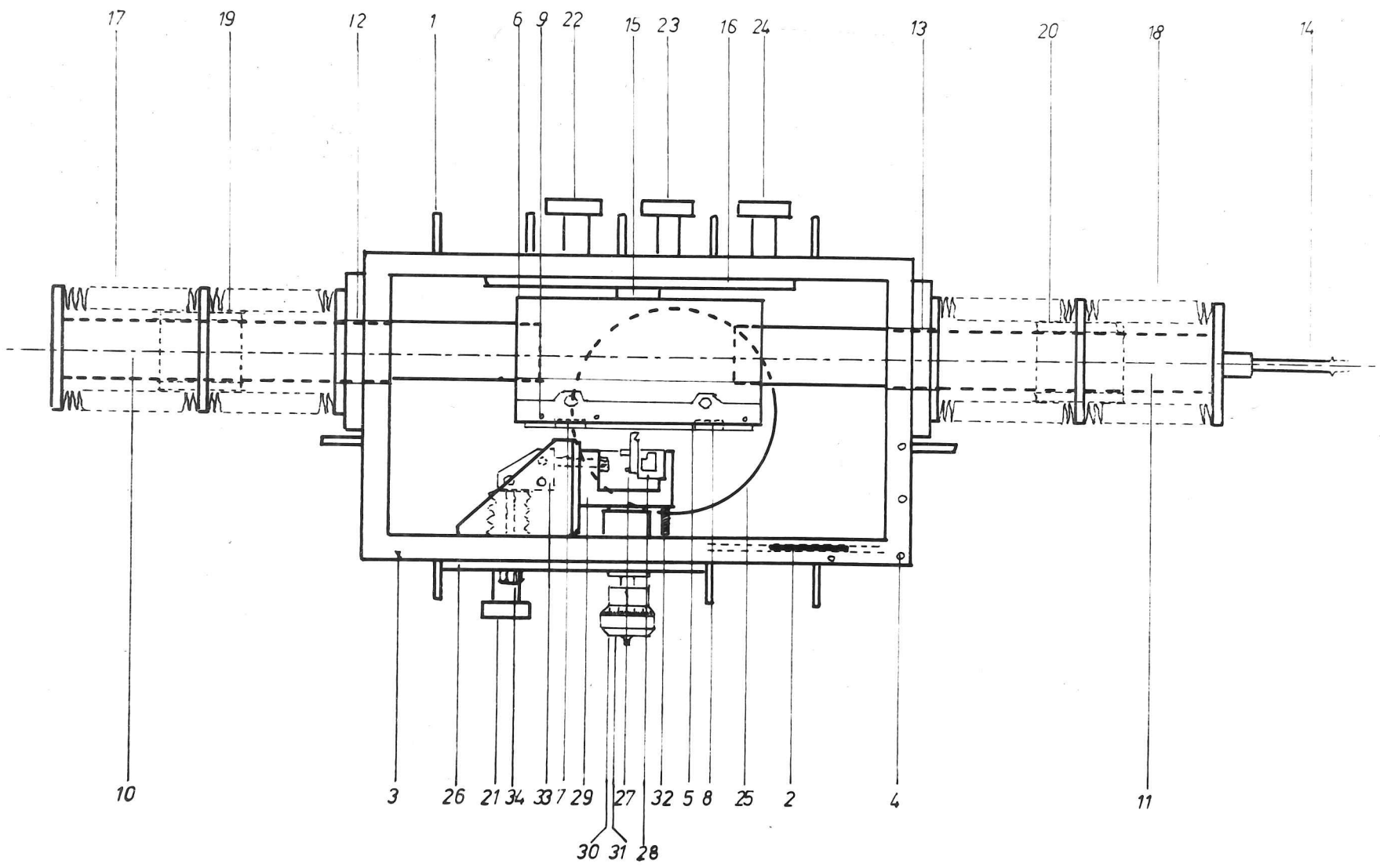

The front plate (26) which carries components (27-34) is removable and is sealed to the chamber by a Viton "O"-ring. The tool (27) is clamped to the load cell (28) which is attached to a bracket (29). Rams bear on the front and bottom faces of the bracket and are operated by micrometer adjustments ((30) and (31) below). The depth of cut may be set using one micrometer (30) and the tool moved up and down, parallel to the cutting edge, using the other (31), which operates through a rocker mechanism. The bracket (29) is held in place against the rams by a spring (32) and clamped in position via the clamping arrangement (33) by tightening the nut (34) outside the chamber.

With the exception of the tool, the workpiece, the load cell and other components where specified above, fabrication of the chamber is in stainless steel with Viton "O"-rings to seal demountable parts. This ensures a good vacuum performance and also provides resistance to chemical attack by gases and vapours applied during cutting experiments.

3.1.2 Vacuum System

A conventional high vacuum pumping system (Figure 3.3) is employed to evacuate the chamber. An Edwards model ES 330 single-stage rotary pump, P, is connected to the system by the flexible connection, F. The solenoid valve, S, provides automatic system isolation, together with air admittance to the pump, when the pump is switched off. The valve, R, connects the chamber, C, to the roughing line which incporates a bakeable foreline trap, B, and air admittance valve, A.

The high vacuum valve, V, type Edwards H9L6B, connects the chamber through the liquid nitrogen vapour-trap, T, to the diffusion pump, D, type Edwards E06 charged with Silicone oil. Foreline and backing pressures are monitored by Pirani gauge heads at G. Chamber pressure

Figure 3.3 Vacuum planing machine - diagram of vacuum system.

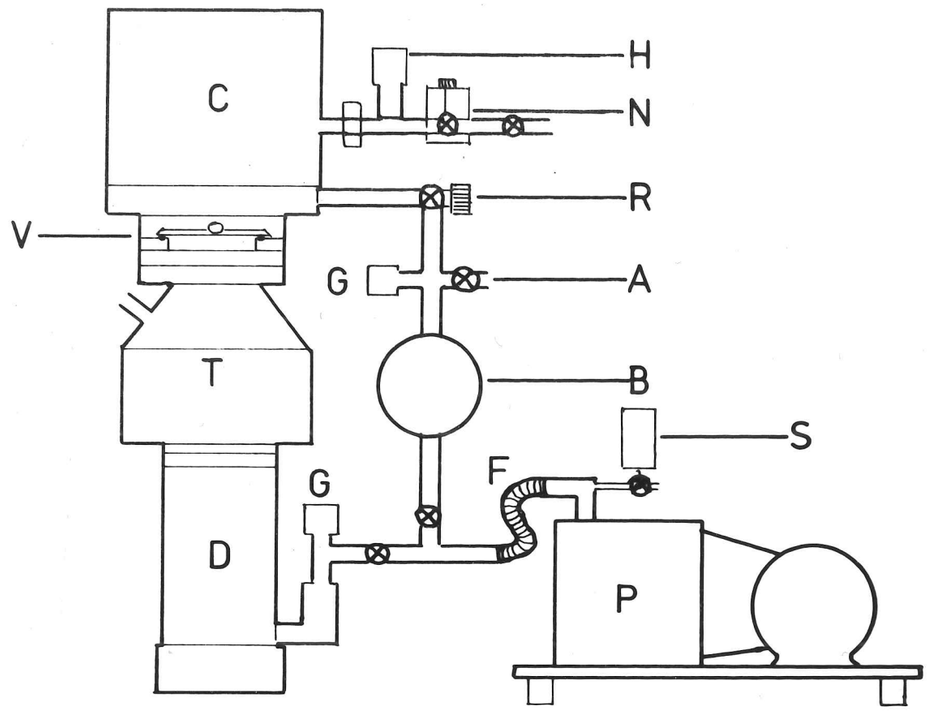

3.3

Figure 3.5 Vacuum planing machine - schematic diagram of hydraulic system.

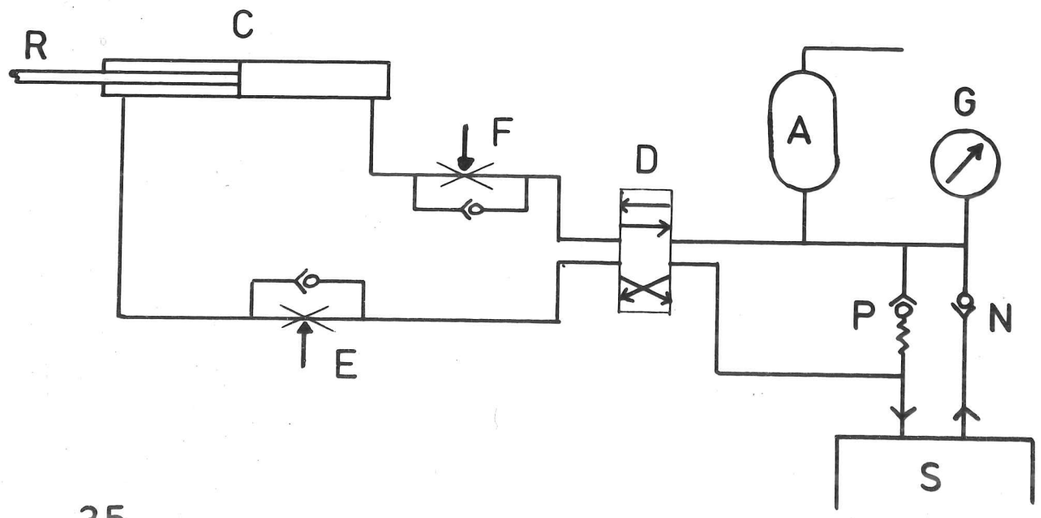

3.5

at high vacuum is monitored by the hot cathode ionisation gauge, H, connected to the U.H.V. flange (Figure 3.2 (23)). A leak valve, N, connected to the adjacent flange (24) allows gases or vapours to be bled into the system. Instrumentation for the vacuum gauges consists of an Edwards Pirani-11 dual head control unit and Ion-7 ionisation gauge unit with IG5M twin-filament heads.

The third UHV flange at the rear of the chamber, (22), carries a high voltage feedthrough for a 1000 V power supply. This is used together with an argon leak to provide glow discharge cleaning. The glow discharge electrode is mounted when required close to the cutting tool. The provision of a hot box (Figure 3.4) allows the entire chamber to be baked in order to achieve the highest vacua.

3.1.3 Hydraulic System

The ram (Figure 3.2, (14)) driving the cutting process is operated by means of the hydraulic system seen in Figure 3.5. The ram, R, is driven in the cutting or return direction by the cylinder, C. A hydraulic power pack, S, of capacity 5 litres/min delivers oil (Shell Tellus 27) to the cylinder at a pressure of 1000 psi regulated by the valve, P, and displayed on the pressure gauge, G. The three-position changeover valve, D, determines the direction of ram travel. The speed of the ram is regulated in the cutting direction by the valve, F, and in the return direction by the valve, E. E is a simple needle valve, while F is a temperature-compensated valve, type VJTVC3 by Pratt Hydraulics, with digital readout for accurate speed control.

At high cutting speeds, i.e. high rates of ram travel, the flow rate required by the cylinder exceeds the capacity of the power pack. The deficiency is made up by the hydraulic accumulator, A, which is

charged from a cylinder of nitrogen. The valve, N, prevents the contents of the accumulator from being discharged into the power pack.

3.1.4 Load Cell

Measurement of the forces acting on the tool during cutting is by a strain gauge dynamometer, which takes the form seen in Figure 3.6. This was designed at the Cambridge University Engineering Department and is machined from a single block of Dural HE15W aluminium alloy.

The force acting on the tool may be specified relative to the direction of cutting by a normal load N and a parallel load T. These give rise to compressive strains in the webs D and E and tensile strains in the webs A, B and C respectively. In practice, in common with all load cells of a similar design, there is some cross-effect on one set of webs of a load applied in the perpendicular direction and the dynamometer must be calibrated for this interaction as described in section 3.4.1.

Monitoring of the strains in A to E is achieved by the use of miniature strain gauges whose impedances vary with the strain imposed. In general, the webs may carry both a pure strain and a bending moment and hence carry two gauges on each web, one above and one below. Using the bridge arrangement seen in Figure 3.7 (for tangential strain) it is possible to measure the pure strain only. The components R are highly stable resistors which are mounted on a circuit board near to the load cell, to provide accurate temperature compensation. Au, Al etc. refer to the upper and lower gauges on each web. The bridge circuit for the normal strain is similar.

Connections to the strain gauge bridges are made via the electrical feedthrough on the front plate flange (Figure 3.2, (21)). Measurement of

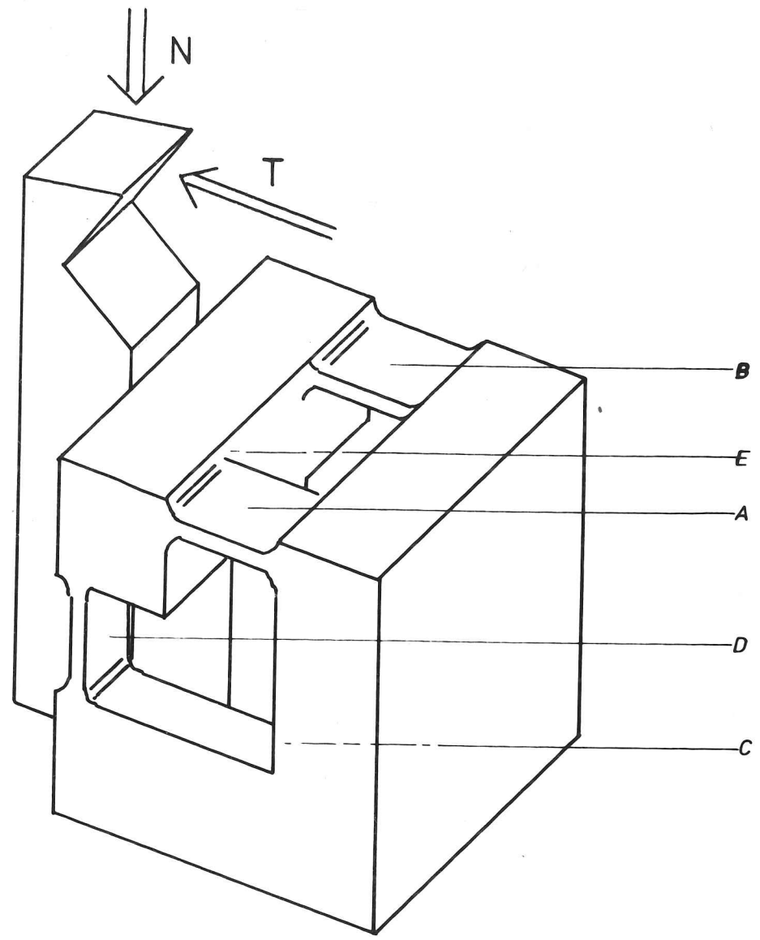

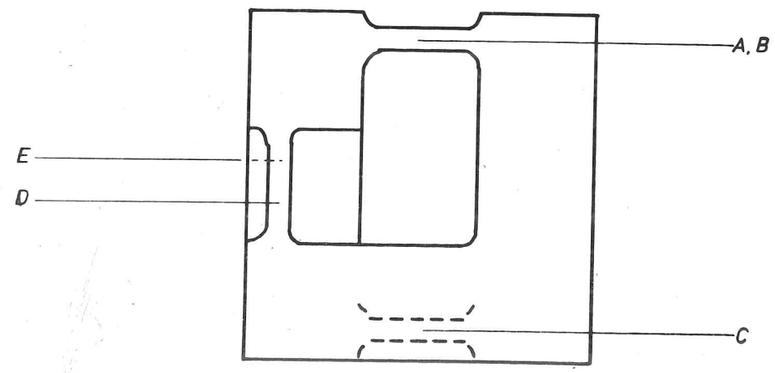

Figure 3.6 Load cell dynamometer block, showing the tool in position.

N and T are the normal and tangential forces acting upon the tool.

A to E are the webs carrying the strain gauges.

changes in the strain gauge impedance is by two Philipps PR9307 carrier wave bridges, one for each direction, and the output of these bridges is fed via a matching circuit to the UV Recorder, SE 6008 (Figure 3.8). Thus a deflection is produced on the recorder trace which is directly proportional to the strains in the load cell members and may, once calibrated, be related to the cutting forces.

3.1.5 Use of the Vacuum Planing Machine

The cutting machine used in this investigation was designed and commissioned with good vacuum performance as the prime requirement (Williams, 1975). In general, cylindrical vessels are preferred to rectangular boxes in vacuum work, but the extensive use of welded stainless steel in construction and the provision of UHV seals for demountable parts ensured that a vacuum in the region of 10^{-6} torr was readily obtained. With the use of an oven for baking-out and extended pumping times, vacua of better than 10^{-7} torr were achieved in this investigation.

However, certain deficiencies are apparent when the rig is considered simply as a machine tool. These in general relate to the low stiffness between tool and workpiece, arising from the mounting of the tool on the side of the box. This tends to flex slightly under the action of cutting forces and is also subject to a deflection upon evacuation. The operation of the clamping device also causes movement of the tool relative to the workpiece. It was found possible to overcome these uncertainties regarding the location of the tool and hence obtain control of the depth of cut. However, the general problems of stiffness remain and most of the cutting work has been performed on relatively soft materials. Fortunately, the investigation being undertaken did not demand the use of hard workpieces or heavy cuts.

Figure 3.7 Impedance bridge circuit for measurement of tangential force.

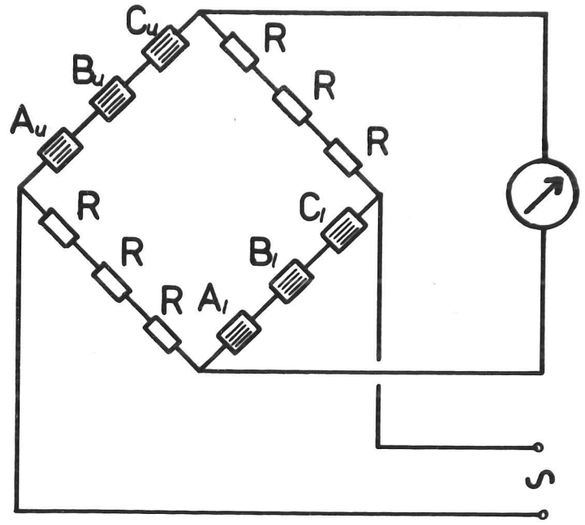

Figure 3.8 Load cell instrumentation.

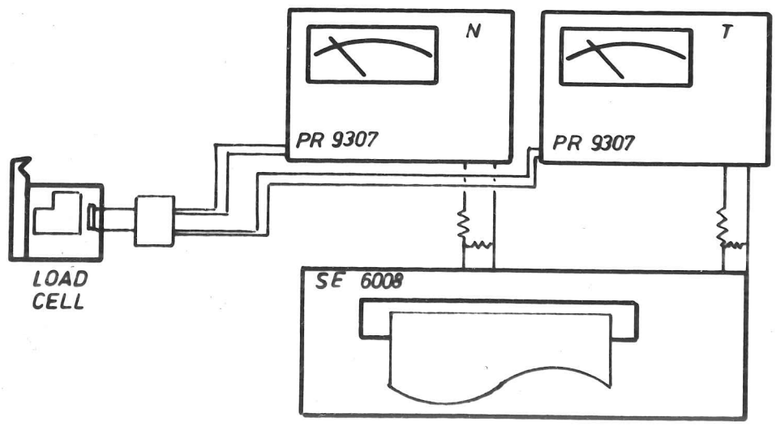

3.2 TOOLING

Introduction

High speed steel tools with a positive rake angle, about 10^{o}, are frequently employed in practical cutting situations, where good surface finish and tool life are desired. However, at high rates of stock removal, i.e. cutting speeds in excess of about 2 $m.sec^{-1}$, the temperatures generated at the tool rake face are too high for high speed steel to retain sufficient hardness and cemented carbide tools are employed. Since brittleness is a characteristic feature of these materials, they require negative rake angles in order to be sufficiently robust, commonly of the order of -10^{o}.

Since the maximum speed of the planing machine is less than 1 $m.sec^{-1}$, steel tools were employed in this investigation, but some examination was made of the effects of negative rake.

3.2.1 Tool Geometry

The geometry of the tool in orthogonal cutting is specified by three parameters - the rake angle, α, the clearance angle and the nose radius. (See Section 2.1.2 and Figure 2.1). For much of the experimental work in this investigation, a rake angle of 10^{o} was employed. However, various pure metals were machined, often in the annealed state, when rake angles as small as 10^{o} give rise to side-spreading effects. Accordingly, much sharper cutting tools of 40^{o} rake were prepared for machining these materials.

The clearance angle was 5^{o} in all cases; although at the lower end of the practical range this was held to be adequate since flank wear was not anticipated. The techniques of tool preparation ensured

that the cutting edge was always very sharp, with radii less than 1 μ. Under these circumstances, the force arising from the "ploughing" interaction at the tip in, say, a cut of 100 μ depth is small (Albrecht, 1960) and may be ignored.

3.2.2 Steel Tools

The high speed steel tools with rake angles of 10° and 40° were machined from T1 steel and oil hardened and tempered to a hardness of 850 VPN prior to grinding to the final dimensions. Further lapping of the rake face was sometimes employed. Tools of plain carbon steel were also manufactured, with the same rake angles, and hardened and lightly tempered to 770 VPN. These were in the form of inserts, which could readily be removed from the holder for study in the Scanning Electron Microscope.

3.2.3 Transparent Tool

In order to render the interactions at the chip/tool interface available for direct observation, a transparent cutting tool was designed, based upon an original conception by Dr. N. Gane. The basic geometry of this tool is seen in Figure 3.9. The tool has a rake angle of 10° and a clearance angle of 5°. The image of the cutting edge is internally reflected at the lower, angled face, to emerge parallel to the cutting edge through the "top" of the tool.

Two prototype tools were produced in fused silica, but the remainder of those manufactured were of the harder synthetic sapphire, with the "C-axis" perpendicular to the rake face. These tools were made by Agate Products of London and the faces were polished at a high pressure using diamond paste on a soft metal lap. The cutting edge is

Figure 3.9 Transparent insert - geometrical details.

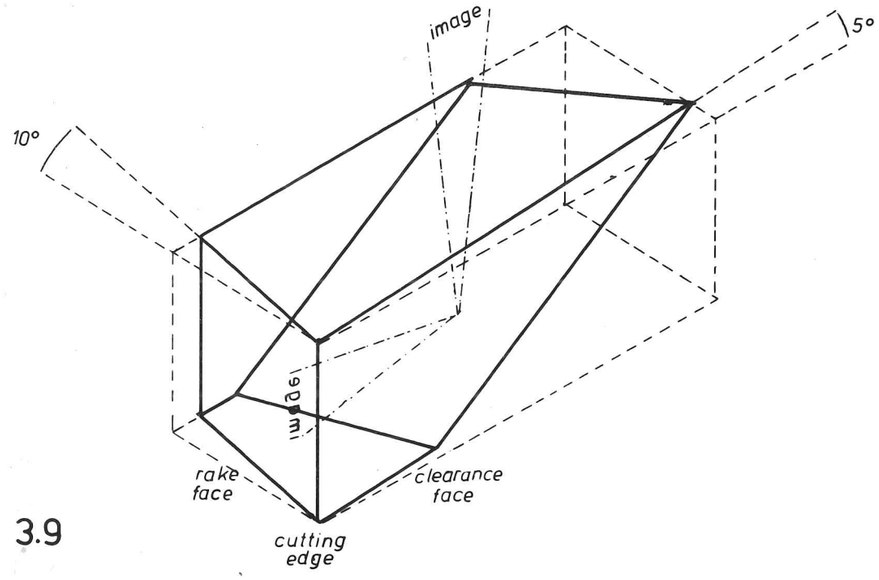

3.9

Figure 3.10 Method of mounting the transparent insert for use as a cutting tool.

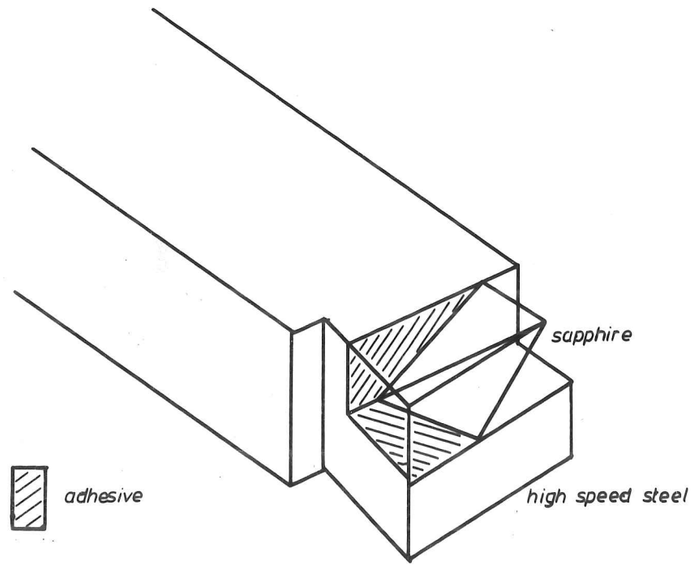

3.10

as sharp as can be achieved by this method, while the remainder of the edges carry a 0.5 mm chamfer.

The tool is held in a 12.5 mm square section steel holder, similar to the high speed steel tools described in Section 3.2.2. The transparent insert is held in place by epoxy adhesive as seen in Figure 3.10. The adhesive mix was carefully controlled to ensure that the bond failed before the tool tip, helping to preserve the expensive sapphires in the event of excessive loading. The cutting edge of the sapphire is in line with a steel cutting edge of the same geometry, enabling cleaning and preparatory cuts to be made with the steel edge under the same experimental conditions as with the transparent tool. The operation of the transparent tool is shown schematically in Figure 3.11.

Multiple reflections arise whenever an observer looks into an acute angle made by polished faces and the image obtained with the transparent tool requires some clarification. (Figure 3.12). AB is an image of the cutting edge itself; above and below it are two images of the rake face. The upper image (X) is unconfused, being the result of a single reflection at the clearance face (and angled (bottom) face). The lower image (Y) is a direct view of the rake face with a reflected image of the clearance face superimposed upon it; this however falls away rapidly and hence the rake face image dominates the field of view. Where lighting conditions give a good upper image (X), one may concentrate on this for a view of the chip/tool interaction at the rake face.

A typical view of the tool during cutting is seen in Figure 3.13. At the top of this picture is the workpiece; the chip may clearly be seen on the right with the transparent tool in the centre. The cutting edge is identified by small features arising from imperfections in the

Figure 3.11 The transparent tool in use, showing the direction of viewing.

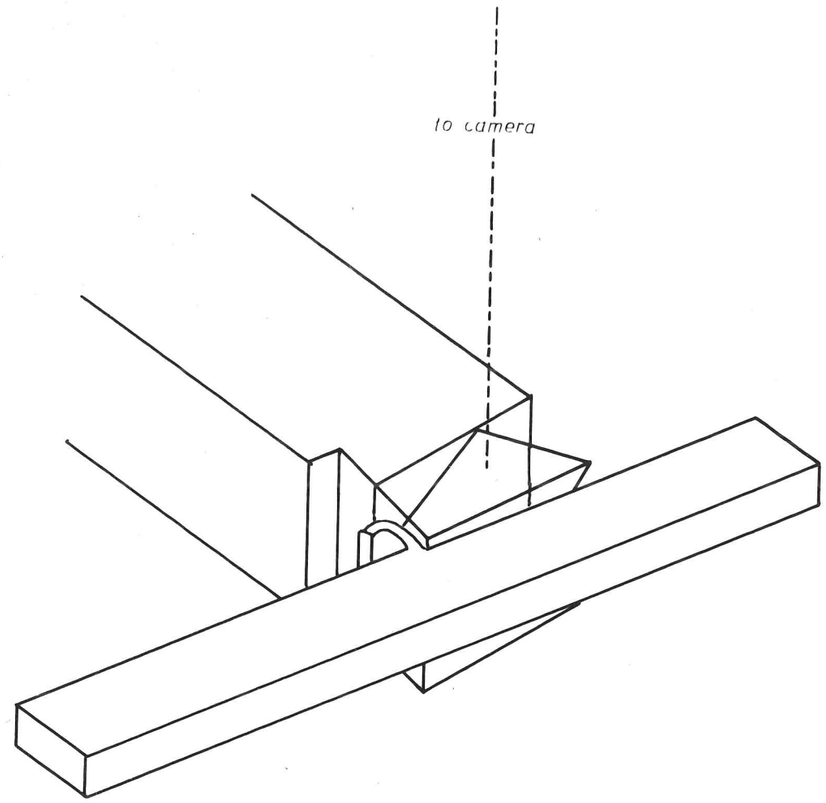

3.11

Figure 3.12 Schematic diagram of the view from above during cutting with the transparent tool.

(x) is an image of the rake face contact.
(y) is an image of the rake and clearance face contacts.

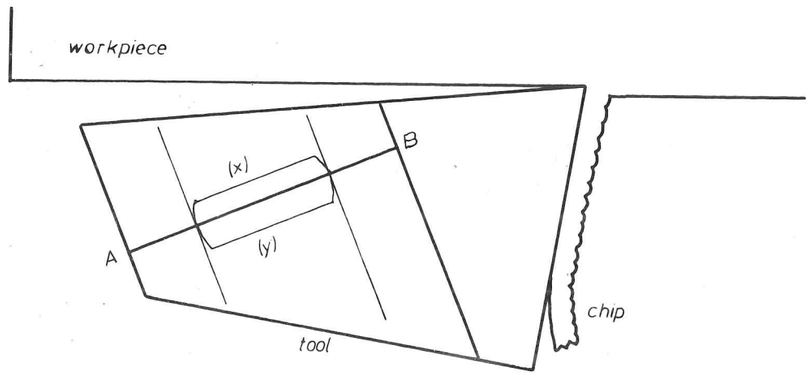

3.12

Figure 3.13 Photograph of the transparent tool in use; dry cut on lead workpiece.

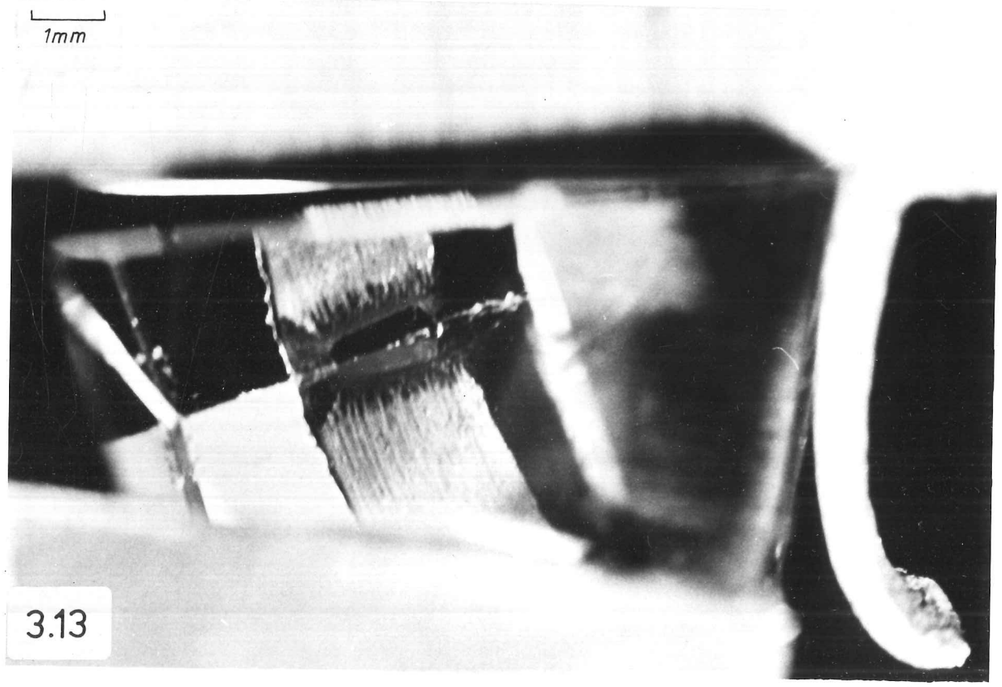

cutting edge, this tool having been given considerable use. The two images of the chip/rake face contact are seen, with the underside of the chip visible but gradually going out of focus where contact between chip and tool is not maintained.

3.2.4 Quick-Stop Device

Tool holding devices equipped with some mechanism for rapid tool disengagement are frequently employed where an understanding of the chip/tool interaction during cutting is sought. The tool is frequently supported against a shear pin or diaphragm which fails rapidly when an explosive charge pushes the tool out of engagement. The partially-formed chip is carried away with the workpiece. A simplified version of this device, operated mechanically, is available for use with the vacuum planing machine (Figure 3.14). Striker plates, clamped with the workpiece in the carrier, make contact with the tool, causing the shear pin to fail. Although the acceleration of the tool is not as high as with explosive devices, it is suggested that the distance moved by the tool before it has achieved the speed of the workpiece/chip is still small compared with the depth of cut (Williams, 1975).

Direct studies using transparent tooling give the majority of the observations of the chip/tool interface in this study. However, some use was also made of the quick-stop facility to provide additional information about conditions at the interface when using steel cutting tools and to allow comparison with the experimental results of other workers.

Figure 3.14 Cutaway drawing of quick-stop device fitted in place of the load cell.

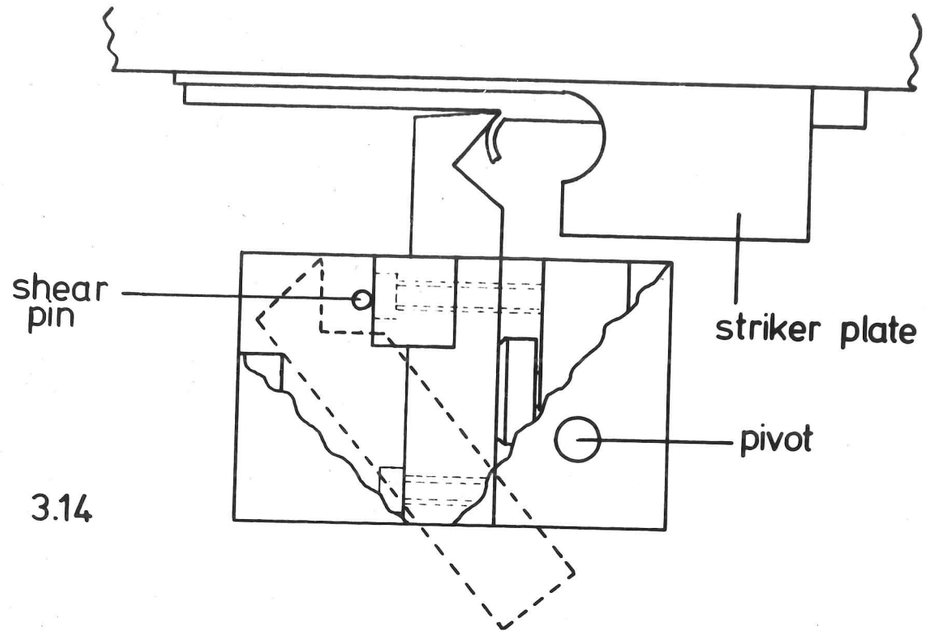

3.14

Figure 3.15 Method of calibrating the load cell.

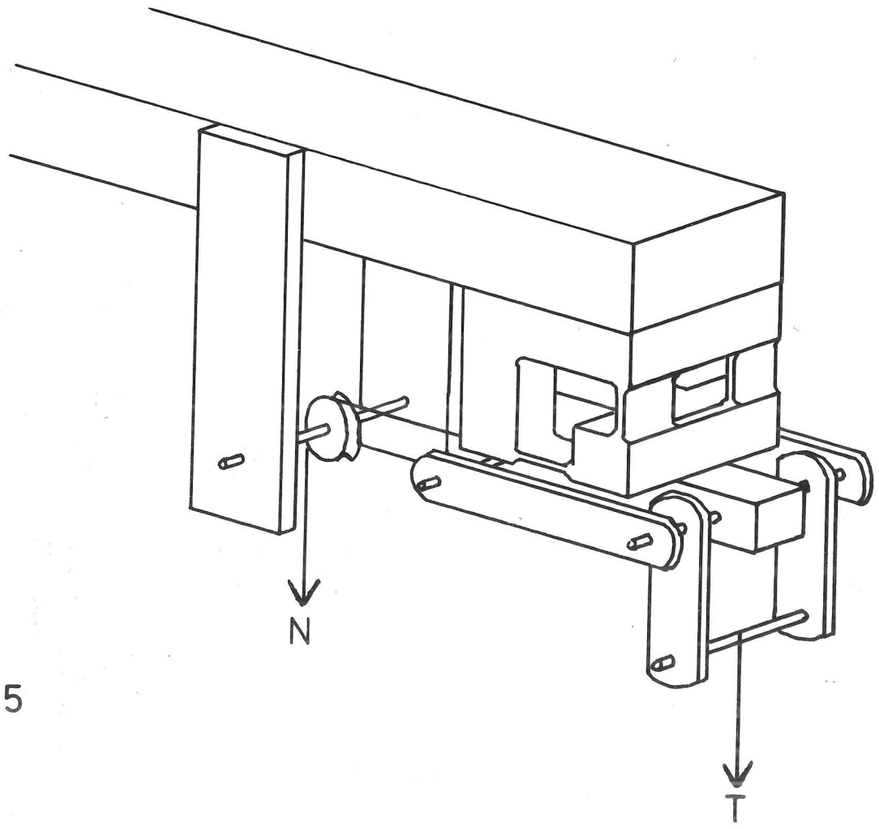

3.15

3.3 PHOTOGRAPHIC EQUIPMENT

Live observations with the transparent tool were made using a binocular microscope clamped to the top of the planing machine. For recording purposes, two pieces of equipment were employed, one for still photography and the other for making cine films. Still photographs were obtained with a Pentax 35 mm camera equipped with a f/1.8, 55 mm Super Takumar lens attached to extension bellows of length 125 mm, giving a magnification in excess of x2 on to the film. 16 mm cine films were made with a Bolex H16 professional camera and Zoomar f/2.8, 90 mm macro-zoom lens at a magnification of 1. In both cases a polarising filter was incorporated in the optical system since sapphire is bi-refringent. Some use was also made of the Hi-Speed camera manufactured by John Hadland (London), with the Zoomar 90 mm lens.

3.4 ANALYTICAL PROCEDURES

3.4.1 Calibration

The arrangement shown schematically in Figure 3.15 was employed to calibrate the strain gauge bridges. Forces were applied by adding weights to the pans hanging from the wires N and T and the galvanometer deflections produced at the UV recorder were measured directly on the trace. Separate calibrations were made of the deflections produced by pure normal and tangential applied loads, together with calibrations for the effect of simultaneous loading. Rotation of the load cell by 180^{o} in the horizontal plane permitted negative normal loads such as those occurring in some cutting situations to be calibrated. Dynamic loading characteristics of the dynamometer were also investigated but were found not to deviate greatly from the dead loading behaviour.

The deflections resulting from these applied loads for various bridge sensitivities were plotted on rectangular axes and force contours drawn, which approximated to straight lines. Calibration diagrams such as Figure 3.16 were prepared. These could be used to provide a graphical force conversion for experimental data, but it was found that the quickest method was to use a pair of equations, describing the relationship between the applied loads and recorder deflections. A simple programme to solve these equations was prepared for the Hewlett-Packard 9825A desk computer.

Frequent reassessments of the load cell behaviour were anticipated but it was found that a simple test with a few values of applied load was sufficient to check the calibration. "Action limits" of $\pm 5\%$ were set beyond which recalibration would be conducted but this was never necessary.

The value controlling the cutting speed (Figure 3.5, F) was calibrated by cutting a workpiece of known length and measuring the distance on the recorder paper between the beginning and end of the force trace; the timing marks made by the recorder are known to be very accurate. The calibration was checked from time to time and found to be consistent to within about 3%.

3.4.2 Measurements of Cutting Geometry

The depth of cut, d, was set by the micrometer adjustment on the front plate, and the clamping nut tightened to the same torque every time to minimise the variation in the slight tool movement that clamping produced. A further check on the depth of cut was made by recording the position of the cut surface with a clock gauge before and after each cut.

Figure 3.16 Typical load cell calibration diagram, for conversion of galvanometer deflection readings to cutting tool forces.

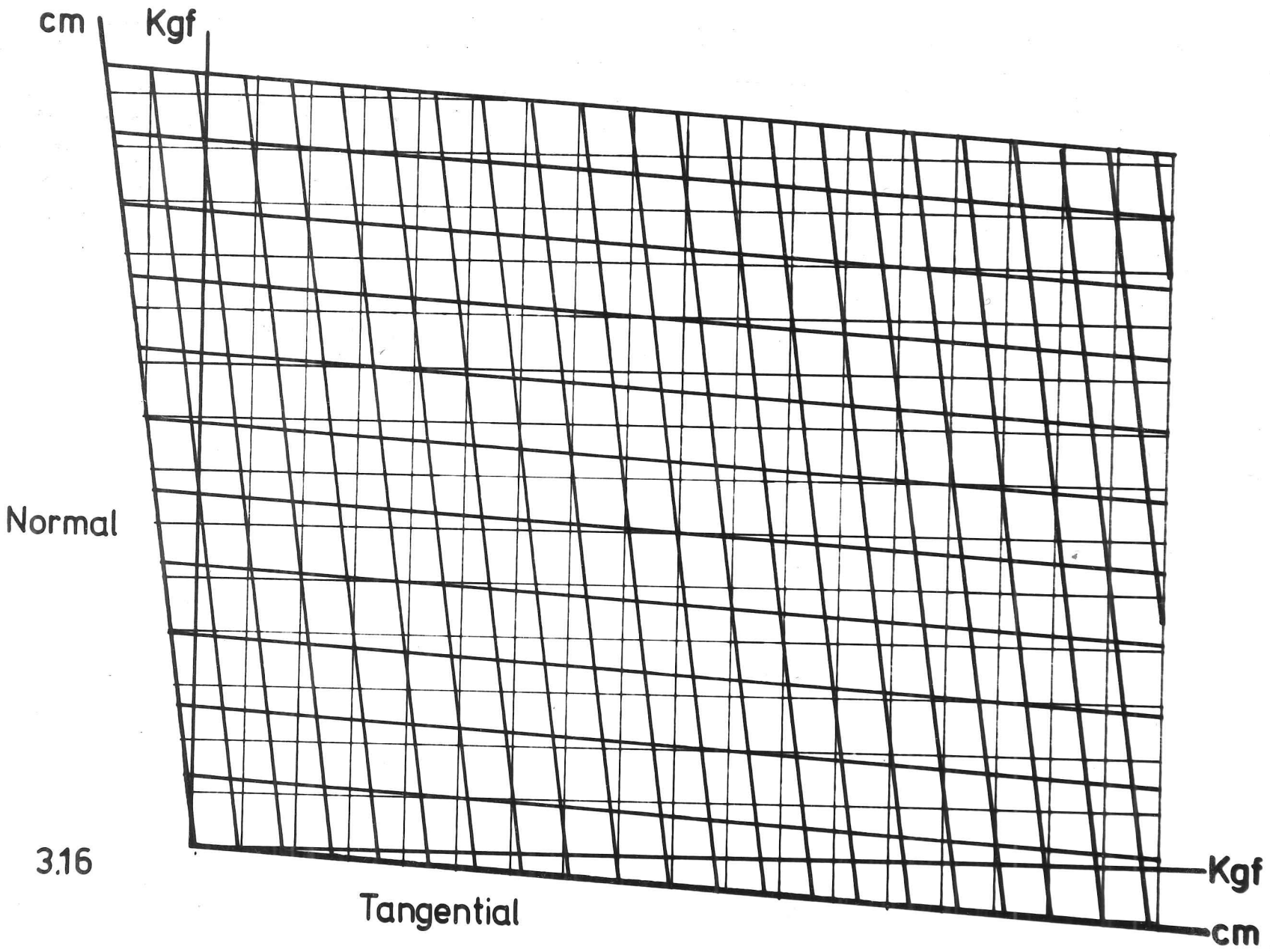

The chip thickness, t, was measured by means of a clock gauge equipped with a sharp stylus and mounted on an anvil; the chip was placed with its (smoother) tool-side to the anvil and several thickness measurements made with the stylus applied to the free surface. The "contact length", l, on the rake face was measured directly when required by careful study of chips from quick-stop experiments.

3.4.3 Summary of Measured and Derived Quantities

Measured quantities:	Normal trace deflection	D_N
	Tangential trace deflection	D_T
	Width of cut	w
	Depth of cut	d
	Chip thickness	t
	Contact length	l
	Rake angle	α
Calculated quantities:	Normal load	N
	Tangential load	T
	Cutting ratio	r_c
	Shear plane angle	ϕ
	Force on shear plane	F_s
	Stress on shear plane	k
	"Friction" force on rake face	F
	Normal force on rake face	W
	Notional friction angle	λ
	"Friction" stress on rake face	k_f

Relationships:

$$N = aD_N + bD_T$$

$$T = cD_N + dD_T$$

$$r_c = d/t$$

$$\tan \phi = \frac{r_c \cos \alpha}{1 - r_c \sin \alpha}$$

$$F_s = T \cos \phi - N \sin \phi$$

$$k = \frac{F_s \sin \phi}{dW}$$

$$F = N \cos \alpha + T \sin \alpha$$

$$W = T \cos \alpha - N \sin \alpha$$

$$\tan \lambda = F/W$$

$$k_f = F/wl$$

3.4.4 Numerical Accuracy

The main emphasis in the experimental work has been placed on careful qualitative observation of the cutting process. Cutting forces have been measured, most frequently, more to illustrate trends than to yield accurate data. However, some estimates of mechanical properties relating to the machining process have been calculated and these should be viewed in the light of the errors expected in measurement.

Force measurements are probably accurate to about $\pm 5\%$ while rake angle and width of cut are known very precisely. Cutting ratio, r_c, and contact length on the rake face, l, are subject to the largest errors due to the uncertainties in direct measurement of the chip. These could be as high as $\pm 10\%$ in some cases. This leads to an expected error in k, the resolved shear stress, as high as $\pm 20\%$. Most probably the accuracy is rather better than this, but errors of the order of 10% are likely.

CHAPTER FOUR

THE CHIP-TOOL INTERFACE IN CONTINUOUS CUTTING

4.1 DIRECT OBSERVATIONS OF THE INTERFACE

Introduction

In preliminary studies of the interface, the transparent tool was used to cut lead at low speeds in air and in vacuum. Visual observations were made and the effects recorded photographically. These experiments were repeated using aluminium workpieces and some attempts were also made to cut copper.

4.1.1 Cutting in Air

When cutting lead and aluminium workpieces in air, there was initially a short contact length on the rake face accompanied by a tight chip curl. This contact length increased rapidly during the first few millimetres of cut to about three times the depth of cut. The region of apparent contact between the rake face of the tool and the workpiece was featureless during this initial establishment of contact, but within the first five millimetres of cutting, particles of material appeared to become attached to the rake face within the contact region, towards the point at which the chip separated from the tool. At the sides of the cut (i.e. the faces of the workpiece) this transfer extended to the cutting edge.

The underside of the chip, viewed through the transparent tool, also developed features as this interaction occurred. While the initial chip surface was featureless and the chip curled smoothly away from the rake face, this onset of transfer resulted in grooving of the chip which

Figure 4.1 Sequence of views through the transparent tool, showing the contact conditions that develop when machining lead in air.

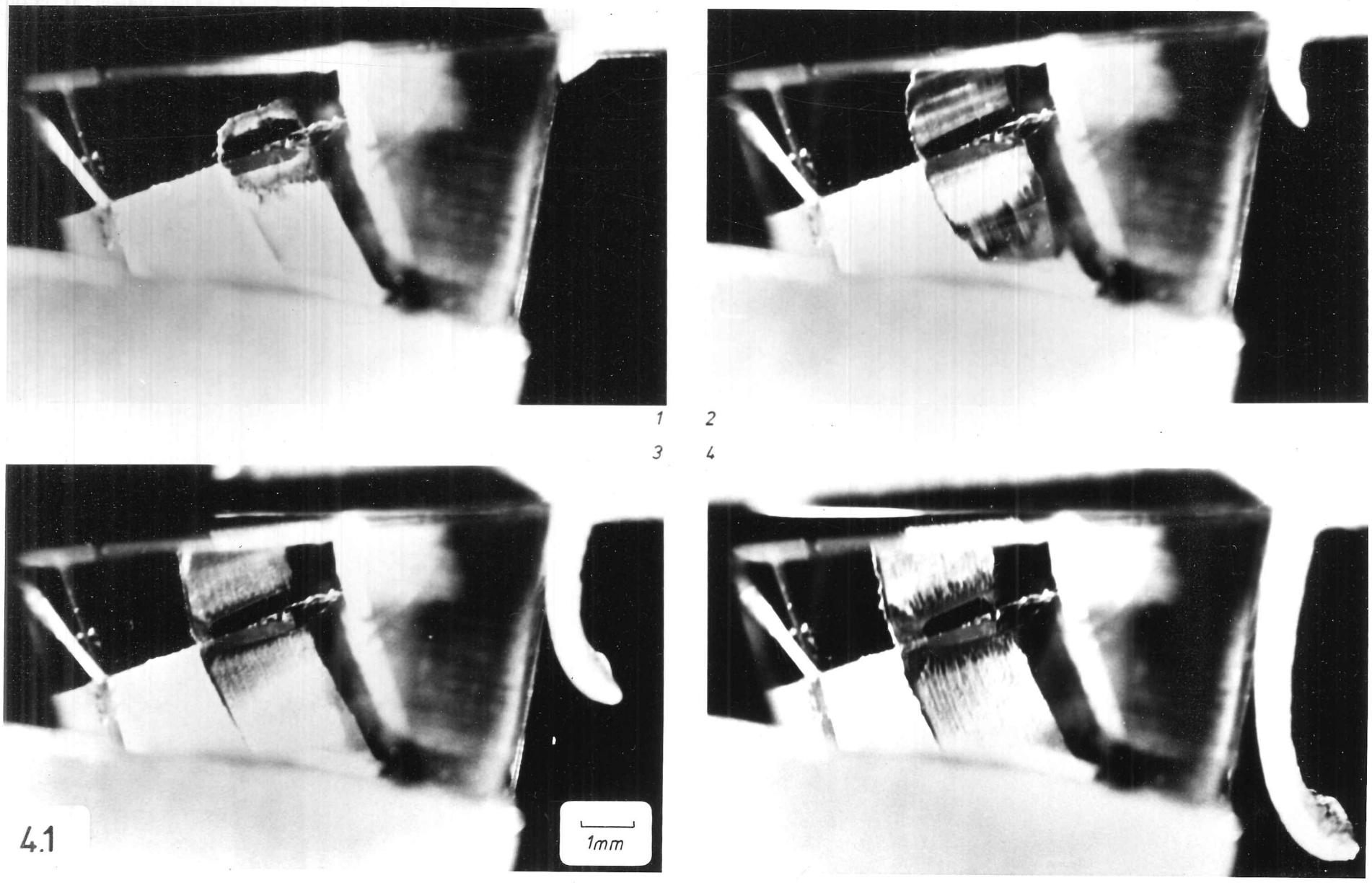

Figure 4.1 Sequence of views through the transparent tool, showing the contact conditions that develop when machining lead in air.

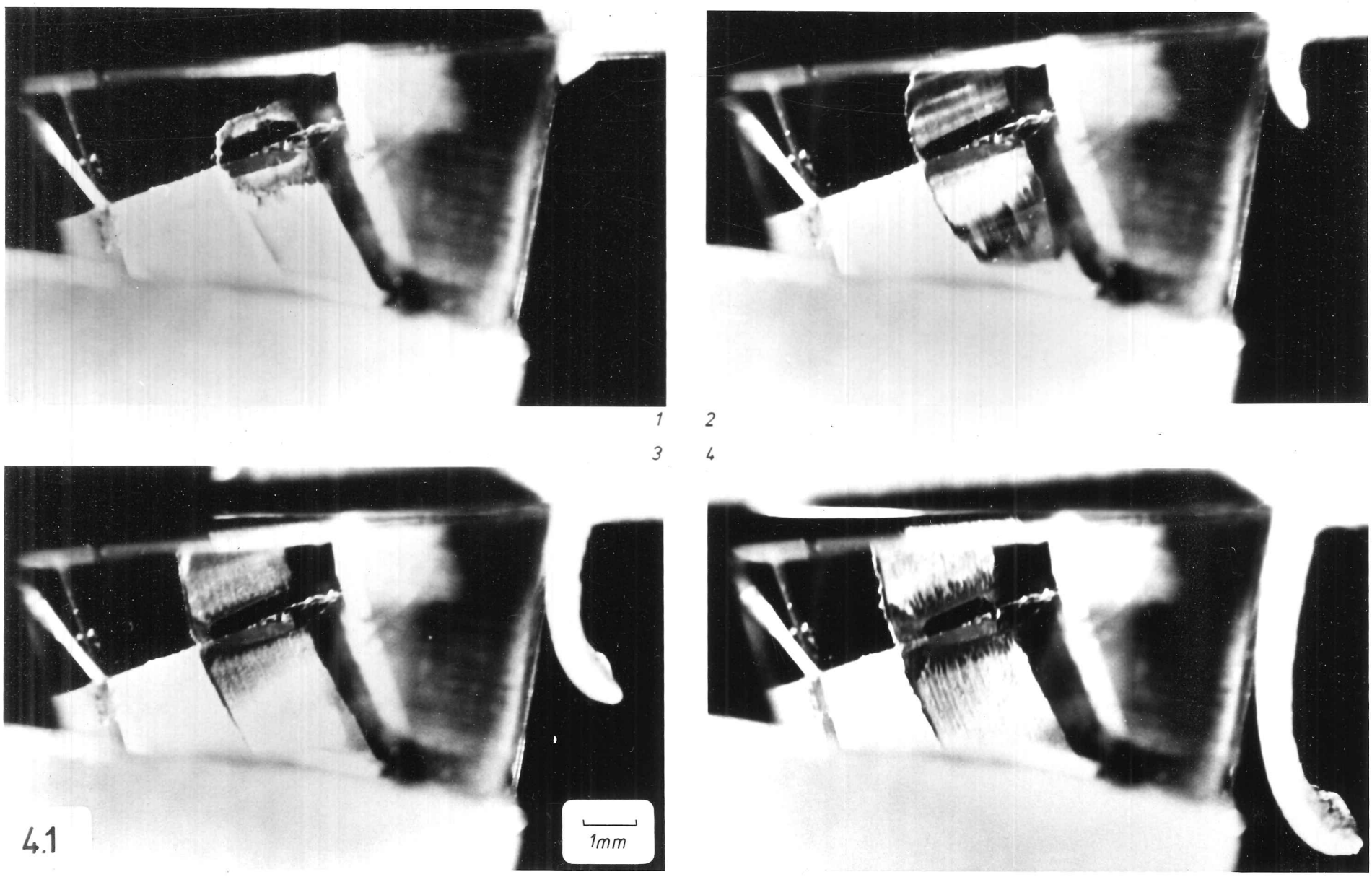

Figure 4.2 Transparent tool; aluminium machined in air.

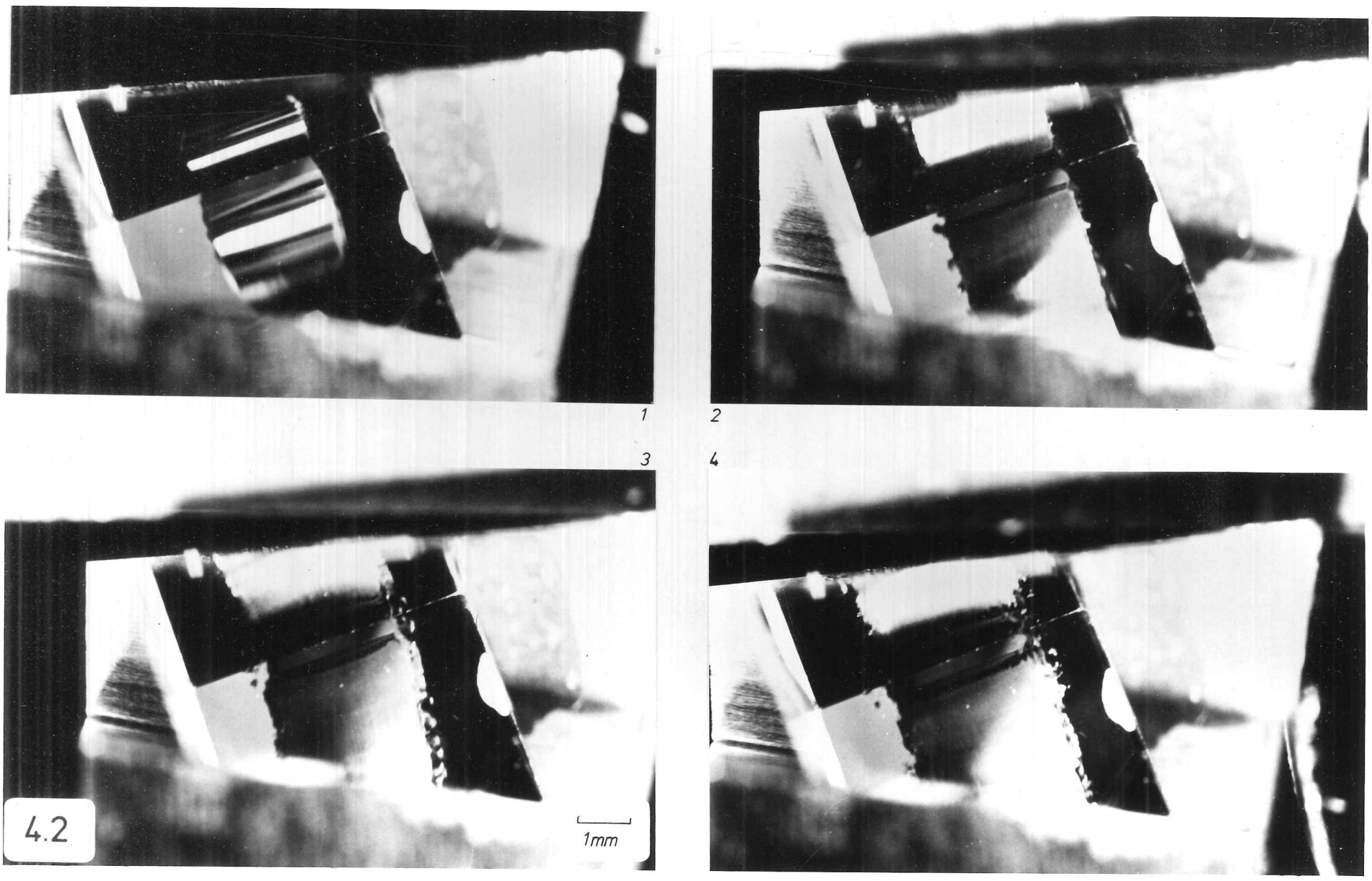

rapidly spread to cover the entire width. The chip also appeared to straighten. The region of transfer became more extensive but did not move any closer to the cutting edge. It appeared to reach an equilibrium size after about 20 mm of cutting.

During the remainder of the cut, this appearance of two zones of contact remained unaltered. The featureless region of apparently intimate contact adjacent to the cutting edge was from two to three times the depth of cut in length. The zone of transfer, commencing at the end of this first zone, reached about five times the depth of cut in length and appeared to undergo disruption during the cut. At the sides, transferred material extended to the cutting edge and also grew outwards slightly as side-spreading of the workpiece became evident.

This sequence is illustrated in Figures 4.1 and 4.2 and in the cine film Sequences 1 and 2. At the end of the cut the tool was allowed to "run out" and then removed from the planing machine for examination. The chip was attached to the tool and required a pull-off force estimated at about 100 gmf for lead and 0.5 Kgf for aluminium (100 μ cuts).

Examination of the sapphire after the cut revealed that the transferred material in the second zone had remained largely attached to the tool, while the first zone had left the rake face clean (Figure 4.3).

The end of the chip, examined by optical microscopy (Figure 4.4) and in the Scanning Electron Microscope (Figure 4.5) also showed the two regimes of contact. Zone 1 appears to be featureless and this suggests intimate contact with the polished sapphire surface. Zone 2, however, carries an impression of the transferred material on the tool and also some lumps of Zone 2 matter which have adhered preferentially to the chip. The remainder of the chip surface, the "finished" chip,

Figure 4.3 Rake face of transparent tool, after machining lead in air.

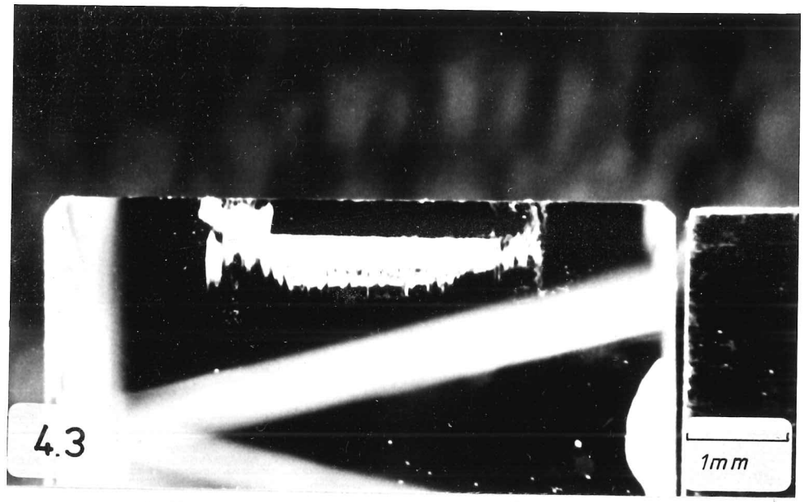

Figure 4.4 Lead chip produced in air with the transparent tool, showing the end of the chip after detachment from the tool.

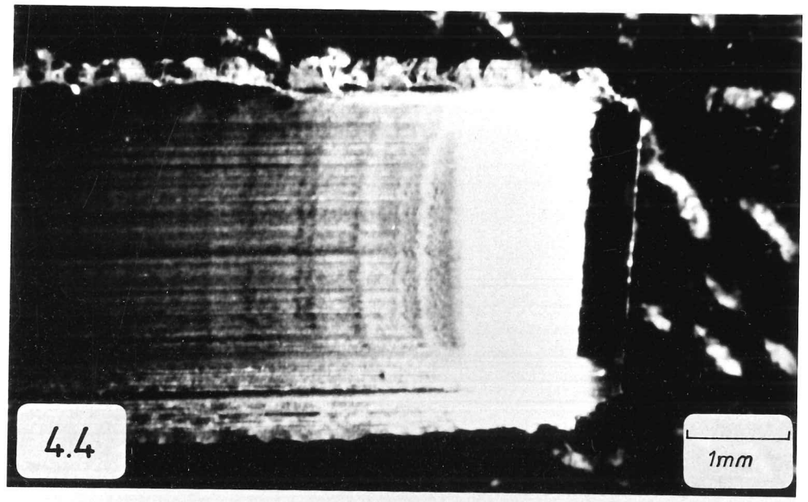

Figure 4.7 Lead chip produced in air with the transparent tool, showing the tightly-curled portion generated at the start of the cut.

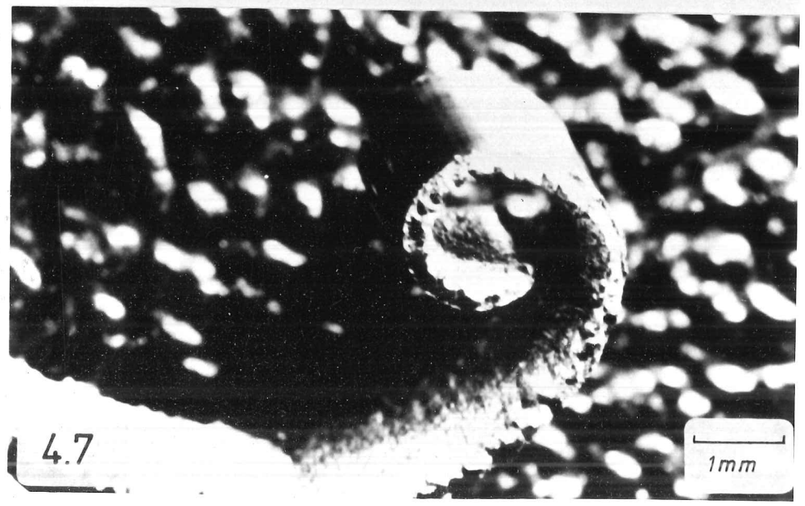

Figure 4.5 Lead chip produced in air with the transparent tool - scanning electron micrograph of the end of the chip seen in Figure 4.4.

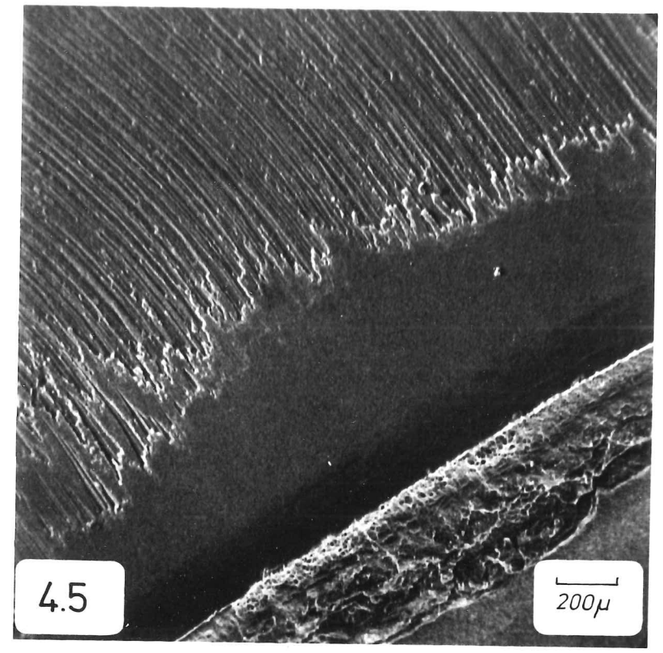

Figure 4.6 As above - central portion of chip showing scoring and redeposition.

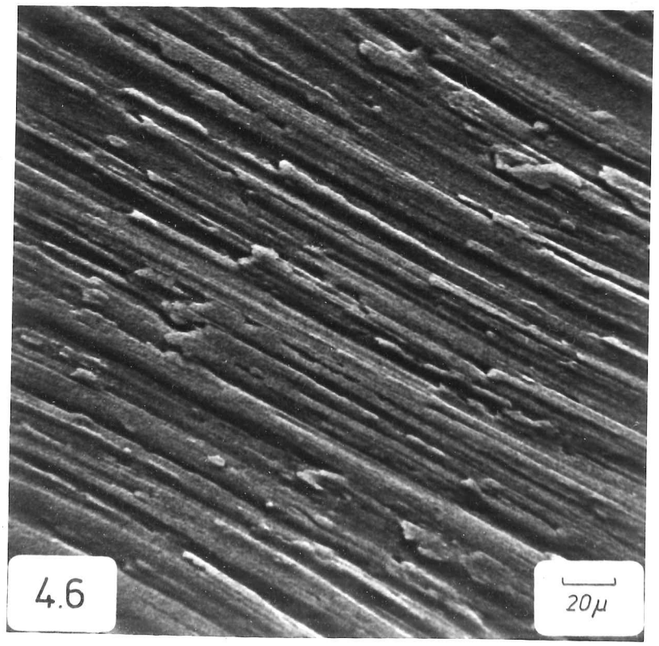

is heavily scored as seen in Figure 4.6. The chip is virtually straight. However, the first portion of chip, machined with the initially clean tool, is tightly curled in contrast and almost smooth (Figure 4.7) with grooves appearing to develop progressively over the first few mm.

4.1.2 Cutting in Vacuum

When the same materials were machined in vacuum, at a pressure of 10^{-5} torr, a marked contrast in behaviour was noted. An initially short contact length and tight curl were again observed and the apparent contact length grew rapidly to about two to three times the depth of cut. This "zone 1" situation continued, however, for the remainder of the cut, with no "zone 2" transfer developing. There was no transfer of chip material to the tool at the edges, either; there was also less "side-spreading" of the workpiece than that noted in air cutting.

The curl radius again increased but the chip did not straighten-out completely. The underside of the chip was featureless and, indeed, it was not always possible to detect the point at which the chip lost contact with the tool. The angle of illumination was found to be critical in this respect. Sequences in vacuum are seen in Figure 4.8 and cine film Sequences 3 and 4.

The chip fell away from the tool at the end of the cut; the sapphire surface was completely free from transfer (Figure 4.9). The chip had a specularly reflecting surface as seen in Figure 4.10.

Examination of the chip by Scanning Electron Microscope was difficult due to the problems of focusing the instrument on a very smooth surface. Figure 4.11 shows a chip produced with a tool which had suffered damage at the edge, giving a feature to focus on. No boundary of contact is evident.

Figure 4.8 Transparent tool; lead machined in vacuum.

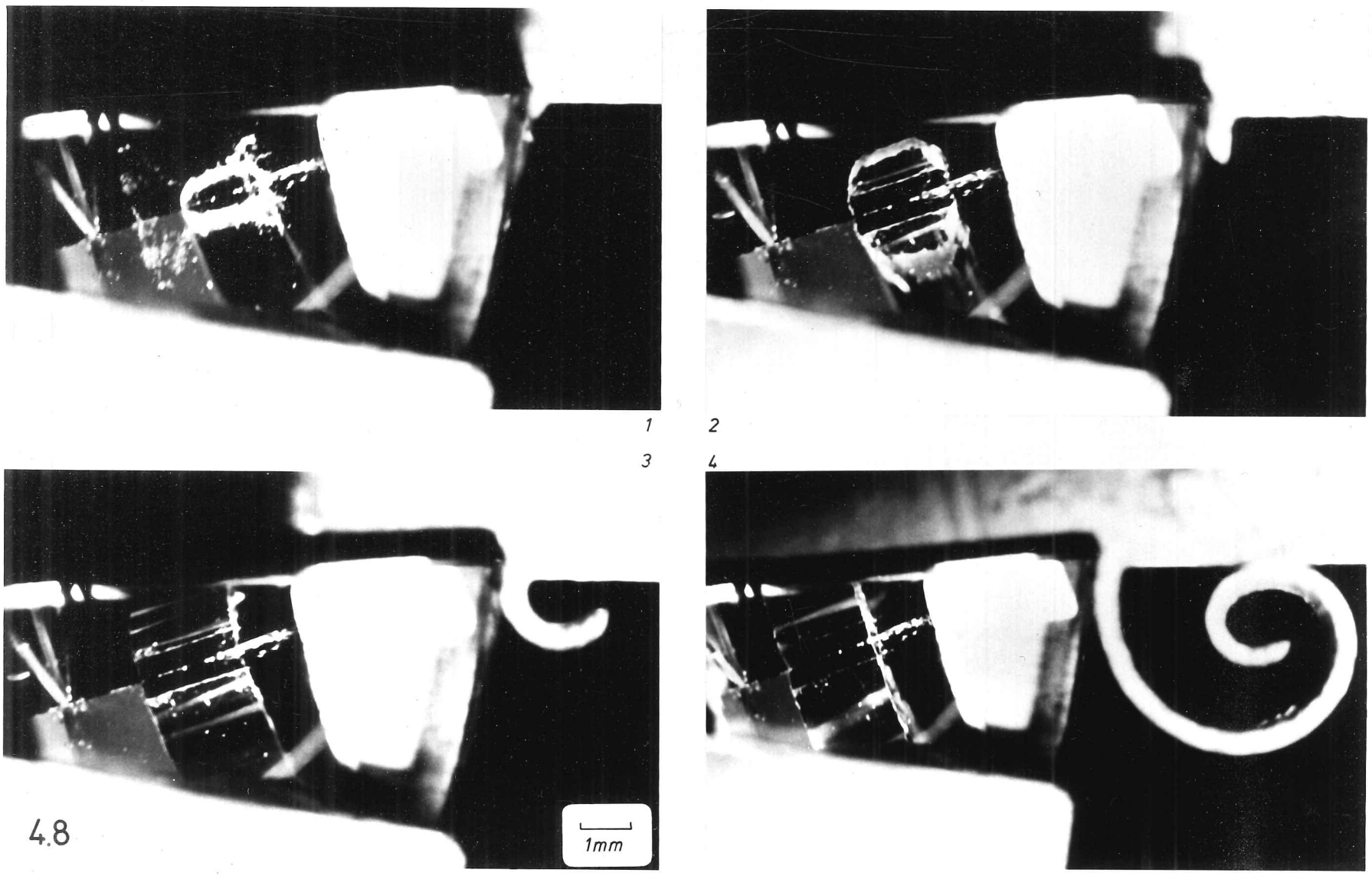

Figure 4.9 Rake face of transparent tool, after machining aluminium in vacuum.

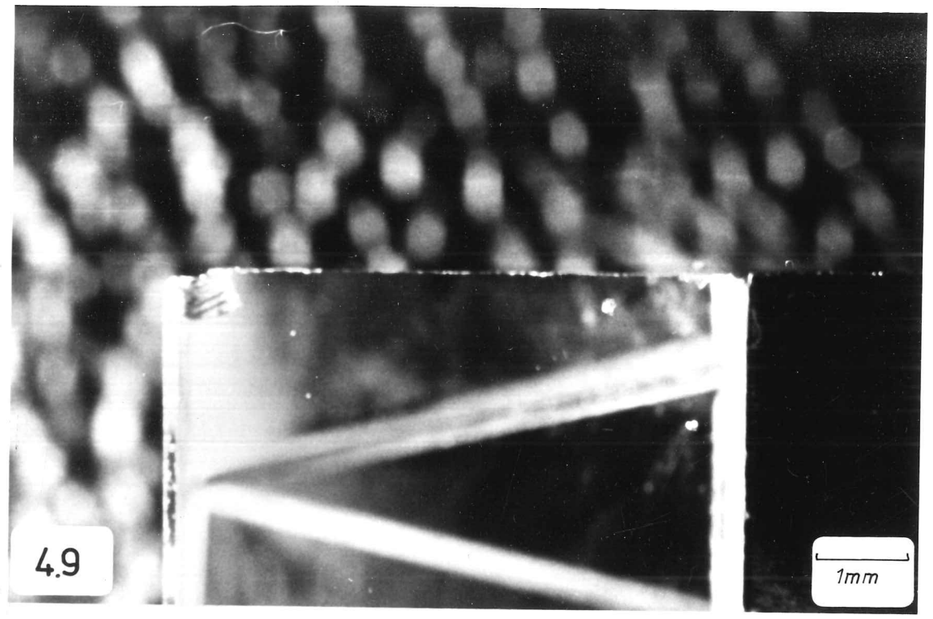

Figure 4.10 Aluminium chip produced in vacuum, showing the extremely smooth surface generated on the side adjacent to the tool rake face.

4.2 ZONE 2 AND THE FORCES IN AIR AND VACUUM CUTTING

The forces acting on the tool were significantly reduced by machining these materials in vacuum rather than in air. Table 4.1 gives the rake face drag force, F, for sapphire and steel tools cutting lead and aluminium. It is seen that cutting in vacuum greatly reduces the rake face drag, consistent with the elimination of zone 2 transfer and the easier passage of the chip up the tool. Machining at higher speeds reduces the severity of the transfer but the behaviour is essentially the same. The forces observed at higher speeds are given for steel tools.

Behaviour similar to vacuum cutting was noted when machining in atmospheres of argon or nitrogen. Zone 2 transfer was found to be related to the pressure of oxygen and the cutting forces with high speed steel tools were recorded at various oxygen pressures (Figure 4.12). The pressure at which the transition in behaviour occurred is markedly similar for aluminium and lead. Machining at higher speeds displaces the transition to higher pressures. Aluminium was machined at a low speed in an atomosphere of pure oxygen at 150 torr and the chip and tool condition compared with those obtained in air, where the partial pressure of oxygen is approximately the same. Gross and rapid zone 2 transfer is observed with pure oxygen.

Close examination of the underside of a chip produced in air (Figure 4.6) reveals that the grooves have a rough, torn appearance and contain lumps of material presumably plucked out of the zone 2 deposit. A vacuum cut was conducted with a tool previously used in air and carrying a zone 2 deposit. A quite different appearance of the

TABLE 4.1 Forces in air and vacuum cuts

Rake face drag force F, Kgf per mm width, Depth of cut 100 μ
Speed 20 mm sec^{-1}, *500 mm sec^{-1}.

Workpiece	Tool	Air	Vac
Lead	10^{o} sapphire	1.22	0.51
Lead	10^{o} steel	1.29	0.82
Aluminium	10^{o} sapphire	8.6	5.7
Aluminium	10^{o} steel	8.4	6.4
Aluminium	40^{o} steel	6.1	3.4
Aluminium*	40^{o} steel	4.5	3.6

Figure 4.11 Lead chip produced in vacuum with the transparent tool - scanning electron micrograph of the end of the chip.

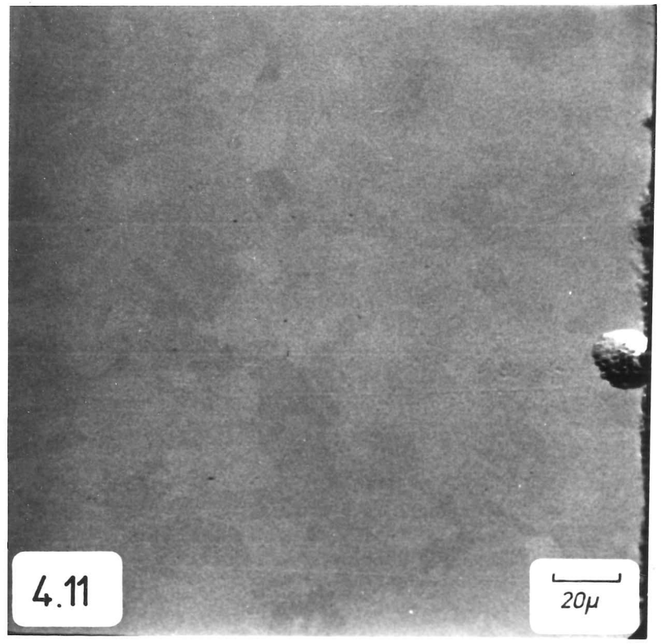

Figure 4.13 Lead chip produced in vacuum with the transparent tool carrying a "zone 2" deposit from a previous air cut - scanning electron micrograph of central portion of chip.

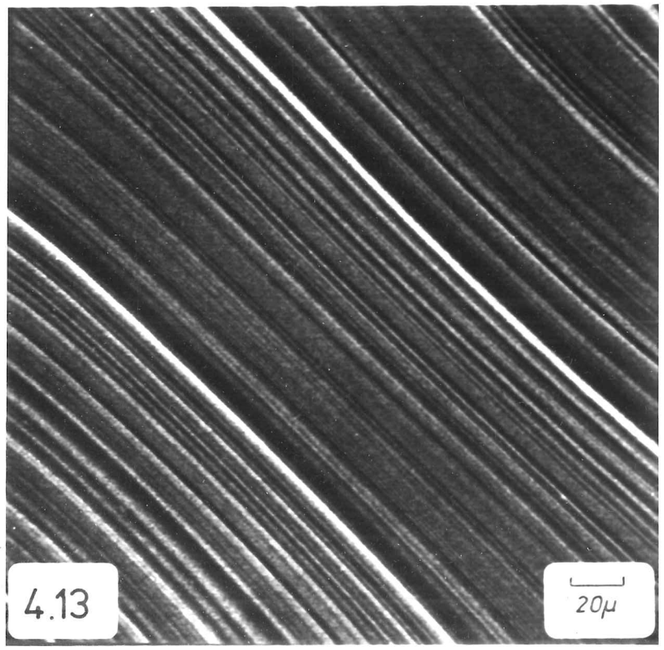

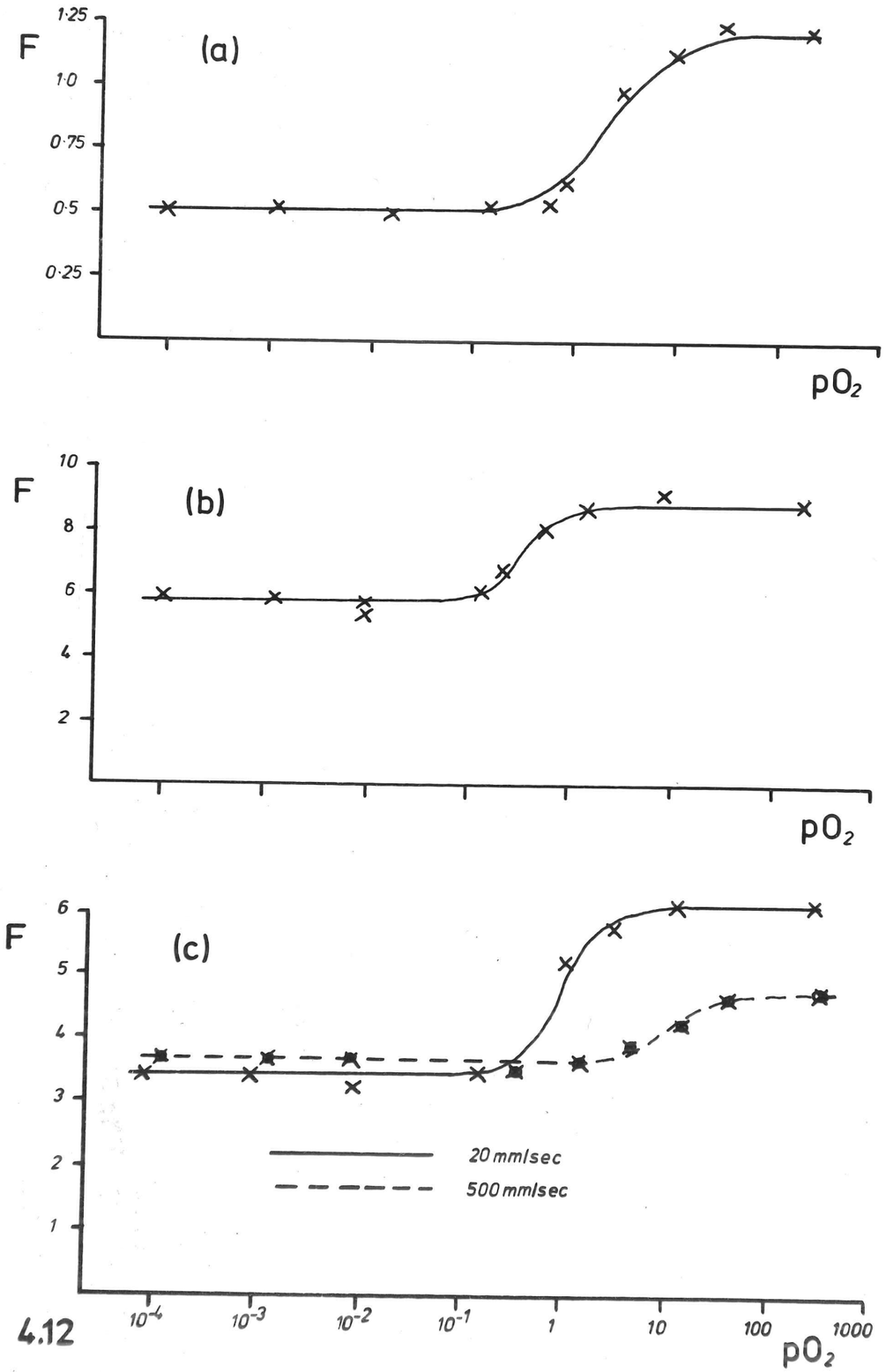

Figure 4.12 Variation of rake face drag force, F, with pressure of oxygen, pO_2.

F in Kgf per mm width, 100 μ cut. pO_2 in torr.

(a) Lead machined with the transparent tool.

(b) Aluminium machined with the transparent tool.

(c) Aluminium machined with a 40° steel tool, showing the effect of increasing the speed of cutting.

underside of the chip resulted in this case (Figure 4.13). These grooves are smooth and continuous indicative of no interaction other than a simple mechanical scoring.

4.3 DETECTION OF MOTION IN ZONE 1

Introduction

During direct observations of transparent tool cuts by binocular microscope, the impression gained was that the chip material was moving in zone 1 and not static at the interface. However, the dynamic resolution of the eye is extremely good compared with that of conventional moving photography and this impression is not recaptured when the cine films are studied. Various special workpieces were prepared in attempts to demonstrate this movement.

4.3.1 Split Workpiece

A workpiece was made consisting of two strips of lead clamped together, with grooves formed in the mating surfaces by first pressing the strips against brass rack (Figure 4.14). This afforded some indication of the sliding situation in zone 1 by the side-to-side movement of the junction. (Cine Sequence 6). This appears to occur even at the cutting edge. The technique is, however, subject to the criticism that the integrity of chip/tool contact in zone 1 is lost at the junction and that static conditions may prevail within the lead strips themselves.

4.3.2 Laminated Workpiece

It was hoped that a suitable eutectic would be found giving sufficient macroscopic contrast in the unetched state. This was not forthcoming and a synthetic laminated specimen was prepared consisting

Figure 4.14 Machining the split workpiece with the transparent tool.

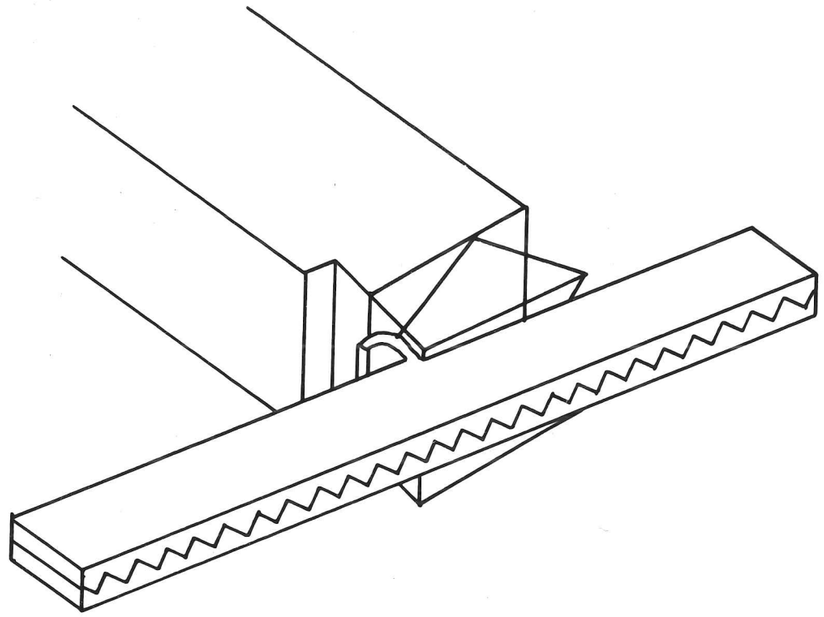

4.14

Figure 4.15 Machining the laminated workpiece with the transparent tool.

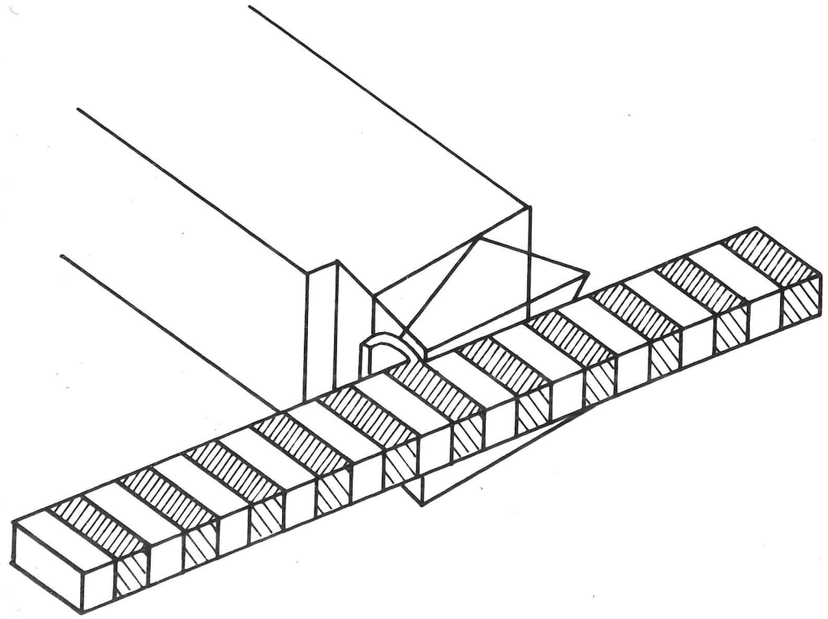

4.15

of alternate layers of tin and lead (Figure 4.15). This was prepared by casting the tin into an evacuated graphite mould containing strips of lead 3 mm wide at a spacing of 3 mm. Precise control of the supercooling of the tin resulted in eutectic formation in a thin interlaminar layer, giving mechanical integrity to the bond.

When this material was cut, the two metals were easily distinguished by a difference in colour and by the porosity of the tin. Movement of the junction was observed to occur from the cutting edge (Cine Sequences 7 and 8 and Figure 4.16). Tin and lead exhibit very similar cutting behaviour under these conditions and a coherent, continuous chip is formed (as seen at the end of Sequence 7 in the film). However, it could be argued that the sliding conditions at the rake face are disrupted by the alternation of chip material, and that interfacial seizure could still prevail when a single metal is being machined.

4.3.3 Dispersed Particle Workpiece

A specimen of lead containing fine inclusions was obtained for use with the transparent tool. These were in the range of 0.5 to 5 microns in size and could not readily be resolved under normal illumination conditions. Oblique illumination of the transparent tool resulted in the inclusions showing up as bright specks and these were clearly moving through zone 1 during cutting. The effect was hard to capture on film and the film contains the best sequence achieved (Cine Sequence 9).

It is considered that this is the nearest approach to an homogeneous workpiece that gives some definite contrast in zone 1 in continuous cutting. These inclusions would not be expected to modify the machining characteristics of the lead and are, indeed, rather smaller than the

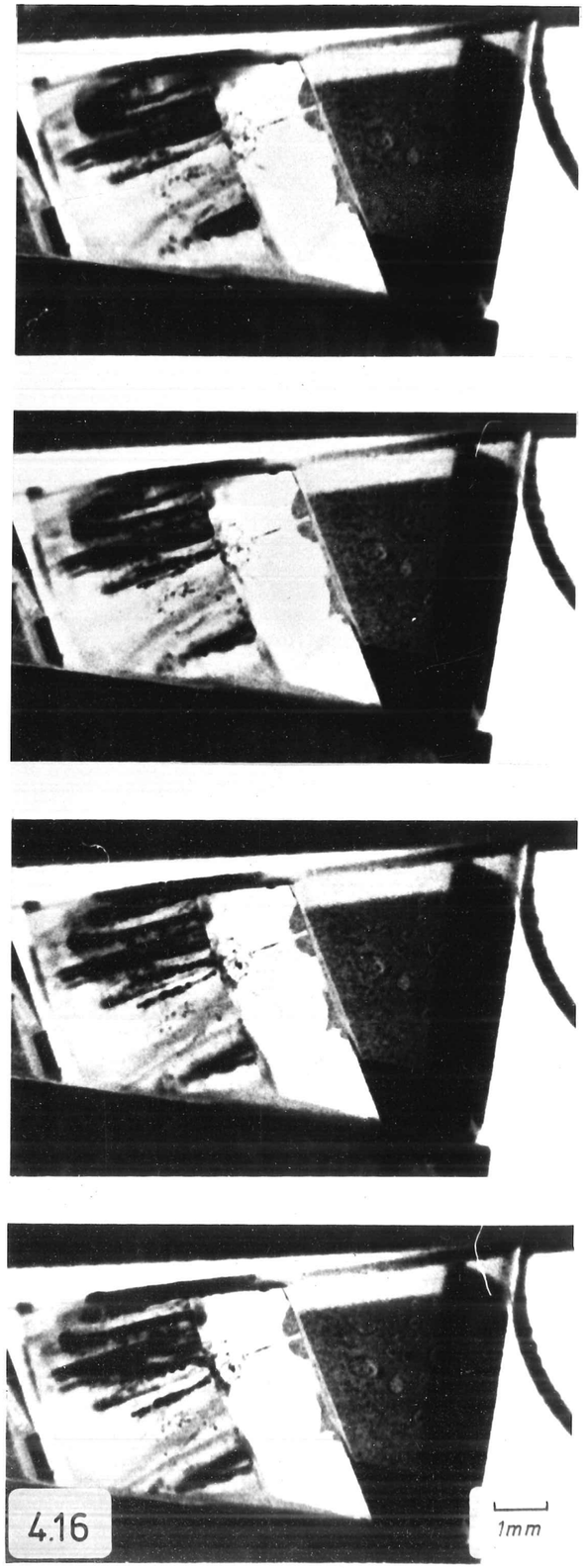

Figure 4.16 Sequence of stills taken from the cine film, showing the laminated workpiece being machined. The tin/lead boundary is moving from the cutting edge along the rake face of the tool.

interlamellar spacing (about 15 μ) on the free surface. Any seized layer on the rake face would have to be very much smaller than 1 μ otherwise stationary particles would have been observed.

4.4 FURTHER EXAMINATION OF THE CONTACT CONDITIONS

Introduction

The use of the transparent tool on harder materials proved to be rather costly in sapphire inserts and only a few runs were attempted. Failure generally occurred by chipping of the cutting edge at the beginning or end of the cuts, reflecting the poor impact properties of ionic crystals. Treatment of the tool in hydrofluoric acid prior to cutting was found to be beneficial, probably due to the blunting of microcracks. Some successful runs were made with copper workpieces and an air cut on copper is seen in the cine film (Sequence 5). Behaviour was very similar to aluminium and lead, with the same zones developing. Aspects of copper cutting using steel tools are investigated in section 4.5. Further investigations of continuous cutting with the transparent tool were limited to materials no harder than aluminium, but varying the cutting conditions gave much additional information about the interface.

4.4.1 Indium

Indium is a very soft metal, renowned for its ready adhesion to many surfaces. A clean glass sphere pressed against indium adheres strongly to the metal and pieces of indium are attached to the glass upon separation. The surprising observation that there is a region of intimate contact without transfer at the tool tip, noted above for

interlamellar spacing (about 15 μ) on the free surface. Any seized layer on the rake face would have to be very much smaller than 1 μ otherwise stationary particles would have been observed.

4.4 FURTHER EXAMINATION OF THE CONTACT CONDITIONS

Introduction

The use of the transparent tool on harder materials proved to be rather costly in sapphire inserts and only a few runs were attempted. Failure generally occurred by chipping of the cutting edge at the beginning or end of the cuts, reflecting the poor impact properties of ionic crystals. Treatment of the tool in hydrofluoric acid prior to cutting was found to be beneficial, probably due to the blunting of microcracks. Some successful runs were made with copper workpieces and an air cut on copper is seen in the cine film (Sequence 5). Behaviour was very similar to aluminium and lead, with the same zones developing. Aspects of copper cutting using steel tools are investigated in section 4.5. Further investigations of continuous cutting with the transparent tool were limited to materials no harder than aluminium, but varying the cutting conditions gave much additional information about the interface.

4.4.1 Indium

Indium is a very soft metal, renowned for its ready adhesion to many surfaces. A clean glass sphere pressed against indium adheres strongly to the metal and pieces of indium are attached to the glass upon separation. The surprising observation that there is a region of intimate contact without transfer at the tool tip, noted above for

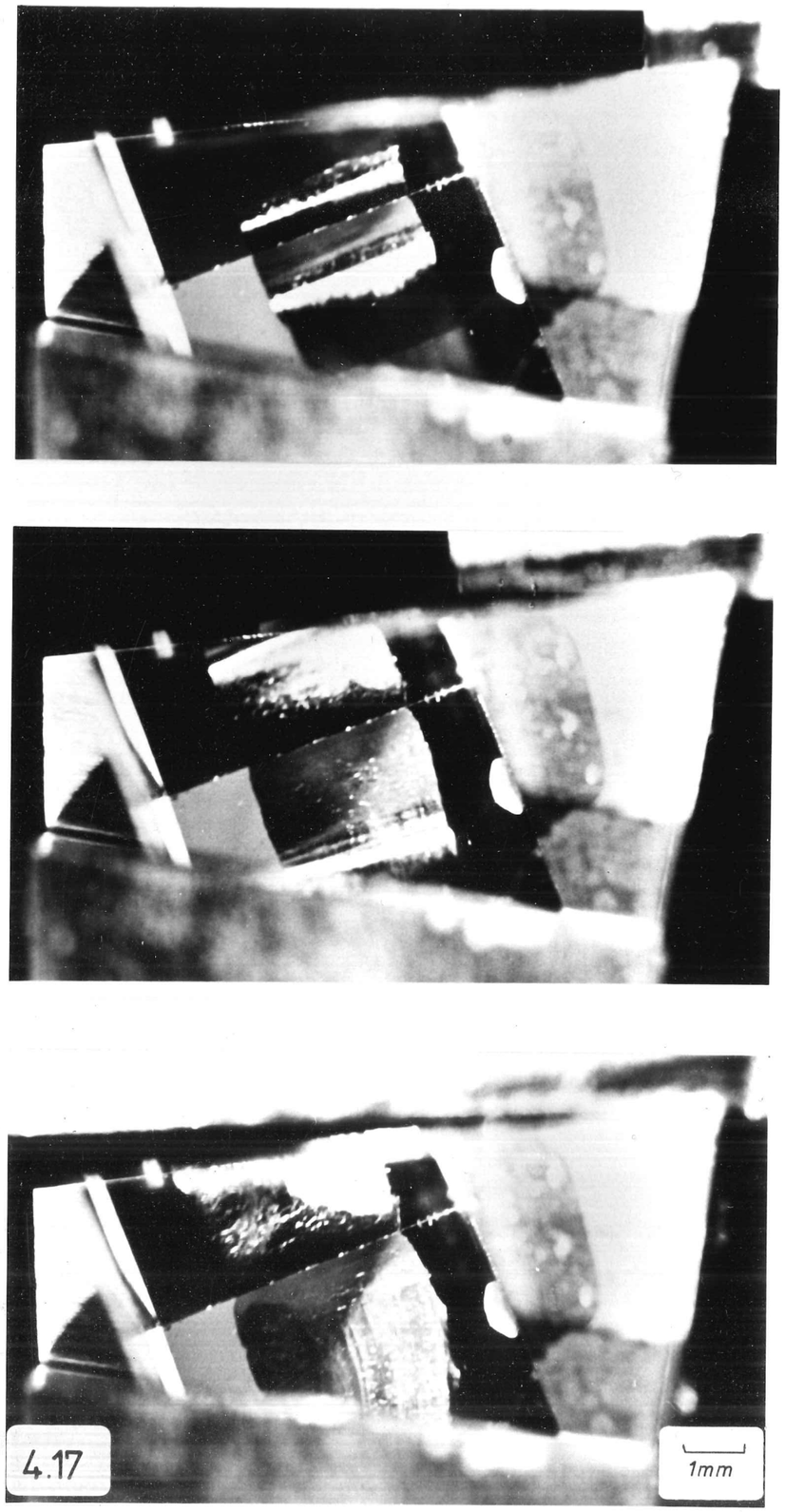

Figure 4.17 Transparent tool; indium machined in air.

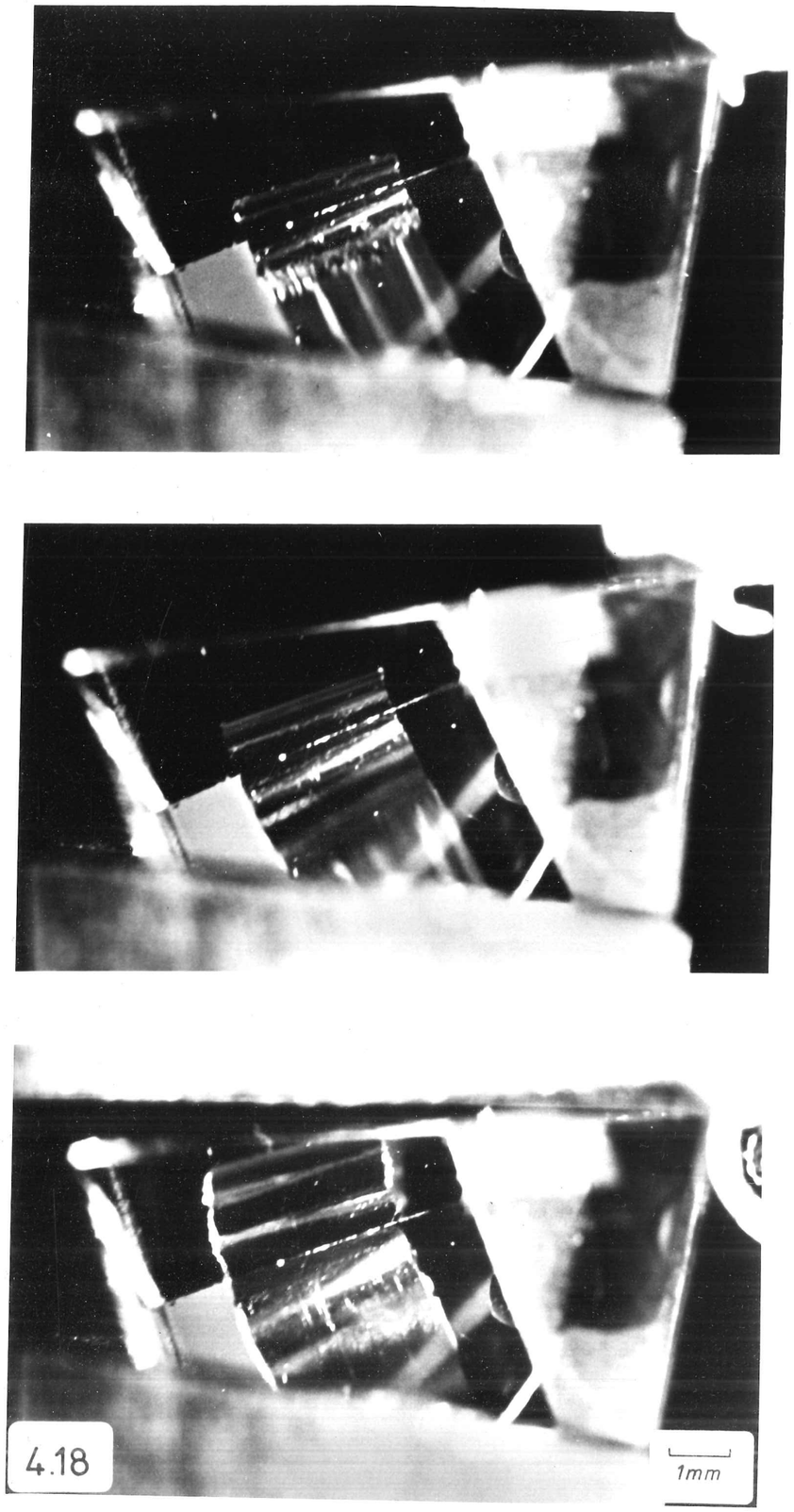

Figure 4.18 Transparent tool; indium machined in vacuum.

lead and aluminium workpieces, is hardly to be expected for indium. However, cuts with the transparent tool did proceed in a similar way (Cine Sequence 10, Figures 4.17 and 4.18). Once more, transfer of chip material to the tool was associated with the presence of oxygen. The chip under-surface displayed features indicative of recrystallisation (Figure 4.19) but did not stick to the tool in vacuum.

The workpiece was rather too short for equilibrium to be reached and the zone 2 deposit produced when cutting in air was light (Figure 4.20). An air cut was arrested half-way and the tool was withdrawn, yielding the effect seen in Figure 4.21.

4.4.2 Copper-Coated Tool

Cuts on lead and aluminium workpieces were performed with the transparent tool coated on the rake face with a thin ($\sim$ 500 Å) layer of copper. The evaporative deposition of metals on sapphire surfaces is a critical process and good substrate cleaning techniques are necessary. It was found that cleaning with solvent (iso-propyl alcohol) only, prior to evaporation, produced the least adherent films, while substrate heating and glow discharge cleaning before coating progressively improved the strength of the interface. For the most adherent films, a very high vacuum was required; argon R.F. glow discharge was followed by rapid pumpdown and fast deposition.

The appearance of the cut when viewed through the tool depended on the coating quality. With poor adhesion, the copper was removed immediately over the entire contact area between chip and tool. When cutting in air, zone 2 transfer formed partly on the clean sapphire but also on top of the copper at the end of the initial contact length.

Figure 4.19 Indium chip produced in vacuum with the transparent tool, showing recrystallisation features.
(Chip "unwound" after cut).

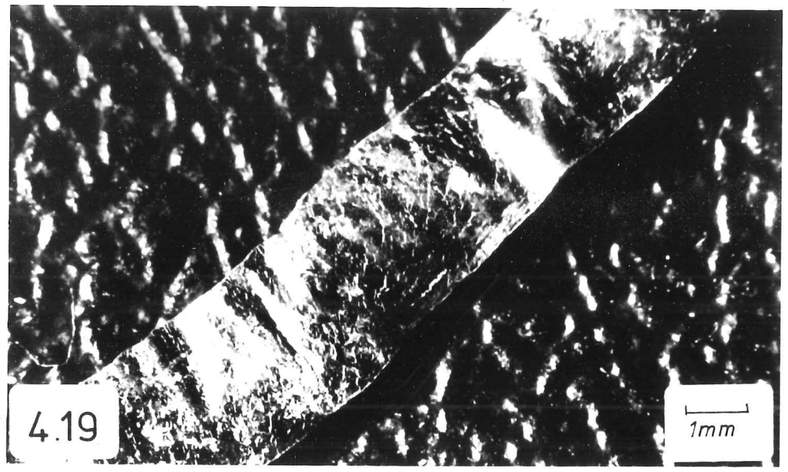

Figure 4.20 Rake face of transparent tool, after machining indium in air.

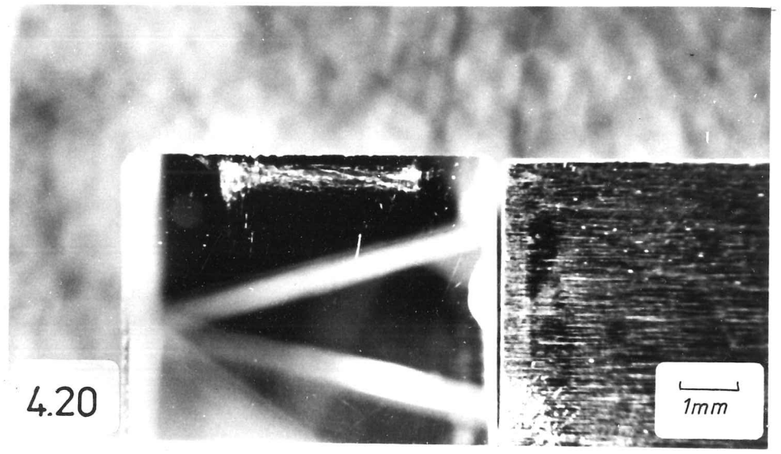

Figure 4.21 Rake face of transparent tool, after stopping and slowly disengaging the tool when machining indium in air.

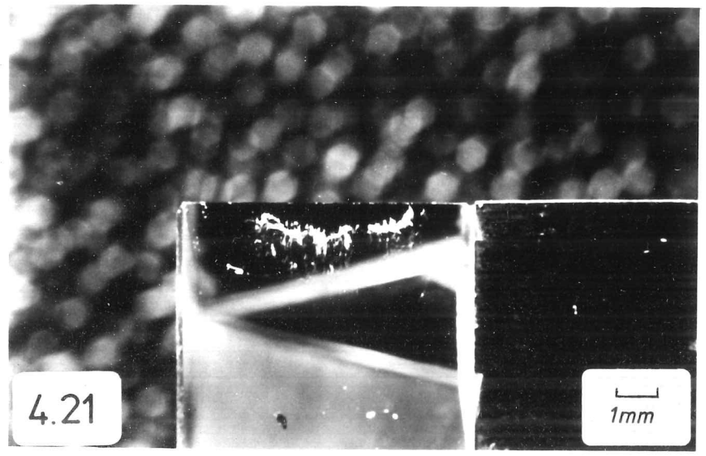

Well adhered coatings appeared initially to remain intact, but after a few millimetres of cut, the copper was removed in part of zone 1. The region where copper was removed extended from about one to about three times the depth of cut along the rake face. The copper at the tip remained attached to the tool. When cutting in air, zone 2 transfer formed mostly on top of the copper. When the cut ran out, the thin strip of copper remaining at the tip sometimes stayed on the tool and in other instances came away with the chip, as seen in Figures 4.22 and 4.23. These effects are summarised in Figure 4.24.

The cine film contains sequences showing all these variations (Sequences 11 - 13). With extremely well-adhered coatings and lead cuts, the copper survived over the entire tool surface (Sequence 14) but this behaviour was not exhibited with aluminium workpieces. Removal of copper appeared to be by bodily detachment of flakes, which were found on the chip, rather than by a wearing-away process.

These results lead to a sub-division of zone 1 (Figure 4.25). Zone 1a is the region at the tip, of approximately the depth of cut in length, in which the copper remains in place during the cut. Zone 1b is the remainder of zone 1.

4.4.3 Quick-Stops with Steel Tools

High speed steel tools with ground finishes were used in quick-stop experiments, to establish whether the same zones of contact described for sapphire were obtained with conventional tooling. These carried grinding marks parallel to the cutting edge.

A tool used, on separate portions of the cutting edge, for one cut in vacuum and one in air is seen in Figure 4.26. The workpiece

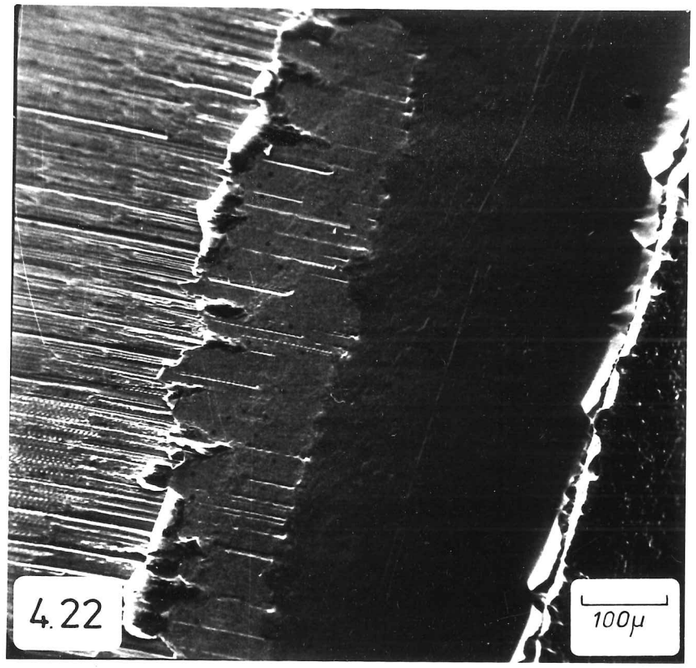

Figure 4.22 Lead chip produced in air with the transparent tool carrying a copper coating on the rake face. This scanning electron micrograph of the end of the chip shows that the copper has transferred to the chip in "zone 1a".

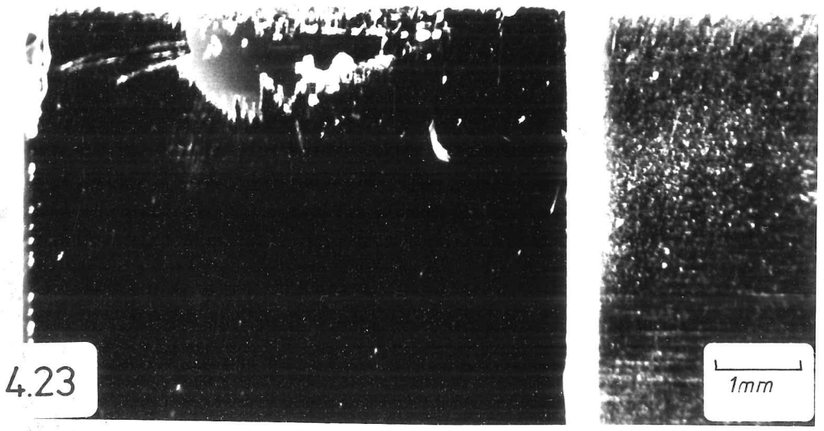

Figure 4.23 Rake face of the transparent tool after machining lead in air , showing that the copper has remained on the tool in "zone 1a".

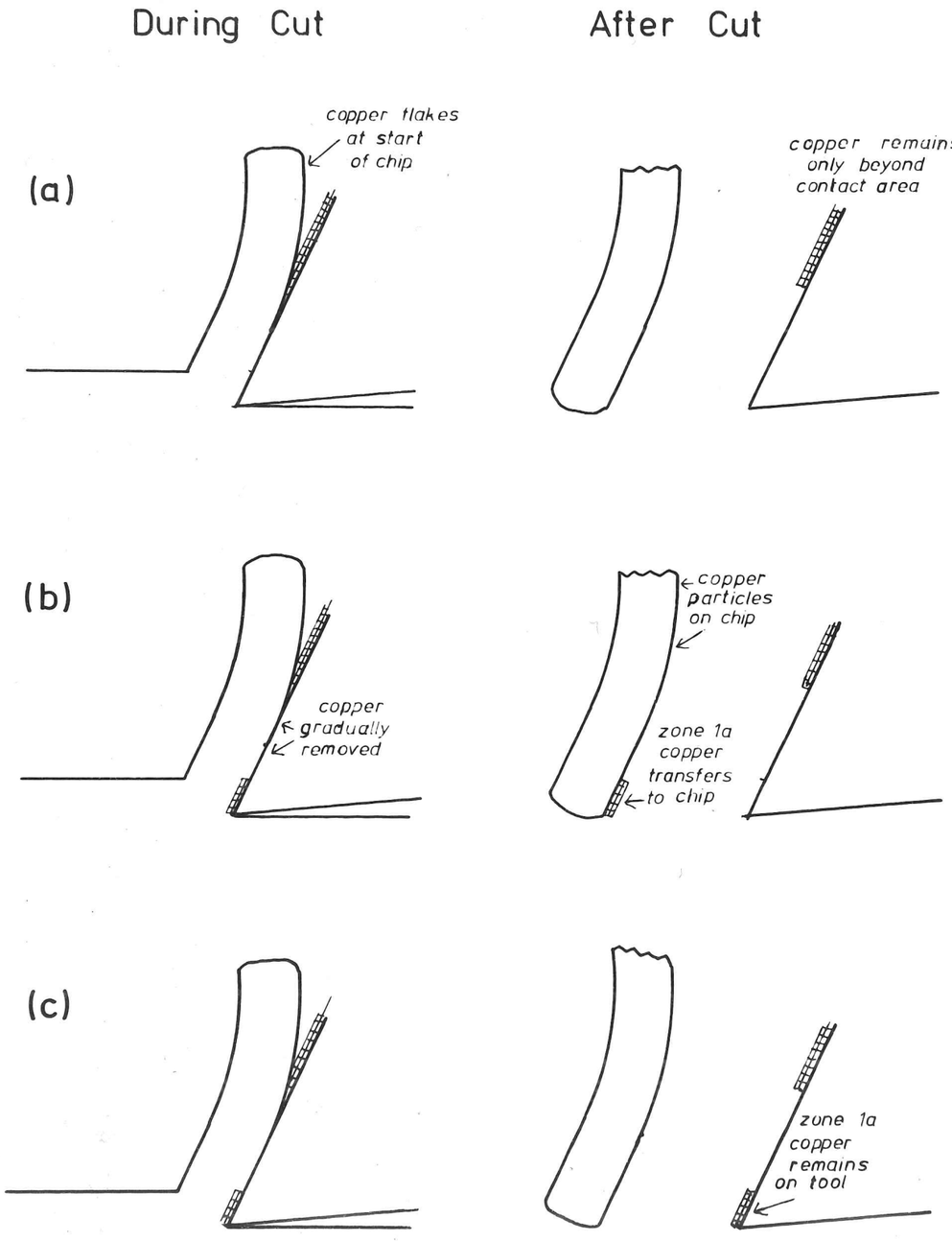

Figure 4.24 Summary of behaviour of copper-coated tools

(a) poor coating adhesion

(b) improved coating adhesion

(c) best coating adhesion

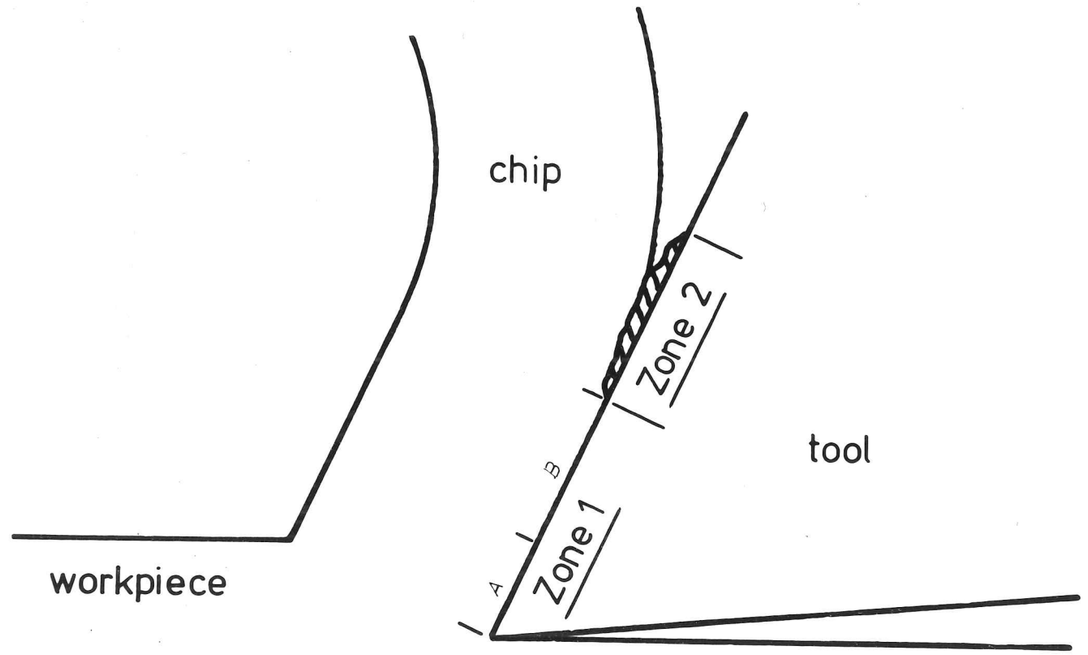

4.25

Figure 4.25 Zones of contact in continuous cutting, based on observations made with the transparent tool.

was of pure aluminium. Both edges have aluminium deposits, but the air cut has a gross, lumpy transfer of material (zone 2) while the vacuum cut has yielded a light ghosting. In both cases, a thin strip at the tip is free from transfer. X-ray analysis of the tool in the S.E.M. also indicated that this region is free from deposited aluminium. Figure 4.27 is a Scanning Electron Micrograph of the chip from the cut made in vacuum. In the region immediately adjacent to the cutting edge, the grinding marks on the tool are faithfully replicated on the chip. These undergo increasing distortion with distance from the edge, so that further up the rake face only a few points seem to be in intimate contact with the tool. The chip acquires a generally smoother appearance and eventually the surface is almost featureless (Figure 4.28). To the naked eye, in fact, the chip appears to be very shiny except at the root. In contrast, an air cut produces a zone 2 deposit (Figure 4.29).

4.4.4 Glow Discharge Cleaning

The effect of prior glow discharge cleaning of the rake face of the tool on cutting in vacuum was studied. Sapphire and steel cutting tools were employed and cleaned in a 1000 V D.C. discharge at 0.05 torr Argon for 5 minutes. This was followed by rapid pumpdown to cutting pressure of less than 1×10^{-5} torr.

Seen through the transparent tool, the vacuum cutting of aluminium after discharge cleaning appeared not markedly different from vacuum cutting with an uncleaned tool (Cine Sequence 15). Some slight disruption of the chip surface was evident as it passed over the tool, but there was no obvious zone 2 build-up. The appearance of the chip and tool confirms this view (Figures 4.30 and 4.31). There is a light ghosting of aluminium all over the contact area except in zone 1a. The chip under-surface is

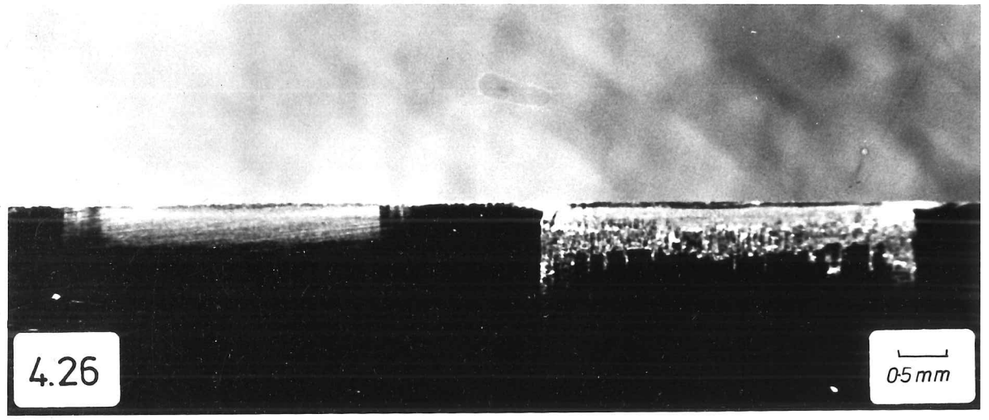

Figure 4.26 Rake face of high speed steel tool used to cut pure aluminium in vacuum (left) and in air (right). Depth of cut 100 μ.

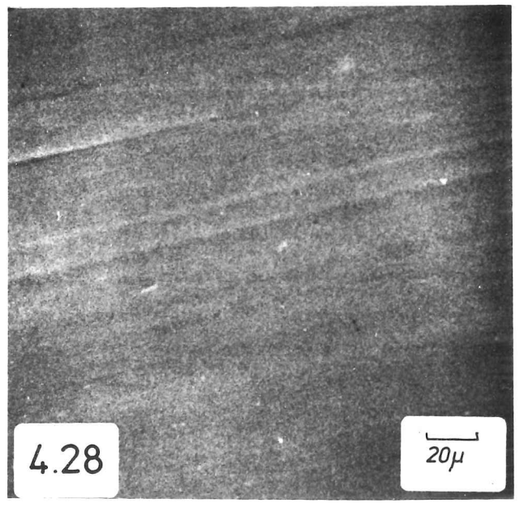

Figure 4.28 Pure aluminium chip produced in vacuum using a high speed tool - scanning electron micrograph of the central portion of chip.

Figure 4.27 Pure aluminium chip produced in vacuum using a high speed steel tool and quick-stop device - scanning electron micrograph of the chip root.

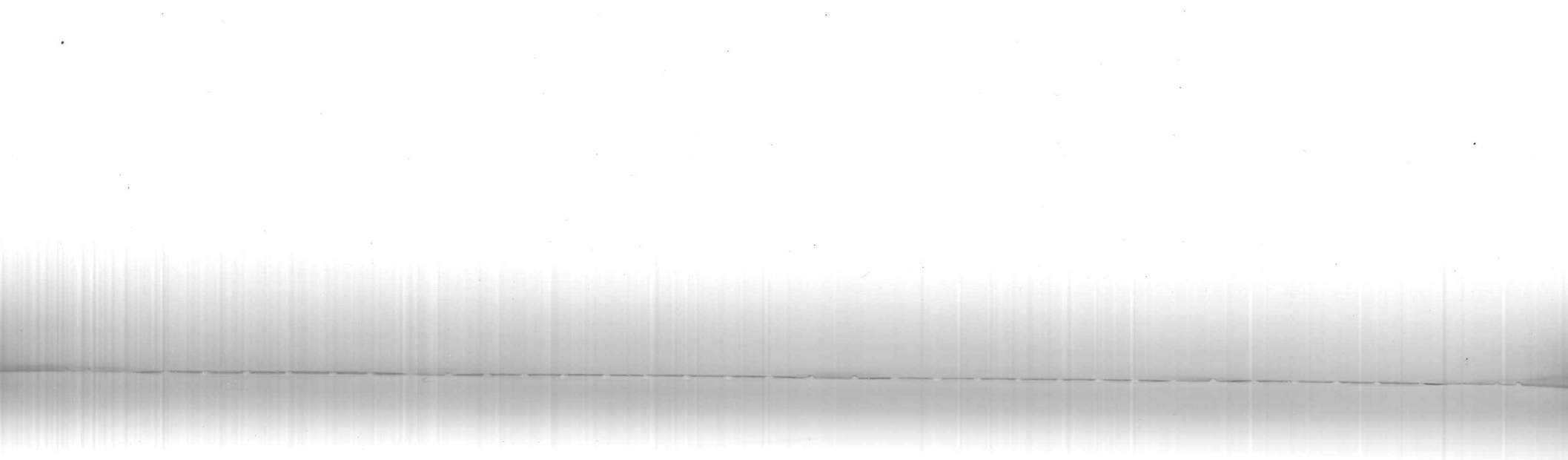

Figure 4.29 Lead chip produced in air using a high speed steel tool - scanning electron micrograph of the chip root.

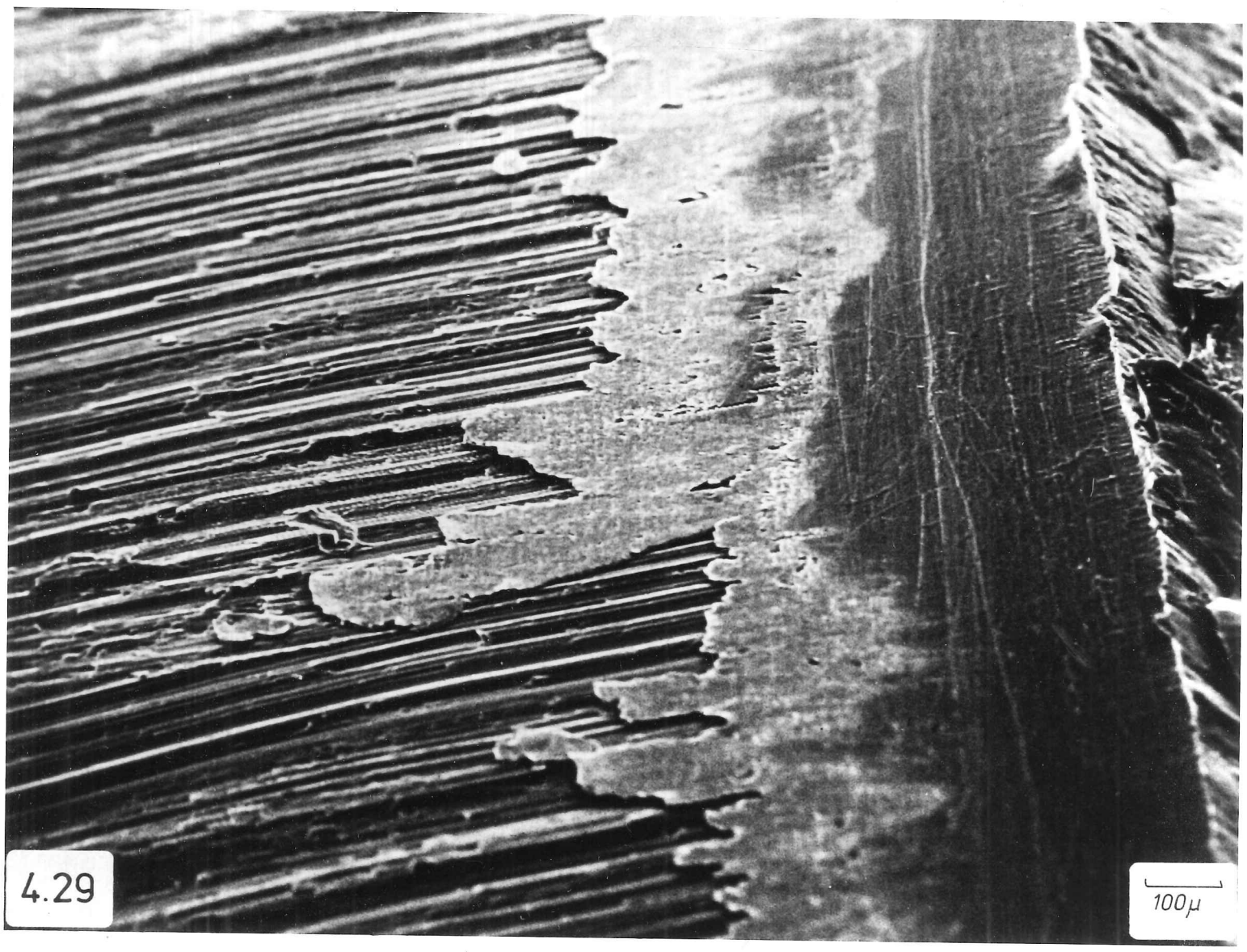

lightly scored, but is much smoother than the chip from a cut conducted in air.

Results with steel tools were similar (Figure 4.32). The ghosting on the tool is extensive but very light. Forces measured during cuts with discharge-cleaned tools are given in Table 4.2.

4.4.5 Negative Rake

The special holder for transparent inserts seen in Figure 4.33 was employed to investigate the influence of negative rake geometry on the contact conditions. Cine film Sequence 16 is an air cut on a lead workpiece. The rake face of the tool, after this cut, is seen in Figure 4.34. Use of negative rake did not appear to alter the zones of contact.

4.5 MACHINING OF COPPER WITH STEEL TOOLS

High speed steel (HSS) tools with 40° rake angle were used to cut pure copper in air and vacuum and the cutting forces were recorded. These experiments were repeated using tools manufactured from a plain carbon steel (PCS). The results are summarised in Table 4.3.

When using HSS tools in air, chip material transfers to the tool some distance from the cutting edge (Figure 4.35). In vacuum, there is reduced transfer to the tool and a smoother underside on the chip (Figure 4.36). This reduction in the resistance to the chip is reflected in the cutting forces, which are lower in vacuum than in air.

The PCS tools exhibit gross transfer of copper to the tool in air cuts and the underside of the chip has a torn appearance (Figure 4.37). In vacuum, the situation is rather worse, the region of chip/tool

lightly scored, but is much smoother than the chip from a cut conducted in air.

Results with steel tools were similar (Figure 4.32). The ghosting on the tool is extensive but very light. Forces measured during cuts with discharge-cleaned tools are given in Table 4.2.

4.4.5 Negative Rake

The special holder for transparent inserts seen in Figure 4.33 was employed to investigate the influence of negative rake geometry on the contact conditions. Cine film Sequence 16 is an air cut on a lead workpiece. The rake face of the tool, after this cut, is seen in Figure 4.34. Use of negative rake did not appear to alter the zones of contact.

4.5 MACHINING OF COPPER WITH STEEL TOOLS

High speed steel (HSS) tools with 40° rake angle were used to cut pure copper in air and vacuum and the cutting forces were recorded. These experiments were repeated using tools manufactured from a plain carbon steel (PCS). The results are summarised in Table 4.3.

When using HSS tools in air, chip material transfers to the tool some distance from the cutting edge (Figure 4.35). In vacuum, there is reduced transfer to the tool and a smoother underside on the chip (Figure 4.36). This reduction in the resistance to the chip is reflected in the cutting forces, which are lower in vacuum than in air.

The PCS tools exhibit gross transfer of copper to the tool in air cuts and the underside of the chip has a torn appearance (Figure 4.37). In vacuum, the situation is rather worse, the region of chip/tool

Figure 4.30 Aluminium chip produced in vacuum with the transparent tool following glow discharge cleaning of the tool.

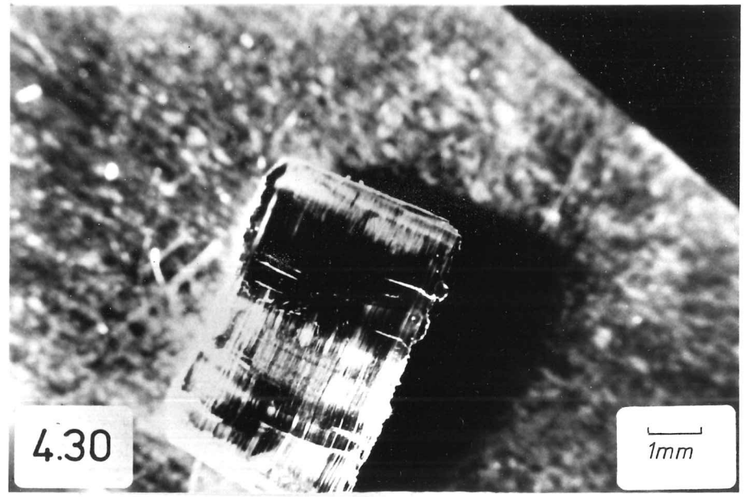

Figure 4.31 Rake face of transparent tool after the above experiment.

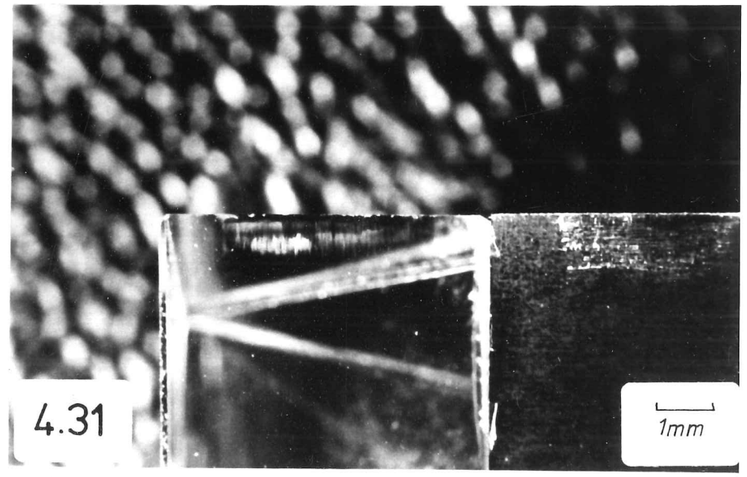

Figure 4.32 Rake face of high speed steel tool used to cut pure aluminium in vacuum, without (left) and with (right) prior glow discharge cleaning of the tool.

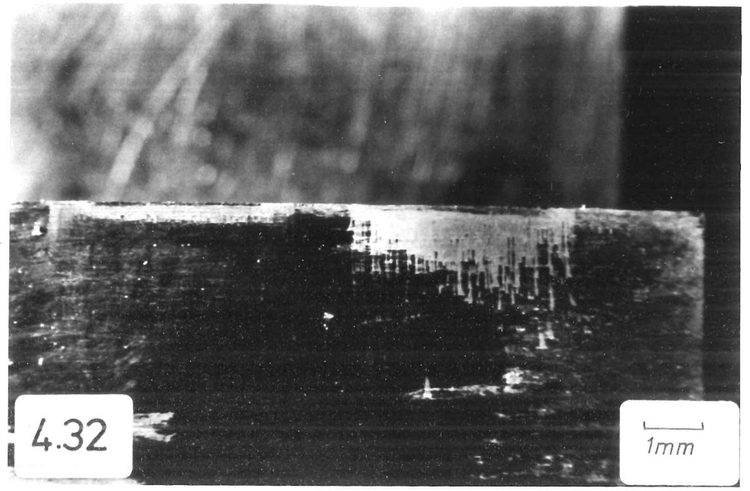

TABLE 4.2 Effect of glow discharge cleaning on cutting of pure aluminium

Forces in Kgf per mm width. Depth of cut 100 μ.
Cutting speed 20 mm sec^{-1}.

Conditions	N	T	F
In air	2.0	7.1	6.1
In vacuum	0.61	4.5	3.4
In vacuum after g.d.	0.63	4.8	3.6

TABLE 4.3 Cutting of copper with steel tools

Forces in Kgf per mm width. Depth of cut 100 μ.
Cutting speed 20 mm sec^{-1}.

Conditions		N	T	F
HSS tool	Air	1.80	11.7	8.9
	Vacuum	0.86	10.1	7.2
PCS tool	Air	4.6	16.8	14.3
	Vacuum	11.0	26.3	25.3

Figure 4.33 Transparent insert holder for negative rake machining.

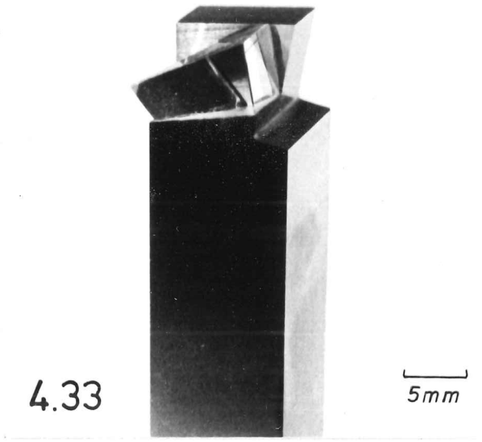

Figure 4.34 Rake face of transparent tool following negative rake machining of lead in air.

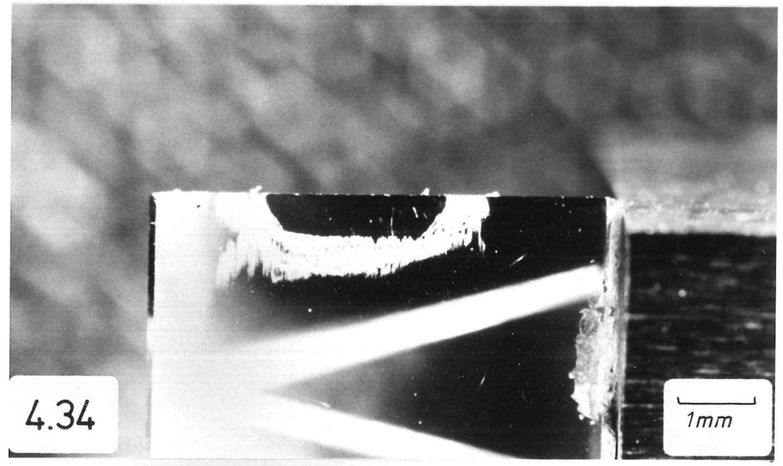

End of chip from the above experiment.

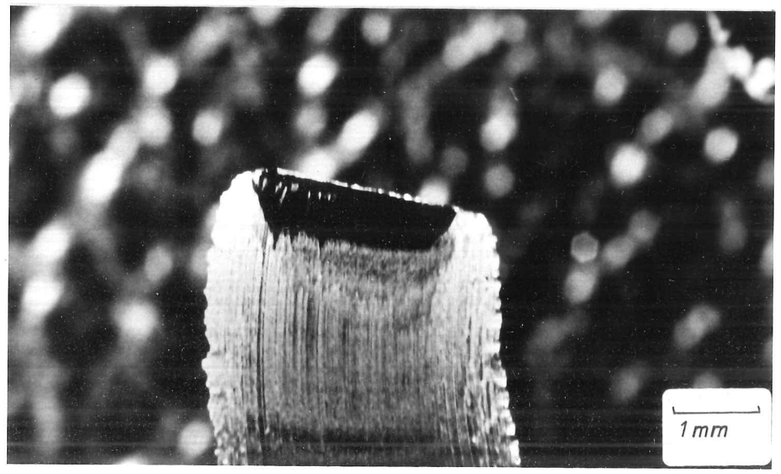

Appearance of the end of the chip and the rake face of the cutting tool, when copper is machined under various conditions.

Figure 4.35 HSS tool
Air

Figure 4.36 HSS tool
Vacuum

Figure 4.37 PCS tool
Air

Figure 4.38 PCS tool
Vacuum

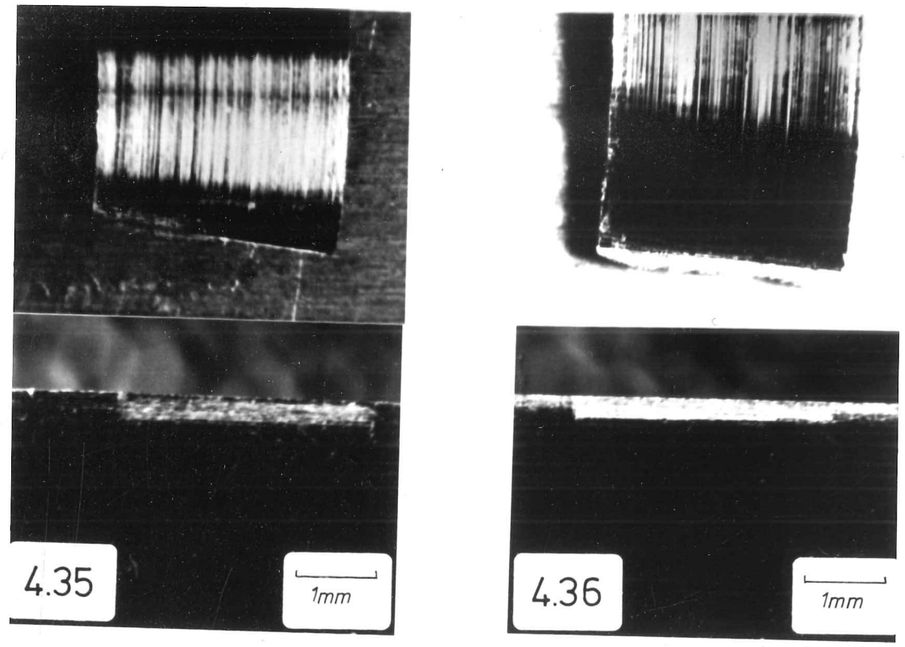

adhesion and transfer being very extensive. The cutting forces are correspondingly higher in vacuum than in air. There is, however, a region free from copper build-up adjacent to the cutting edge (Figure 4.38).

4.6 DISCUSSION

Introduction

The first observations of continuous cutting with the transparent tool lead to the conclusion that there are two regimes of contact at the chip/tool interface. These may be described as follows:

Zone 1: Intimate contact between chip and tool. No transfer of chip material after the cut.

Zone 2: Region of transfer to the tool, associated with the presence of oxygen.

4.6.1 The Role of Oxygen

The increased cutting forces in air, compared with vacuum, appear to be due to zone 2 formation. The transition from air to vacuum behaviour and its dependence on cutting speed were previously reported by Williams (1975), who suggested that the access of sufficient oxygen to form a layer of oxide on the underside of the chip was necessary to promote adhesion of these materials to high speed steel tools. Using lead and aluminium workpieces, the same was found to be true when plain carbon steel tools were used.

Further evidence for this dependence on oxygen access is provided by the observation that pure oxygen promotes more rapid and severe transfer than the same partial pressure of oxygen in atmospheric air.

The nitrogen balance in the air acts as a partial barrier to the oxygen diffusing into the narrow wedge at the interface.

The most compelling evidence for a transport-controlled mechanism concerns the remarkably consistent values of pressure at which the transition in behaviour occurs, for a given cutting speed. This is reported for the case of lead and aluminium and by Williams (1975) for a range of materials. The critical factor is the access or availability of oxygen at the end of zone 1 rather than the oxidation characteristics of the metal.

The dynamic nature of the zone 2 interaction is demonstrated in the Scanning Electron Micrographs of Figures 4.6 and 4.13. The oxygen appears to promote not only adhesion of chip material to the tool, but also to the transferred material. A redeposition process results, leading to the establishment of an equilibrium zone 2 size. Any explanation of the role of oxygen must take this dynamic feature into account.

The newly-generated (tool-side) surface of the chip emerging from zone 1 meets the atomosphere (if present). We can see from Figure 4.27 that the chip may make and then lose contact with the tool several times, before final separation, without adhering in vacuum. Clearly there is no tendency for the unoxidised chip to adhere to the tool and a smooth, undisrupted chip surface results. When oxygen is present, material becomes attached to the tool; thus, the oxidised surface is adherent. This may be because of an inherent "stickiness" of the oxidised surface, or due to some feature of the oxidation process itself.

Williams (1975) suggests that the tool is normally covered in a thin contaminant layer, which remains intact when cutting in vacuum and prevents adhesion of the chip. The presence of oxygen causes oxide scale to form which, being harder than the metal, abrades away the contaminant

and allows the chip to adhere to the clean tool. To test this hypothesis, some zone 2 material from a cut on pure aluminium was removed from the sapphire tool using cellulose acetate softened in acetone. This material was thin enough, in places, to allow Transmission Electron Microscopy (Figure 4.39). No evidence of any oxide "scale" or island oxide was found. However, oxide layers only a few molecules thick would not be detected by this method. It is considered that effective abrasion by scales of such dimensions would be unlikely. It is also difficult to explain the dynamic features of zone 2 (i.e. the redeposition of zone 2 material on to the chip) in terms of oxide abrasion.

The evolution of heat in the oxidation reaction was considered as a mechanism for increasing adhesion. It is difficult to see how heat alone could increase the strength of an interfacial bond. Greater flow of surface layers due to thermal softening might increase the true contact area, but the high normal loads must result in a substantial area of intimate contact and some local adhesion would be expected. Further, we have suggested that there is intimate contact in zone 1, but there is no adhesion in this region.

The important observation that oxidation reactions can lead to an increase in adhesion was reported by Pepper (1976), who studied the adhesion and sliding friction of alumina against copper, nickel and iron in ultra high vacuum at slow speeds of sliding. When the clean metal surfaces were exposed to oxygen sufficient to form a monolayer of oxide on the surface, increases in adhesion and sliding friction coefficient were observed. Pepper interprets these as due to some reaction of metal oxide with alumina producing strong interfacial bonds. This increase in adhesion was demonstrated in static tests so the oxide-abrasion theory would not seem to apply in this case.

Figure 4.39 Transmission electron micrograph of "zone 2" material taken from the transparent tool, following a cut on pure aluminium in air.
Shows a fine aluminium grain size with no evidence of island oxide.

Sapphire is aluminium oxide and the high speed steel tools would certainly carry an oxide layer, which could exhibit similar behaviour. Similar suggestions concerning interfacial adhesion increased by oxygen were made by Coffin (1959) and De Gee (1965, 1967).

When cutting in air, the zone 2 deposit itself would also be covered in an oxide layer and hence the observation of smooth grooving over zone 2 material in vacuum (Figure 4.13) may be understood, if adhesion between metals and oxides is inherently low. A neat demonstration of this phenomenon occurs in the cold welding process, in which two metal surfaces carrying oxide films are forced together at high pressure (Figure 4.40). In a peel test conducted before good metallic bonding has been obtained, it is found that the broken-up oxide particles stick together and failure occurs at the metal/oxide interface.

Further aspects of the role of oxygen in promoting the adhesion of the chip to oxide tools are treated in Chapter 7.

4.6.2 Movement in Zone 1

The question of movement in zone 1 with the transparent tool has been discussed in Section 4.3 and it appears that, in the case of the materials studied, any stationary layer present during cutting must be extremely thin, probably only a few hundred Angströms. Surface irregularities, even on the polished sapphire, are of this order. Unambiguous study of such a thin layer trapped between large bodies being impossible, then effectively we can conclude that observable interfacial seizure does not occur. This view is supported by several further pieces of evidence:

(a) the difficulty in detecting the position of the end of zone 1, in chips from vacuum cutting with sapphire tools;

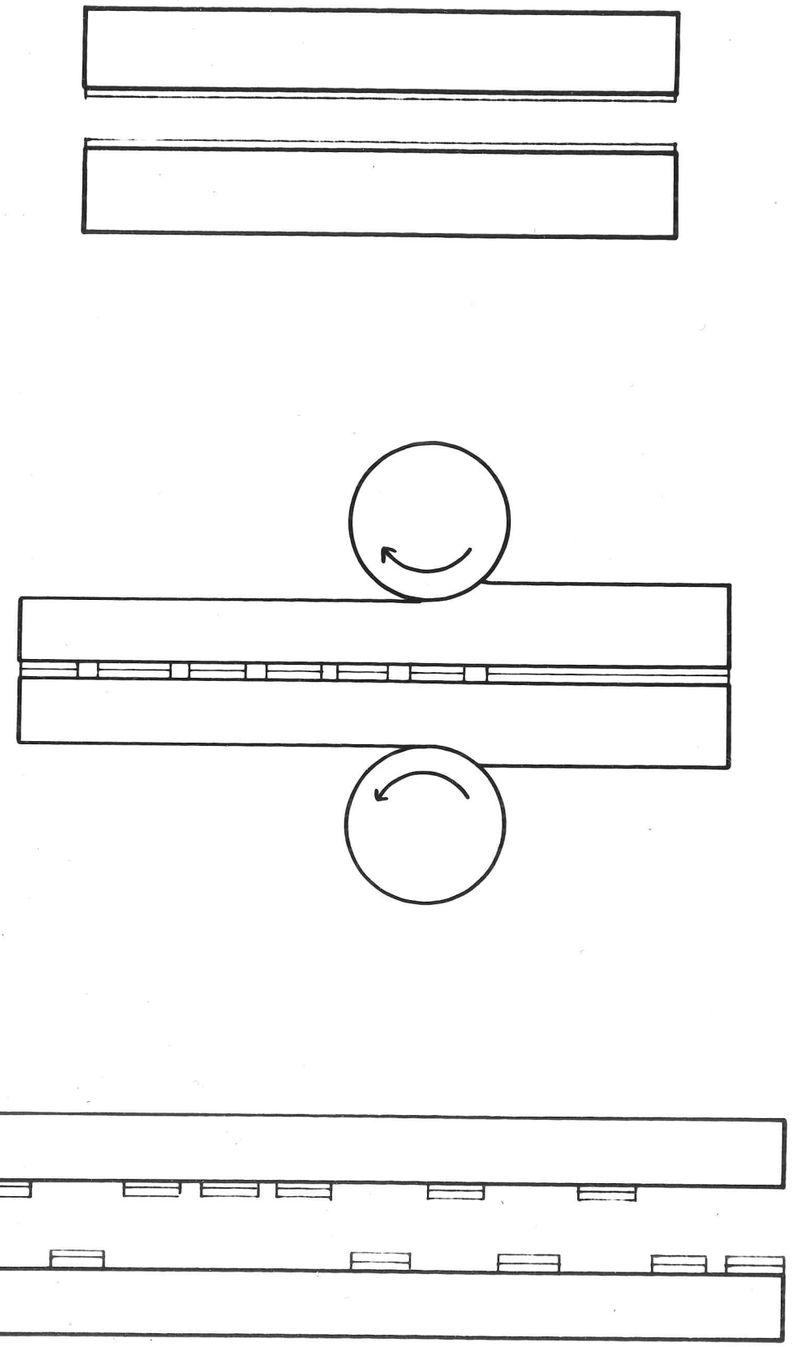

Figure 4.40 Adhesion of air-formed oxide films during the early stages of cold-welding.

(b) the way tool grinding marks are "ironed-out" in chips from vacuum cutting with steel tools;

(c) the lack of transferred material in zone 1 after the cut.

4.6.3 Zones 1a and 1b

Undertaken initially in an attempt to mask the rake face from view, to study the clearance interaction, the experiments with copper coatings on the tool yielded intriguing results. A division occurred within zone 1 which was not evident during cuts without the coating. The non-removal of copper in a length corresponding to the depth of cut was at first attributed to an initial indentation effect, but it was noted that chip/tool contact was sometimes established over a distance considerably greater than the length of zone 1 before any copper was removed, eliminating this possibility. The removal of the copper in zone 1a with the chip, at the end of the cut, suggests that there may indeed be conditions of seizure at the interface. However, a slight improvement in the coating practice leads to the retention of this film on the tool. The removal of the copper film in the remainder of zone 1, i.e. in zone 1b, clearly demonstrates that there is interfacial sliding in this region. The fact that this can occur without chip material sticking to the tool, while zone 2 transfer is laid down on top of the copper, casts further doubt on the oxide-cleaning hypothesis.

The clearance interaction was not illuminated by this technique and, with the sharp tools in use, appeared to be negligible, no contact length or transfer zone being observed. Further applications of copper coatings are described in Chapters 7 and 8.

The proposed sub-division of zone 1 is given further support by the micrograph of the chip root (Figure 4.27) in vacuum with quick-stop.

The undistorted region corresponds to zone 1a, with intimate contact between chip and tool. In zone 1b the chip appears to slide without adhesion, interacting with progressively less of the tool surface until there is contact only at a few high-spots. Clearly both non-contact and seizure may be ruled out as explanations of the lack of adhesion in vacuum and the strength of the interface must be lower than that of the chip material. This contact at high-spots does, however, produce light "ghosting" on the tool in zone 1b (Figure 4.26). This is quite unlike a zone 2 deposit and, it is proposed, occurs by "micromachining" of the chip by the edges of the tool grinding marks. No light transfer is found in zone 1a, because there is always contact.

4.6.4 Glow Discharge Cleaning

The effect of discharge cleaning of the tool prior to cutting in vacuum is to promote a light transfer of chip material, wherever contact with the tool is made, except in zone 1a. A small increase in the cutting force is observed, but not comparable to the effect of oxygen (Table 4.2). The transfer experienced with glow discharge was much easier to remove from the sapphire tool than a zone 2 deposit, and could be cleared away from the sapphire simply by wiping with cotton wool. The light transfer on the steel tool is again associated with grinding marks, but now extends to regions where there is only transient contact. It is considered that glow discharge cleaning causes loosely-held particles of chip material, generated in the rubbing contact, to adhere to the tool. This contrasts with the view of Williams (1975) who proposes that the glow discharge, in removing contaminants, simulates the effect of oxygen. If this were true, one would expect a gross, zone 2 transfer to be promoted, but this is not the case.

4.6.5 Effect with Different Tool Materials

The remarkable contrast in the performances of high speed steel (HSS) and plain carbon steel (PCS) tools in the cutting of copper compounds the confusion over contact conditions. Since both tool materials are much harder than the workpiece, and both composed of alloyed iron, differences in the surface film seem to be the most likely cause of these differences in behaviour.

High speed steel tools produce effects with copper workpieces not markedly different from those experienced with indium, lead and aluminium. The zone 2 deposit is smaller and less well attached to the tool, but still associated with oxygen which produces an increase in the cutting forces. It has been suggested (in Section 4.6.1) that these tools would carry an oxide film, which might be resistant to wear by the chip.

The PCS tools produce the opposite effect, with increased chip/tool interaction in vacuum. The apparently "lubricating" action of vacuum, previously encountered with the softer metals, is reversed. However, the metal is transferred in a different region on the tool from zone 2 transfer and appears, on initial inspection, to extend to the tip. Only close scrutiny reveals the presence of a clean region on the tool and corresponding features at the chip root. This is of the same dimensions as zone 1a, i.e. it corresponds to the depth of cut. Adhesion, therefore, occurs in zone 1b and is diminished, rather than promoted, by oxygen. The interface between the chip and the tool in zone 1b is now stronger than the chip, causing flow to occur within the metal.

It is proposed that the oxide films present on the PCS tool are less well adherent and/or weaker than those on the HSS tool. These are

removed by the passage of the copper chip, but not by that of a softer metal such as lead or aluminium. Analysis of the tool surface by X-ray electron spectroscopy supports this view; the oxide layer on the PCS tool is iron oxide, but the HSS tool appears to be covered by some other oxide. Figure 4.41 shows the X-ray spectra of the HSS tool surface at two different electron voltages. True surface analysis of steel specimens is complicated by the difficulties in surface cleaning, but this technique conveniently displays the trend as the penetration depth is reduced. Table 4.4 gives the bulk analysis of the material. It seems likely that the surface oxide layer on the HSS is vanadium oxide.

TABLE 4.4 Specification of Ti tool steel

	%
Carbon	0.7
Chromium	4
Tungsten	18
Vanadium	1.0

When the oxide film is removed by the chip, metal/metal contact occurs and the interfacial strength is intermediate between that of the chip and the tool (Bowden and Tabor, 1964). The lubricating action of oxygen is then explained since oxide formation on the deposit serves to diminish the adhesion. It is not particularly effective, however, since oxide/oxide bonding is also fairly strong. Further aspects of lubrication by oxygen and of the machining of copper with these tools are treated in Chapter 7.

Figure 4.41 X-ray analysis of high speed steel tool surface, showing the effect of decreasing the depth of penetration.

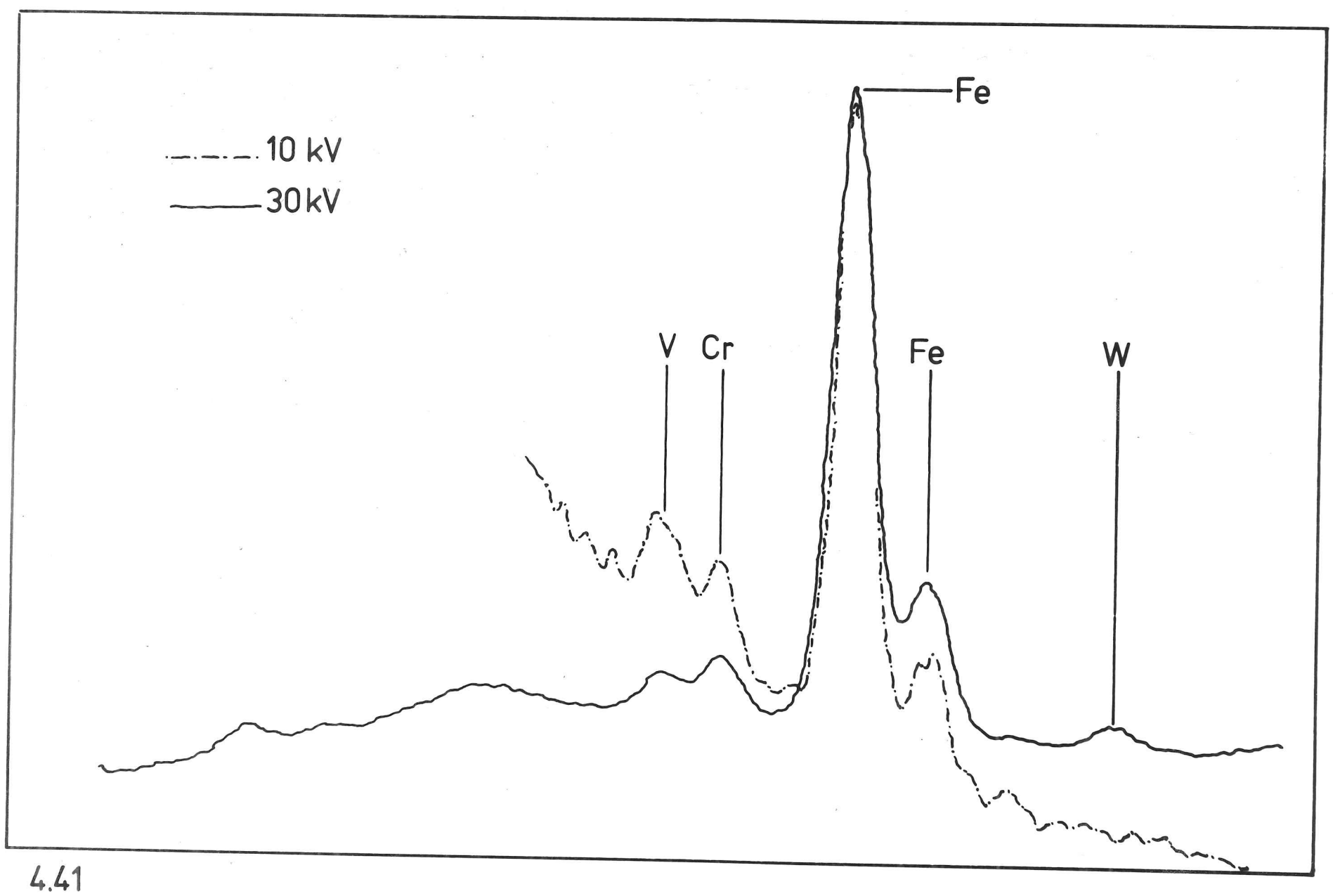

4.41

Similar effects to those described above are reported by Williams (1975) who used an iridium tool to cut aluminium, lead and copper. The cutting behaviour of the first two materials in air and vacuum was similar to that observed with HSS tools. The copper, however, exhibited very much higher cutting forces with the iridium tool in air and in vacuum they rose even higher. This was attributed to the lack of oxide film on the noble iridium; however, if this is a correct explanation, one might expect all workpiece materials to produce the same effect. Perhaps the iridium carries a very thin oxide film which is still effective with the softer materials. De Gee (1967) proposed that even monomolecular films might act in this way. It is noted that Williams observed tool/chip adhesion up to the cutting edge, i.e. in zone 1a when performing quick-stop experiments on copper with iridium tools.

The action of oxygen in the cutting of steel with HSS tools is similar to its effect on copper with PCS tools, i.e. it acts as a lubricant (Rowe and Smart, 1963; Williams, 1975). At the speeds investigated, a build-up edge is formed, so this situation will be treated in the next Chapter.

4.7 A DESCRIPTION OF THE INTERFACE

In summary, we may describe the chip/tool interface in continuous cutting in the following way:

Zone 1a Corresponds approximately to the depth of cut. Intimate contact between the chip and the tool, with the real and apparent areas of contact being equal. However, separation occurs at the interface after the cut. There appears to be movement at the interface, but no severe rubbing since surface films are not worn away. Treated further in Chapter 8.

Zone 1b Sliding under a gradually diminishing normal load. Adhesion and hence the severity of sliding contact depend on the nature of the tool surface and sometimes indirectly on the hardness of the material being cut. Sticking and transfer in this region occur if metal-to-metal contact can be established. In such cases, the presence of oxygen reduces the growth of the adhered junction.

Zone 2 Region of chip/tool transfer at the end of zone 1b associated with access of oxygen to the newly-exposed under-surface of the chip. Only observed with oxide or oxide-covered tools and eliminated in vacuum, due to the inherent weakness of metal/oxide bonding.

CHAPTER FIVE

CONTINUOUS CUTTING WITH BUILT-UP-EDGE FORMATION AND DISCONTINUOUS CUTTING

5.1 THE EFFECT OF BUILT-UP-EDGE ON CONTINUOUS CUTTING

With certain combinations of workpiece material and machining conditions, the continuous cutting process becomes complicated by the appearance of a built-up-edge (BUE). (See Chapter 2 and Figure 2.5). This serves to modify the cutting geometry, increasing the effective rake angle and thereby increasing the shear plane angle and reducing the chip thickness and cutting forces. Unfortunately this wedge of workpiece material is unstable and intermittently breaks away, pieces of the BUE being carried away with the chip or the workpiece, resulting in poor surface finish. Many commercially important materials exhibit this variation of continuous cutting, including the precipitation-hardened aluminium alloys and most steels. The formation of small, stable BUE's is frequently preferred and is aimed for when establishing the cutting conditions. It is also found (with steel) that the BUE becomes modified at higher cutting speeds due to thermal effects.

Attempts to arrive at an understanding of the interface conditions giving rise to BUE formation and the factors governing its size and shape were made in the present study. The transparent tool could not be employed with steel workpieces but was used to cut Duralumin (aluminium alloy). High speed steel cutting tools were used with steel workpieces and the effects of free machining additives were studied.

5.2 OBSERVATIONS ON DURALUMIN WITH THE TRANSPARENT TOOL

Introduction

Due to the problems anticipated when using the sapphire to cut this harder material, two different alloys were investigated. First attempts were made with Duralumin H, (HS 30) which is a relatively soft material. Further cuts were then made on Duralumin S, (HS 15) which is harder and rather less ductile.

5.2.1 Alloy H

Cutting of this material in air was viewed through the transparent tool. The appearance of such a cut was initially very similar to the cutting, in air, of the materials described in the previous chapter. There was an initial tight curl region, followed rapidly by the onset of transfer to the tool and grooving of the chip. It was observed, however, that the contact length was much shorter than with the pure metals and the chip was very much thinner and retained a degree of curl. Soon after the beginning of the cut, the impression of movement in zone 1 was suddenly lost. This is seen in Figure 5.1 and Cine Sequence 17.

At the end of the cut, the chip was removed from the tool and the BUE was found to adhere mostly to the chip (Figure 5.2). The tool itself carried transfer only in a region at the end of the chip/tool contact, the rake face being almost clean near the edge (Figure 5.3).

In vacuum, similar effects were observed, with the rapid establishment of a "dead zone" of static material adjacent to the cutting edge. The BUE was again attached to the chip after the cut, with the rake face retaining only small flakes of material which were found to be loosely held to the tool.

Figure 5.1 Transparent tool; Duralumin H machined in air.

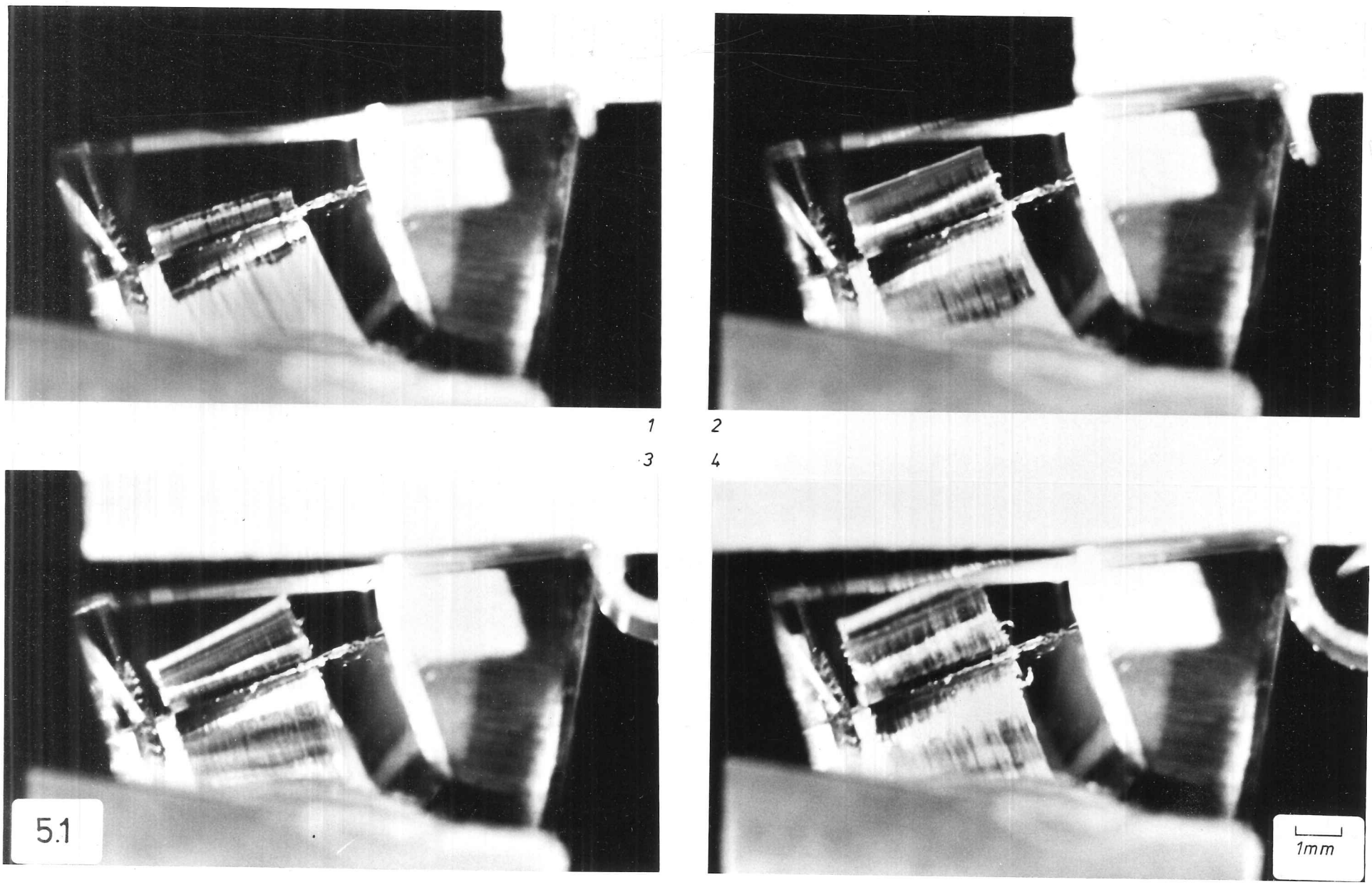

Duralumin H chip attached to the transparent tool, produced when machining in air.

Figure 5.2 End of the chip when removed from the tool.

Figure 5.3 Rake face of the transparent tool after removal of the chip.

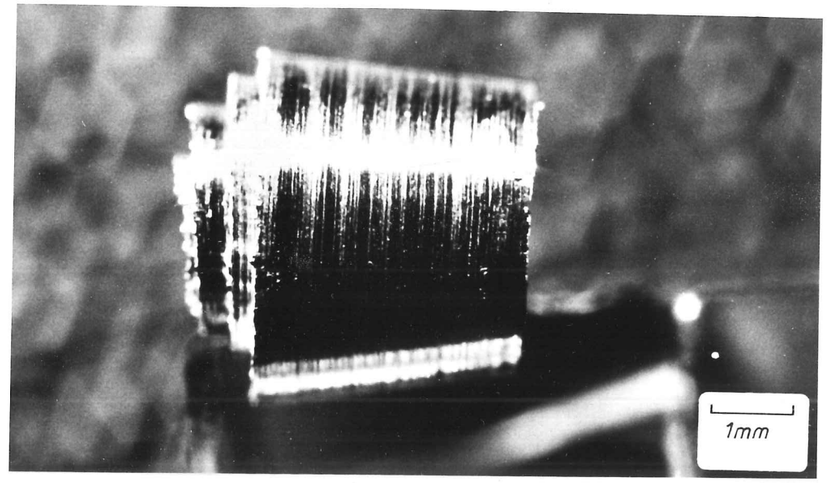

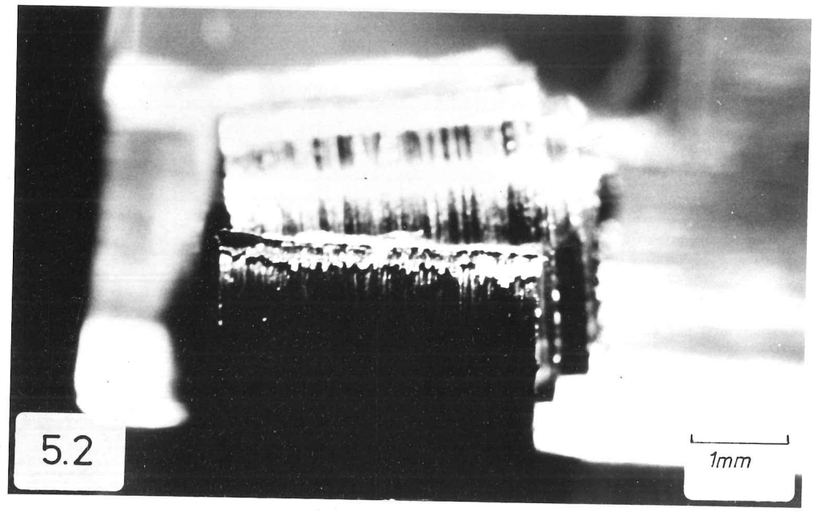

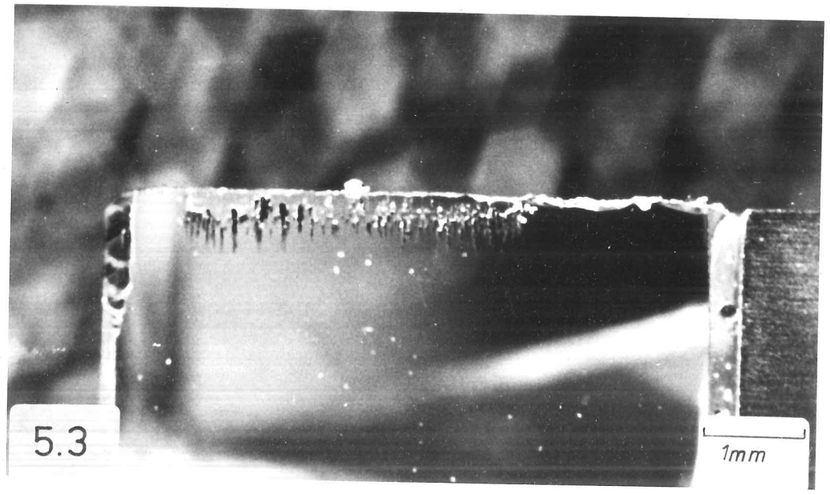

5.2.2 Alloy S

When this harder alloy was cut in vacuum, (Cine Sequence 18) smooth chip sliding and the lack of BUE was again followed by the establishment of a static region and scoring of the chip. Tighter curl accompanied the onset of BUE behaviour. A rather larger BUE was formed than with alloy H. The BUE was again largely transferred to the chip after the cut but this time the tool carried more debris (Figure 5.4). The chip was heavily segmented indicative of tearing and the machined surface had a very rough appearance (Figure 5.5).

The air cut on this material (Cine Sequence 19) proceeded in a progressively more difficult manner, the built-up-edge growing in size and the chip becoming more segmented until eventually the forces became too great and the sapphire insert was removed from its holder due to failure of the adhesive. This time a substantial layer of material was left adhering strongly to the tool (Figure 5.6). The machined surface was also markedly more disrupted (Figure 5.7).

Due to the large forces and the risk of damage, further investigations of the machining properties of the alloy were made with the use of cutting fluid and are described in Chapter 7.

5.3 CUTTING OF MILD STEEL WORKPIECES

Mild steel specimens were machined with HSS tools and the tool and chip studied after the cut (Figures 5.8 and 5.9). The BUE is attached to the chip but some steel is transferred to the tool further up the rake face. The chip root, with BUE adhering, from a quick-stop experiment, is seen in section in Figure 5.10. The BUE is more extensive in vacuum than in air and, as a result, the vacuum-machined chip is very irregular

Figure 5.4 Rake face of the transparent tool after machining Duralumin S in vacuum.

Figure 5.5 Cut surface of the Duralumin S workpiece after machining in vacuum.

Figure 5.6 Rake face of the transparent tool after machining Duralumin S in air.

Figure 5.7 Cut surface of the Duralumin S workpiece after machining in air.

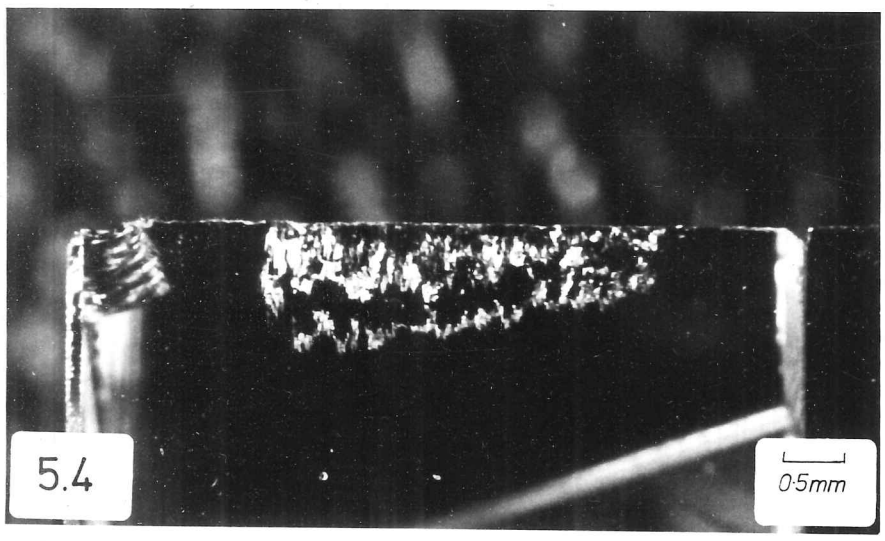

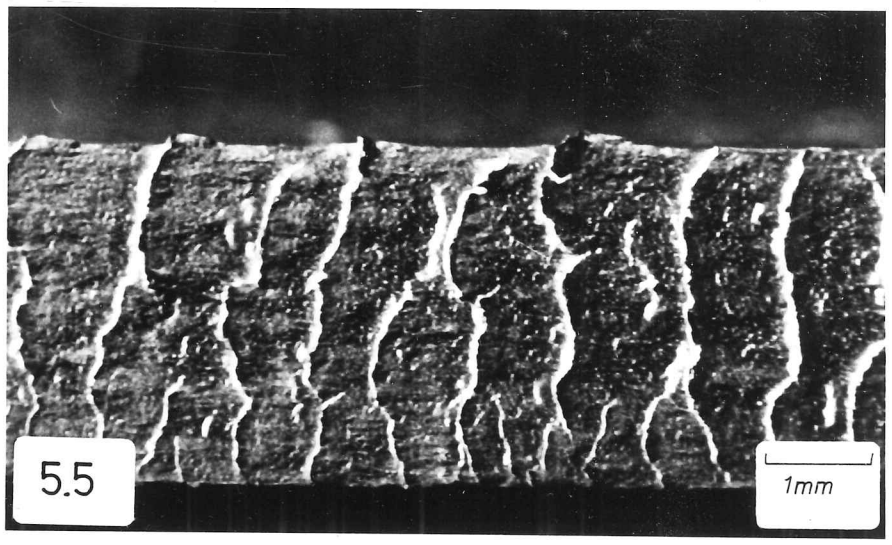

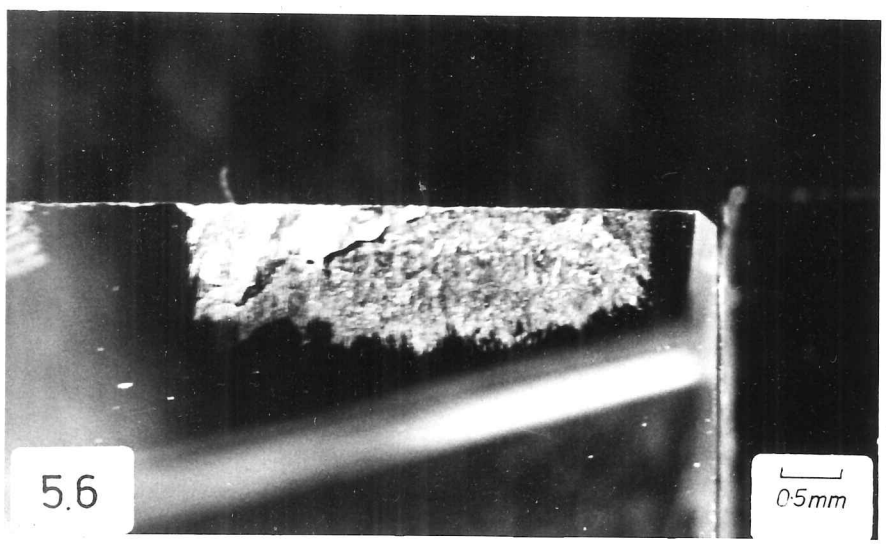

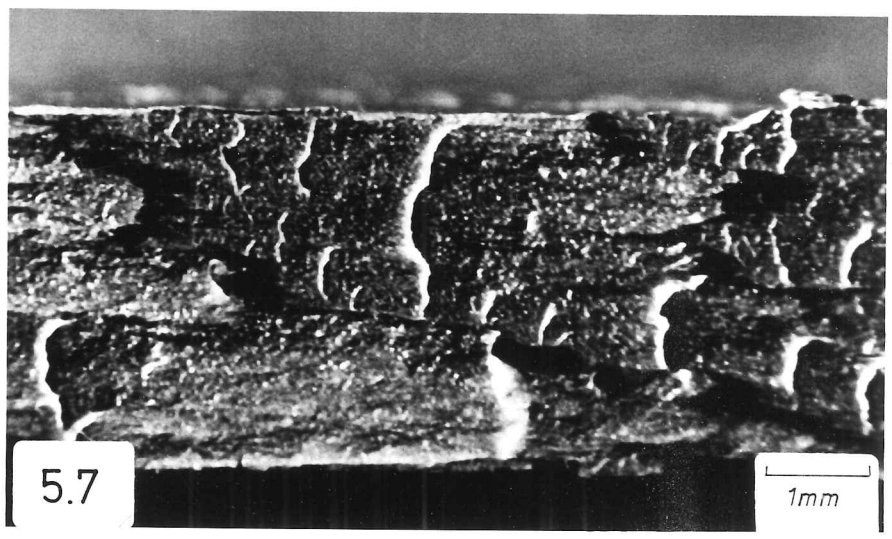

and the cut surface extremely uneven. The effect of oxygen on the cutting forces was studied and a summary of the results is presented in Table 5.1, together with the results for a resulphurised steel of slightly higher carbon content.

TABLE 5.1 Cutting of steel in air and vacuum

Forces in Kgf per mm width. Depth of cut 100 μ.
Cutting speed 165 mm sec^{-1}. H.S.S. tool

Material	Conditions	N	T	F
Mild steel	Air	5.9	14.4	13.8
	Vacuum	11.1	18.3	20.2
Resulph. steel	Air	7.1	16.5	16.1
	Vacuum	7.1	16.8	16.3

5.4 DISCUSSION OF BUILT-UP-EDGE

When cutting with the transparent tool, initial movement was observed in zone 1, followed by the establishment of an apparently stationary layer. It was initially supposed that the BUE could only form after some transfer of workpiece material to the tool, further up the rake face, had taken place and increased the resistance to sliding of the chip. This was supported by the observation that grooving of the chip preceded BUE formation. This view that it is resistance to chip movement, rather than seizure at the tool tip, that causes the BUE to form was also strengthened by the following observation: careful study of Figures 5.4 and 5.5 reveals that the broken boundary of the BUE

Figure 5.8 Rake face of high speed steel tool after machining mild steel in air.

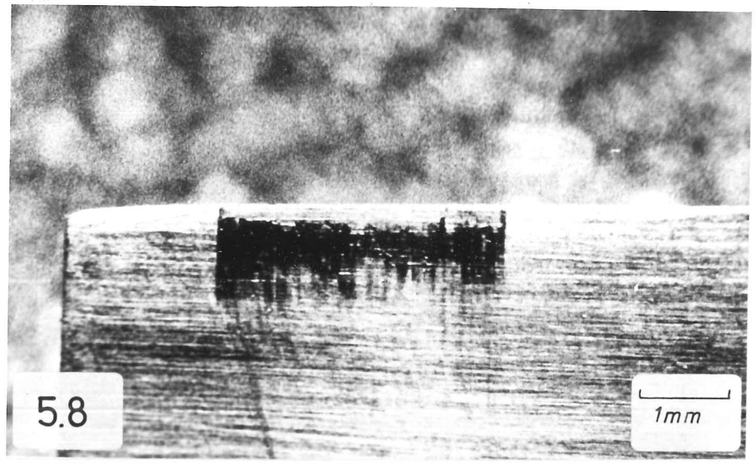

Figure 5.9 Views of the mild steel chip root from a quick-stop experiment, with built-up-edge adhering.

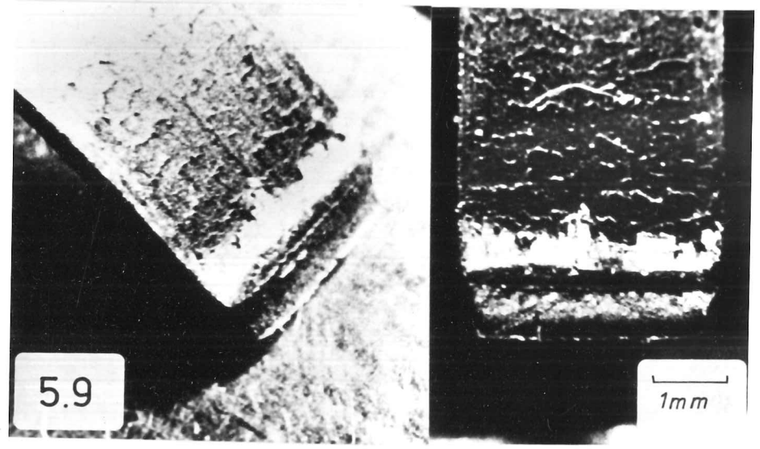

Figure 5.10 Section through the chip and built-up-edge.

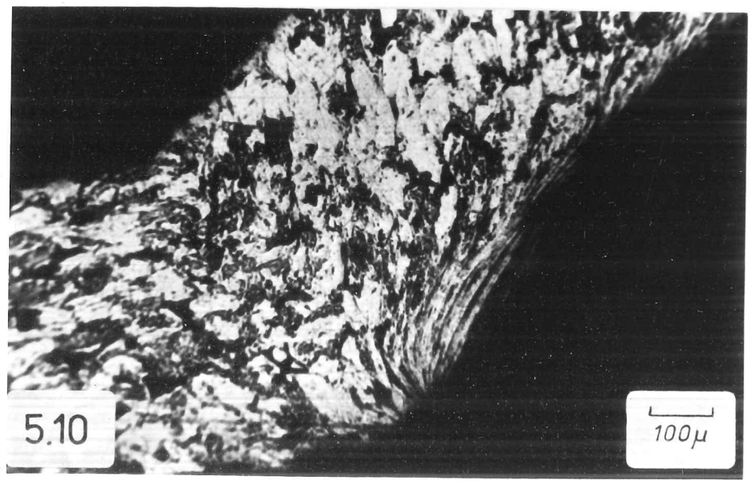

adhering to the chip exactly matches the boundary of the clean region on the tool. Thus the transfer on the rake face and the BUE were once one body of material in contact with the tool. This suggests that the greater adhesion may be at the end away from the cutting edge.

If, however, it is assumed that a zone 2 transfer is responsible for the BUE, then cutting in vacuum, with an oxide tool, should eliminate BUE formation. This is not found. However, as indicated by the attempts to cut the harder alloy, oxygen may still serve to increase adhesion and make the situation more severe.

It is suggested that the process of BUE formation is such that the establishment of a static body of workpiece material at the tool tip may occur even when the chip/tool interface is weaker than the bulk. In an homogeneous material, this weakness leads to interfacial sliding, as we have observed in Chapter 4 in, for example, the cutting of pure aluminium with a sapphire or HSS tool. However, with the introduction of second-phase particles acting as stress concentrators, the localised load transmitted to the chip through interfacial sliding could cause fracture to occur at a rake face stress lower than the yield point, as depicted in Figure 5.11. Once the BUE is formed, it is stable despite the apparent weakness of the BUE/tool bond. This is because the new stress at the interface, resulting from the modified shape of the cutting tool, is low, as shown schematically in Figure 5.12.

However, at the end of the cut, or when the tool is withdrawn in a quick-stop experiment, the weakness of the interface becomes evident and the BUE remains affixed to the chip. This does not occur in places where a strong BUE/tool bond has formed, for example, in the case of oxide tools, the region accessible to oxygen. With tools that lose a

Figure 5.11 Fracture within the chip resulting from the rake face drag, producing the separation of a built-up-edge.

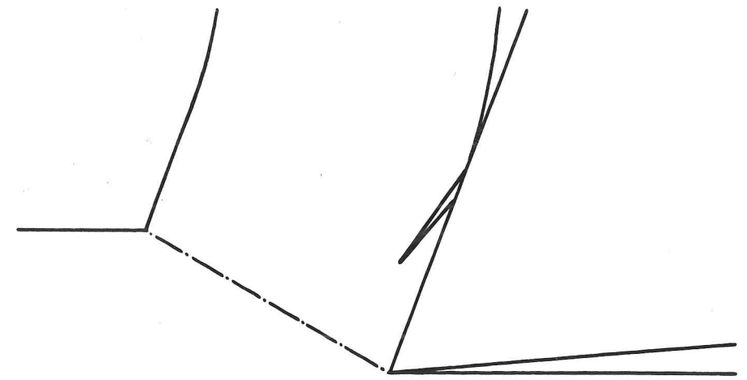

5.11

Figure 5.12 Forces acting on the built-up-edge, showing that the built-up-edge may remain stable despite the apparent weakness of the built-up-edge/tool interface. The built-up-edge is the rigid body PNO. The shear stress acting over PN is greater than that over ON.

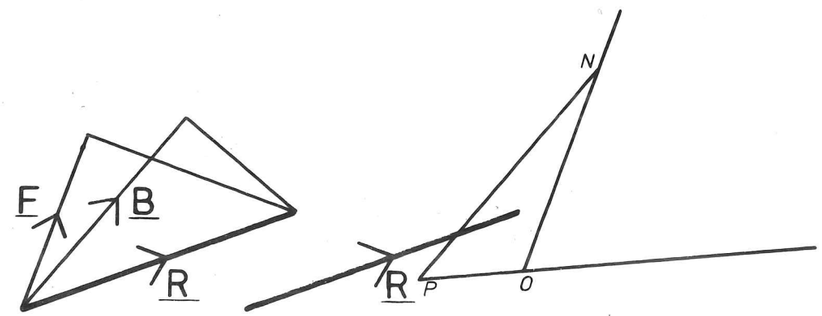

$$\frac{B}{PN} > \frac{F}{ON}$$

5.12

surface oxide layer, strong bonding of the BUE to the tool would be evident in such areas. Thus the occurrence of a BUE is due mainly to the fracture properties of the workpiece material, but its growth is governed by interfacial adhesion.

The steel-cutting experiments tend to support this view. The action of oxygen is found to be lubricative, reducing the growth of the BUE by restricting metal-to-metal contact. This may be compared with the situation of a copper workpiece and plain carbon steel tool described in Chapter 4.

The steel containing manganese sulphide inclusions does not appear to be affected in its machining behaviour by the presence of oxygen. In such a steel, the growth of the BUE is limited by the MnS inclusions themselves.

5.5 DISCONTINUOUS CUTTING

Metals of insufficient ductility to sustain the large shear strains in continuous chip formation produce discontinuous chips by periodic fracture. (See Chapter 2 and Figure 2.6). Many "difficult-to-machine" materials fall into this category, for example the Nimonics. Other alloys contain free-machining additivies which modify the behaviour of the material to one of discontinuous chip formation e.g. leaded brasses.

The use of the transparent tool for many of these materials was precluded by the vulnerability of the sharp cutting edge to damage by the repeated impacts. However, it was possible to obtain an insight into discontinuous cutting by machining magnesium, which demonstrates this mode of chip formation together with very low cutting forces.

5.6 CONTACT CONDITIONS IN THE MACHINING OF MAGNESIUM

5.6.1 Cutting in Air

The cine film (Sequence 20) shows the cutting of polycrystalline pure magnesium in air, viewed through the transparent tool. Still photographs taken at the beginning and after a short length of cut are seen in Figure 5.13.

The process of indentation and release accompanying the formation of each segment is clearly seen in the cine film. The region adjacent to the cutting edge becomes rapidly obscured by debris and gradual transfer of chip material further up the rake face is noted. The segments fall away from the tool soon after formation, the longest pieces of chip containing only four or five individual segments. These chips have a rough appearance on the underside.

The appearance of the sapphire tool after the cut is seen in Figure 5.14. There is magnesium adhering to the rake face in a region of about 1 mm length. A light cleaning operation produces the effect seen in Figure 5.15.

5.6.2 Cutting in Vacuum

This is seen in Sequence 21 and Figure 5.16. Although the process of chip formation appears to be the same, some influence of the vacuum is clearly evident. The segments are smaller and hold together in greater numbers before falling away from the tool. Although some debris again appears on the rake face during the cut, this obscures less of the field of view and the chips have a smoother appearance on the underside.

The appearance of the tool before and after a light cleaning operation is seen in Figures 5.17 and 5.18.

Figure 5.13 Transparent tool; magnesium machined in air.

Figure 5.14 Rake face of the transparent tool after machining magnesium in air.

Figure 5.15 The same after a light cleaning operation.

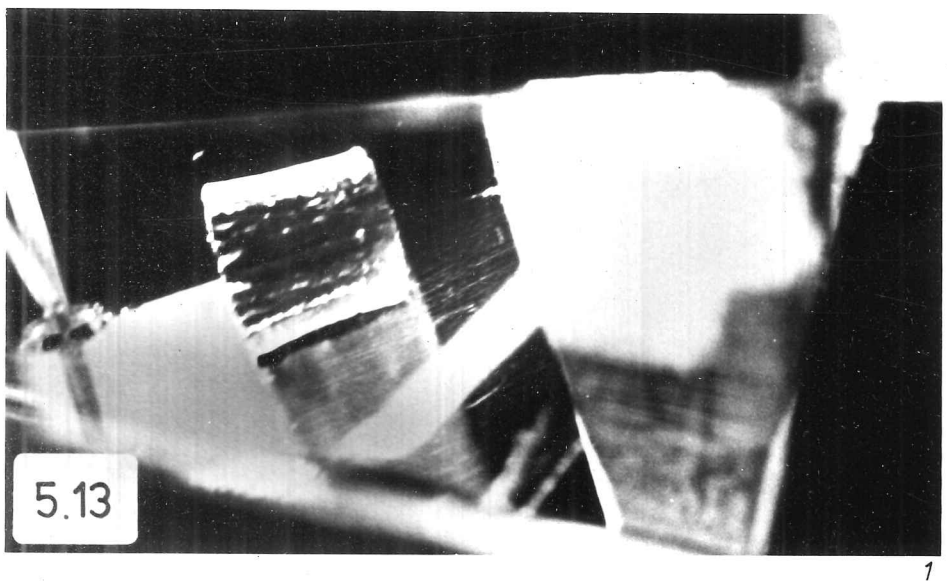

1

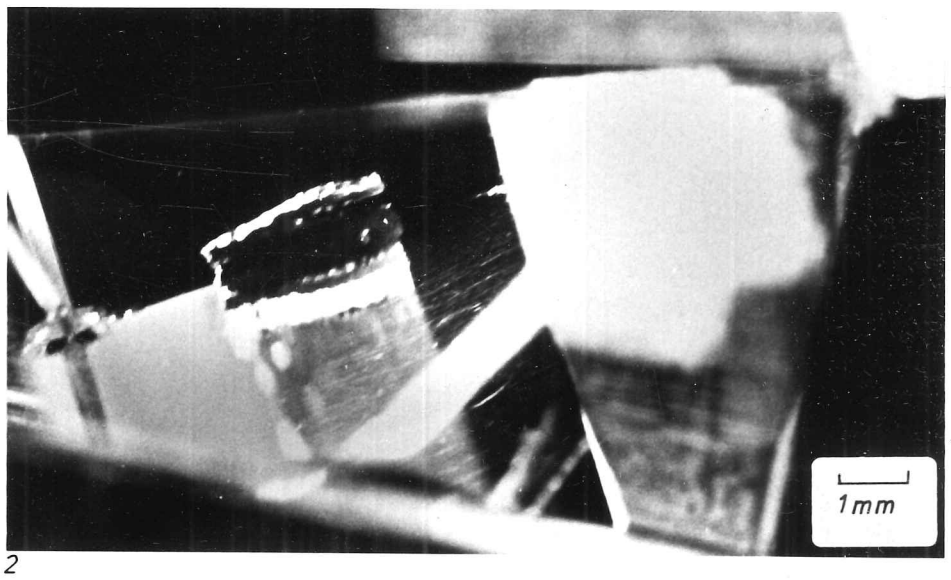

2

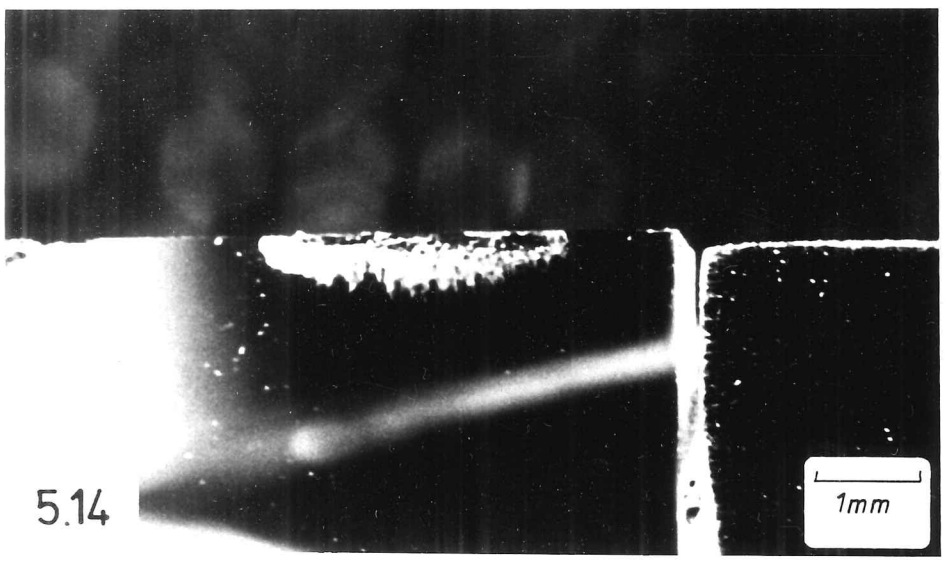

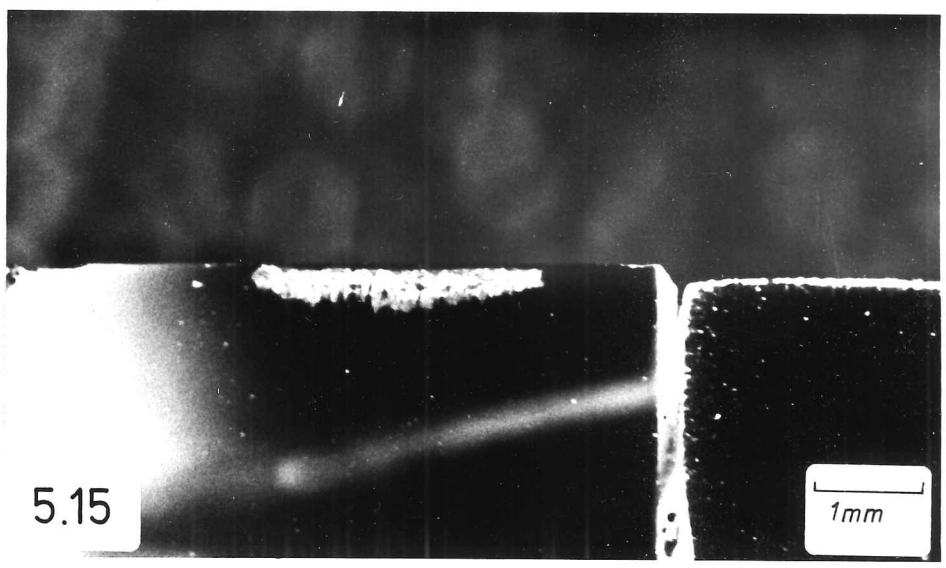

Figure 5.16 Transparent tool; magnesium machined in vacuum.

Figure 5.17 Rake face of the transparent tool after machining magnesium in vacuum.

Figure 5.18 The same after a light cleaning operation.

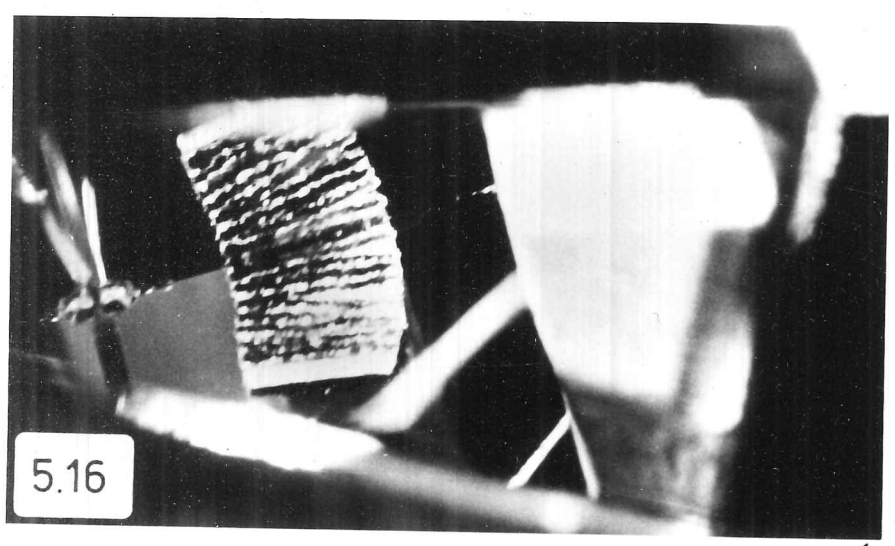

1

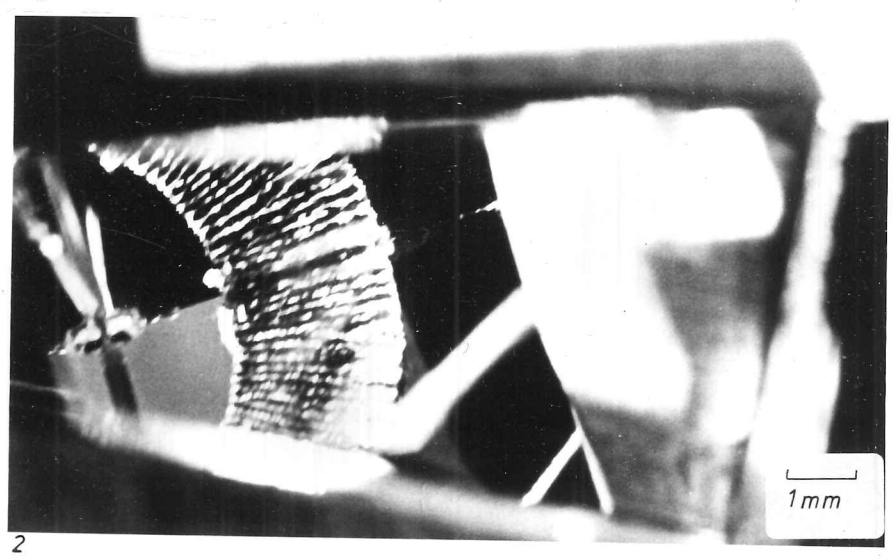

2

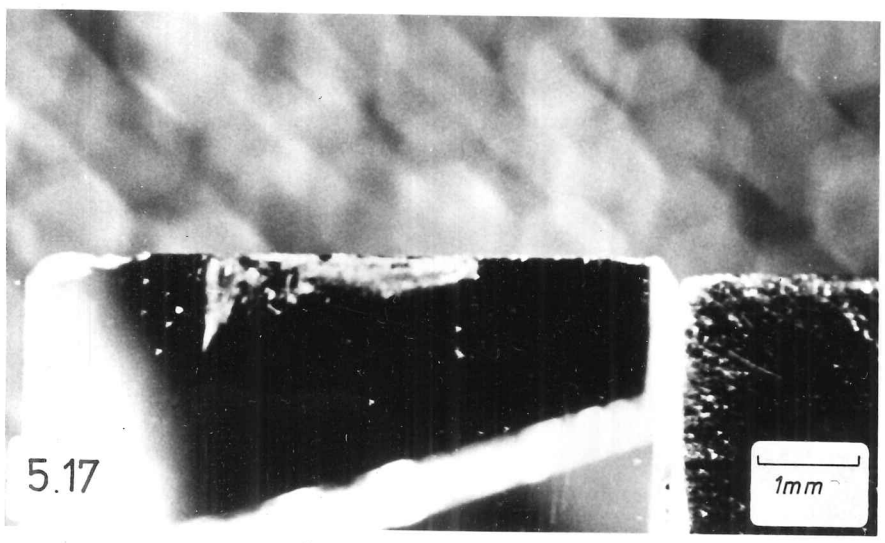

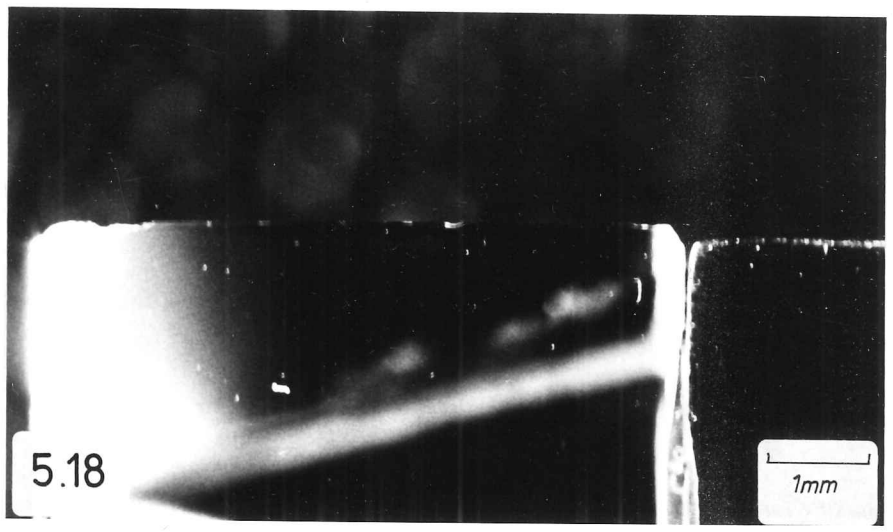

5.6.3 Cutting Forces

Table 5.2 gives the forces in air and vacuum. These are mean values since the measured force naturally fluctuates during the cut. There appears to be a marked increase in the rake face drag force when machining this material in air rather than in vacuum. However, with an initially clean tool, there is a brief period of cutting in air when the cutting forces are comparable to those in vacuum.

TABLE 5.2 Cutting magnesium in air and vacuum

Forces in Kgf per mm width. Depth of cut 100 μ.
Cutting speed 10 mm sec^{-1}.

Conditions	N	T	F
Air	3.78	3.29	4.30
Vacuum	2.70	3.17	3.21
Air (at start)	2.77	3.08	3.26

5.7 FREE MACHINING BRASS

Small depths of cut ($< 50\ \mu$) with the 40° HSS tool produce tightly-curled, ribbon-like chips from the leaded brass workpiece. Increasing the depth of cut results in the appearance of discontinuous chips (Figure 5.19). These are in the form of short lengths of connected segments. The underside of the chip is generally smooth and some of the "cracks" between segments holding together as a chip have been obliterated. A Scanning Electron Micrograph of one of these "cracks" between segments

is seen in Figure 5.20. The tool carries a deposit, after cutting this material, in the region adjacent to the cutting edge.

5.8 DISCUSSION OF INTERFACE IN DISCONTINUOUS CUTTING

Interfacial conditions in discontinuous chip formation display marked differences from those observed in the continuous case. The indentation/release cycle leads to intermittent chip/rake face contact at the tip of the tool, rather than continual contact over this region.

In the vacuum cutting of magnesium, loosely held particles of workpiece material are found on the rake face in the region close to the edge. This transferred material is readily removed and appears to be fracture debris. However, cutting in air produces a gross deposit which is more firmly attached to the tool. This is like a "Zone 2" deposit, but is found at the tip, because oxygen gains access through the intermittent contact. The cutting forces are increased in the presence of oxygen, as found in the continuous cutting of metals using oxide tools. Another effect of the oxygen is to cause break-up of the chip, apparently due to the interaction with transferred magnesium on the tool. The vacuum chip holds together rather better and this demonstrates that the fracture process has not caused complete separation within the machined layer. Particularly when only partially discontinuous chips are formed, adhesion at the chip/tool interface may still be an important influence on machining behaviour.

Similar effects to those seen with magnesium are noted with F.M. brass, material becoming attached to the tool in the indentation region. The remainder of the rake face is relatively free from chip/tool interaction, as indicated by the absence of build-up and the smooth undersurface of the chip. This is consistent with lubrication by thin

Figure 5.19 Free-machining brass chips produced with the 40° high speed steel tool; depth of cut 40 μ (left) and 150 μ (right).

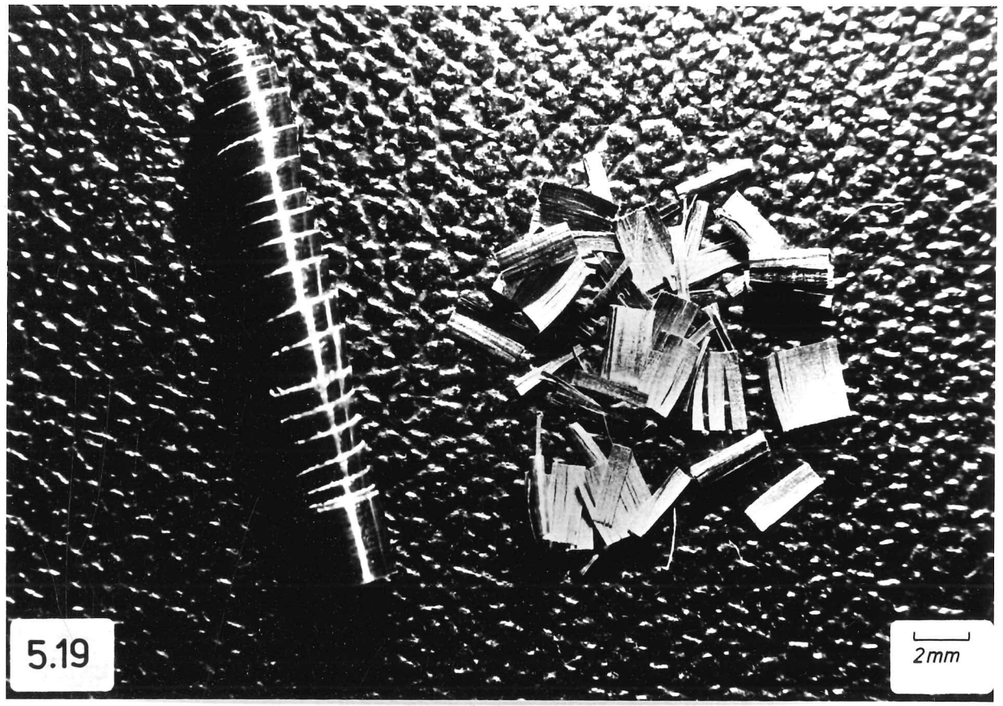

Figure 5.20 Scanning electron micrographs of discontinuous chips of free-machining brass, showing the shear failure surface between segments.

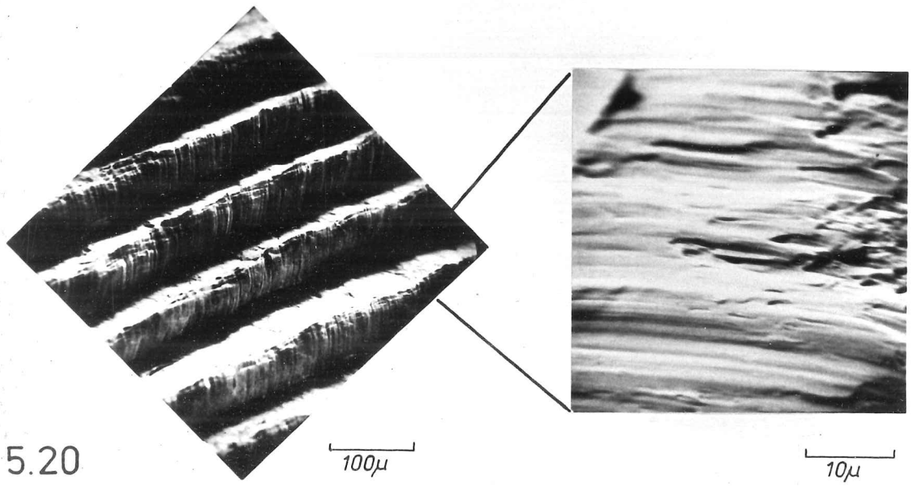

layers of lead (Williams et al., 1970).

The shear surfaces between segments resemble those of ductile rupture (Figure 5.20). It has been suggested (Doyle, 1974) that this rupture occurs by linking of voids around second-phase particles, accounting for discontinuous behaviour. The depth of cut was found to influence the mode of chip formation. This has been noted by Atkins (1974) who suggests that the discontinuous cutting behaviour of free machining brasses is the result of a reduction in fracture toughness caused by additions of lead. Unfortunately, further study of this area was beyond the scope of this investigation.

CHAPTER SIX

MECHANICS OF THE CHIP-FORMING PROCESS

6.1 THE EFFECT OF ORIENTATION ON CUTTING

Introduction

The microscopic processes of slip which give plastic behaviour in metals are crystallographic in origin, so one would expect any metal deformation process, such as cutting, to proceed according to the crystal orientation. Manufactured metallic components are almost invariably polycrystalline and it is frequently desirable, because of the effect on mechanical properties, to obtain a fine grain structure. Hence the cutting behaviour of polycrystals is of the greatest general interest. However, many metal forming processes, such as rolling, introduce texture (preferred orientation), so crystallographic effects may become important. There are also advantages when studying the basic mechanisms of the shear process in using workpieces of known initial slip geometry.

6.1.1 Observations With a Coarse-Grained Polycrystalline Specimen

Pure aluminium workpieces with an equiaxed structure of grains approximately 5 mm in diameter were machined in vacuum, using 40° rake high speed steel tools. Fluctuations in the cutting forces, shear plane angle (as indicated by chip thickness) and lamellae spacing with grain orientation were observed (Figure 6.1). When the free surface of the chip is studied in the S.E.M., the positions of grain boundaries are revealed (Figure 6.2).

Orientation effects are also found on the cut surface of the workpiece, even though no nominal nose radius was employed (Figure 6.3).

Figure 6.1 Etched coarse-grained pure aluminium workpiece, showing the variation of tangential cutting force with variations in the grain structure. The central narrow strip is the cut surface.

Figure 6.2 Free surface of pure aluminium chip produced from the coarse polycrystalline specimen; scanning electron micrograph showing a grain boundary and differing lamellae spacings in the two grains.

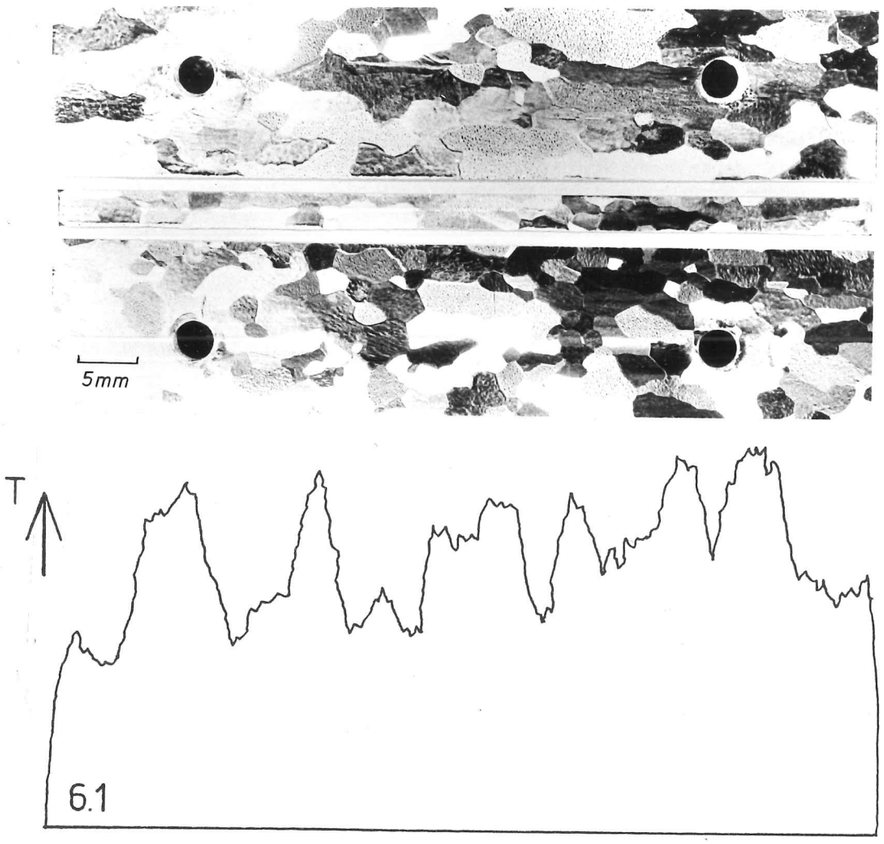

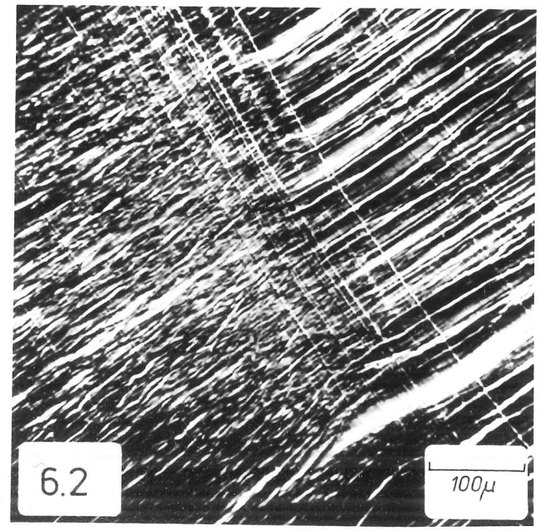

These are in the form of bands across the workpiece, parallel to the cutting edge and of constant spacing within any particular grain. This gives the cut surface an "etched" appearance, although not every grain displays these features. Since they do not extend across the whole workpiece, meeting the edges only when the grain meets one or both sides, they could not be attributable to tool movements induced by fluctuation of the shear plane angle. They must, therefore, have some direct crystallographic origin, in the region of the cutting edge. These effects were not investigated further, but could be of some importance in relation to surface finish.

Previously macro-etched specimens were also machined. These had a faceted surface prior to the cut, in which the cube planes were revealed, regardless of grain orientation (Figure 6.4). The manner in which these facets deform in cutting is rather unusual. In many cases, the etched features are lost and a typical lamellae pattern results. Some grains, however, appear to preserve their etched appearance (Figure 6.5) although the "blocks" are distorted. Very close examination of these blocks was made in the S.E.M. (Figure 6.6). It is suggested that these grains were in a suitable orientation for slip on a single slip system and that the large strains in the initially smooth-surfaced blocks produced these remarkable effects.

6.1.2 The Notion of a Constant Resolved Shear Stress

Two pieces of experimental work on the cutting of single crystals are reported in the literature. Ramalingam and Hazra (1973), machining pure aluminium, obtained results indicating that the resolved shear stress on the shear plane has a constant value, although shear plane angle might vary with orientation. They consider that shear in cutting

Figure 6.3 Cut surface of coarse-grained pure aluminium workpiece.

Figure 6.4 Scanning electron micrograph of coarse-grained pure aluminium after macro-etching treatment, showing cube planes.

Figure 6.5 Free surface of pure aluminium chip produced when machining on etched specimen, showing some regions of typical lamellae and some apparently almost undistorted "blocks".

Figure 6.6 As Figure 6.5; higher magnification of one of the etched "blocks".

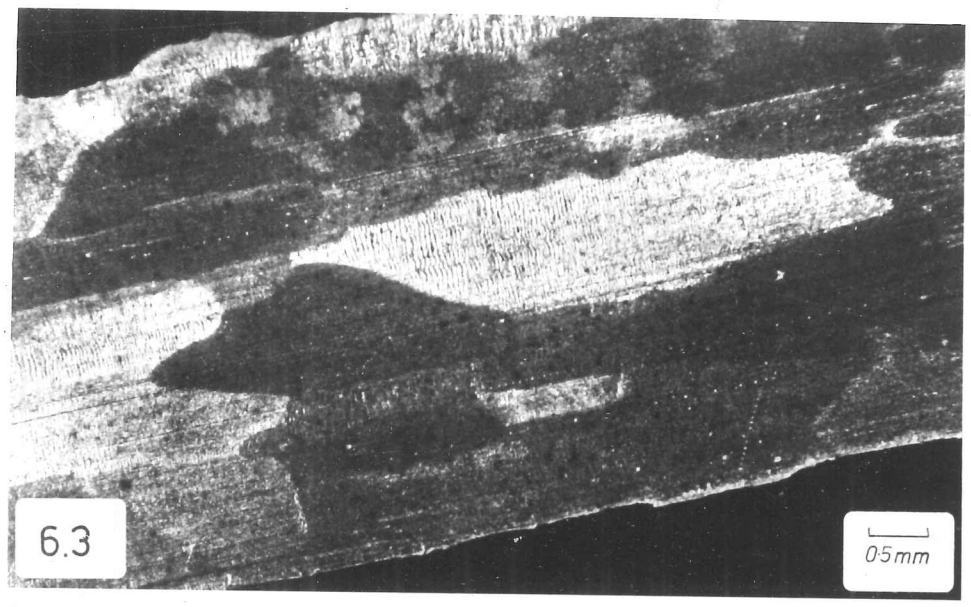

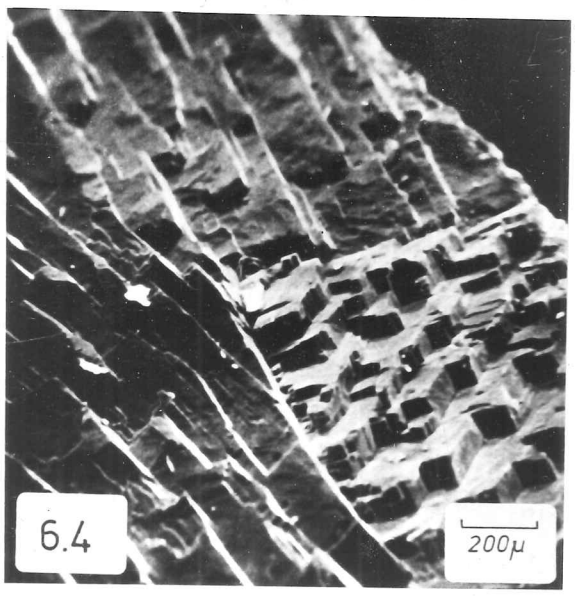

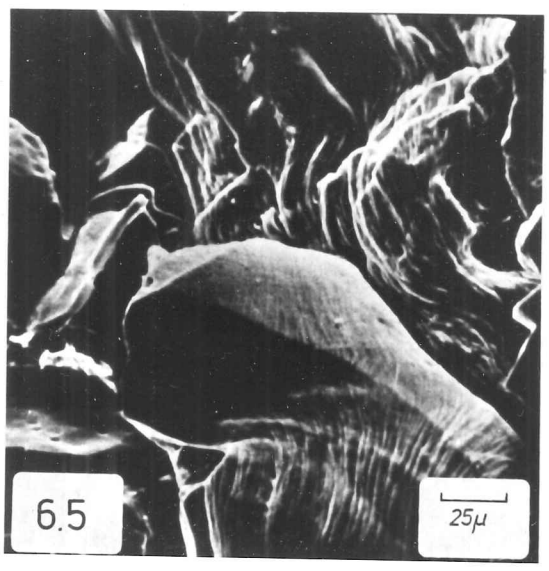

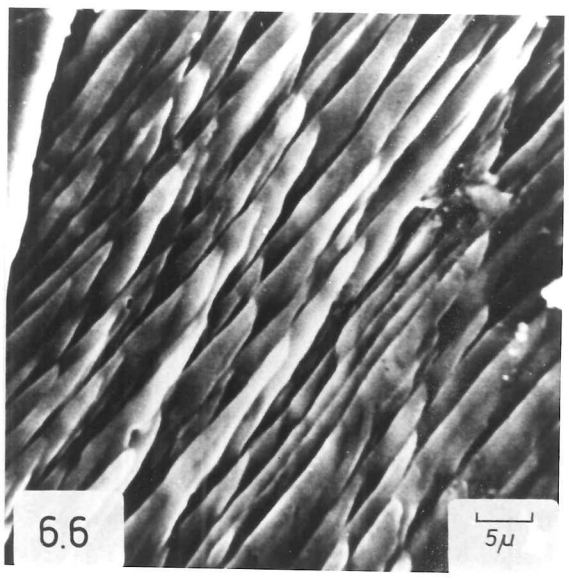

occurs on a crystallographic plane, of non-specific Miller indices, by the operation of multiple slip on a number of slip systems. Thus variations in cutting force with crystal orientation are due to variations in the angle of the most favourable shear plane. The resolved shear stress is an invariant, material property.

Williams and Gane (1977) in a study of the microtoming of pure copper crystals of two known orientations, conclude that the resolved shear stress is dependent on the orientation and has a lower value when a slip plane is aligned with the shear plane. Thus the flow stress in multiple slip is considered to be higher than in single slip.

Some work was conducted in the present study in an attempt to resolve this conflict. Both aluminium and copper crystals were cut in the same type of machine and in several orientations. Great care was taken to obtain an accurate value of the cutting ratio and hence of the shear plane angle. Some new work is also reported in which the cutting behaviour of magnesium single crystals was investigated.

6.2 COPPER AND ALUMINIUM SINGLE CRYSTAL CUTTING

6.2.1 Experimental Details

The single crystal workpieces were grown from a high-purity melt using seed crystals and subsequently checked for orientation by x-ray diffractometry. They were strips 3 mm thick and initially 20 mm wide, cut by spark erosion into lengths of approximately 80 mm. All the strips had a $\{110\}$ face and differed from one another by the indices of the cutting direction $\langle x, y, z \rangle$. Copper crystals of $\langle 100 \rangle$, $\langle 110 \rangle$ and $\langle 211 \rangle$ orientations and aluminium $\langle 100 \rangle$ and $\langle 211 \rangle$ crystals were prepared. The $\{110\}$ $\langle 211 \rangle$ crystals, being non-symmetrical, were

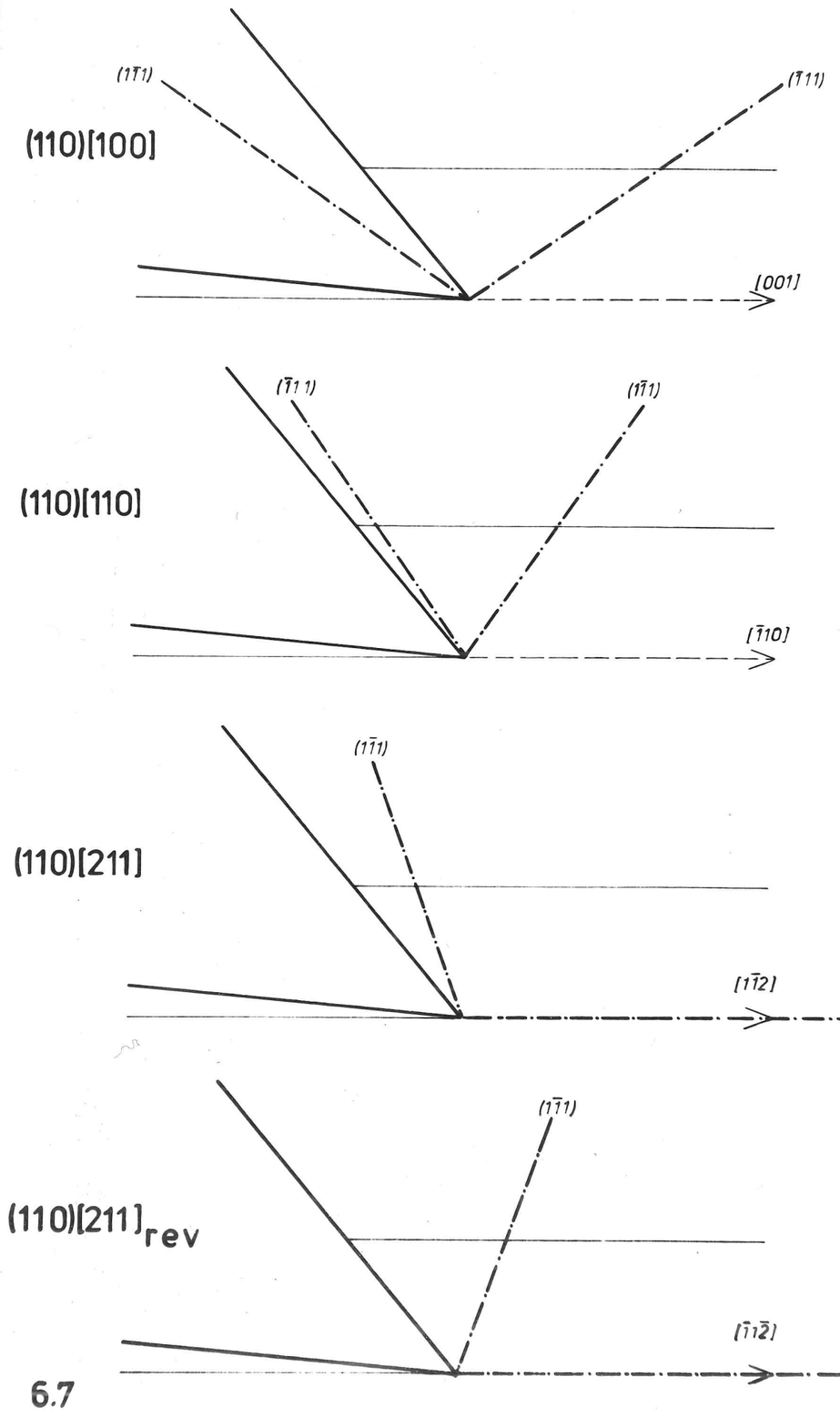

Figure 6.7 Orientations employed in studying the cutting behaviour of copper and aluminium single crystals, showing the positions of the $\{111\}$ planes.

cut in two directions. These orientations, and the positions of the slip planes $\{111\}$ are seen in Figure 6.7.

All cuts were made with ground HSS tools of 40^{o} rake angle. Both air and vacuum runs were performed at a cutting speed of 20 mm sec^{-1}. A constant depth of cut, of 100 μ, was intended, but this in fact varied by about 15% due to the uncertainties inherent in the setting mechanism. The true depth obtained was determined by clocking the cut surface and further verified by weighing the chip. The thickness of the chips and and also some lengths of chips were measured to yield a value for the cutting ratio and hence the shear plane angle. This was verified in some cases by direct measurement of shear angle on the workpiece (after a quick-stop experiment).

No attempts were made to remove the damaged layer between runs so all the cuts were made on previously cut surfaces. It is considered that the orientation 50-100 μ below the cut surface is unlikely to have been altered by the previous cuts, the main effect at this depth being work-hardening. The workpiece material is necessarily heavily work-hardened when it approaches the shear zone. No nominal nose radius was used, greatly reducing any ploughing effect, but some rotation of the upper 10 μ or so may possibly have occurred.

6.2.2 Results

The values of shear plane angle and resolved shear stress for the single crystal runs, together with those for a fine-grain annealed poly-crystal of the same purity, are presented in Tables 6.1 and 6.2. The errors quoted refer to scatter in the data.

Scanning Electron Micrographs of the free surfaces of some copper chips are seen in Figures 6.8 - 6.11. In the case of the copper $\{110\}\langle 110\rangle$

TABLE 6.1 Copper single crystal cutting

Shear plane angle ϕ degrees. Resolved shear stress k Kgf mm^{-2}.

Crystal Orientation	Air		Vacuum	
	ϕ	k	ϕ	k
Polycrystal	16.6 ± 0.5	30.4 ± 0.7	20.5 ± 1.1	30.3 ± 1.1
(110) [100]	13.0 ± 0.7	29.4 ± 0.9	14.3 ± 0.6	26.2 ± 1.2
(110) [110] (a)	5.9 ± 0.4	23.4 ± 0.8	8.0 ± 0.5	22.5 ± 0.9
(110) [110] (b)	30.1 ± 2.5	29.2 ± 1.5	24.1 ± 1.0	29.0 ± 2.0
(110) [211]	22.2 ± 1.3	32.6 ± 0.5	25.1 ± 2.2	33.9 ± 0.5
(110) [211] rev	36.3 ± 0.9	26.6 ± 1.1	45.2 ± 1.6	22.5 ± 0.4

TABLE 6.2 Aluminium single crystal cutting

Shear plane angle ϕ degrees. Resolved shear stress k kgf mm^{-2}.

Crystal Orientation	Air		Vacuum	
	ϕ	k	ϕ	k
Polycrystal	9.2 ± 0.3	10.3 ± 0.4	10.8 ± 0.2	9.5 ± 0.2
(110) [100]	9.2 ± 0.3	9.7 ± 0.3	10.4 ± 0.3	9.6 ± 0.2
(110) [211]	7.3 ± 0.2	10.0 ± 0.4	7.6 ± 0.2	9.6 ± 0.1
(110) [211] rev (a)	8.6 ± 0.2	10.0 ± 0.1	17.7 ± 0.2	8.7 ± 0.3
(110) [211] rev (b)			31.1 ± 1.6	9.5 ± 0.3

Figure 6.8 Free surface of copper chip, $\{110\}$ $\langle 100 \rangle$ orientation.

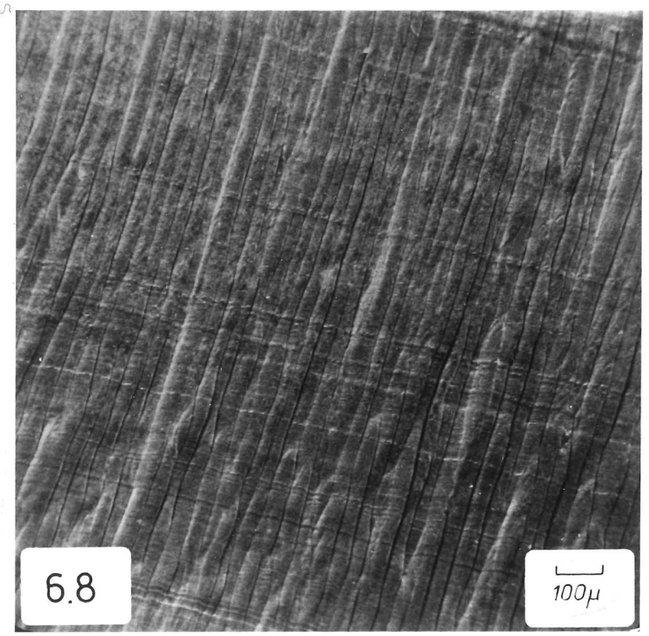

Figure 6.9 Free surface of copper chip, $\{110\}$ $\langle 110 \rangle$ orientation, showing the effect of two different shear plane angles.

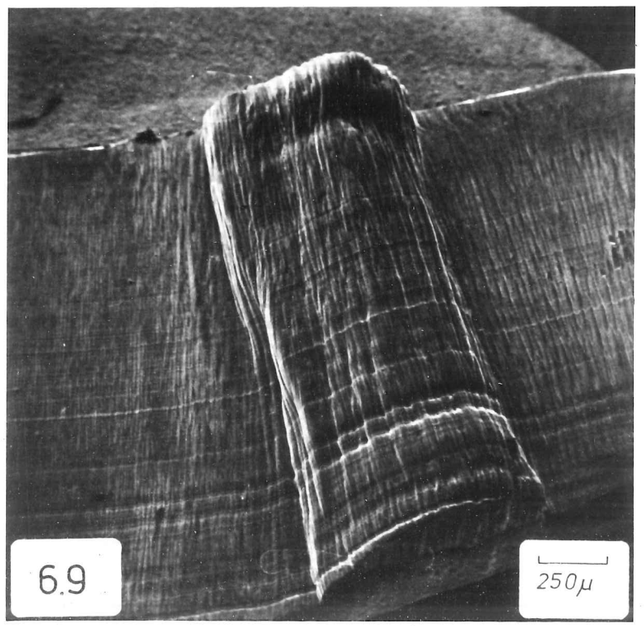

Figure 6.10 As Figure 6.9, low shear plane angle region.

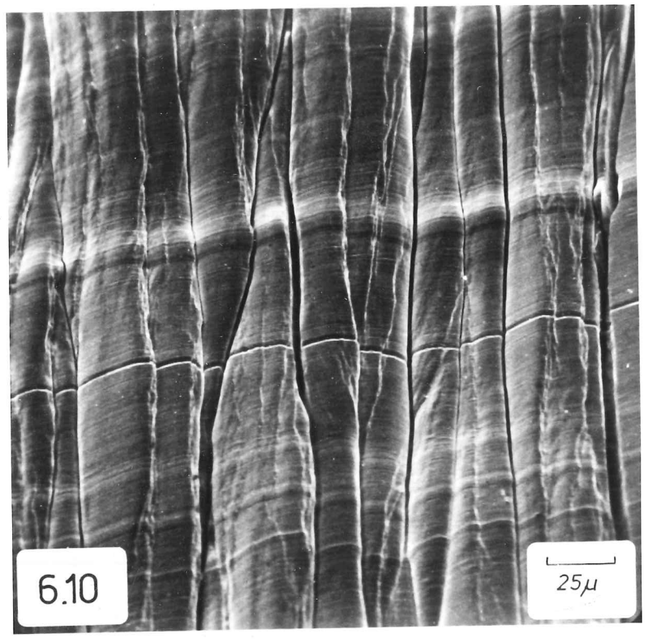

Figure 6.11 As Figure 6.9, high shear plane angle region.

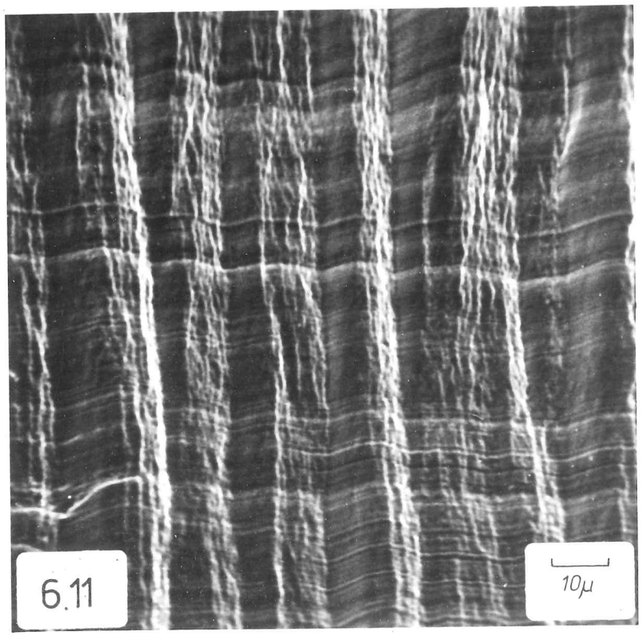

and the aluminium $\{110\}\ \langle 211\rangle$ specimens, the shear plane angle appeared to take two approximate values, with corresponding changes in chip thickness as seen in the photograph. This "flipping" of the shear plane could occur two or three times in the course of a cut of 80 mm. In the aluminium case, this behaviour was only observed in vacuum cuts, a lower shear plane operating in air.

6.2.3 Discussion

Copper exhibits variations in resolved shear stress (RSS) with orientation, as previously described by Williams and Gane (1977). The $\{110\}\langle 100\rangle$ crystal (described by Williams and Gane as the "easy" orientation) gives a RSS value lower than the $\{110\}\langle 211\rangle$ crystal (described as "difficult"). However, the contrast is not so marked in this work, being of the order of 12% compared with 30%. The polycrystal has RSS values intermediate between the single crystals, instead of being equivalent to the "difficult" crystal as noted by Williams and Gane. The values of RSS encountered by Williams and Gane are all lower than those found in the present study. This disagreement is almost certainly due to the difference in scale between planing and microtoming experiments, in relation to dislocation structures.

The new orientations provide further evidence for the dependence of cutting stress on orientation. In the case of the $\{110\}\ \langle 110\rangle$ crystal, there appear to be two planes which are favourable for slip. The higher-angled plane operates at a RSS similar to the $\{110\}\langle 100\rangle$ and polycrystal specimens. The lower plane leads to very high cutting forces but the RSS is low. This figure, however, must be subject to a large error due to the large shear plane area and the difficulty of measuring a small shear plane angle accurately. There may also be in

this case greater departures from idealised plane shear.

It is proposed that the "flipping" behaviour is due to variations in the rake face friction. Increased resistance to chip flow would favour the operation of the lower shear plane, but should the resistance to chip movement subsequently fall - possibly because the structure resulting from the primary shearing process now makes slip along the rake face crystallographically more favourable - there is a return to the higher plane. Obviously shear planes of intermediate angle must all require greater cutting force, since they are not observed. This offers further support for the concept of "easy" shear directions.

The reversed $\{110\}\langle 211\rangle$ crystal, not used by Williams and Gane, gives the most striking demonstration of reduced RSS in favourable orientation, with a reduction of 15% over the polycrystal. Thus easier orientations may be found than $\{110\}\langle 100\rangle$. It also appears that polycrystal specimens may be expected to produce an "averaging" effect in planing experiments, rather than a tendency to reflect the most difficult orientations. This suggests that texture in copper work-pieces could well result in variations in the machining behaviour. However, "cube" texture (frequently encountered in rolling) should not be expected to produce much departure from an untextured structure.

The aluminium experiments also confirm the published work (Ramalingam and Hazra, 1973). Variations in shear plane angle are found and the flipping behaviour is again observed, although only in vacuum where the rake face drag is low. This reinforces the view that critical rake face processes might govern this behaviour. However, there is no marked dependence on orientation of the RSS values. The scatter is rather less than that seen in Ramalingam and Hazra's work.

Thus the apparent contradiction in the previously published work

on single crystal cutting appears not to be due to differences in the cutting configuration, as suggested by Williams and Gane. Real differences in behaviour between copper and aluminium are found when they are studied in identical cutting situations. Copper displays a dependence of RSS on $\{111\}$ plane orientation, aluminium does not.

This difference must relate to the processes of dislocation movement which contribute to shear on a particular shear plane. The ability of individual dislocations to glide on more than one $\{111\}$ plane, in the process known as "cross-slip", is critical in this context.

Consider the dislocation:

$$\tfrac{1}{2}\ [1\bar{1}0]\quad (111)$$

This is also free to move in $(11\bar{1})$ which is approximately 70^{o} away. However, it may dissociate into partials

$$1/6\ [1\bar{2}1]\ +\ 1/6\ [2\bar{1}\bar{1}]$$

These partials repel each other and, as they separate under the action of a diminishing repulsive force, a sheet of stacking fault is formed between them. The energy of this fault prevents them from separating and, effectively, gives them a constant attraction, leading to an equilibrium spacing. Glide of the dissociated dislocation is confined to the (111) plane, but should the partials be brought together, reducing the width of the stacking fault to zero, the dislocation may then glide in another plane. Cross-slip is therefore more unlikely as the width of the stacking fault increases.

The stacking fault energies and equilibrium spacings for copper and aluminium are given in Table 6.3 (Hirsch, 1975). It is predicted that cross-slip should occur very readily in aluminium, small local fluctuations in the stress field around a pair of partials, due to

the presence of nearby dislocations, solute particles, precipitates or grain boundaries frequently causing constriction and recombination. This would be less likely with copper and most dislocations would therefore be confined to one glide plane. (In fact, some pairs of partials in copper can also interact with one another to form "locks" e.g. the Lomer-Cottrell lock 1/6 [110] which are unable to glide at all).

TABLE 6.3 Stacking fault energies.

	Stacking fault energy (ergs cm^{-2})	Equilibrium spacing (atom distances)
Copper	55	10 - 15
Aluminium	200	2

It is proposed that the apparent conflict between the results of previous workers in this field may be the effect of stacking fault energy. The same processes of dislocation mobility that contribute to the low strength of pure aluminium cause its flow stress in machining to be substantially constant with workpiece orientation. Since dislocations are less mobile in the stronger copper, favourable orientation of a glide plane reduces the flow stress.

6.3 MAGNESIUM SINGLE CRYSTAL CUTTING

6.3.1 Experimental Details

Pure magnesium single crystal strips were prepared, 3 mm thick and initially 20 mm wide. Three specimens were made, giving four

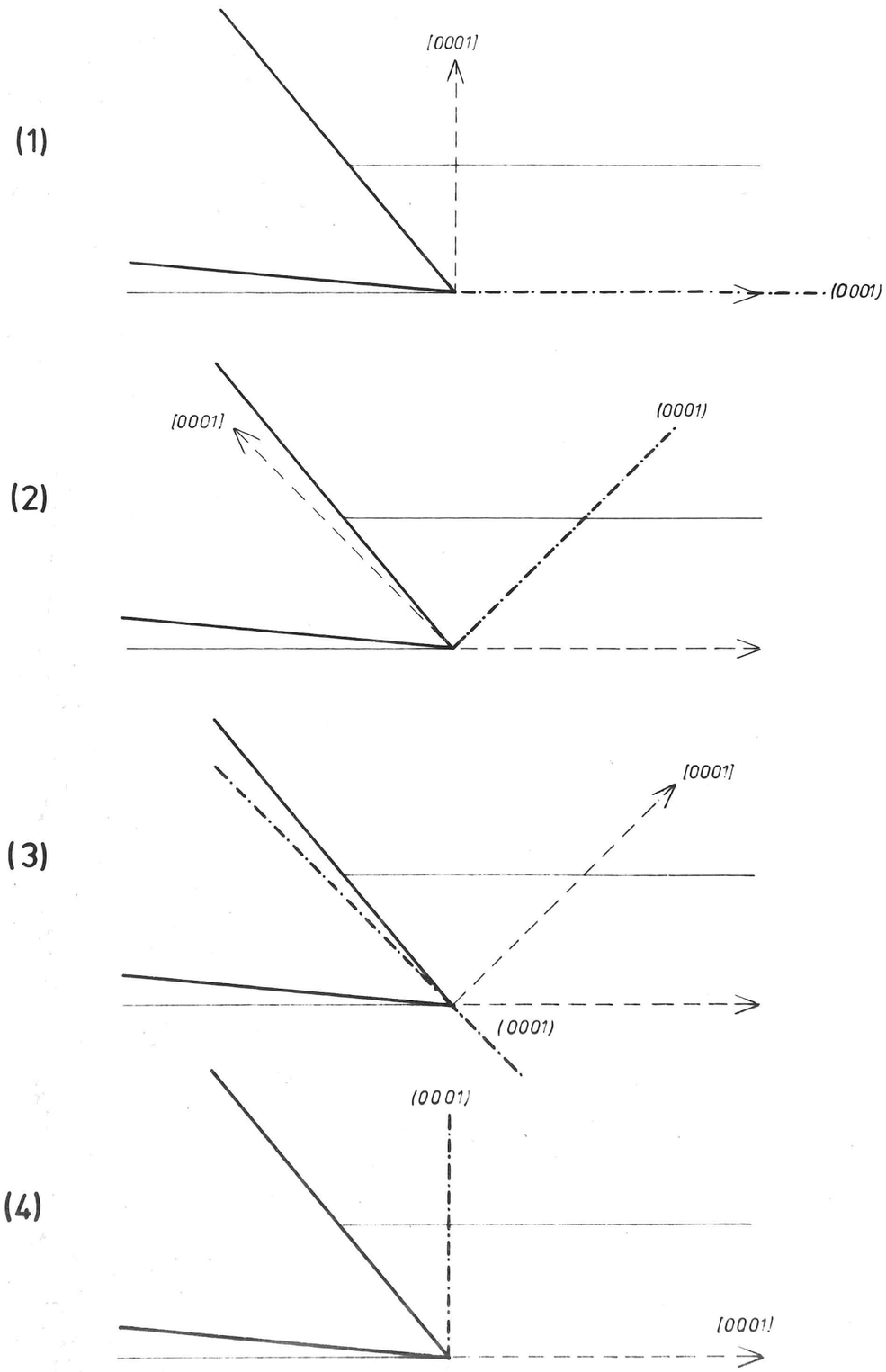

Figure 6.12 Orientation employed in studying the cutting behaviour of magnesium single crystals, showing the position of the (0001) plane.

different cutting orientations. Magnesium has a hexagonal close-packed structure; the strips had a $(10\bar{1}0)$ face. The major slip plane is (0001) perpendicular to the $[0001]$ direction and specimens with this plane parallel; perpendicular and at 45^{o} to the cutting direction were employed (Figure 6.12) together with a pure polycrystalline specimen. The rake angle was 40^{o}.

6.3.2 Results and Discussion

Not only the cutting force, but also the mode of chip formation is found to vary with the crystal orientation. A summary of the cutting behaviour is given in Table 6.4, together with the measured forces, chip geometry and resolved shear (or fracture) plane stress, all for cuts of 100 μ depth.

1. With the major slip plane coincident with the cutting direction, dislocation glide can not contribute to chip formation. Discontinuous chips are produced by fracture along the direction of maximum shear stress.

2. Plastic flow by means of dislocation glide becomes possible when the slip plane is rotated to the $\pm 45^{o}$ position. It is found that the RSS required to produce the chip is reduced by this change of mechanism. However, some fracture seems to be involved since the chip is in segmented form.

3. With the slip plane at -45^{o}, fracture along this plane results in the tool digging into the work (Figure 6.13). If allowed to continue, lumps of magnesium would be removed from the workpiece, as the restoring force on the tool arrested its movement. This observation indicates that the basal plane in magnesium can be a plane for cleavage as well as for slip.

TABLE 6.4 Cutting behaviour of magnesium single crystals

Orientation	(0001) plane angle degrees	Mode of chip formation	Tool forces		t μ	ϕ degrees	k Kgf mm^{-2}
			N Kgf	T Kgf			
1	0	Discontinuous	0.9	7.1	(120)	54	9.1
2	45	Continuous, segmented No curl	0.2	3.4	150	43	5.4
3	-45	No chip formed Digs in	-	-	-	-	-
4	90	Continuous. Tight curl	0.2	5.5	80	79	4.4
Polycrystal	varies	Discontinuous	0.6	6.6	(120)	54	9.3

Figure 6.13 Magnesium single crystal, -45° specimen; tool digs-in, no chip produced.

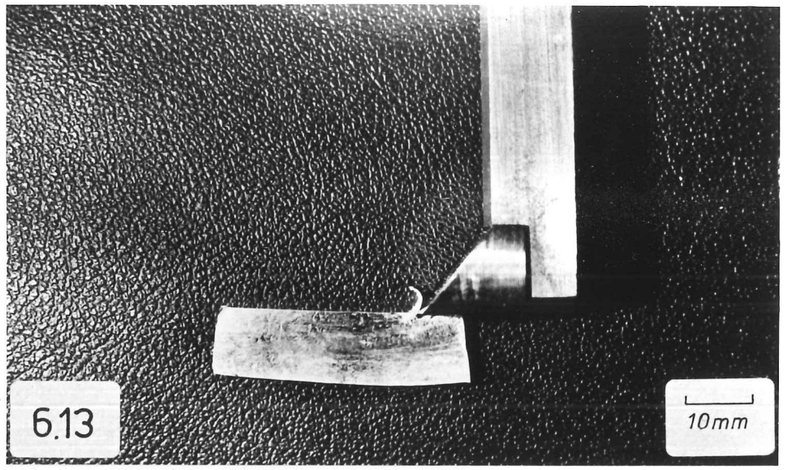

Figure 6.14 Magnesium single crystal
Left - segmented continuous chip, +45° specimen
Right - fully continuous chip, 90° specimen

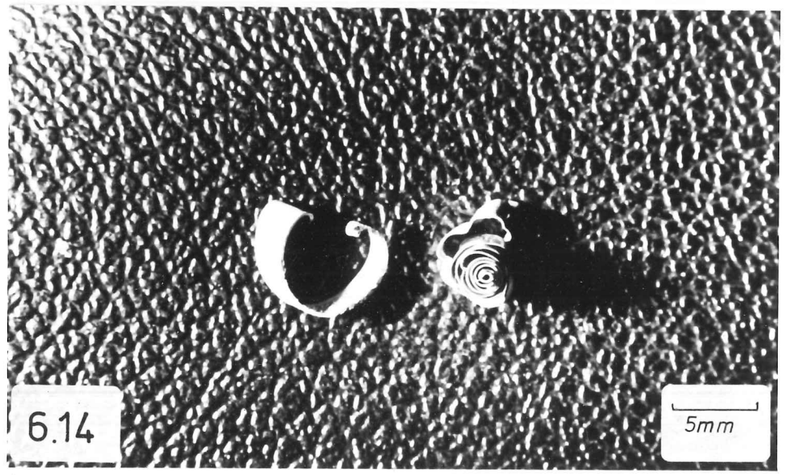

Figure 6.15 Chip from 90° specimen uncurled, showing that the chip is longer than the workpiece.

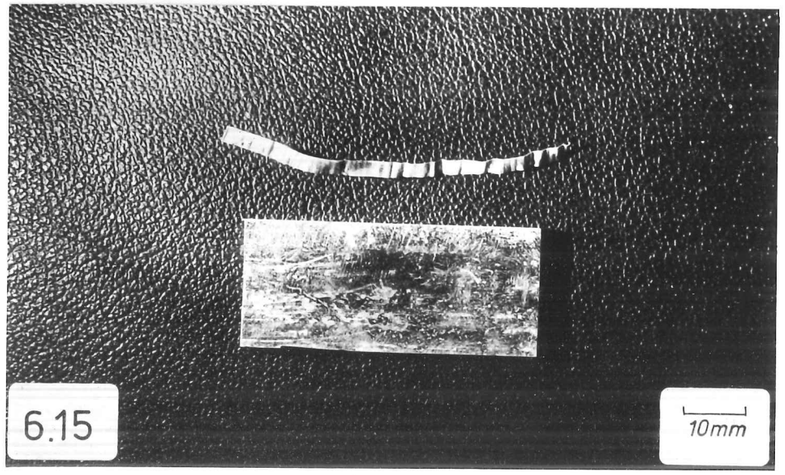

4. Finally, a vertical slip plane leads to rather surprising behaviour, with chip formation apparently fully continuous. The chip is tightly curled (Figure 6.14); when straightened-out it is found to be longer than the workpiece from which it was generated (Figure 6.15), consistent with the high shear plane angle and a cutting ratio r_c more than one. The RSS required to produce the chip is further reduced, although the measured cutting force is higher than in specimen 2.

5. The polycrystalline specimen forms chips by fracture, at a RSS comparable to specimen 1. This is because only a few grains are oriented for slip. Magnesium, therefore, owes its discontinuous machining behaviour to the singular major slip plane.

6.4 INSTABILITIES IN THE CUTTING PROCESS

Introduction

A typical lamellae structure on the free surface of a continuous chip is seen in Figure 6.16. This feature indicates that the cutting system can not be truly continuous, some cyclic process occurring at a frequency corresponding to the lamellae frequency. This could occur either by vibration of the cutting tool or because of some oscillation in the cutting process itself. The lamellae were investigated with these possibilities in mind.

6.4.1 Tool Vibrations

The possibility that tool vibration might be responsible for the lamellae was investigated in two ways: in the planing machine, by cutting at different speeds, and on a lathe, by varying the tool overhang. The results are summarized in Table 6.5.

It is clear from this data that any tool vibration connected with lamellae formation must be a forced, rather than a natural vibration. However, there are marked variations in the lamellae spacing with variations in the crystal orientation across the width of the workpiece (Figure 6.2) and no apparent correspondence between the lamellae and any features on the cut surface (Figure 6.3). Movement of the tool would be expected to produce a constant spacing across the width of the workpiece and corresponding features on the cut surface. Thus it is clear that tool movements, themselves caused by some other mechanism, do not produce the lamellae.

TABLE 6.5 Variation in lamellar spacing with cutting speed and tool overhang.

Depth of cut 100 μ. Rake angles: 40° (planing machine); 10° (lathe).

Material	Speed mm sec^{-1}	Overhang mm	Lamellar spacing μ
Lead	5		25
Lead	500		14
Pure aluminium	5		4.0
Pure aluminium	500		2.4
Mild steel	20		1.4
Mild steel	500		2.0
Copper	375	20	6.7
Copper	375	100	5.3
Mild steel	375	20	4.4
Mild steel	375	100	4.5

6.4.2 Source of the Instability

Some instability must occur in the processes of primary shear, or in the sliding of the chip against the tool, or in both. Continuous cutting has been described (von Turkovich and Black, 1970) in terms of heterogeneous plastic flow in which the shear process occurs in an

Figure 6.16 Lamellae on the free surface of a metal chip; workpiece - polycrystalline annealed copper.

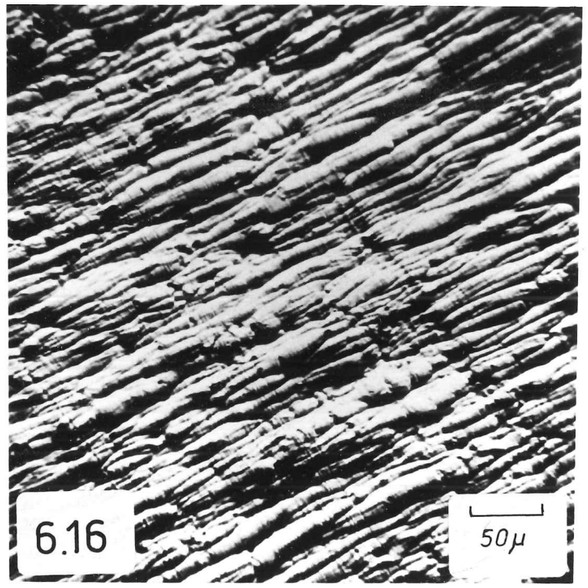

Figure 6.17 Lamellae on the free surface of a non-metal chip; workpiece - butter at a temperature of 10° C.

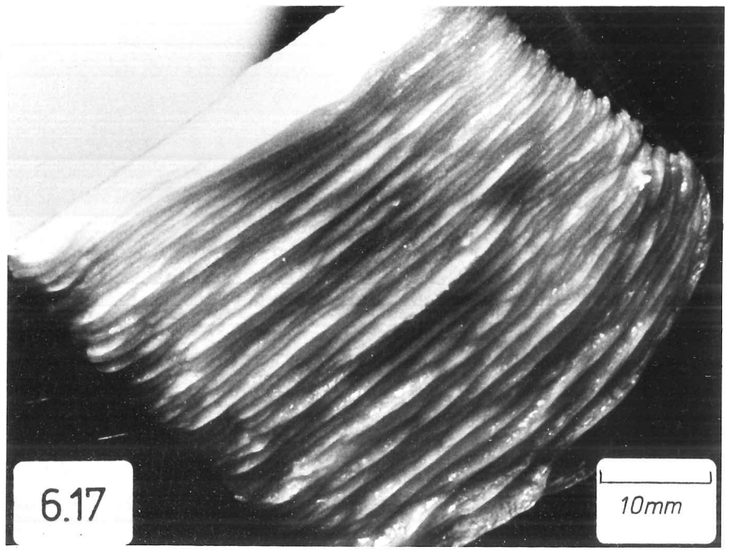

intermittent fashion, producing well-defined lamellae separated by very thin "plates"of concentrated shear (Black, 1971, 1972). These workers propose that, during the compression phase of the process, large numbers of dislocations are created at points of stress concentration. This is followed by shear in a narrow band. If the periodic structure is not generated in the workpiece prior to the instability, some periodic local fall in the material's yield stress, leading to local flow, is required. Without such a mechanism, there would be no reason for shear to be concentrated in bands. Von Turkovich (1970) postulates the adiabatic generation of heat during the compressive deformation. Once initiated, shear continues catastrophically within the shear band until the stress falls to below the flow stress at the current temperature, when the cycle recommences.

Evidence for adiabatic shear, in the form of "white layers" on the shear plane in etched steel workpieces, has been offered (Recht, 1964; Lemaire and Backofen, 1972) but is held to be ambiguous (Doyle and Samuels, 1976). Further, lamellae are produced even at the slowest possible cutting speeds and at similar spacings to those in fast cuts.

It is worth noting, in passing, that non-crystalline materials which can be machined to form continuous chips also display lamellae (Figure 6.17). In these cases it seems likely that a "stick-slip" movement of material up to the rake face is occurring. This approach has been adopted for metals (Rubenstein, 1974). However, the indentation-release cycle described by Rubenstein incorporates cyclic deflection of the tool. It is proposed here that the actual mechanism of sliding of the chip against the rake face should also be considered as a possible source of the cycle.

6.4.3 Direct Observations of Lamellae

Investigations into the lamellae process were conducted by means of high-speed photography. High speed cine films were made with the transparent tool, cutting pure aluminium and lead. A framing speed of 1000 pps and cutting speed of 5 mm sec^{-1} gives several frames per lamella.

No new features of the chip-tool contact were revealed by this method. The appearance of zone 1, seen through the tool, was unaltered during the time scale of the production of a single lamella.

The outer surfaces of the chip and workpiece during cutting were studied using the arrangement seen in Figure 6.18. The formation of individual lamellae was observed to occur by bulging of workpiece material ahead of the tool, followed by a "release" which began another bulging operation. During this event, the chip was sliding continuously up the rake face (Figure 6.19).

6.4.4 Discussion

It appears from these observations that the lamellae are the result of heterogeneous plastic flow in the primary shear zone, rather than heterogeneous sliding up the rake face, since chip/tool sliding is continuous. However, the adiabatic shear concept is not the only description which could satisfactorily explain these features. Some further speculations on the mechanism of lamellae production are made in section 6.5.2.

Figure 6.18 Arrangement used for high-speed filming of the outer surfaces of the chip and workpiece during the cut.

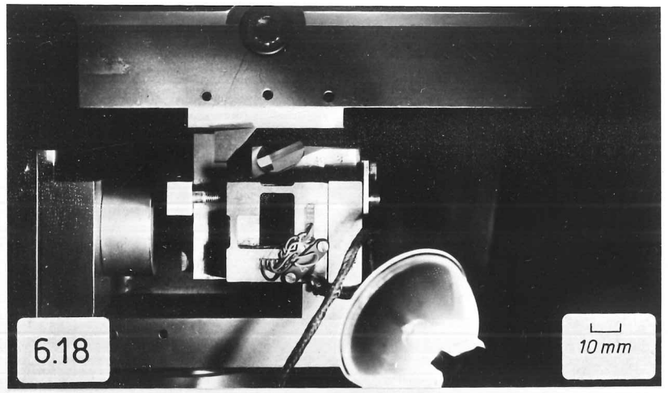

Figure 6.19 Sequence of stills taken from the high-speed film. Workpiece - aluminium. A line has been scribed across the workpiece to facilitate interpretation of the photographs; in the original film, the individual lamellae may be distinguished.

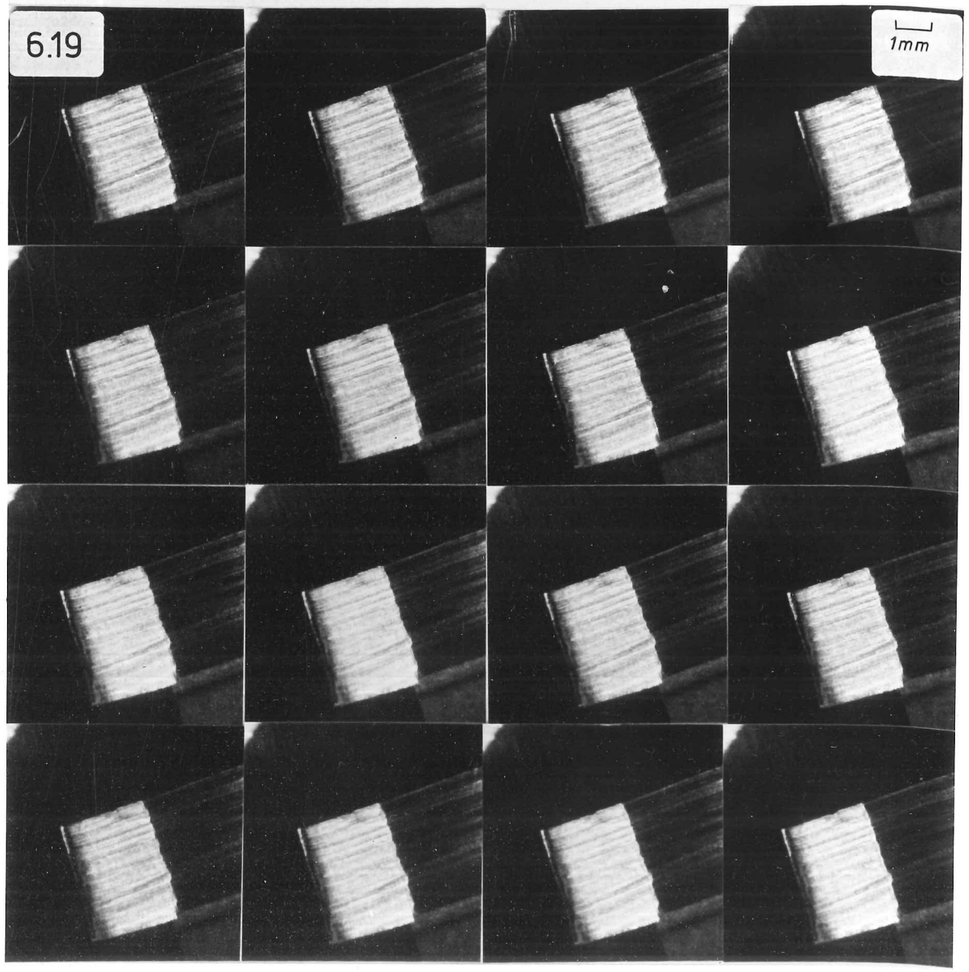

Figure 6.18 Arrangement used for high-speed filming of the outer surfaces of the chip and workpiece during the cut.

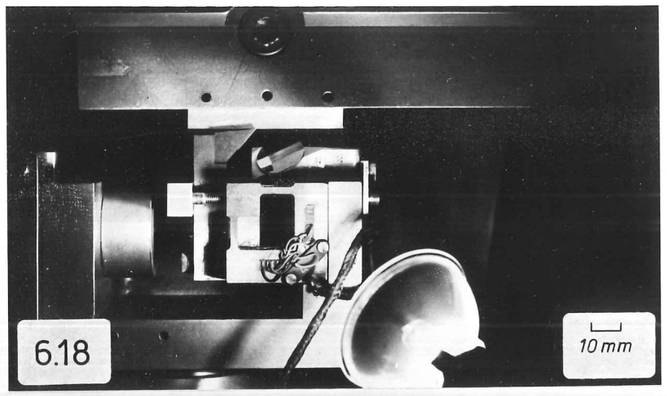

Figure 6.19 Sequence of stills taken from the high-speed film. Workpiece - aluminium. A line has been scribed across the workpiece to facilitate interpretation of the photographs; in the original film, the individual lamellae may be distinguished.

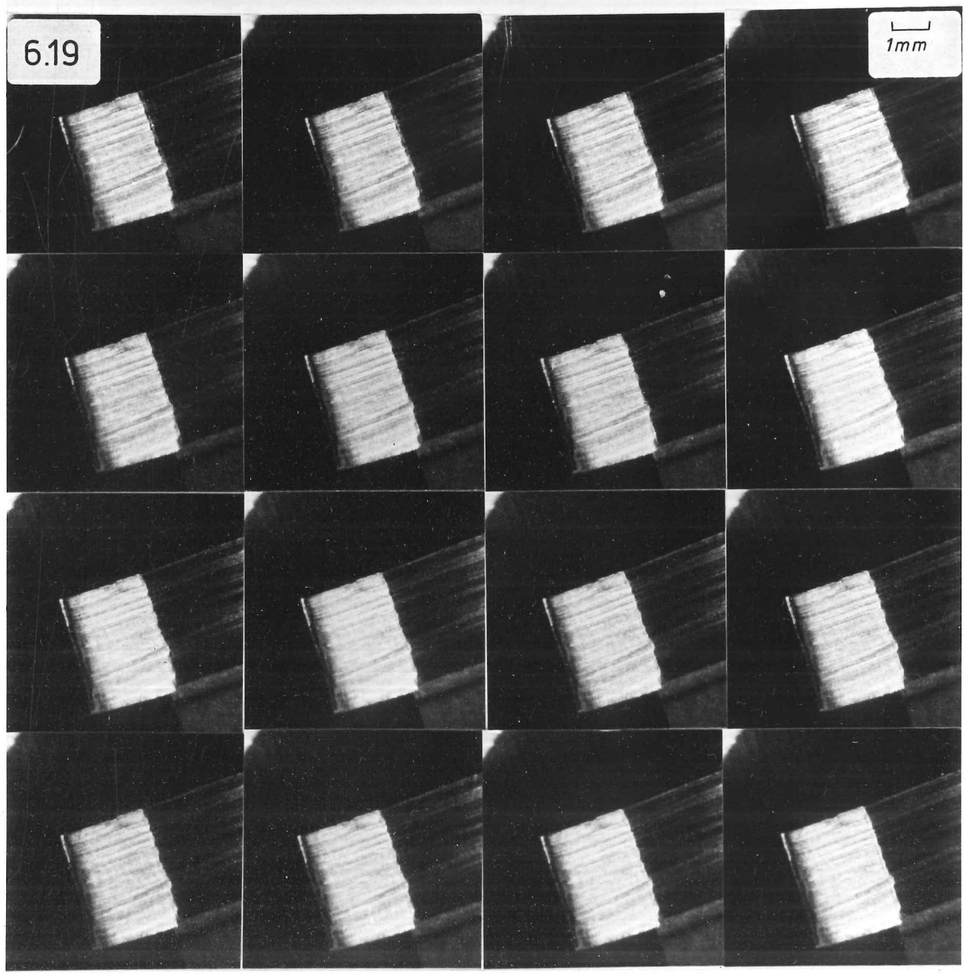

6.5 CHIP CURL

6.5.1 Initial and Equilibrium Curl

The observation was made in Chapter 4 that the curvature of the chip in continuous cutting is tightest at the start of the cut, the chip straightening-out as the contact area on the rake face grows to an equilibrium value. An increase of resistance on the rake face, for example when machining with oxide tools in air rather than vacuum, leads to a further increase in the chip radius, producing almost straight chips with small rake-angle tools. Conversely, the appearance of a built-up-edge (Chapter 5) increasing the rake angle and hence the shear plane angle, or lubricated conditions (Chapter 7) tend to reduce the chip radius.

It might be suggested that tight curl is an integral part of the primary deformation rather than the consequence of the shearing processes on the rake face. The chip curvature observed under equilibrium conditions is always less pronounced than the natural curl, because of the retarding effect of rake face interactions.

The sequence in Figure 6.20 shows the first few millimetres of a cut of 200 μ made on lead with the sapphire tool. It illustrates that the chip curl occurs before the full zone 1 contact has been established and even before the tool has indented to the full depth of cut, i.e. before establishment of the full length of zone 1a. This effect is shown schematically in Figure 6.21. The radius is constant during the development of zone 1a contact, but once zone 1b contact starts to develop, there is an increase in the curl radius. (This observation offers further support for the proposal that the chip/tool interaction in zone 1a does not involve severe rubbing contact).

Figure 6.20 Transparent tool; first few millimetres of a cut made on lead, showing the rake face contact conditions during initial curl.

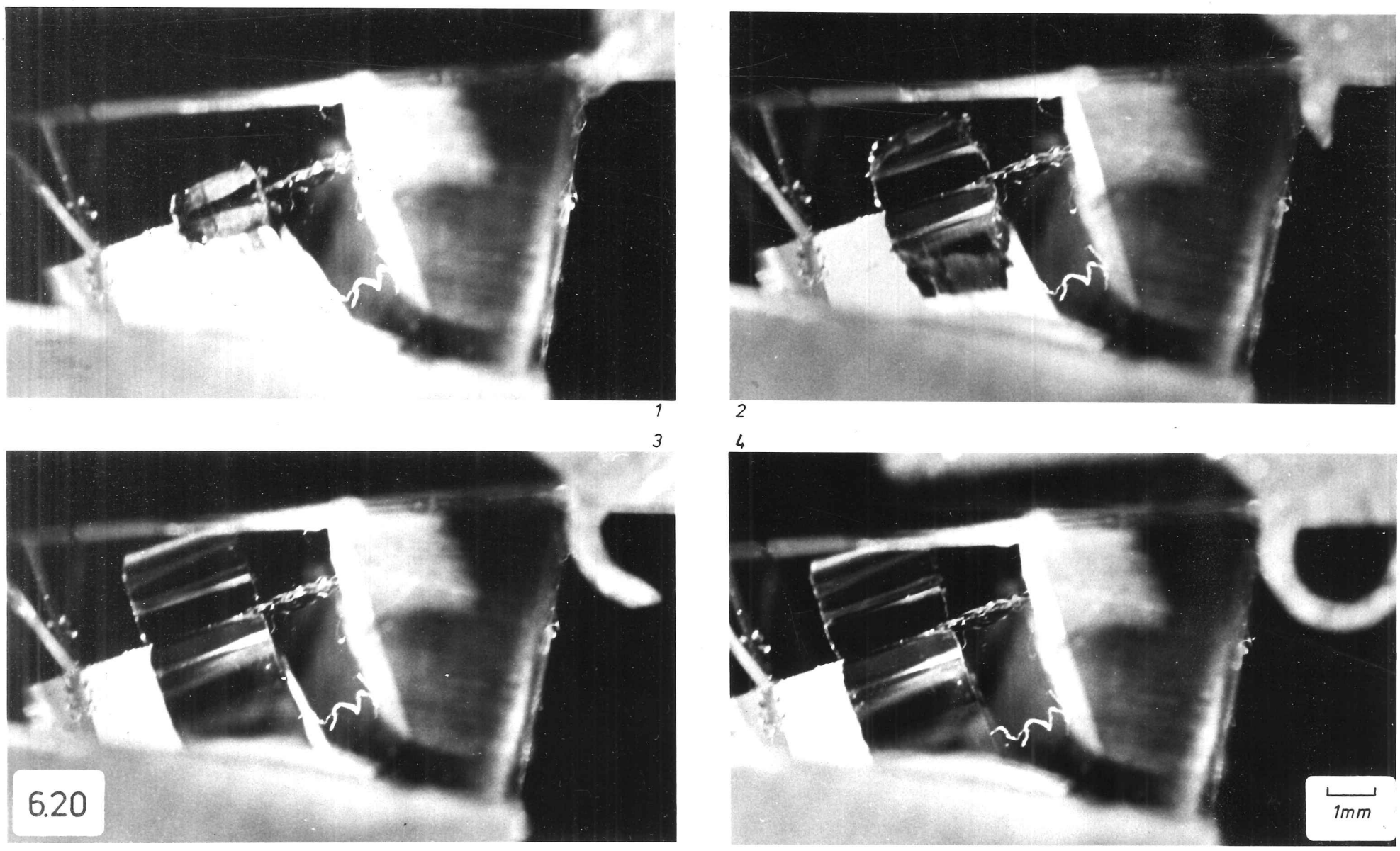

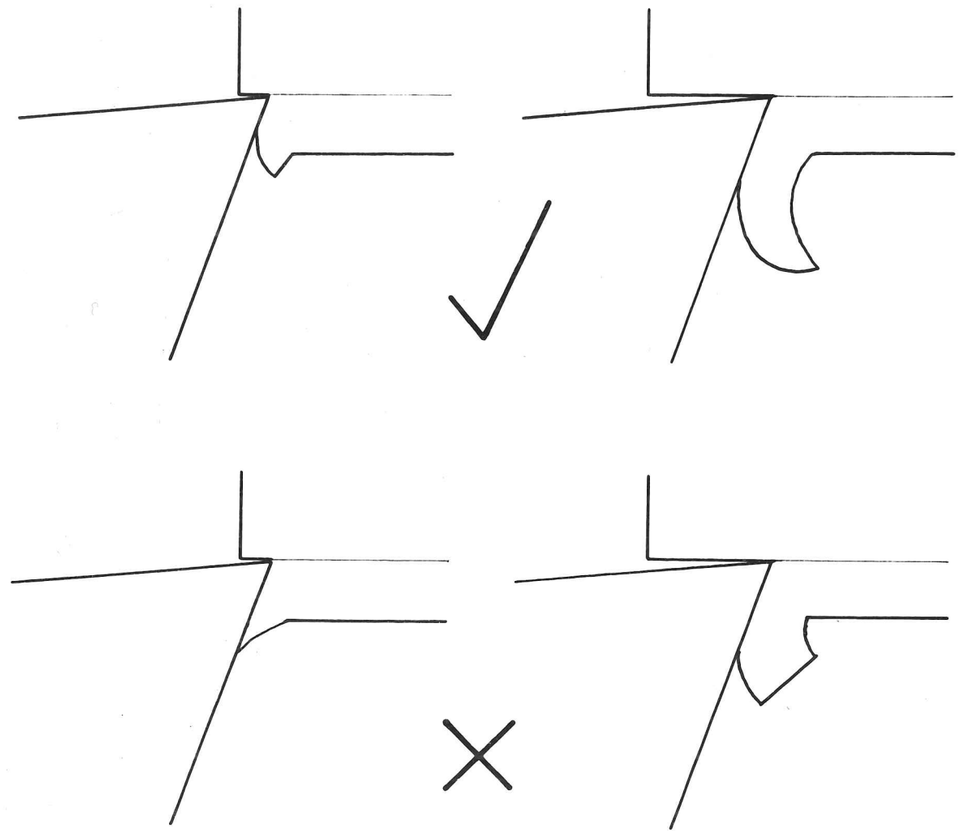

6.21

Figure 6.21 Diagram to facilitate interpretation of Figure 6.20.

6.5.2 Natural Curl

It appears, from observations of initial chip curl in continuous cutting, that natural curl is quite tight, with a radius of curvature of about 20 times the depth of cut. Residual elastic strains in a finished straight chip, as seen in Figure 6.22, would yield a minimum chip radius of perhaps 1000 times the depth of cut. There is therefore substantially more material in the tool side of the chip than in the free-surface side. Starting from the unmachined strip of workpiece, this implies large differences in the strains introduced on the shear plane at the tool tip and at the free surface. Considerations of stress equilibrium on a straight shear plane (Figure 2.1) require homogeneous strains in the chip and hence lead to straight chip geometry. Curly chip formation has consequently been described in terms of curved shear surfaces (Kudo, 1965; Dewhurst, 1978). However, in such models, it is the stresses imposed by secondary shear that are held to be responsible for the shape of the slip line fields. This type of model does not account for the transient tight curl, nor does it dispense with the friction angle to characterize the rake face contact zone.

A new model is presented, which considers chip curl in the light of the heterogeneous nature of continuous chip formation. As indicated in section 6.4, the chip is usually considered to form by a regular series of discrete shear events, giving a straight chip made up of small parallel segments (Figure 6.23 (a)). In this picture, however, no account is taken of the workpiece material that moves "past" the tool between shear events (the shaded triangle in Figure 6.23 (b)). In the treatment that follows, the chip curl is the consequence of this "missing" material.

The material is pushed ahead of the tool between shear events in

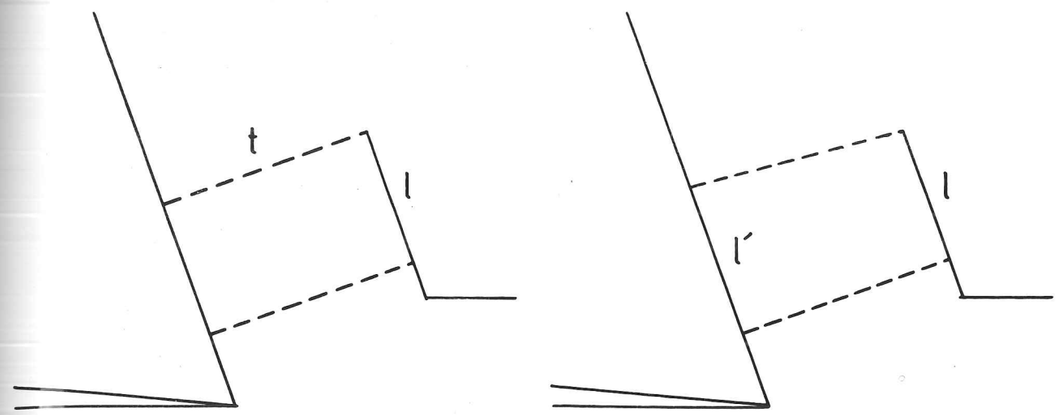

$$l' = l(1 + \varepsilon_{elastic})$$

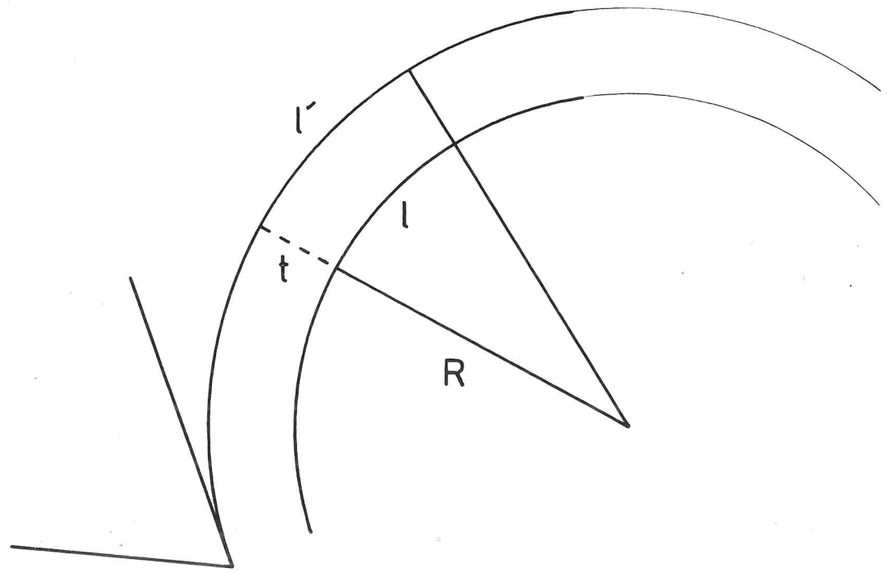

$$\frac{R+t}{R} = \frac{l'}{l} = 1 + \varepsilon_{el}$$

$$R = \frac{t}{\varepsilon_{el}}$$

6.22

Figure 6.22 Calculation of the chip curl radius resulting from the release of elastic strain in an initially straight chip.

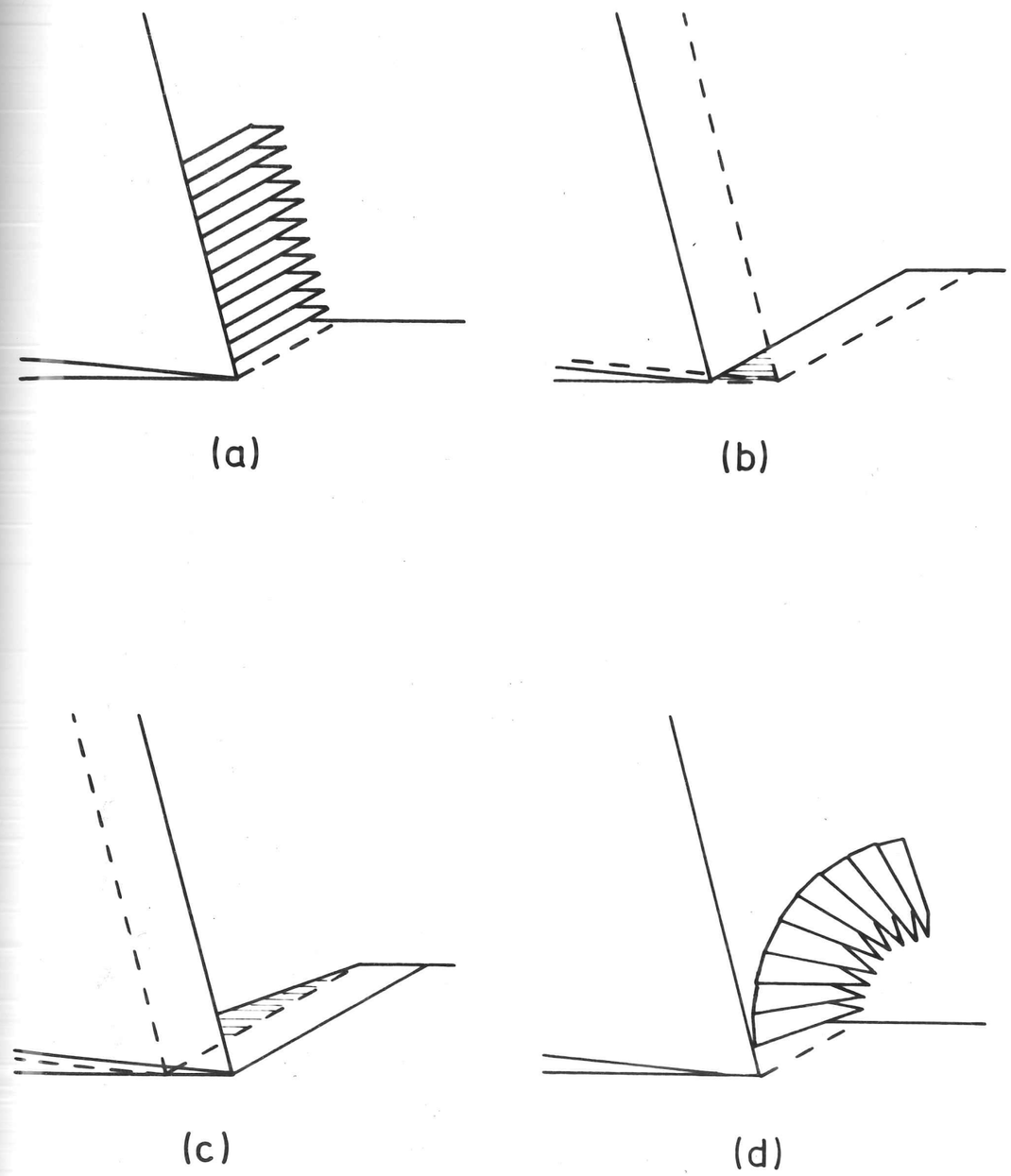

Figure 6.23 Instabilities in the cutting process giving curl of the chip

(a) simple representation of the mechanism of lamellae formation

(b) "missing" material that moves past the tool between shear events (shaded portion)

(c) material pushed ahead of the tool, showing the area equivalent to the shaded portion in (b)

(d) chip curl resulting from the modified shape of the chip segment.

a "bulging" operation, modifying the shape of the chip segment. This is idealised in Figure 6.23(c), with the new material forming the shaded triangle "above" the shear plane. In reality, of course, it is pushed into the segment from the base. If it is assumed that no material "escapes" under the tip of the tool, the areas of the shaded triangles in Figures 6.23(b) and (c) will be equal. The chip now curls away from the rake face as seen in Figure 6.23(d), since each element contains a small wedge angle. It is a matter of simple geometry to derive an expression for the radius.

Referring to Figure 6.24: during one complete cycle, the tool moves forward from point A to point D. The operative shear plane, AC, rotates to HC during the indentation, as material from the triangle ABD is pushed into the segment. At point D, shear along DF commences and the segment DHCF is complete. HC and DF meet at R, the centre of the chip segment circle. Since the angle HRD is small, RD may be taken as the chip radius. Triangles ABD and HBC are equal in area.

Depth of cut FG = d

Interlamellar spacing CE = BD = s

Chip thickness (between lamellae) TC = t

Rake angle SBD = α

Shear angle BAD = ϕ

Angle HCT = θ

Chip radius RD = r

Figure 6.24 Geometry of the curly chip segment.

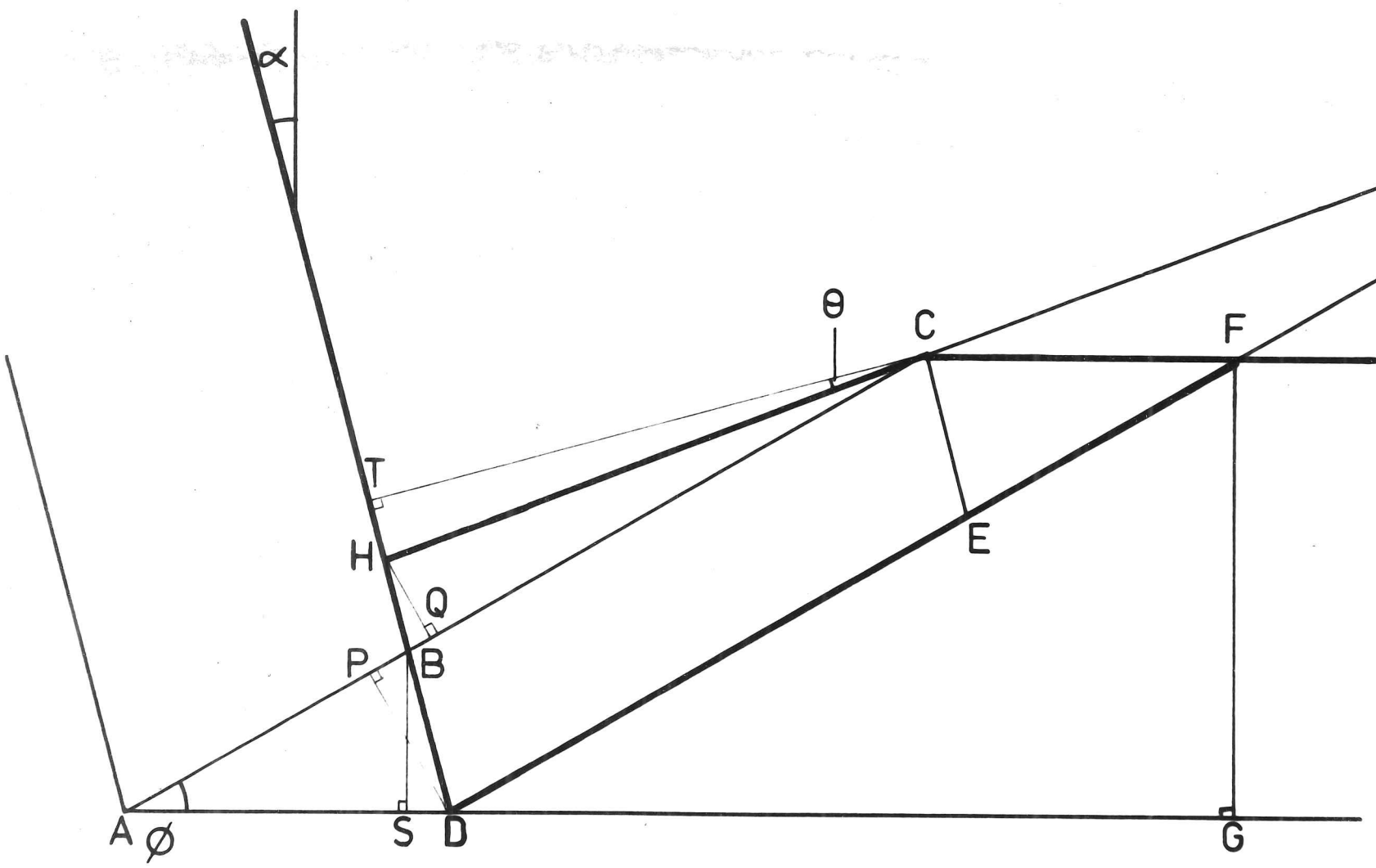

6.24

Calculation of r :-

$$\underline{DP = s \cos (\phi - \alpha)}$$

$$BS = s \cos \alpha ; \qquad AB = \frac{BS}{\sin \phi}$$

$$\underline{AB = \frac{s \cos \alpha}{\sin \phi}}$$

$$AC = DF = \frac{d}{\sin \phi}$$

$$BC = AC - AB = \frac{d}{\sin \phi} - \frac{s \cos \alpha}{\sin \phi}$$

$$\underline{BC = \frac{(d - s \cos \alpha)}{\sin \phi}}$$

Areas of $\triangle$'s ABD and HBC are equal

$$AB \cdot DP = BC \cdot HQ$$

$$HQ = \frac{AB \cdot DP}{BC} = \frac{s \cos \alpha}{\sin \phi} \cdot s \cos (\phi - \alpha) \cdot \frac{\sin \phi}{(d - s \cos \alpha)}$$

$$\underline{HQ = \frac{s^2 \cos \alpha \cos (\phi - \alpha)}{(d - s \cos \alpha)}}$$

$$HB = \frac{HQ}{\cos (\phi - \alpha)} = \frac{s^2 \cos \alpha}{(d - s \cos \alpha)}$$

$$HD = HB + BD = \frac{s^2 \cos \alpha}{(d - s \cos \alpha)} + s$$

$$\underline{HD = \frac{sd}{(d - s \cos \alpha)}}$$

$$HC = \frac{TC}{\cos \theta} = \frac{t}{\cos \theta}$$

$$\underline{\sin HRD} = \sin HCB = \frac{HQ}{HC} = \underline{\frac{s^2 \cos \alpha \cos (\phi - \alpha) \cos \theta}{t(d - s \cos \alpha)}}$$

$$\underline{\sin DHR} = \sin THC = \underline{\cos \theta}$$

Using the sine rule in triangle HRD

$$\frac{RD}{\sin DHR} = \frac{HD}{\sin HRD}$$

$$RD = r = HD \frac{\sin DHR}{\sin HRD} = \frac{sd}{(d - s\cos\alpha)} \cdot \frac{\cos\theta \cdot t(d - s\cos\alpha)}{s^2 \cos\alpha \cos(\phi - \alpha)\cos\theta}$$

$$r = \frac{dt}{s\cos\alpha\cos(\phi - \alpha)}$$

If the lamellar width s is small compared with the chip thickness, we can use the expression for continuous cutting

$$\frac{d}{t} = \frac{\sin\phi}{\cos(\phi - \alpha)} \qquad \text{(See Chapter 2)}$$

to derive

$$\frac{t}{\cos(\phi - \alpha)} = \frac{d}{\sin\phi}$$

$$r = \frac{d^2}{s\cos\alpha\sin\phi}$$

This is the expression for natural curl. It will be noted that it still predicts a positive chip radius at negative rake angles.

It is considered that the approximations made in this calculation are insignificant in comparison with those arising from the use of a single shear plane. One point that merits further discussion is the assumption that none of the "missing" material passes under the tool. The suggestion that forced tool vibrations, occurring due to stick-slip processes on the rake face, account for the appearance of lamellae on the free surface of the chip has been discussed in section 6.4.1 and discounted on the basis of several pieces of evidence. Consequently, any regular event involving

the passage of material under the tool bears no relation to the process being considered in this model, and "tool chatter" may be disregarded.

Cuts were made on several materials in order to compare predicted radii with measured values. The results are summarized in Table 6.6. Considering the approximations, this agreement is remarkably good and indicates that the tight chip curl that occurs prior to any significant frictional interactions on the rake face may well arise from the proposed mechanism.

If this description of natural curl is correct, it offers a new interpretation of the lamellar structure on the free surface of the chip and of the microscopic processes accounting for continuous chip formation. Referring again to Figure 6.24: as the tool moves from A towards D and the shear plane rotates from AC towards HC, the amount of material being pushed into the segment ahead of the tool progressively increases. When the energy required to push more material into the segment (along HD) and also maintain shear along HC exceeds that required to shear along DF, the cycle starts again.

6.5.3 Ultra-tight Curl

In the observations made on continuous cutting behaviour without lubricant, the initial tight curl was usually followed within a few centimetres of cutting by a marked increase in the chip radius, associated with rubbing contact between the chip and the rake face beyond zone 1a (see Chapter 4). However, when there was effective lubrication of zone 1b (see Chapter 7) the radius continued to be close to that of natural curl.

When cutting some materials in vacuum, extremely tight chip curl

TABLE 6.6 Calculated natural curl radii compared with measured radii.

Material	Rake Angle	Shear Angle	Depth of cut (μ)	Mean Lamellar Spacing (μ)	Calculated Curl (mm)	Observed Initial Curl (mm)
Commercial Lead	40°	23°	110	14	2.9	4.0
as above	10°	18°	110	18	2.2	2.5
as above	-10°	12°	100	19	2.6	2.5
Pure Aluminium	40°	37°	120	4.0	7.8	7.0
Pure Copper	40°	26°	50	4.6	1.6	1.0
Mild Steel	40°	45°	50	1.9	2.4	1.5

Figure 6.25 Normal chip form, produced when lead is machined in vacuum.

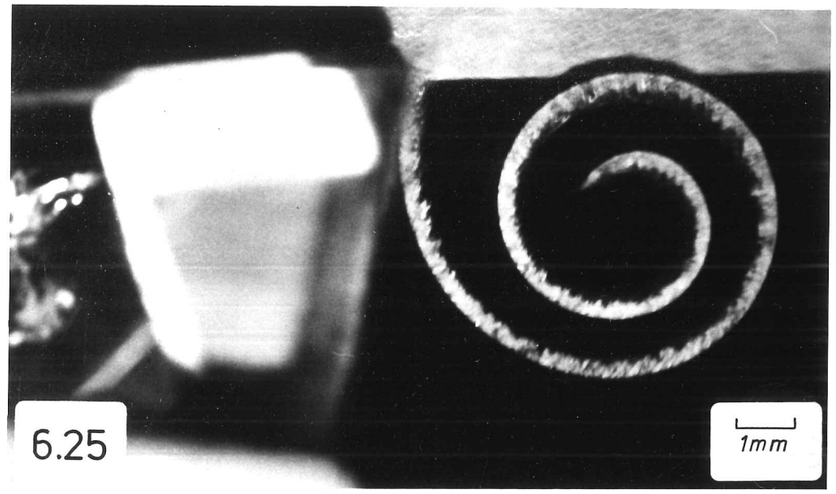

Figure 6.26 Ultra-tight chip curl, experienced when lead is re-cut, i.e. immediately after a previous cut, in vacuum.

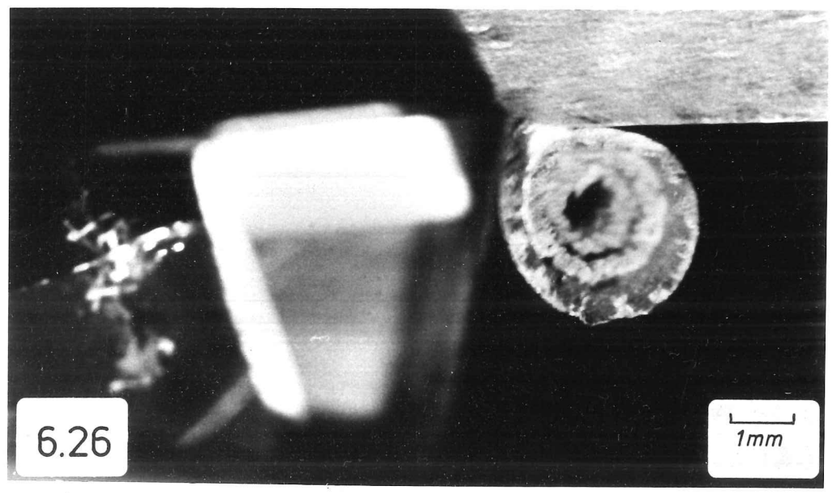

was experienced throughout the cut. This effect, previously reported by Williams (1975) in the case of lead, was investigated further.

The first of a series of cuts on lead workpieces in vacuum always exhibited the pattern of tight, initial curl followed by an increase in the chip radius. This is described in section 4.12 and is seen in cine Sequence 3. Subsequent cuts, however, frequently gave a tightly-curled chip which it was impossible subsequently to unravel. These chip forms are shown in Figures 6.25 and 6.26. It was observed that a delay between cuts resulted in a return to the large radius behaviour. The duration of the required delay was found to be related to the oxygen pressure in the chamber, Figure 6.27.

To determine whether or not some contamination of the tool between cuts accounted for this behaviour, the special workpiece of Figure 6.28 was employed. This introduced an interruption of the cut, in which the chip fell away from the tool and a "new" cut was made immediately on the second half of the workpiece. It was found that the machining behaviour of the two halves of this interrupted workpiece was always identical, i.e. after a delay, both gave large-radius, while immediate re-cutting produced ultra-tight curl from both.

This indicates that the important effect of the delay is the degree of oxygen access to the cut surface of the workpiece. The chip curls over and the underside touches the previously cut surface ahead of the tool (Figure 6.29). If the oxide layer here is not too thick, the surfaces "bond together" and the chip rolls up ahead of the tool. If there is a thick enough layer of oxide on the surface, there is no tendency for bonding to occur, so the usual increase in chip radius is able to proceed.

Figure 6.27 Graph showing the delay between cuts needed to eliminate ultra-tight curl, plotted against the chamber pressure.

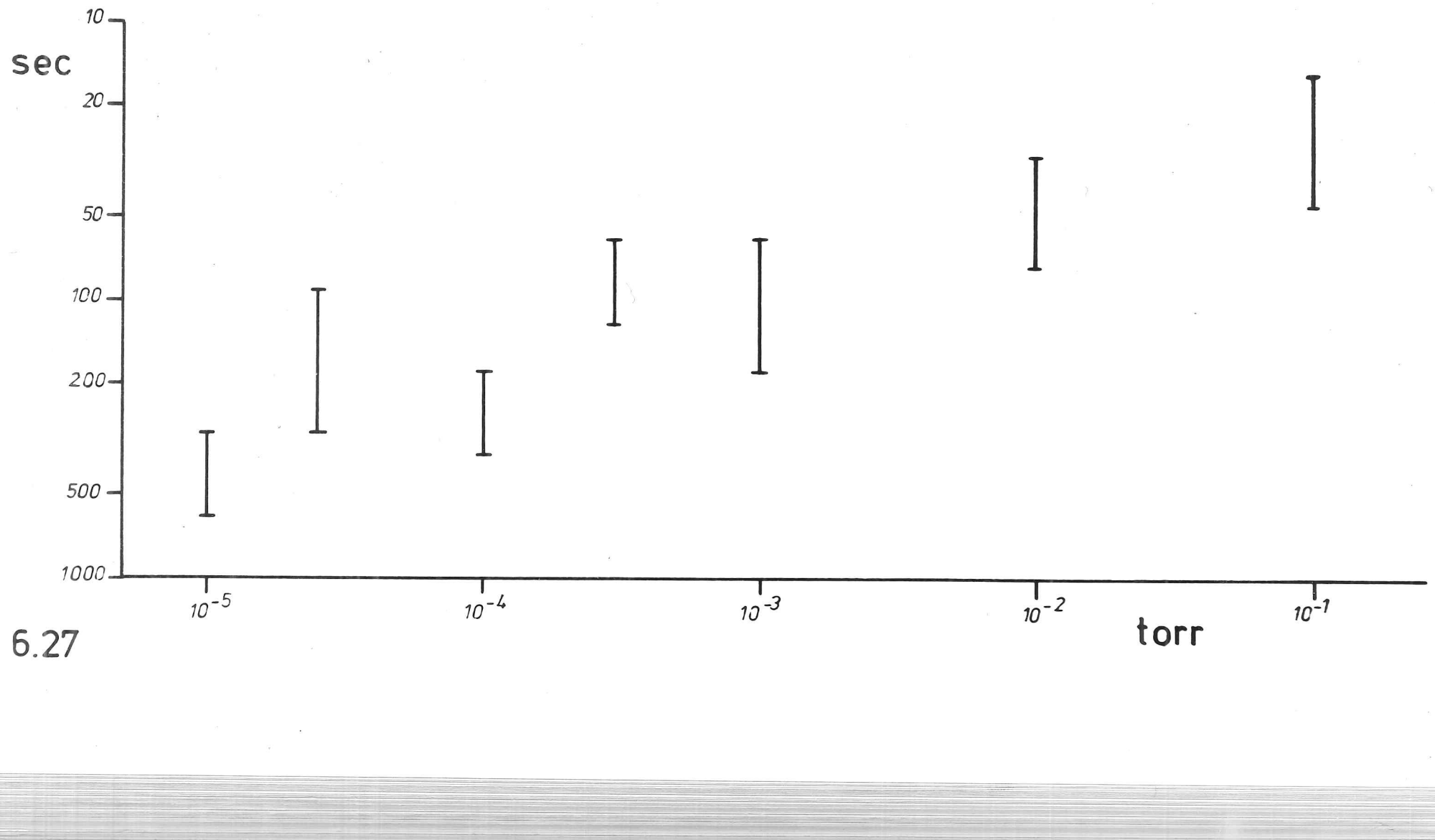

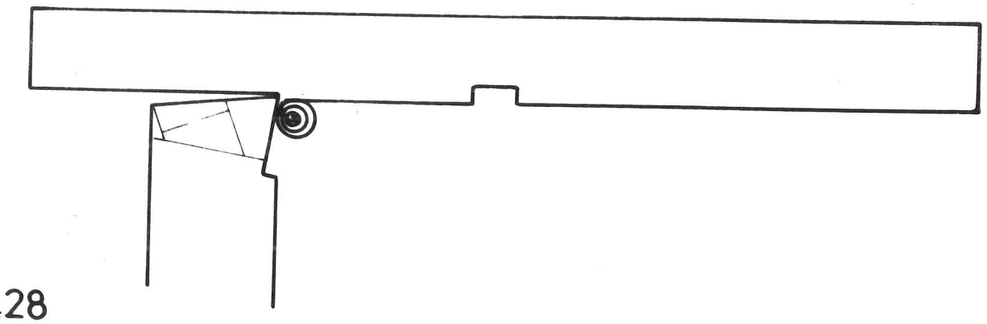

6.28

Figure 6.28 Special workpiece used to demonstrate that the condition of the workpiece, rather than the tool, determines whether ultra-tight curl shall occur.

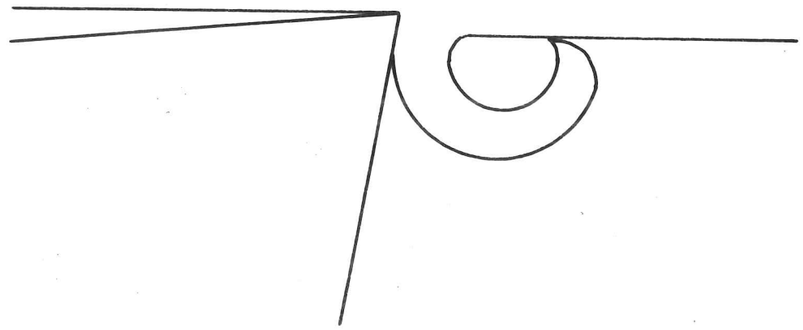

6.29

Figure 6.29 Chip curls over and touches the workpiece during the initial stage of cutting.

It is reasonable to assume that, at the pressures in use, the underside of the chip (and the cut surface in rapid re-cut experiments) will be covered by at least a monolayer of oxide. Thus it is rather thicker oxide layers on the cut surface that inhibit the bonding. It is suggested that thinner layers of oxide are readily disrupted allowing metal/metal bonding to occur. Indeed unpublished work in micro-adhesion studies (Pethica, 1978) strongly supports this view. With thicker oxide on the cut surface, only the near monolayer on the chip would be disrupted, giving metal / oxide contact.

Indium workpieces give ultra-tight curl when cut in air if re-cut immediately, but a delay of a few minutes eliminates the effect. This may reflect both the greater ductility of the metal and its lower rate of oxide formation. Aluminium, on the other hand, can not be made to exhibit the ultra-tight curl effect at the lowest oxygen pressures that can be achieved in the apparatus.

This mechanism offers further support for the proposal that metals do not adhere readily to oxides (even to their own oxides). The establishment over large areas of metal/metal contact is necessary for two metal surfaces to bond together. (As we have seen in Chapter 4, oxide/oxide contact also greatly increases the adhesion, but the mechanical integrity of the bond is low due to the brittleness of the oxide film, and also perhaps the poor oxide/metal bond beneath).

CHAPTER SEVEN

LUBRICANTS IN METAL CUTTING

Introduction

A region of intimate contact between the chip and the tool has been identified adjacent to the cutting edge. This is considered in the next chapter. Between the end of this zone and the point at which the chip loses contact with the tool is the region in which changes in the environment may affect the chip/tool interaction, modifying the geometry and energy consumption of the chip-forming process. This is the subject of the present chapter.

7.1 LUBRICATION BY GASES AND VAPOURS

7.1.1 The Role of Oxygen

Observations of "dry" cutting behaviour described in Chapter 4 led to the suggestion that the effect of oxygen on machining is dependent on the chemical nature of the surface of the tool.

Oxide tools. Oxygen promotes the adhesion of the chip to the tool, causing transfer and the build-up of a gross deposit (zone 2). There is no tendency for chip material to adhere to the tool in vacuum cutting.

Metal tools. Oxygen reduces the extent of the sticking zone, close to but not at the cutting edge, (zone 1b) compared with vacuum cutting. Thus it acts as a lubricant.

Both these effects are most pronounced at low cutting speeds and high speed cutting in air or oxygen more closely resembles that in vacuum.

It was proposed in Chapter 4 that this behaviour is attributable to low adhesion at a metal/oxide interface compared with an oxide/oxide or a metal/metal interface. The effect has been reported elsewhere (Coffin, 1959; De Gee, 1967; Pepper, 1976, 1978). Explanations have been offered in terms of a reaction between the oxides, possibly forming a spinel-type compound (Pepper, 1976). However, recent work in quartz-metal systems points to a surface electronic mechanism (Pepper, 1978). At the time of writing, the situation is still very unclear, but low adhesion between metal/metal oxide pairs has been established in a wide range of experimental situations.

Some intriguing evidence of longer term oxide/oxide reactions at the interface is furnished by considering the ease of cleaning away the zone 2 transfer on the sapphire tool. This was performed using cotton wool, isopropyl alcohol and rouge. When performed immediately after the cut, this was accomplished with ease, but became very difficult after a delay of some hours. Aluminium deposits were then very firmly attached and had to be cut away using a new scalpel blade and the fine deposit removed by polishing. Takeyama and Ono (1968) remark that, in the Japanese work with a glass tool, it was necessary to use acid to remove the lead from the tool surface.

7.1.2 Lubrication by Vapours

Several extensive investigations have been made into the lubricating action of organic vapours (Rowe and Smart, 1965; Williams, 1975; Williams and Tabor, 1977). In the work of Williams, carbon tetrachloride vapour was introduced into the vacuum planing machine when cutting several materials with high speed steel tools. The effect was to reduce the cutting forces, compared with unlubricated cutting, except

in the case of lead, when the forces were increased. CCl_4 vapour was employed both with and without oxygen present. In the case of aluminium, the cut proceeded in a manner similar to vacuum cutting, but with a shorter chip/tool contact length and tighter chip curl. The effect of CCl_4 seemed to be to reduce the length of the region of sliding contact, (i.e. zone 1b in our notation). Childs (1972) remarks that the "elastic portion" of the contact area is greatly reduced in length when CCl_4 is employed as the cutting lubricant.

It is noted (Williams, 1975) that CCl_4 is less effective, when cutting aluminium, in the presence of oxygen. This may be explained as a "barrier" effect in much the same way as the influence of nitrogen in air, which reduces the promotion by oxygen of zone 2 transfer by restricting the access of oxygen to the fresh metal surface (see Chapter 4). In this case, however, it may be that the species are in competition and that some of the oxygen reacts with the freshly-exposed aluminium to form oxide in minute areas. These are inert to the CCl_4 and may tend to increase the adhesion of the chip to the tool. The question of chemical reactions will be discussed in a later section.

In contrast, it is found that CCl_4 vapour is more effective in the presence of oxygen than in its absence when cutting steel with high speed steel tools (Rollason, 1967). This indicates that the lubricating effects of CCl_4 and oxygen in the "metal tool" case are additive.

The action of CCl_4 has been described (Cassin and Boothroyd, 1965) as the formation of films of low shear strength in the region of sliding contact by reaction with the chip. Pepper (1976) found that exposure to chlorine reduced the adhesion of copper, nickel and iron to clean sapphire in ultra-high vacuum. The failure of CCl_4 to lubricate in the cutting of lead has been ascribed (Shaw, 1958) to the

lower reactivity of the lead or the fact that lead chloride may have a higher shear strength than lead itself.

It appears from these experiments by other workers that CCl_4 vapour is a "zone 1b lubricant", reducing the severity of sliding contact between the chip and the tool, whether metal or oxide, by the formation of weak chloride layers on the surface of the chip. Its particular effectiveness as a cutting fluid has been interpreted as due to its good penetration into this region of imperfect contact (see Chapter 2). Williams and Tabor (1977) suggest that the vapour diffuses into the contact region through a network of microcapillaries between the chip and the tool. However, it has been noted (Rowe and Smart, 1965; Williams, 1977) that the liquid is generally more effective than the vapour, indicating that the controlling factor is the supply of sufficient lubricant close to the contact region.

7.2 DIRECT OBSERVATIONS OF LIQUID LUBRICANT ACTION

7.2.1 Mechanism of Access

Lead was cut in air with the transparent tool under flood lubrication conditions using a light mineral oil. It was observed that, in the initial contact prior to any significant amount of lead transfer in zone 2, oil slowly "seeped-in" from the sides of the chip at the perimeter of zone 1. Eventually, the two oil films joined up, approximately in the middle of the chip. This sequence was repeated several times in the cutting of a 250 mm long specimen and is seen in Figure 7.1 and in Cine Sequences 22 and 23.

It appears from these observations that the liquid lubricant gains access to the rake face contact by being "sucked-in" from the

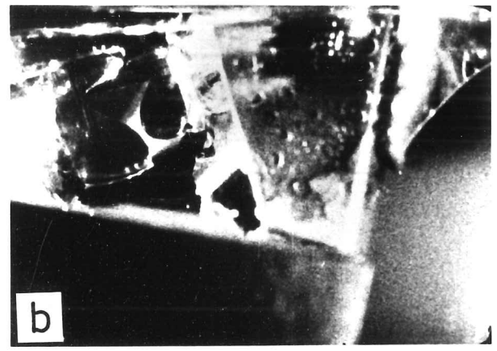

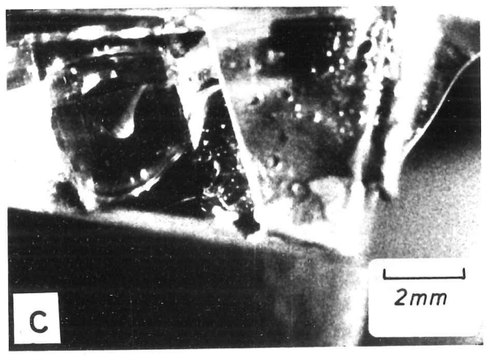

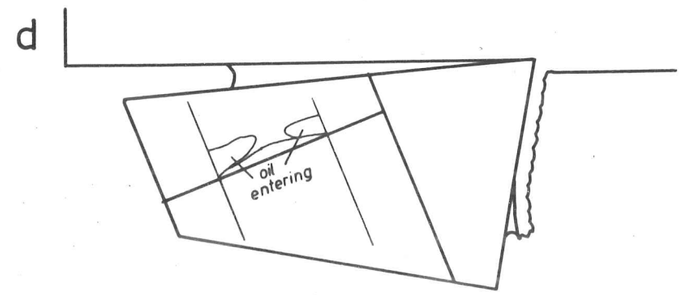

Figure 7.1 Transparent tool; lead machined in the presence of a plain mineral oil, showing liquid lubricant access to the rake face

(a) to (c) Oil films enter at the sides of the contact, joining in the middle and leaving an oil-free region at the cutting edge.

(d) Diagram to facilitate interpretation of (a) to (c).

sides to the wedge opening up between the chip and the tool, presumably due to the surface tension. Clearly the degree of penetration by this mechanism will depend on the surface energy and viscosity of the liquid. Even at the low cutting speeds employed in these experiments, there was no indication that flow of liquid against the flow of the chip might be involved.

7.2.2 Carbon Tetrachloride

Pure aluminium was machined in the presence of liquid CCl_4 using the transparent tool. Considerable numbers of bubbles were observed around both the rake and clearance faces (Figure 7.2). These were evolved continuously during the cut, as seen in the cine film (Sequence 24). It was noted that the bubbles appeared to originate at the cutting edge in the clearance face contact, while in the rake face contact there was a region close to the cutting edge in which no bubbles were seen. The clearance face bubbles also appeared to be more copious. This was confirmed by repeating the experiment with the rake face coated with an opaque (1000 Å) layer of copper, thereby modifying the double lower image and revealing only the clearance interaction, the rake face image now consisting of a featureless copper sheet. (Cine Sequence 25). It will be noted from this sequence that a few bubbles continued to be evolved at the machined surface after the cut had "run-out".

When lead was machined with liquid carbon tetrachloride present, no bubbles were seen and zone 2 transfer developed on the rake face (Cine Sequence 26).

7.2.3 Water

Distilled water was employed as the cutting fluid with the same

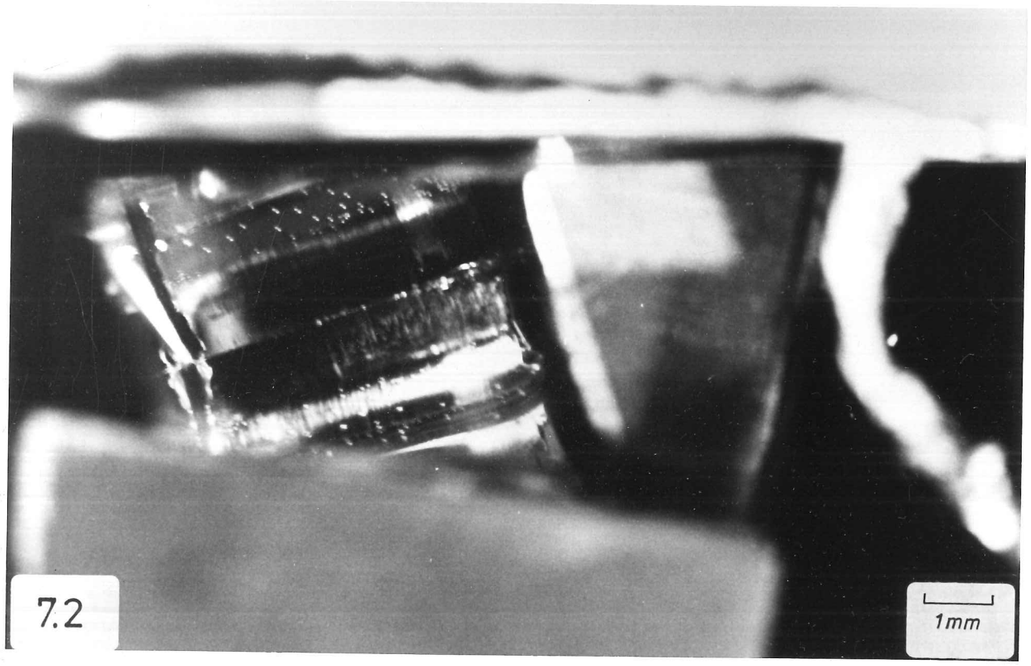

Figure 7.2 Transparent tool; pure aluminium machined in the presence of CCl_4.

materials and the lubrication behaviour was reversed. Bubbles were again observed with pure aluminium but now with severe transfer developing in zone 2 (Cine Sequence 27). The cutting forces were increased compared with cutting in air. With a lead workpiece, (Cine Sequence 28) no bubbles were observed but zone 2 transfer was eliminated and the water was as effective as oil in reducing the cutting forces relative to dry cutting in air. Indeed, it was found that, if cutting was started dry and then water introduced half way through the cut, the zone 2 build-up that had developed was "stripped-away" and the tool was left clean. This effect is seen in the film, Sequence 29. Such behaviour could not be induced in the cutting of pure aluminium using any liquid lubricant.

7.2.4 Range of Organic Liquids

To approach the question of bubble formation, a range of organic liquids was employed in cuts with pure aluminium workpieces. The liquids were de-aerated prior to use and the cuts were studied by binocular microscope. Water, acetone, three secondary alcohols and three paraffins were used. The results are summarised in Table 7.1.

7.2.5 Discussion

Carbon tetrachloride liquid behaves in a manner similar to its vapour, lubricating the cutting of pure aluminium and greatly reducing the length of zone 1b, but not lubricating the cutting of lead. Water provides an abundant supply of oxygen in aluminium cutting and promotes severe transfer in zone 2. Recent work (Doyle, 1978) using sensitive detection techniques has shown that hydrogen is evolved when pure aluminium is machined in the presence of water. With the less reactive

TABLE 7.1 Summary of observed behaviour when cutting pure aluminium with various fluids

Cutting Fluid	Cutting Behaviour	Bubbles	Boiling Point °C
Water	Severe transfer	Yes	100
Acetone	Well-lubricated	Yes	56
2-Propanol	Well-lubricated	Yes	82
2-Butanol	Well-lubricated	Yes	99.5
2-Pentanol	Well-lubricated	Yes	119
n-Pentane	Lubricated	No	36
n-Hexane	Lubricated	No	69
n-Heptane	Lubricated	No	98

lead, water behaves similarly to oil in excluding oxygen from the contact. This is noted by Shaw (1958).

Water added half-way through the cut on lead produces an unusual effect. Under these circumstances the chip appears to "cold-weld" to zone 2 deposit, breaking through the thin oxide layer and forming a strong metal/metal bond in the manner described in Chapter 4. This results in the removal of the zone 2 deposit by the chip, due to failure at the surface of the sapphire. This behaviour is only observed with lead and reflects the great ductility of the metal.

The appearance of the bubbles, while spectacular, is rather difficult to interpret. It appears that one or more of three mechanisms may be responsible, namely (a) cavitation, (b) boiling and (c) chemical reaction evolving a gas.

(a) The cavitation theory depends on the reduction in pressure in a wedge of liquid formed between two surfaces, one of which is moving relative to the bulk of the liquid, away from the apex. The observation that the same speed, configuration and liquid in the clearance wedge produces bubbles with aluminium but not with lead appears to invalidate this interpretation.

(b) It would be reasonable to suppose that the temperatures generated on the cut surface and the underside of the chip might be higher with aluminium than with lead, since its yield stress is much higher. Thus the bubbles with CCl_4 and water might be due to boiling. The use of several organic solvents appears to support this view; for example, 2-Butanol (b. pt. 99.5^{o}C) also yields bubbles. However, the range of paraffins did not produce this effect, suggesting that surface temperatures alone are not responsible.

(c) The alcohols may well react with aluminium, evolving hydrogen and producing a lubricating film. The paraffins, however, should be inert and indeed, they showed no bubble formation. Chemical reaction may thus be accepted as the source of the bubbles. CCl_4 may give rise to C_2Cl_6 as suggested by Shaw (1942) or, in the presence of oxygen, to $COCl_2$. The more copious bubbles on the clearance face may be understood in terms of the more favourable geometry for access of the liquid to the freshly generated surface. The lack of bubbles with lead indicates that any chemical reactions occurring must yield different reaction products, which are not gaseous or are soluble in CCl_4.

7.3 LUBRICANT CHEMISTRY

Introduction

Two basic categories of chip/tool interaction having emerged, it was decided to investigate fully the effect of various cutting fluids in a system of workpiece, tool materials and lubrication conditions representative of both categories. The system chosen was pure copper, cut with high speed steel (HSS) and plain carbon steel (PCS) tools. The conditions of cutting employed were: in air, in vacuum and in the presence of distilled water, plain mineral oil, chlorinated oil, sulphonated oil, a water-based surface-active synthetic (RT 105) and carbon tetrachloride. The fluids were applied in flood lubrication in atmospheric conditions.

It has already been suggested in Chapter 4 that the marked differences in behaviour when machining copper with these two tool materials are due to the removal during the cut of oxide layers from the PCS, but not from the HSS, tool. With the system chosen, it was

possible to study the effect of cutting fluids on both the zone 1b and the zone 2 interactions, without changing workpiece material.

7.3.1 Experimental

The cuts were made with 40° rake tools at a cutting speed of 20 mm sec^{-1}. At least eight and an average of ten cuts were made under each set of conditions at a nominal depth of 100 μ. The actual depth of cut taken was measured by "clocking" the cut surface. The best-fit curve was obtained, by computer analysis, between depth of cut and the readings of cutting forces, chip thickness and rake face contact length and the value at 100 μ obtained from the graph.

The results are given in Tables 7.2 and 7.3 and in Figure 7.3. (Note that the forces apply to the full 3 mm width of the workpiece). The repeatability in these experiments was always better than $\pm$5% but in view of the uncertainties regarding chip geometry measurements, errors as high as $\pm$10% might be expected in some of the data. For clarity of presentation, all the data is quoted to two significant figures.

7.3.2 Discussion

Several important points emerge from consideration of these results:

(a) With the oxide layer on the HSS tool remaining intact, adhesion and transfer of chip material to the tool does not occur in zone 1b. Zone 2 transfer is induced by the presence of oxygen. Hence vacuum cutting proceeds with lower forces than air cutting.

(b) Water acts as a source of oxygen and promotes zone 2 transfer with HSS tools. The chip/tool contact length is slightly greater than

TABLE 7.2 Lubricants in cutting of copper with high speed steel tools

Conditions	Normal load N Kgf	Tangential load T Kgf	Chip thickness t μ	Shear angle ϕ deg	Resolved shear stress k Kgf mm^{-2}	Rake force W Kgf	Rake friction F Kgf	Contact length μ	Rake pressure Kgf mm^{-2}	Rake traction K_f Kgf mm^{-2}	Rake face friction coeff. μ
AIR	5.4	35	310	18	32	23	27	320	24	28	1.14
VAC	2.6	30	270	20	31	21	21	240	30	30	1.00
WATER	5.9	36	320	17	32	24	28	340	23	27	1.16
N-OIL	2.3	27	200	29	36	19	19	230	27	27	1.00
Cl-OIL	1.6	25	210	27	33	18	17	220	28	27	0.95
S-OIL	2.0	26	230	25	32	19	18	240	26	26	0.98
RT 105	3.5	30	240	23	34	21	22	250	27	29	1.06
CCl_4	-0.6	20	150	42	34	16	12	140	38	30	0.79

TABLE 7.3 Lubricants in cutting of copper with plain carbon steel tools

Conditions	Normal load N Kgf	Tangential load T Kgf	Chip thickness t μ	Shear angle ϕ deg	Resolved shear stress k Kgf mm^{-2}	Rake force W Kgf	Rake friction F Kgf	Contact length μ	Rake pressure Kgf mm^{-2}	Rake traction K_f Kgf mm^{-2}	Rake face friction coeff. μ
AIR	14	51	410	13	34	30	43	500	20	29	1.44
VAC	33	79	600	8	35	39	76	850	15	30	1.93
WATER	12	41	340	16	33	24	35	430	19	28	1.49
N-OIL	17	52	400	13	35	29	46	560	17	27	1.59
Cl-OIL	15	51	430	12	32	29	45	490	20	30	1.52
S-OIL	20	52	410	13	34	27	49	530	17	31	1.82
RT 105	2.9	28	230	25	35	20	20	240	28	29	1.03
CCl_4	-0.5	21	170	37	35	17	13	140	40	32	0.80

TABLE 7.3 Lubricants in cutting of copper with plain carbon steel tools

Conditions	Normal load N Kgf	Tangential load T Kgf	Chip thickness t μ	Shear angle ϕ deg	Resolved shear stress k Kgf mm^{-2}	Rake force W Kgf	Rake friction F Kgf	Contact length μ	Rake pressure Kgf mm^{-2}	Rake traction K_f Kgf mm^{-2}	Rake face friction coeff. μ
AIR	14	51	410	13	34	30	43	500	20	29	1.44
VAC	33	79	600	8	35	39	76	850	15	30	1.93
WATER	12	41	340	16	33	24	35	430	19	28	1.49
N-OIL	17	52	400	13	35	29	46	560	17	27	1.59
Cl-OIL	15	51	430	12	32	29	45	490	20	30	1.52
S-OIL	20	52	410	13	34	27	49	530	17	31	1.82
RT 105	2.9	28	230	25	35	20	20	240	28	29	1.03
CCl_4	-0.5	21	170	37	35	17	13	140	40	32	0.80

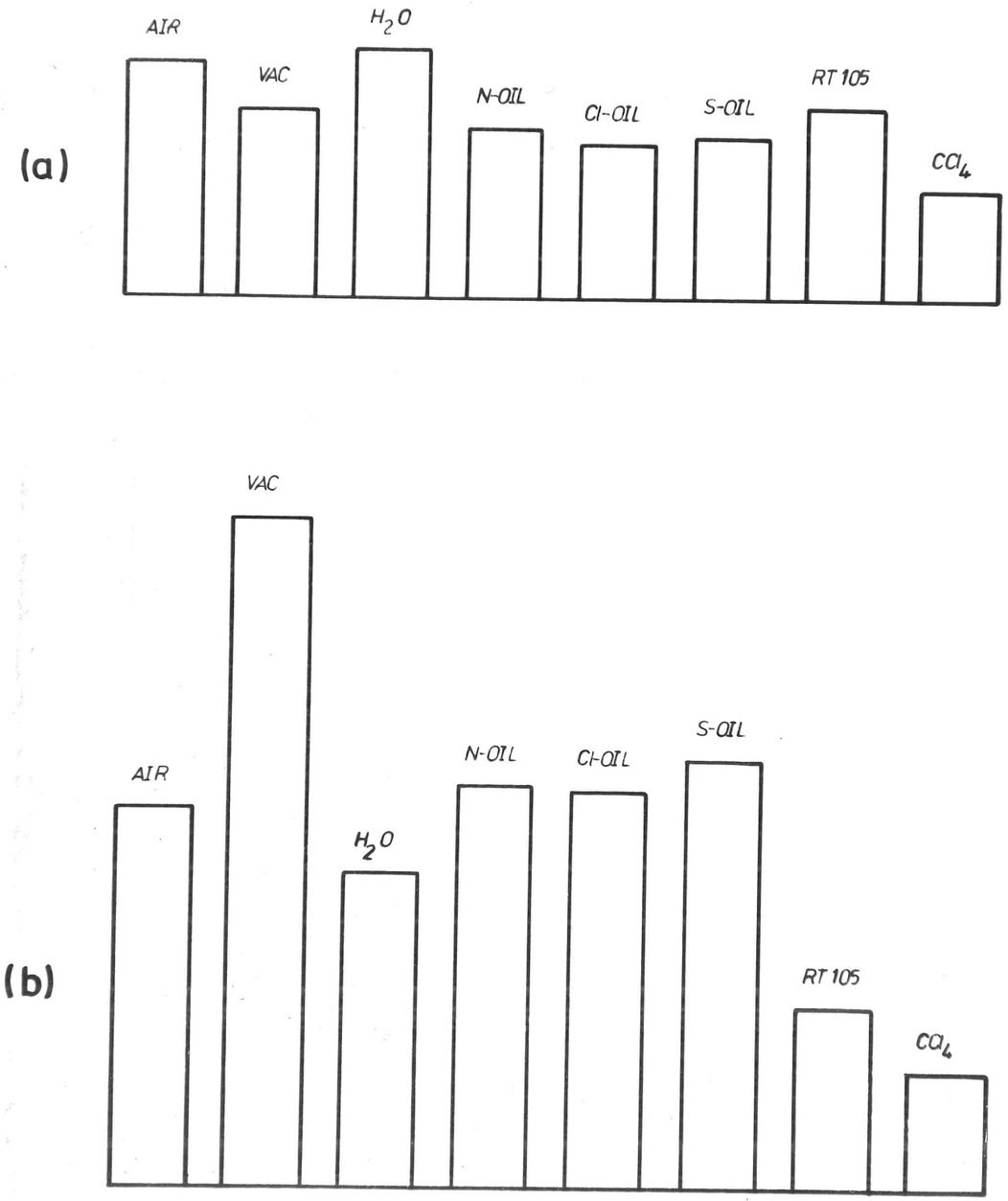

Figure 7.3 Rake face drag force, when copper is machined in the presence of various lubricants

(a) using high speed steel tools

(b) using plain carbon steel tools.

in air and there is a corresponding slight increase in the cutting force.

(c) Oil acts to exclude oxygen from the chip/tool contact and prevent the transfer of chip material to the HSS tool in zone 2. There is also evidence of a slight effect of the oil as a boundary lubricant in zone 1b, since the contact length and cutting force are slightly reduced relative to vacuum cutting. However, this effect is slight due to poor penetration of the oil into zone 1b.

(d) The surface-active synthetic cutting fluid is water-based and again acts as a source of oxygen, promoting zone 2 transfer with the HSS tool. However, the surface-active constituent reduces the extent of the chip/tool interaction and the forces are intermediate between air and vacuum cutting.

(e) CCl_4 produces an enormous reduction in the cutting force due to lubrication of the sliding contact in the zone 1b region. The limit of contact is close to the depth-of-cut line (130 μ) i.e. the contact area is almost all zone 1a.

(f) Cutting in vacuum with the PCS tool is extremely difficult due to gross development of chip/tool adhesion in zone 1b. (It is noted that the length of zone 1b is much greater than the length of zone 2 in the HSS/air case). The effect of oxygen is to reduce considerably the extent of zone 1b, but possibly due to the difficulty of access of sufficient oxygen to this region, the cutting force is still high with regard to the HSS tool.

(g) It is clear that water is a slightly better source of oxygen than atmospheric air in this case, since it produces a further reduction in cutting force.

(h) Cutting in oil flood with the PCS tool reduces the growth of zone 1b compared with vacuum cutting, due to the restriction of metal/metal contact by a boundary lubrication mechanism. However, the oil is not as effective as air or water which act as E.P. lubricants.

(i) The synthetic fluid RT 105 acts both as a source of oxygen and as a surface-active agent, greatly restricting the growth of adhesion in zone 1b and reducing the cutting force with PCS tools to values comparable to the HSS case. The drag force on the rake face is actually lower, due to the absence of any zone 2 transfer.

(j) CCl_4 supplies lubrication of zone 1b due to good penetration into this region. Cutting with the PCS tool is now exactly equivalent to cutting with the HSS tool since both zone 1b and zone 2 adhesion interactions have been eliminated.

(k) At the low cutting speeds employed, there is no significant difference in the performance of the three oils. This is probably because insufficient heat is generated to break down the additives, or induce reactions with the chip. It is suggested that the effect of the additives would be experienced at higher cutting speeds.

(l) Despite a large range of values of the cutting forces, the resolved stress on the shear plane varies by only about 5% with differences in cutting conditions, due to a corresponding range of shear plane angles.

(m) In particular, the lack of a reduction in the resolved shear stress when CCl_4 is employed casts doubt on any hypothesis that this fluid may act by weakening the workpiece.

(n) The traction stress on the rake face also does not vary greatly and is always comparable to but rather less than the resolved shear

stress. This is true even when the chip/tool contact is almost entirely in zone 1a (i.e. when using CCl_4 lubricant).

(o) However, the notional friction coefficient, an average over the entire contact area, varies considerably. For instance, it has a value of approximately 1 in the cases of "mechanical" sliding (i.e. no adhesion) in zone 1b and a higher value (up to 2) when severe adhesion occurs in this zone.

Further support for the proposed description of the interface between the chip and the tool is provided by these experiments. Clearly the data would be amenable to other interpretations. In particular, it is noted that the concepts of constant rake face traction stress together with variable contact length, or of variable rake face friction coefficient can be used to describe the chip/tool interaction. This underlines the uncertainties that are inherent in physical descriptions based upon derivations from measurement rather than upon direct observation.

7.4 LUBRICANTS IN BUILT-UP-EDGE AND DISCONTINUOUS CUTTING

7.4.1 Lubrication in Continuous Cutting with Built-Up-Edge

The effect of CCl_4 flood on the cutting of Duralumin was studied using the sapphire tool. (Cine Sequence 30). The BUE appeared still to be formed and at the conclusion of the cut, the chip was still attached to the tool (Figure 7.4). However, upon removal of the chip (Figure 7.5) no chip material was stuck to the sapphire (Figure 7.6). The BUE was also substantially smaller than in unlubricated cutting (c.v. Figure 5.2) and the surface finish on the workpiece was much finer, without evidence of BUE fragments.

Figure 7.4 Duralumin H chip attached to the transparent tool, produced when machining in the presence of CCl_4.

Figure 7.5 End of the chip when removed from the tool.

Figure 7.6 Rake face of the transparent tool after removal of the chip.

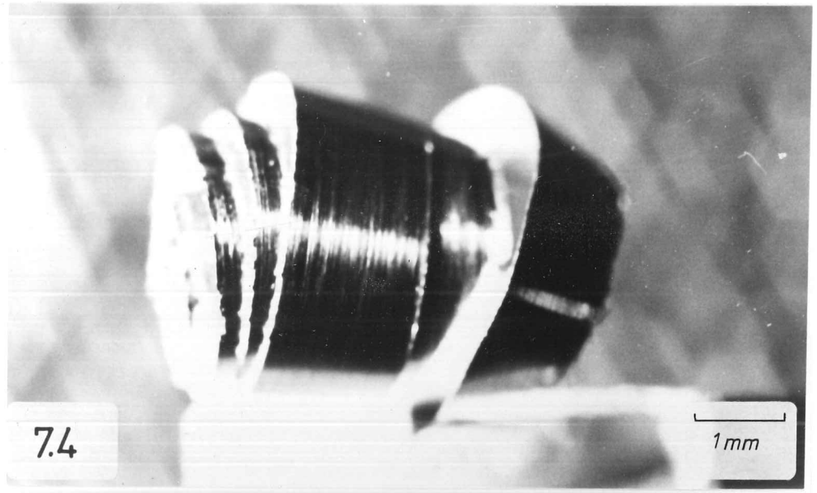

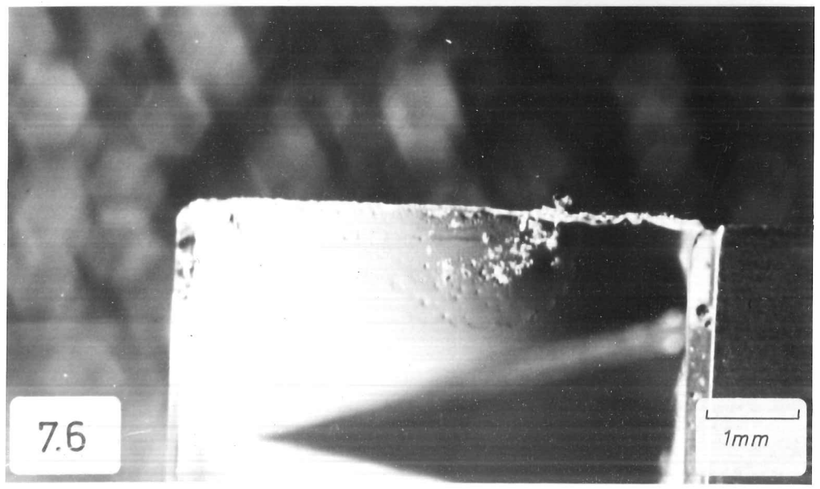

The influence of CCl_4 lubrication on the cutting forces was investigated using a 40° rake angle steel cutting tool. The results are presented in Table 7.4.

TABLE 7.4 Effect of CCl_4 on cutting of Duralumin

Forces in Kgf per mm width. Dept of cut 100 μ. Cutting speed 10 mm sec^{-1}.

Conditions	N	T
Air	1.1	6.3
Vacuum	0.78	5.7
CCl_4 flood	0.13	4.5

Trent (1977) suggests that the action of cutting fluids in BUE cutting is to reduce the adhesion between the layers of the BUE. This explanation should be treated with caution since it is not certain that the BUE forms in this way. One might expect the BUE to be eliminated altogether, since in this case the lubricant prevents adhesion of chip material to the tool.

If the BUE is considered as a "new" tool nose, one might postulate regions analogous to zones 1a and 1b in the interface between the chip and the BUE. Since the cutting forces with CCl_4 flood are substantially lower than those in dry cutting, it is suggested that the CCl_4 operates as a "zone 1b" lubricant, penetrating the region between the BUE and the chip and restricting the growth of the BUE. Thus the tendency is for cutting lubricants to promote small, stable BUE's rather than to eliminate them completely.

7.4.2 Lubrication in Discontinuous Cutting

The influence of oxygen on the cutting behaviour of magnesium, using the transparent tool, is noted in Chapter 5. Oxygen is found to increase the adhesion between magnesium and the sapphire promoting transfer of chip material at the tip. This behaviour is eliminated in vacuum.

The cutting performance in CCl_4 flood is found to be very similar to vacuum conditions, as seen in Table 7.5. The fluid does not further reduce the cutting force over the force in vacuum. This is presumably because there is no zone 1b region of sliding contact for the CCl_4 to lubricate. This also suggests that the proposed weakening of workpiece material, in this case via crack behaviour, does not in fact occur with CCl_4.

TABLE 7.5 Effect of CCl_4 on cutting of magnesium

Forces in Kgf per mm width. Depth of cut 100 μ. Cutting speed 10 mm sec^{-1}.

Conditions	N	T	F
Air	3.8	3.3	4.3
Vacuum	2.7	3.2	3.2
CCl_4 flood	2.8	3.1	3.3

Free-machining brass was cut with a 10° rake angle HSS tool under flood conditions using oil and CCl_4. (This material is machined without cutting fluid in normal workshop practice). The effect on the cutting forces compared with unlubricated cutting is indicated in Table 7.6. It appears that neither fluid has a pronounced effect on the cutting

forces when compared with cutting in vacuum. Indeed, using a highly leaded brass (3%) CCl_4 was found to increase the drag force on the rake face compared with unlubricated conditions (Doyle, 1978). This is presumably due to the extruded layer of lead on the underside of the chip; the observation that CCl_4 does not act as a lubricant with lead has been noted in section 7.2.

TABLE 7.6 Effect of lubricants on cutting of free-machining brass.

Forces in Kgf per mm width. Depth of cut 100 μ. Cutting speed 50 mm sec^{-1}.

Conditions	N	T	F
Air	5.5	8.7	6.8
Vacuum	3.9	8.8	5.5
CCl_4 flood	3.6	9.4	5.2
Oil flood	3.9	9.1	5.6

The lubricating action of cutting fluids in fully discontinuous cutting is thus, as one might expect, limited to the prevention of adhesion in the indentation region.

CHAPTER EIGHT

THE ZONE 1a PROBLEM

Introduction

Chapter 4 was concluded with a classification of the chip/tool contact zones in continuous cutting. Zones 1b and 2 have been examined in Chapter 7 and described in terms of:

(a) the strength of the interface between the tool and the chip;

(b) the effect of surface films and contaminants and

(c) the influence of the environment.

Zone 1a will now be considered.

8.1 NATURE OF THE PROBLEM

We are concerned with a region of chip/tool contact on the rake face, adjacent to the cutting edge, corresponding roughly to the depth of cut. It might alternatively be described as the region of workpiece/tool contact on the rake face. Experimental evidence in this investigation suggests that it has the following properties:

(i) Conditions of intimate contact prevail at the interface, the real and apparent areas of contact being equal.

(ii) During the cutting process there is a high normal load acting over this area.

(iii) There is relative movement between the chip and the tool at the interface.

(iv) When the chip and tool are separated, there is no tendency for chip material to adhere to the tool in this region.

(v) Surface films on the tool do not appear to be worn away.

These properties do not appear to be consistent with the accepted understanding of sliding contact. Under the contact conditions (i) and (ii) above, one is inclined to predict that failure will occur within the weaker material - in this case the workpiece material - leaving a "seized" layer on the tool and a velocity gradient into the chip. This is the current popular conception of the chip/tool contact in the region adjacent to the cutting edge.

Since this is the first comprehensive study of the chip/tool interface by means of direct observation, no verification of (iii) may be found in the literature. It is important, then, to recognise that we have only observed interfacial movement in a very limited number of cutting situations. However, observation (iv) is widely reported and this alone should cast the greatest doubt on the seizure hypothesis. If according to the conventional view the interface is so strong that flow occurs within the chip during cutting, then why does failure occur at the interface in, for example, a quick-stop experiment? The interface could be strong in shear and weak in tension, but this is not a property usually associated with metals. It might be proposed that the strength of the interface during the cut is increased by the presence of a high normal load. It is difficult to imagine, however, how a normal force could increase adhesion except by increasing the area of real contact. Studies of quick-stop chip and tool surfaces in the SEM indicate that total interfacial contact existed at the instant of separation, although of course microscopic relaxation effects would not be revealed in this way. In any case, even islands of strong interface should produce local adhesion.

If there is interfacial sliding, however, then why are surface

films (v) not worn away? This includes oxide films on metal tools, since we would expect strong adhesion in zone 1a analogous to that experienced in zone 1b if true metal/metal contact were established. (Indeed, using an iridium tool with copper, this is exactly what was experienced). This leads to the proposal that there is interfacial sliding without high surface traction. But the shear stresses parallel to the rake face in zone 1a are high, as we measured in cuts lubricated by carbon tetrachloride and as confirmed by many other workers using a wide range of stress measurement techniques.

Here, then, is the zone 1a problem. This is clearly a fundamental problem in the understanding of all continuous metal cutting situations and not solely when we use a sapphire tool. It is particularly significant in relation to interrupted cutting, "internal lubrication" and crater wear. In all three situations, the lack of chip/tool seizure in zone 1a is very important.

8.2 FURTHER EXAMINATION OF THE EVIDENCE

Introduction

Before attempting to resolve these difficulties, it is prudent to review the experimental basis for the above description of zone 1a.

8.2.1 Contact

One possibility which has been considered at length is the presence of a "crack" ahead of the tool, such that the chip and tool are not really in contact adjacent to the cutting edge. Apart from the thought that the propagation of such a large crack in, say, lead, is inherently unconvincing, there are several good reasons why this solution

can not be adopted.

Clearly a crack can not transmit any normal load to the tool, so the cutting force would have to be supported further up the rake face - beyond the depth-of-cut line - with the zone 1a portion of chip acting as a "lever" (Figure 8.1). It would seem to be much easier to bend this chip back against the tool than to cause shear in the primary shear zone - especially at low shear plane angles. When zone 1b is effectively lubricated using CCl_4, the chip/tool contact is almost all zone 1a (see Chapter 7). We rapidly approach the suggestion that the chip and tool are not touching at all.

The clearest indication of the contact geometry is furnished by studies of chips from quick-stop experiments. The grinding marks on the tool are always replicated on the chip in zone 1a, indicating that there is intimate contact on separation. Even the most rapid disengagement devices fail to reveal any fracture markings in this zone. In order to obliterate any trace of a crack, the tool would have to impress the chip perfectly during the disengagement. For these reasons, we may accept the proposed intimate chip/tool contact.

8.2.2 Stress

In this study, only the total load acting on the tool has been measured. Many workers have attempted to reveal the stress distribution using a variety of techniques (see Chapter 2, section 2.3.2) and generally agree on a distribtuion similar to Figure 2.4. This would suggest that the normal load acting over zone 1a is high and exceeds the yield strength close to the edge. When the chip/tool contact length is comparable to the depth of cut, the zone 1a load approaches the total load. In Chapter 7 the mean normal load was found to increase as lubrication of zone 1b

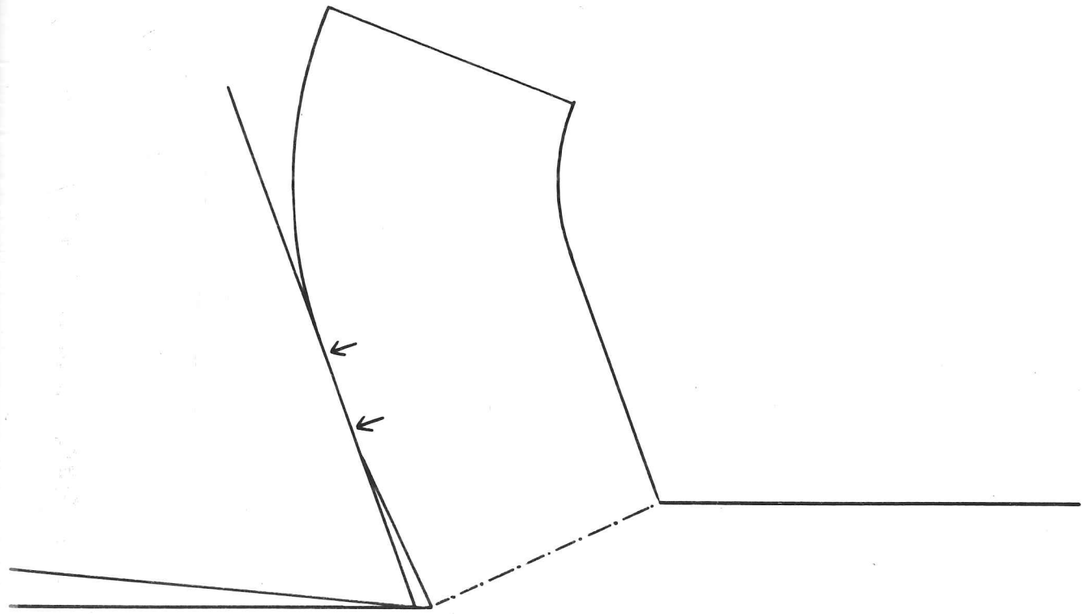

8.1

Figure 8.1 Non-contact, a possible description of zone 1a, showing the region which would transmit the normal load to the tool.

improved and this situation was approached. The shear stress in zone 1a (often termed the "sticking zone") is generally considered to have a constant value, close to but always less than the shear yield strength. This was again experienced in these experiments.

8.2.3 Movement

The difficulties in detecting movement have been discussed earlier (Chapter 4). It was concluded that, in the rather limited number of situations that could be studied, any stationary layer must be so thin as to be transparent. Since there is no doubt that relative movement occurs in zone 1b, we should expect to see some contrast between zones 1a and 1b, if zone 1a is stationary, both with the transparent tool and also after the cut when studying the chip in the SEM. Zone 1 was not, at first, subdivided as indicated by the scheme of numbering.

8.2.4 Adhesion

The frequent occurrence of a "clean" region at the tip of the tool has not escaped the notice of other workers. In a recent survey of the subject, Trent (1977) attributed this effect to the removal with the chip of a built-up edge. We saw in Chapter 5 that the direct view of a BUE is very different from that of zone 1a contact. Furthermore, "clean zone 1a" effects are observed with many materials which do not exhibit BUE formation. The clear conclusion is that the chip/tool interface in zone 1a is weaker than the bulk of the chip. This is in contrast with zone 1b, where the interface is stronger once metal/metal contact is established.

8.2.5 Surface Films

Low adhesion in zone 1a can still prevail when, as a result of the

improved and this situation was approached. The shear stress in zone 1a (often termed the "sticking zone") is generally considered to have a constant value, close to but always less than the shear yield strength. This was again experienced in these experiments.

8.2.3 Movement

The difficulties in detecting movement have been discussed earlier (Chapter 4). It was concluded that, in the rather limited number of situations that could be studied, any stationary layer must be so thin as to be transparent. Since there is no doubt that relative movement occurs in zone 1b, we should expect to see some contrast between zones 1a and 1b, if zone 1a is stationary, both with the transparent tool and also after the cut when studying the chip in the SEM. Zone 1 was not, at first, subdivided as indicated by the scheme of numbering.

8.2.4 Adhesion

The frequent occurrence of a "clean" region at the tip of the tool has not escaped the notice of other workers. In a recent survey of the subject, Trent (1977) attributed this effect to the removal with the chip of a built-up edge. We saw in Chapter 5 that the direct view of a BUE is very different from that of zone 1a contact. Furthermore, "clean zone 1a" effects are observed with many materials which do not exhibit BUE formation. The clear conclusion is that the chip/tool interface in zone 1a is weaker than the bulk of the chip. This is in contrast with zone 1b, where the interface is stronger once metal/metal contact is established.

8.2.5 Surface Films

Low adhesion in zone 1a can still prevail when, as a result of the

removal of oxide films, severe chip/tool adhesion develops in zone 1b. This suggests that surface films are not worn away in zone 1a. This is supported by the work with evaporated films of copper on the transparent tool, when a thin strip of copper was left on the tool in zone 1a. The possibility was raised that this was an artifact of the initial indentation of the tool against the workpiece. This was dispelled, however, by the observation that, with a "well-adhered" film, several millimetres of chip were sometimes generated before anything but the copper layer could be seen through the rake face. Subsequently, the copper was slowly worn away in zone 1b but not in zone 1a. However, it was found that the copper in zone 1a could in some experiments adhere preferentially to the chip on detachment.

8.3 FURTHER EXPERIMENTS

8.3.1 Pulling on the Chip

The effect of applying a pulling force to the chip was investigated. A conventional cut was first conducted for comparison, 150 μ being taken at 2 mm sec^{-1} from an as-rolled copper workpiece using a polished plain carbon steel tool. This produced extremely extensive chip/tool adhesion in zone 1b, as seen in Figures 8.2 and 8.3. Zone 1a was slightly short of the depth-of-cut line and "clean".

The experiment was repeated, while pulling on the chip as seen in Figure 8.6. The load at which the chip broke was determined and another cut was made at a slightly smaller load. In both cases, the zone 1b transfer appeared to be more extensive as a result of the pulling, but did not encroach into zone 1a (Figures 8.4 and 8.5). When pulling hard enough to break the chip, failure occurred in the

Figure 8.2 Rake face of plain carbon steel tool after slow machining of copper in air. Depth of cut 150 μ.

Figure 8.3 Chip root, following a quick-stop; conditions as in Figure 8.2.

Figure 8.4 As above, with a pulling force applied to the chip.

Figure 8.5 Last fragment of chip, following a quick-stop; conditions as in Figure 8.4.

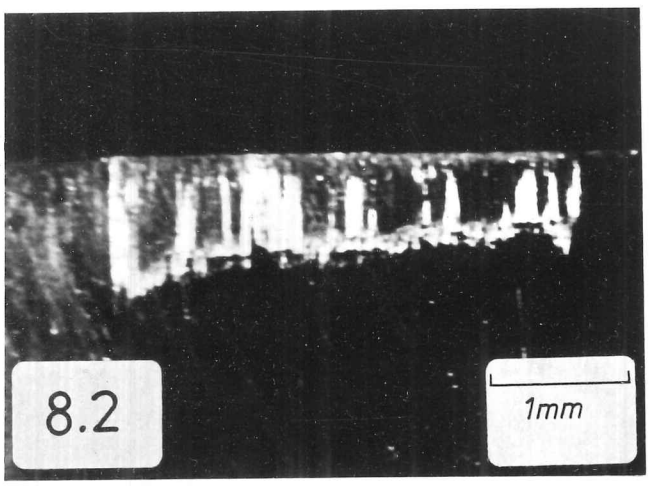

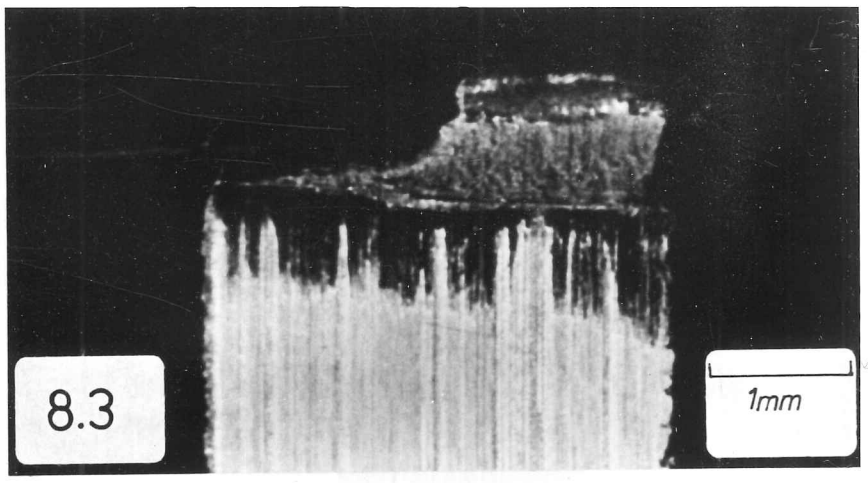

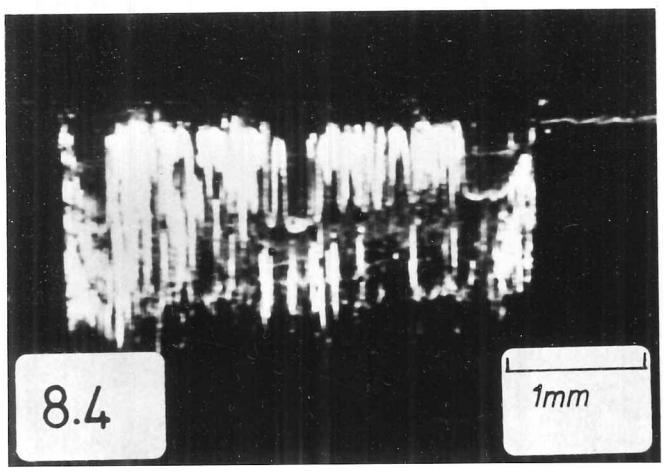

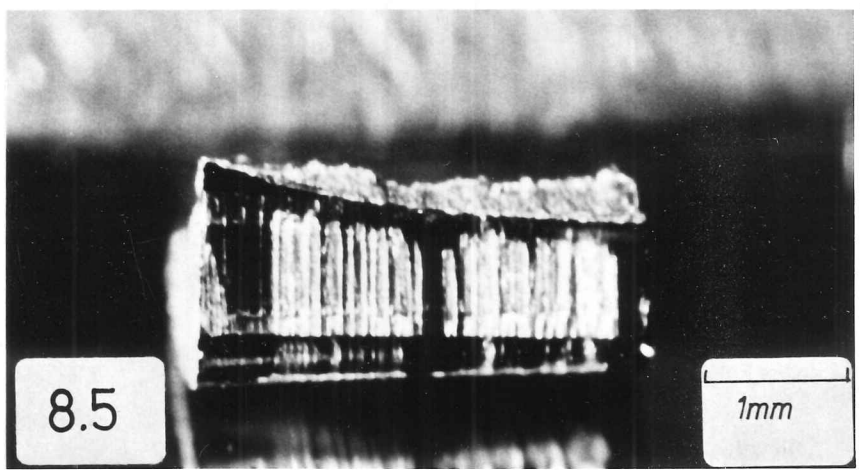

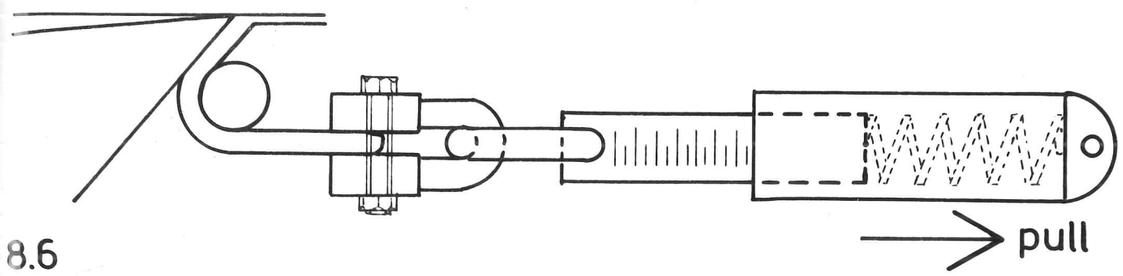

8.6

Figure 8.6 Schematic diagram of arrangement used to apply a pulling force to the chip during cutting.

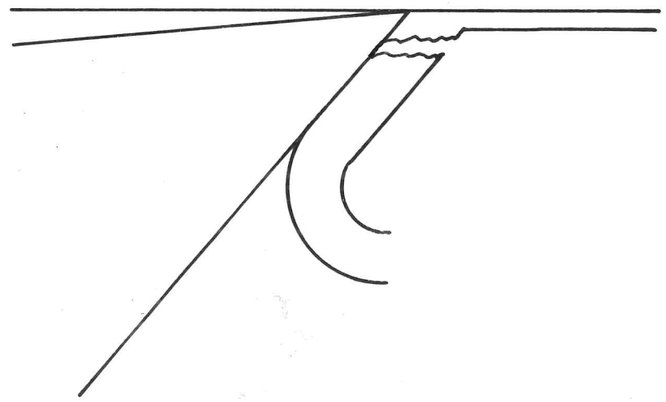

8.7

Figure 8.7 Manner of chip breakage in "pulling" experiment.

manner shown in Figure 8.7.

This experiment produced what might be termed a "negative" result; it would have been more instructive if the zone 1a interface had been affected in some way by applying a force to the chip. It does indicate, however, that the high normal force acting over zone 1a - largely unaffected by pulling on the chip - may be more significant in relation to the zone 1a sliding mechanism than the tangential force along the rake face.

8.3.2 Two Effects in Lubricated Cutting

An entertaining aspect of the sapphire tool work was the fact that novel effects were produced by every slight variation in experimental technique - even an accidental variation. During one cut on pure aluminium lubricated with a saturated hydrocarbon (see Chapter 7) a small piece of debris was embedded in a minute crack in the cutting edge (Figure 8.8a). Lubricant was applied only to the rake face and no bubbles had been observed in previous similar experiments with a clean tool. However, one stream of bubbles was clearly visible in this case, originating at the end of an apparent "scratch" in zone 1 (Figure 8.8b). These clearly resulted from the movement of air from the clearance wedge along a "tube" between the rake face and the chip (Figure 8.8c). The frequency of bubbles suggested that air was being drawn along the tube, presumably by the moving chip. Attempts to repeat this effect and record it on film were unsuccessful.

Another "accidental" observation of some significance was the result of a hurried departure from the laboratory. A high speed steel tool, used to cut copper with CCl_4 lubricant, was left uncleaned on the bench. Figure 8.9 shows the appearance of the tool after 2 days'

Figure 8.8 (a) Minute particle embedded in a crack in the cutting edge of the transparent tool.

(b) Appearances of bubbles seen through the transparent tool.

(c) Probable mechanism accounting for the bubbles.

Figure 8.10 Copper coating on the end of the workpiece.

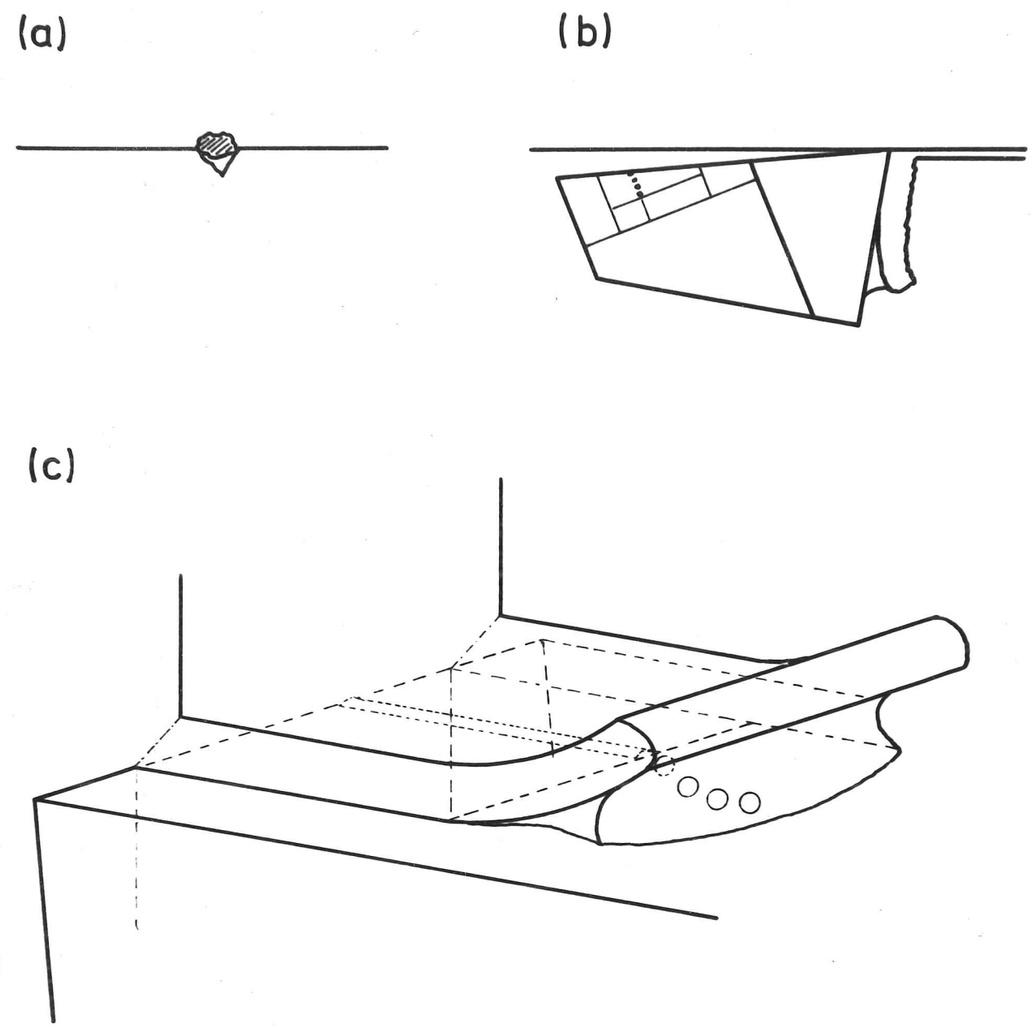

8.8

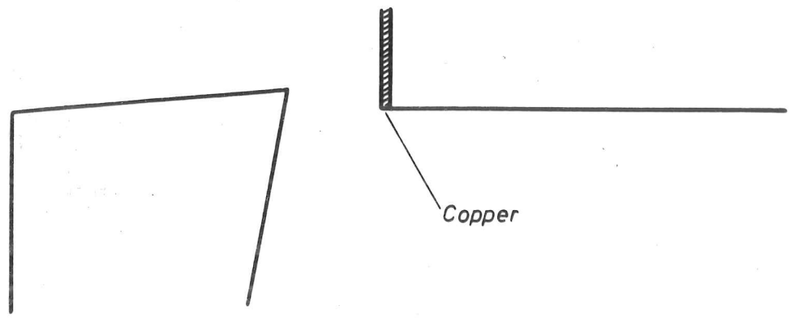

8.10

exposure to laboratory air. Oxide growth has been promoted in the region subject to rubbing contact with the chip in the presence of CCl_4. The deposit appeared on close inspection to be hydrated Fe_3O_4 i.e. rust. It is suggested that the slight ghosting of copper over this area acted with the iron to form a large number of minute galvanic corrosion cells, the rubbing action with CCl_4 having removed insulating contaminants. The interesting feature is the unoxidised area corresponding to zone 1a, where surface films are presumably retained.

8.3.3 More Copper Coatings

Work described elsewhere (Chapters 4 and 7) employed copper coatings on the tool. A series of experiments was conducted using approximately 1000 Å (0.1 μ) copper on the end of a pure aluminium workpiece, as shown in Figure 8.10. The cuts were performed with a 10° rake HSS tool with a range of surface finishes.

The chip root was studied following a quick-stop. When the tool surface had a polished finish, no copper was visible in the chip root. (It was all to be found at the beginning of the chip). The same occurred with a tool wet-finished with "600" SiC paper, surface roughness 0.04 μ C.L.A. However, a tool with a "120" finish, 0.4 μ C.L.A., retained copper in zone 1a. This copper was transferred to the chip at the end of the cut (Figure 8.11). This effect is discussed later, section 8.4.2

8.3.4 Internal and External Grids

Several workers have used engraved grids on the workpiece to reveal flow patterns in cutting (see Chapter 2, section 2.2.3). Here there is always the danger that one may be viewing edge effects, which

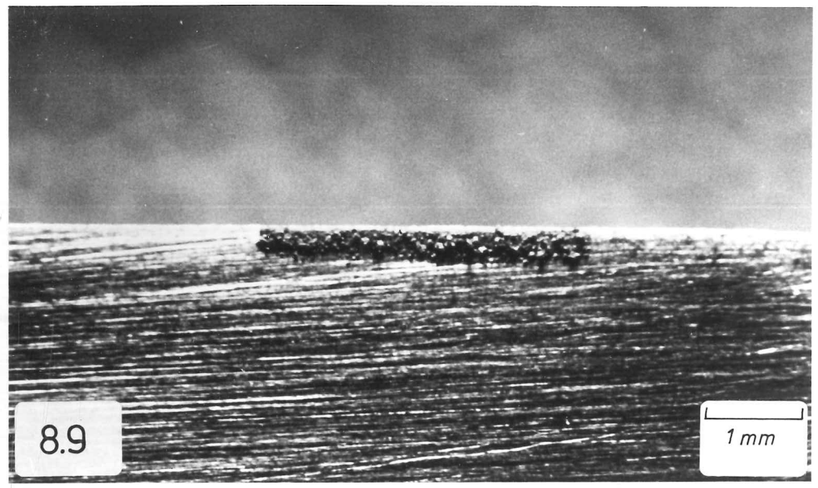

Figure 8.9 Rust formed on the high speed steel tool, after machining of copper in the presence of CCl_4.

Zone 1a is free from rusting.

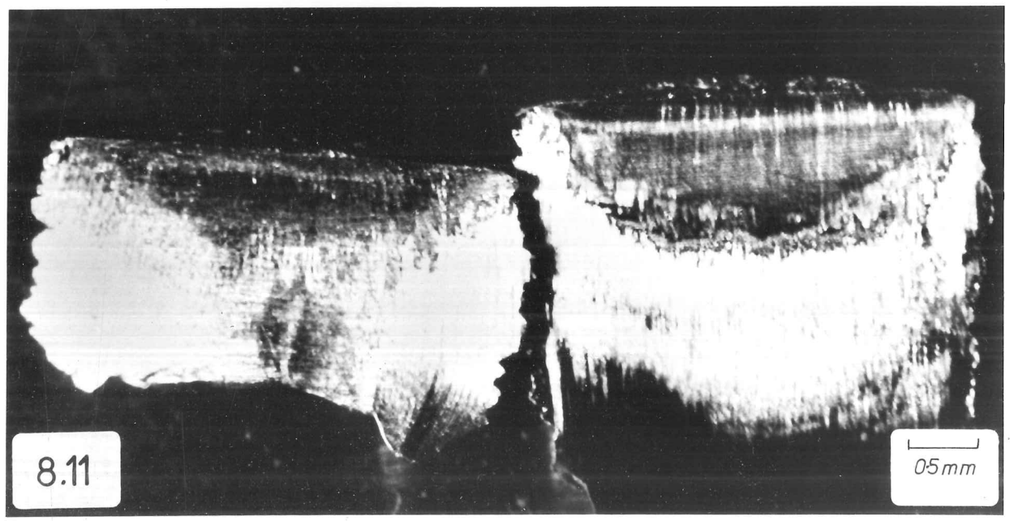

Figure 8.11 Pure aluminium chips produced when machining a workpiece coated with copper as depicted in Figure 8.10.

Left: "120" finish on tool; copper visible in the chip root.

Right: "600" finish on tool; no copper visible in the chip root.

may not be representative of the flow patterns in the body of the workpiece.

Cooke and Rice (1973) reported the use of a directionally solidified Silver-Copper eutectic to examine the shearing process. The same material was used by Williams (1975). These investigations were conducted mainly with the eutectic plates parallel to the direction of cutting. In this study, the plates were normal to the direction of cutting.

A quick-stop section of this material cut with a plain carbon steel tool is seen in Figure 8.12. (This material behaves similarly to copper when machined with HSS and PCS tools). It will be noted that the "bending-round" of the plates is much more pronounced in zone 1b than in zone 1a. The deformed region on the underside of the chip is also much deeper beyond the end of zone 1a.

Two photographs taken from the work of Childs (1972) are reproduced in Figure 8.13 for comparison. It is evident that the substantial rake face "drag" evident in zone 1a in Figure 8.13a at the surface is not reproduced in Figure 8.13b in the body of the chip. These pictures support the proposition that, although as mentioned above, the shear stresses are fairly high, the chip slides over zone 1a without experiencing a large shear strain. This method would not, however, reveal strain in a very thin surface layer next to the tool.

8.4 DISCUSSION - POSSIBLE SLIDING MECHANISMS

8.4.1 Surface Buckling

It is suggested that the stress acting on the chip parallel to the rake face might cause it to buckle and lose contact with the tool

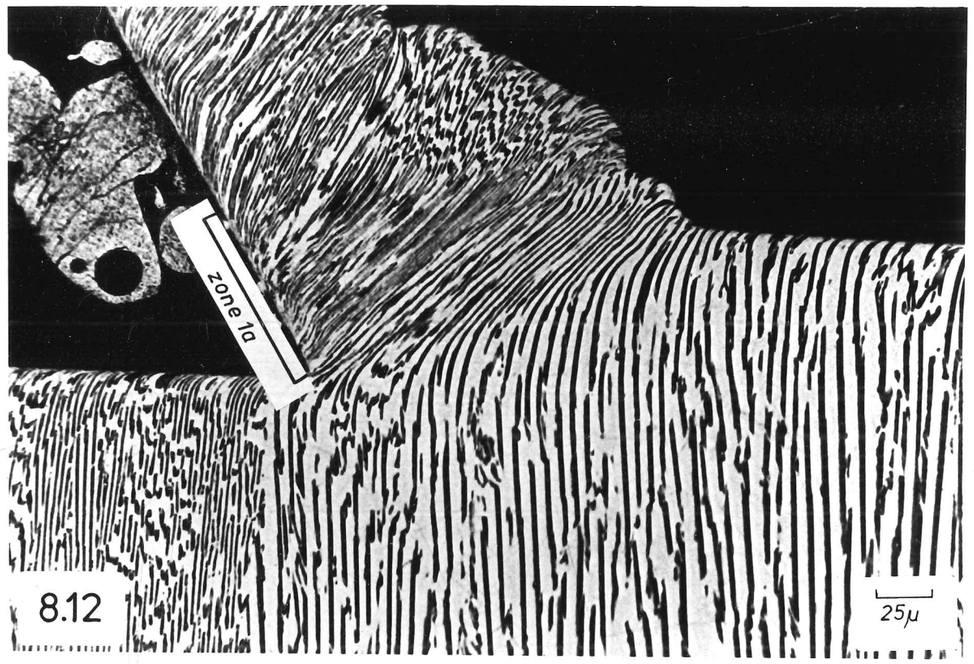

Figure 8.12 Section through chip and workpiece from a quick-stop experiment; copper/silver eutectic machined in air with a plain carbon steel tool. Increased drag in zone 1b, compared with zone 1a, is evident.

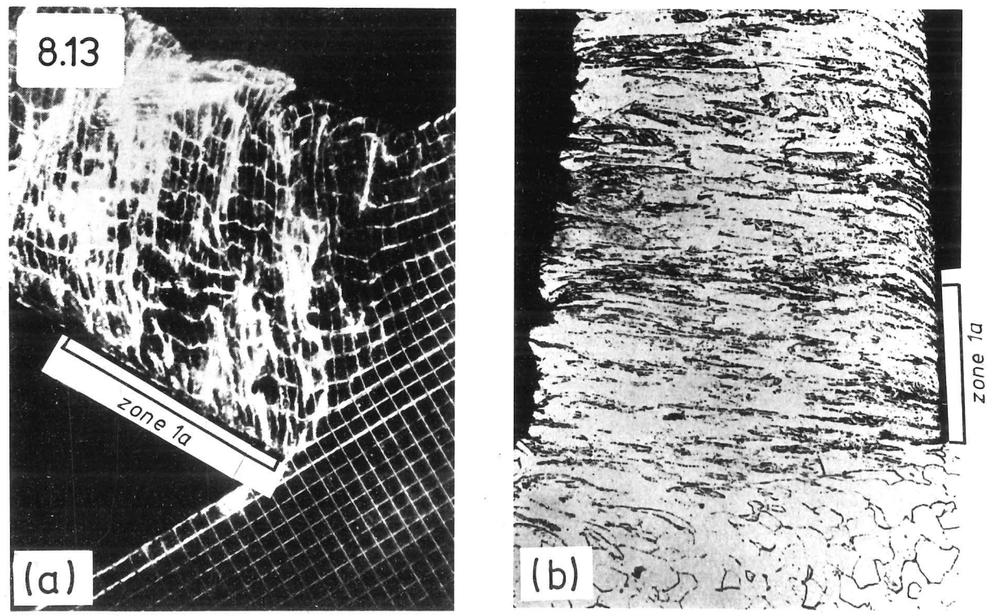

Figure 8.13 Plates taken from the work of Childs (1972)

(a) Side of chip and workpiece inscribed with a grid prior to cutting; mild steel lubricated with CCl_4. There is considerable bending-round of the grid markings in zone 1a.

(b) Section through chip and workpiece; mild steel, unlubricated. Despite the more severe conditions, there is no marked bending-round of the grain structure in zone 1a.

Figure 8.12 Section through chip and workpiece from a quick-stop experiment; copper/silver eutectic machined in air with a plain carbon steel tool. Increased drag in zone 1b, compared with zone 1a, is evident.

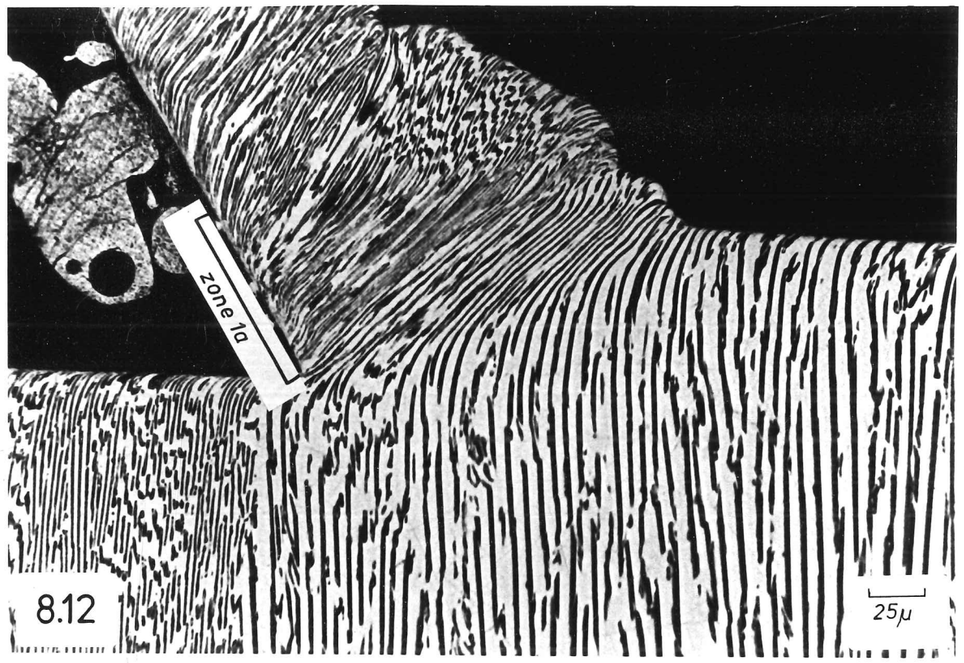

Figure 8.13 Plates taken from the work of Childs (1972)

(a) Side of chip and workpiece inscribed with a grid prior to cutting; mild steel lubricated with CCl_4. There is considerable bending-round of the grid markings in zone 1a.

(b) Section through chip and workpiece; mild steel, unlubricated. Despite the more severe conditions, there is no marked bending-round of the grain structure in zone 1a.

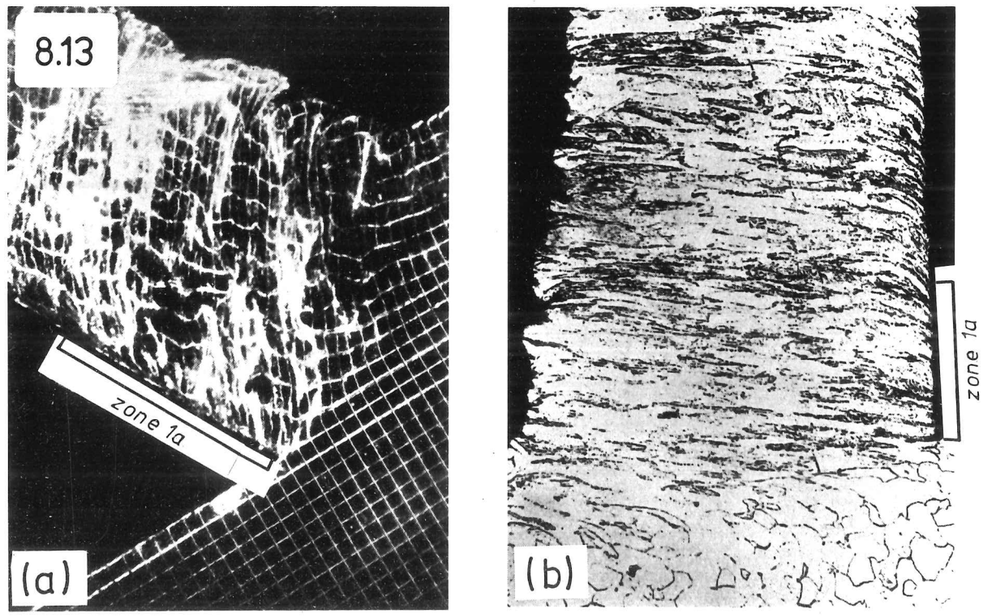

surface, as seen in Figure 8.14a. The high normal stress would, however, prevent the formation of a large single buckle of this type and would favour multiple buckling (Figure 8.14b). Sliding could then take place by the translation of these buckles along the interface in a manner resembling the movement of a ruck in a carpet.

The possibility that there may be circumstances in which frictional sliding occurs by the passage of elastic, non-crystalline dislocations in the interface has recently been proposed by Gittus (1975). These interface dislocations - which he calls "interfaceons" - are stabilised by the high normal pressure. Gittus derives a friction coefficient by considering the energy loss (hysteresis) in the translation of these interfaceons. The model is essentially speculative, but Gittus refers to the observation by Schallamach (1971) of such "waves of detachment" in the sliding of some highly elastic rubbers. There remains considerable doubt, however, whether such sliding mechanisms could operate in metals where the elastic strains that can be accommodated are much smaller.

8.4.2 The Effect of Roughness

Whether we interpret the relative motion of the chip and tool in zone 1a in terms of detachment-and-reattachment, or some form of bodily sliding, our results suggest that the interface is weaker than the bulk and true interface sliding occurs over the whole area, since this consumes the least energy. So far we have considered ideally smooth surfaces, but in reality the tool surface is rough (Figure 8.15). It is perhaps unreasonable to suppose that material "climbs" in and out of all these surface irregularities. Since "extra" material on the underside of the chip would need to be generated (and then consumed) from the body of the chip to match the tool surface, complex flow

(a)

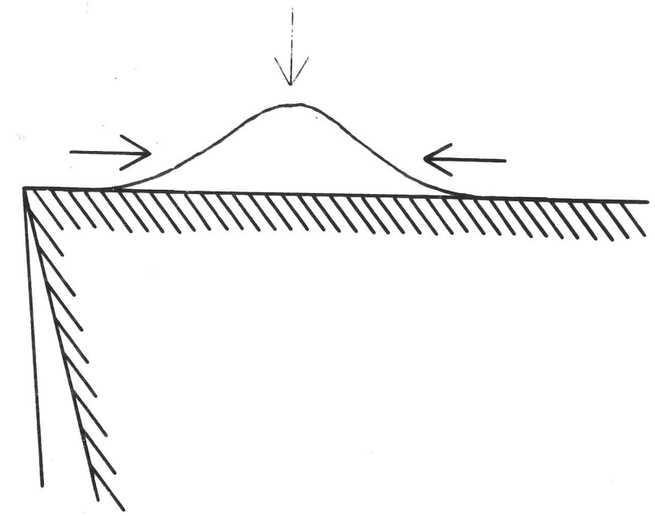

(b)

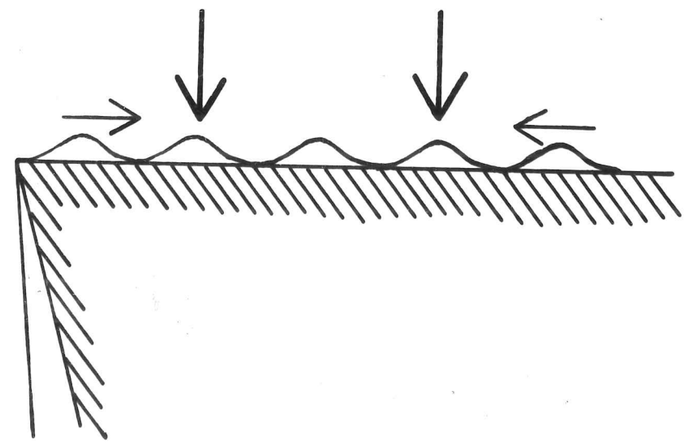

8.14

Figure 8.14 Buckling at the chip/tool interface
(a) single buckle
(b) multiple buckle.

patterns would occur in the chip which would increase the energy of sliding. The magnitude of the increase would depend on the roughness of the surface.

The work with copper coatings on the end of the workpiece (section 8.3.3) confirms the suspicion that the material found in the impressions of tool grinding marks (Figure 4.27) is, in fact, stationary during the cut. Once the "valleys" in the tool surface reached dimensions comparable to the coating thickness, the pieces of copper remained embedded in the tool and chip flow occurred over them. When the chip and tool were separated, however, this mechanical "keying" of material was no longer effective and the chip/tool combination separated at the weakest point.

This observation offers the clue to the mystery of non-removal of contaminant films on the tool. Even minute irregularities in the tool surface in zone 1a are filled-in by chip material, due to the high normal pressure, trapping any contaminant films. (Figure 8.16). For the topological reasons already indicated, local internal shearing of the chip occurs above the stationary material, which is trapped - not seized, since the interface is still weaker than the bulk. In zone 1b, by contrast, sliding occurs only over the asperities; should the chip remove any contaminant or oxide films, real seizure would occur, producing a strong chip/tool bond.

Perhaps this - and not interfaceon movement - is the mechanism of sliding in zone 1a with tools of normal surface structure. It predicts that there should be some tendency for chip material to be retarded on the rake face, but only on a scale comparable to the surface roughness as suggested in section 8.3.4. However, it is difficult to understand why the shearing process within the chip should fail to "drag" material out of the gaps between the asperities, especially

8.15

Figure 8.15 Representation of the roughnesses in the tool surface.

8.16

Figure 8.16 Contaminant films trapped within the roughnesses, as the chip undergoes local internal shearing.

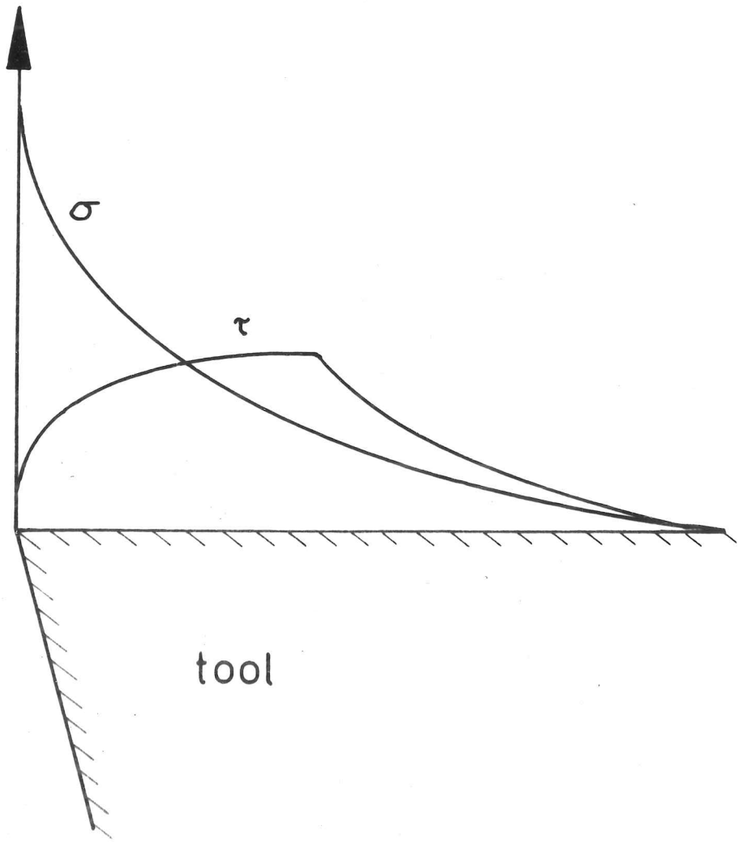

8.17

Figure 8.17 Possible stress distribution on the rake face

τ = shear stress

σ = normal stress

since the slopes may only be of the order of a few degrees.

8.4.3 Shear Stress Distribution

So far we have accepted that the shear stress on the rake face follows the distribution of Figure 2.3. Applying a yield criterion in plane strain (Hill, 1950) to the material at the tip of the tool, we might expect a distribution similar to Figure 8.17. The presence of a high normal stress near the tip reduces the shear stress required to cause flow. If the shear stress required to produce interfacial sliding were unaffected by the normal stress, then there would always be a region of internal shearing close to the tip of the tool, regardless of the surface structure.

This suggests that the length of zone 1a might depend on the stress distribution, the geometry of the surface roughnesses and the interfacial adhesion. It has been noted earlier that the limit of zone 1a contact is not rigidly identifiable with the depth of cut line. In these experiments, it was sometimes possible to obtain an accurate measurement of the length of zone 1a but there was no provision for assessment of the stress distribution on the rake face. Further work on the zone 1a problem might profitably explore these areas.

CHAPTER NINE

SUMMARY OF MAIN CONCLUSIONS

(i) It appears from this and other studies that, while the adhesion of metal-to-metal and of oxide-to-oxide contacts is high, the adhesion between metal and oxide is often lower.

(ii) This has important consequences in the metal cutting process. Virgin metal surface is generated in cutting, but this may be oxidised once exposed to the environment. The tool may be composed of oxide or have an adherent oxide film. Alternatively, surface layers on a metal tool may be abraded-away, exposing metal surface. Thus the strength of adhesion at the chip/tool interface can vary in a complex manner.

(iii) A new description of the chip/tool interface in continuous cutting is proposed, which allows effects previously considered anomalous to be understood. This incorporates some features of earlier descriptions, based on less direct experimental methods, but also attempts to resolve some inconsistencies.

(iv) The interface is divided into two zones, corresponding to regions on the rake face observed directly when using a transparent cutting tool. In zone 1, adjacent to the cutting edge, there is no tendency for chip material to adhere to the sapphire tool. There appears to be relative movement at the interface. In zone 2, around zone 1, chip material adheres to the tool in the presence of oxygen. No zone 2 is seen in vacuum or inert atmosphere.

(v) Zone 1 is sub-divided into zone 1a, nearest the cutting edge corresponding to the depth of cut, and zone 1b, the remainder of zone 1. With the transparent tool, the main distinction is that surface films

on the tool do not appear to be worn away in zone 1a by the rubbing action of the chip.

(vi) Zone 1a is the region, between the cutting edge of the tool and, approximately, the depth-of-cut line,* in which there is intimate contact between the chip and the tool. The real area of contact is equal to the apparent area of contact and large stresses act over this region. The normal component of stress increases sharply towards the cutting edge, while the shear stress over the region has a constant value. This is frequently termed the "sticking region" by other workers.

(vii) There appears to be relative motion between the chip and the tool in zone 1a. This movement is clearly observed in cutting situations that can be studied directly. Also, when the chip and tool are separated, they normally do so at the interface. However, surface films on the tool do not appear to be rubbed away, although they may transfer to the chip on separation.

(viii) These features of zone 1a suggest that it is not a sticking, or seizure region, and that some interfacial sliding occurs under the action of a shear stress rather lower than the flow stress of the chip. The mechanism of sliding in this region has not been fully elucidated, but appears to depend on the presence of a high normal component of stress.

(ix) Beyond this first zone, in zone 1b, the normal load gradually diminishes, such that the chip is no longer in intimate contact with the whole tool surface. This is commonly termed the "sliding region"

---

* In oblique cutting, this would be the feed-line.

by other workers. It is now suggested that the nature of sliding contact between the chip and tool in this region depends on the chemical composition of the tool surface and the surrounding environment.

(x) If the tool is composed of oxide, or has an oxide film which, under the cutting conditions, is retained on the tool, there is no tendency for the chip to adhere to the tool in zone 1b. This is because of the weak adhesion between metal and oxide. Frictional sliding occurs at the interface, which may involve ploughing of the underside of the chip by the asperities on the tool surface.

(xi) If the bare metal of the tool is exposed in zone 1b, the chip adheres to the tool. This is because metal-to-metal adhesion is strong. The adhered region grows by the process of junction growth, such that relative motion between the chip and the tool occurs by shear within the chip itself. Oxygen serves to restrict the growth of the metal-to-metal junction and hence lubricates the cutting process.

(xii) Zone 2 is a region of chip/tool transfer beyond zone 1, seen with oxide tools. It is associated with the access of oxygen to the underside of the chip. Only when sufficient oxygen gains access to the chip/tool interface to form a critical oxide layer on the underside of the chip does chip material adhere to the tool. This is because oxide-to-oxide adhesion is much stronger than oxide-to-metal adhesion.

(xiii) The controlling factor in this zone 2 interaction appears to be the access of oxygen to the interface, via the wedge between the chip and the tool. Different metals exhibit the onset of zone 2 transfer at similar values of oxygen pressure and speed of cutting. This would not be the case if the process were controlled by the kinetics

of the oxidation reaction.

(xiv) Access to the chip/tool interface is also a critical factor in the action of cutting lubricants. It is clear that no lubricant gains access to zone 1a, because there is intimate chip/tool contact. Differences in performance relate to how near the end of zone 1a the lubricant can provide effective lubrication of the contact.

(xv) Liquid lubricants appear to gain access to the interface by being "sucked-in" from the sides to the wedge opening up between the chip and the tool, rather than by movement against the flow of the chip.

(xvi) From the end of zone 1 towards the end of zone 1a it becomes increasingly difficult for the lubricant to penetrate. In this region, lubricant reaches the interface by vapour diffusion. This explains the particular effectiveness of carbon tetrachloride as a cutting fluid. However, because sufficient lubricant must be supplied at the end of zone 1, the liquid may still be more effective than the vapour.

(xvii) A good cutting lubricant reduces the adhesion of the chip to the tool. Thus, for example, plain oil lubricates the cutting of aluminium with an oxide tool by excluding oxygen from the contact and eliminating transfer in zone 2. Water lubricates the cutting of steel with a high speed steel tool by supplying oxygen and thus restricting junction growth in zone 1b.

(xviii) More effective lubrication is provided when the lubricant reacts with the chip to produce a low shear-strength layer. The most effective cutting lubricants penetrate zone 1b by vapour diffusion and hence greatly reduce the length of chip/tool contact.

(xix) Whether or not a built-up-edge develops in continuous cutting depends on the fracture properties of the workpiece. The high stresses

at the chip/tool interface in the region of the tip of the tool cause separation of the BUE by fracture, initiated by second-phase particles. The BUE may not, in fact, be strongly adherent to the tool.

(xx) The growth of the BUE, however, depends upon the adhesion. Thus the shape of the BUE is determined by the chemical composition of the tool surface,of the workpiece and of the environment. Cutting lubricants affect adhesion between the chip and the tool and also between the chip and the BUE.

(xxi) The chip/tool interface in discontinuous cutting is intermittently exposed to the environment. In the indentation region adjacent to the tip of the tool, chip material adheres if metal-to-metal or oxide-to-oxide contact is made.

(xxii) The action of lubricant is to prevent this adhesion. Because the chip is broken-up, there is little resistance to sliding on the rake face. If partially discontinuous chips are formed, lubrication effects similar to those in zones 1b and 2 may be experienced.

(xxiii) Magnesium produces discontinuous chips because it has an insufficient multiplicity of slip planes and directions to show full plastic behaviour. Fracture occurs in the direction of maximum shear stress. If a single crystal specimen is suitably oriented, a continuous chip is formed by slip, at a lower cutting stress.

(xxiv) In continuous cutting, variations in crystal orientation produce variations in the shear plane angle and cutting forces.

(xxv) When cutting aluminium single crystals, the resolved stress on the shear plane is found to remain constant with variations in orientation. Copper single crystals, however, show dependence of resolved shear stress on orientation.

(xxvi) This difference appears to be due to differences in stacking fault energy. Aluminium has a high s.f.e., so partial dislocations do not separate very far. These readily recombine, allowing cross-slip to take place. It is therefore relatively easy for dislocations to move on several slip planes, so that the cutting stress does not depend on slip plane orientation. Copper has a low s.f.e., partials are widely separated and cross-slip occurs less readily. Thus when a slip plane is aligned with the shear plane, the cutting stress is reduced.

(xxvii) Continuous cutting does not proceed in a steady state, instabilities in the shearing process being evident. These produce fairly regular striations or "lamellae" on the free surface of the chip. For a particular workpiece material, lamellar spacing depends primarily on the depth of cut, but also varies between grains of different orientation.

(xxviii) The lamellae appear to be the result of heterogeneous plastic flow in the primary shear zone rather than tool vibrations or stick-slip of the chip along the rake face of the tool. Primary shear is concentrated in thin bands separated by segments of less deformed material.

(xxix) It is suggested that, as the tool advances between shear events, the tool indents into the shear band, pushing material into the base of the segment and causing the shear plane to rotate. The amount of material being pushed into the segment progressively increases, so that eventually it becomes energetically more favourable for shear on the "next" shear band to commence.

(xxx) Natural curl of the chip occurs before there is any significant frictional interaction on the rake face. Indeed, natural curl appears to be very tight and the influence of the rake face interaction is to

reduce the radius. It is proposed that chip curl is the consequence of the wedge angle produced as extra material is pushed into the base of the segment of chip between successive positions of the primary shear plane.

REFERENCES

Albrecht, P. (1960) Trans. ASME 82 B, 348

Atkins, A.G. (1974) Int. J. Prod. Res. 12, 2, 263

Bailey, J.A. (1975) Wear 31, 243

Barlow, P.L. (1967) Proc. Inst. Mech. Eng. 181, 687

Black, J.T. (1971) Trans. ASME 93 B, 2, 507

Black, J.T. (1972) Trans ASME 94 B, 1 307

Boothroyd, G. (1963) Proc. Inst. Mech. Eng. 177, 789

Bowden, F.P. and Tabor, D. (1964) "The Friction and Lubrication of Solids", Part 2, Oxford University Press

Brown, R.H. and Luong, H.S. (1975) Metals Technology 2, 1

Cassin, C. and Boothroyd, G. (1965) J. Mech. Eng. Sci. 7, 1, 67

Chandrasekeran, H. and Kapoor, D.V. (1965) Trans. ASME 87 B, 495

Childs, T.H.C. (1971) Int. J. Mech. Sci. 13, 373

Childs, T.H.C. (1972) Proc. Inst. Mech. Eng. 186, 717

Childs, T.H.C., Richings, D. and Wilcox, A.B. (1972) Int. J. Mech. Sci. 14, 359

Childs, T.H.C. and Rowe, G.W. (1973) Rep. Prog. Phys. 36, 223

Christopherson, D.G., Oxley, P.L.M. and Palmer, W.B. (1958) Engineering 186, 113

Coffin, L.F. (1959) Proc. Symp. "Friction and Wear", Detroit, 1957; Ed. Robert Davies, Elsevier Publ. Co., Amsterdam, 36

Cook, N.H., Finnie, I. and Shaw, M.C. (1954) Trans. ASME 76, 153

Cooke, W.H.B. and Rice, W.B. (1973) Trans. ASME 95 B, 844

De Gee, A.W.J. (1965) Wear, 8, 121

De Gee, A.W.J. (1967) Materialprüf 9, 5, 166

Dewhurst, P. (1978) Proc. Roy. Soc. A360, 587

Doyle, E.D. (1974) Proc. Int. Conf. Prod. Eng., Japan, 1974; Part 1, 522

Doyle, E.D. (1978) Private communication

Doyle, E.D. and Samuels, L.E. (1975) Unpublished 16 mm movie film

Doyle, E.D. and Samuels, L.E. (1976) J. Aust. Inst. Metals 21, 1,2

Epifanov, G.E., Pleteneva, N.A. and Rebinder, P.A. (1954) Dok. Akad. Nauk. USSR 17, 2, 714

Ernst, H. (1938) "Physics of Metal Cutting", Machining of Metals, publ. Amer. Soc. Metals

Ernst, H. and Merchant, M.E. (1941) "Chip Formation, Friction and Finish", Cincinnati Milling Co. Ohio

Field, M. and Merchant, M.E. (1949) Trans. ASME 71, 421

Finnie, I. and Shaw, M.C. (1956) Trans. ASME 78, 1649

Gittus, J.H. (1975) Phil. Mag. 31, 317

Hahn, R.S. (1953) Trans. ASME 75, 581

Hastings, W.F., Oxley, P.L.B. and Stevenson, M.G. (1974) Proc. Inst. Mech. Eng. 188, 245

Heginbotham, W.B. and Gogia, S.L. (1961) Proc. Inst. Mech. Eng. 175, 892

Hill, R. (1950) "Plasticity", Clarendon Press, Oxford

Hirsch, P.B. (1975) (Ed) "The Physics of Metals", Cambridge University Press

Iwata, K., Aihara, J. and Okushima, K. (1971) Annals CIRP 20, 323

Kamskov, L.F. (1959) Vestn. Mashinostroeniya 5, 59

Kobayashi, S., Herzog, R.P., Eggleston, D.M. and Thompsen, E.G. (1960) Trans. ASME 82 B, 333

Kobayashi, S. and Thompsen, E.G. (1960) Trans. ASME 82 B, 324

Kohn, E.M. (1965) Wear 8, 43

Kramer, I.R. (1963) Trans. Met. Soc. AIME 227, 1003

Kudo, H. (1965) Int. J. Mech. Sci. 7, 43

Lee, E.H. and Shaffer, B.W. (1951) J. Appl. Mech. Trans. ASME 73, 405

Lemaire, J.C. and Backofen, W.A. (1972) Met. Trans. 3, 477

Mallock, A. (1881) Proc. Roy. Soc. 33, 127

Merchant, M.E. (1945) J. Appl. Phys. 16, 267 and 318

Merchant, M.E. (1957) Conf. "Lubrication and Wear", Inst. Mech. Eng.

Nakayama, K. (1957) J. Soc. Precision Mechanics, 23, 441

Nakayama, K. (1958) Bull. Fac. Eng. Yokohama University, 7, 1

Nakayama, K. (1962) Bull. Fac. Eng. Yokohama University, 11, 1

Oxley, P.L.B. and Hastings, W.F. (1976) Phil. Trans. Roy. Soc. A282, 565

Oxley, P.L.B. and Hastings, W.F. (1977) Proc. Roy. Soc. A356, 395

Palmer, W.B. and Oxley, P.L.B. (1959) Proc. Inst. Mech. Eng. 173, 623

Pepper, S.V. (1976) J. Appl. Phys. 47, 801 and 2579

Pepper, S.V. (1978) "Shear Strength of Metal-SiO_2 Contacts", (paper in preparation)

Pethica, J.B. (1978) PhD Thesis (in preparation)

Postnikov, S.N. (1967) Wear 10, 142

Ramalingam, S. (1971) Trans. ASME 93 B, 538

Ramalingam, S. and Black, J.T. (1973) Met. Trans. 4, 1103

Ramalingam, S. and Hazra, J. (1973) Trans. ASME 95 B, 939

Rebinder, P.A., Lichtman, V.I. and Karpenko, G.V. (1958) "Effect of Surface Active Media on the Deformation of Metals", HMSO Translation

Recht, R.F. (1964) Trans ASME 31 E, 189

Rollason, E.C. (1967) ISI Special Report No. 94

Rowe, G.W. and Smart, E.F. (1963) Brit. J. Appl. Phys. 14, 924

Rowe, G.W. and Smart, E.F. (1964) Proc. Inst. Mech. Eng. 178, 229

Rowe, G.W. and Smart, E.F. (1965) Proc. 5th Lub. Conf. Inst. Mech. Eng.

Rowe, G.W. and Spick, P.T. (1967) Trans. ASME 89 B, 530

Rowe, G.W. and Wolstencroft, F. (1970) J. Inst. Metals, 98, 33

Rubenstein, C. (1974) Int. J. Mach. Tool Des. Res. 14, 335

Sata, T. (1963) Proc. Conf. CIRP 18

Schallamach, A. (1971) Wear 17, 301

Scrutton, R.F. (1967) Trans. ASME 89 B, 539

Sharma, C.S., Rice, W.B. and Salmon, R. (1971) Trans. ASME 93 B, 441

Shaw, M.C. (1942) ScD. Thesis, cited in Wear 2, 217

Shaw, M.C. (1950) J. Appl. Phys. 21, 599

Shaw, M.C. (1958) Wear 2, 217

Shaw, M.C., Cook, N.H. and Finnie, I. (1953) Trans. ASME 75, 273

Shaw, M.C., Gujral, A. and Usui, E. (1961) Int. J. Mach. Tool Des. Res. 1, 187

Shaw, M.C., Smith, P.A. and Cook, N.H. (1961) Trans. ASME 83 B, 163

Stevenson, M.G. and Oxley, P.L.B. (1970) Proc. Inst. Mech. Eng. 184, 561

Takeyama, H. and Kasuya, U. (1961) Journal of the Government Mechanical Laboratory, 15, 4, 229

Takeyama, H. and Ono, T. (1968) Trans. ASME 90 B, 335

Taylor, F.W. (1907) Trans. ASME 28, 31

Thime, J. (1870) "Resistance of Metals and Wood to Cutting".

Trent, E.M. (1959) J. Inst. Prod. Eng. 38, 105

Trent, E.M. (1967) ISI Special Report no. 94

Trent, E.M. (1977) 'Metal Cutting", Butterworth

Tresca, H. (1878) Proc. Inst. Mech. Eng. June 1878, 310

von Turkovich, B.F. (1970) Trans. ASME 92 B, 151

von Turkovich, B.F. and Black, J.T. (1970) Trans. ASME 92 B, 130

Usui, E. and Takeyama, H. (1960) Trans. ASME 82 B, 303

Usui, E. and Takada, K. (1967) J. Jap. Soc. Precision Eng. 33, 23

Wallace, P.W. and Boothroyd, G. (1964) J. Mech. Eng. Sci. 6, 74

Williams, J.A. (1975) PhD. Thesis, University of Cambridge

Williams, J.A. (1977) J. Mech. Eng. Sci. 19, 5, 202

Williams, J.A. and Gane, N. (1977) Wear 42, 341

Williams, J.A. and Tabor, D. (1977) Wear 43, 275

Williams, J.E. and Rollason, E.C. (1970) J. Inst. Metals 98, 144

Williams, J.E., Smart, E.F. and Milner, D.R. (1970) Metallurgica, 81, 3, 51 and 89

Winter, R.E. (1975) Phil. Mag. 31, 765

Wolak, J. and Finnie, I. (1968) Proc. 8th Int. Conf. Mach. Tool Des. Res., 233

Zorev, N.N. (1958) Proc. Conf. "Techniques Eng. Manuf.", Inst. Mech. Eng. 1958, 237

Zorev, N.N. (1963) Proc. Conf. CIRP, 42

Zorev, N.N. (1966) "Metal Cutting Mechanics", Pergamon Press, Oxford